

ABSTRACT

Title: CHARACTORIZATION OF ORGANIC COMPOUNDS
IN HYDRAULIC FRACTURING FLUID

Jenna Lynn Luek, Doctor of Philosophy, 2018

Disertation Directed By: Dr. Michael Gonsior
Assistant Professor, University of Maryland Center for
Environmental Sciences

Over the past decade, hydraulic fracturing combined with horizontal drilling has become the dominant technique for extracting shale gas in the US, and is increasingly important globally. A complex mixture of chemicals is used in hydraulic fracturing fluid to stimulate natural gas production, but federal regulations have exempted operators from reporting the specific chemicals used in any given well. Recent state-by-state regulations and voluntary disclosures have increased our understanding of these fluids, but knowing this list of chemicals going into a well is just the tip of the iceberg. Once these chemicals are injected, they mix with fluids and naturally occurring chemicals originating in the shale formation and can undergo physical, chemical, and biological transformations. In Chapter 2, I reviewed the literature to date regarding the characterization of organic compounds in injected hydraulic fracturing fluids and waste fluids returning to the surface. I identified a substantial knowledge gap in our understanding of organic compounds in these fluids, particularly non-volatile compounds, and potential

transformations within the organic compound pool over the lifetime of the well. I analyzed a number of different shale gas wastewaters using ultrahigh resolution mass spectrometry and identified halogenated organic compounds in these fluids (Ch. 3), suggesting that these compounds were transformation products. Using a time series of shale gas fluids (Ch. 4), I was able to track changes in halogenated organic compounds and find evidence for both biological and chemical transformation pathways. Hierarchical cluster analyses helped identify sulfur-containing transformation products (Ch. 4), and I then determined that sulfur-containing molecules may be useful tracers of shale gas wastewaters in the environment (Ch. 6). In Chapter 5, I used toxicological tests and photoirradiation experiments to track the fate of organic compounds in shale gas wastewaters. Using a primarily non-targeted approach, I have been able to identify a number of organic compounds that are indicative of biological and chemical transformations occurring within hydraulic fracturing fluids and wastewaters. Understanding how these fluids change within the well and during storage and disposal provides critical information for engineering the safe and effective operation of wells, wastewater treatment techniques, and environmental impacts.

CHARACTERIZATION OF ORGANIC COMPOUNDS IN HYDRAULIC
FRACTURING FLUIDS

by

Jenna Lynn Luek

Dissertation submitted to the Faculty of the Graduate School of the
University of Maryland, College Park in partial fulfillment
of the requirements for the degree of
Doctor of Philosophy

2018

Advisory Committee:

Professor Michael Gonsior, Chair
Professor Lee Blaney
Professor Andrew Heyes
Professor Carys Mitchelmore
Professor Philippe Schmitt-Kopplin

Chapter 2: © Elsevier

<https://doi.org/10.1016/j.watres.2017.07.012>

Chapter 3: © American Chemical Society

<http://pubs.acs.org/doi/abs/10.1021/acs.est.6b06213>

All other materials © Copyright by

Jenna Lynn Luek

2018

For my family

Acknowledgements

I am so thankful for Michael Gonsior for taking me on with our unfunded project, allowing me the flexibility to pursue the questions I was interested in, introducing me to a network of scientists around the world, and guiding me through this crazy process with patience and understanding. I am extremely grateful to Paula Mouser for being the key in making a number of my research project successful by providing us with samples. Thank you to the Gonsior lab and BFL chemistry community for the feedback, support, fun, and snacks! Thank you to my fellow students for the fun and especially Hadley for always listening and keeping me sane. Thank you to my family for the years of support and love, and instilling in me the value of hard work and wanting to make a difference in the world. Thank you to my husband, KG, for everything you do for me and for helping to keep me motivated through this crazy process.

This research was supported by a number of sources of funding: Chesapeake Biological Laboratory Graduate Research Fellowship, Graduate Education Council Ruth Mathes Scholarship, DAAD (German Academic Exchange Service) Research Award, American Chemical Society Doctoral New Investigator Grant, and NSF Environmental Engineering Award #1604475.

TABLE OF CONTENTS

Dedication.....	ii
Acknowledgements.....	iii
List of Tables.....	vi
List of Figures.....	vii
List of Abbreviations.....	ix
Chapter 1 Introduction.....	1
Unconventional Resources.....	1
Environmental Policy.....	3
Hydraulic Fracturing Fluid and Wastewater Lifecycle.....	4
Dissertation Framework.....	7
Chapter 2: Organic compounds in hydraulic fracturing fluids and wastewaters.....	9
Introduction.....	10
Hydraulic Fracturing Fluid Additives.....	12
Flowback and Produced Waters.....	14
Environmental Contamination.....	30
Flowback and Produced Water Treatment.....	39
Considerations and Future Research.....	41
Conclusions.....	43
Chapter 3: Halogenated organic compounds identified in hydraulic fracturing wastewaters using ultrahigh resolution mass spectrometry	44
Introduction.....	45
Materials and Methods.....	49
Results and Discussion.....	54
Chapter 4: Temporal dynamics of halogenated organic compounds in Marcellus Shale flowback.....	68
Introduction.....	69
Methods.....	72
Results and Discussion.....	75
Conclusions.....	94
Chapter 5: Environmental fate and toxicity of organic compounds present in shale gas wastewaters.....	96
Introduction.....	97
Methods.....	100
Results and Discussion.....	105
Conclusion.....	118

Chapter 6: Organic matter fingerprinting techniques for identification of stream contamination arising from hydraulic fracturing activities	120
Introduction.....	121
Methods.....	124
Results and Discussion.....	128
Conclusions.....	141
 Chapter 7: Summary and Conclusions.....	 143
 Appendix 1.....	 150
Appendix 2.....	152
Appendix 3.....	173
Appendix 4.....	205
Appendix 5.....	226
 References.....	 241
 Curriculum Vitae	

List of Tables

Table 1.1 Hydraulic fracturing fluid ingredients	5
Table 2.1 Published reports and peer-reviewed literature analyzing organic compounds in shale gas flowback and produced waters.	16
Table 2.2 Halogenated organic compounds identified in flowback and produced waters.	28
Table 3.1. Selected halogenated organic molecular formulae identified in at least two flowback water samples.	56
Table 3.2 Iodinated compounds identified in FB1 with sufficient intensity to be confirmed using isotopic pattern matching and production of a fragment at m/z 126.9045.	58
Table 4.1 Iodinated molecular formulas identified in MSEEL samples supported with ^{13}C peak.	86
Table 5.1 Toxicity tests performed on daphnid species	103
Table 5.2 Photoirradiation experiments and absorbance data	104
Table 6.1 Molecular formulas assigned to tracer ions	130
Table 6.2 Unassigned tracer ion exact masses	132

List of Figures

Figure 1.1 Unconventional versus conventional natural gas resources	1
Figure 1.2 Shale gas plays in the continental US	2
Figure 1.3 Key policy actions associated with hydraulic fracturing	4
Figure 1.4 Life cycle analysis of hydraulic fracturing fluid waters	6
Figure 2.1 Summary of flowback and produced water samples analyzed to date for organic compounds in 18 studies.	15
Figure 2.2 Concentrations of benzene, toluene, ethylbenzene, and xylene in flowback and produced water samples by days after HVHF well completion from literature.	22
Figure 2.3. Boxplot of acetate/acetic acid concentrations in quantified samples reported in literature.	24
Figure 2.4. Acetone concentrations in flowback and produced water to 90 days compiled from literature values.	26
Figure 3.1 Oxygen to carbon (O/C) versus hydrogen to carbon (H/C) ratios and mass to charge ratio versus H/C ratios of 259 known halogenated disinfection by-products by class.	53
Figure 3.2 Ultrahigh resolution mass spectra of flowback water samples showing exact masses and molecular formula assignments between m/z 266.75-267.05.	55
Figure 3.3 Halogenated organic molecular formulae identified in at least two flowback water samples shown as their oxygen to carbon (O/C) versus hydrogen to carbon (H/C) ratios and mass to charge ratio versus H/C ratio.	56
Figure 4.1 Time series of specific ethoxylate carboxylate homologue abundance in MSEEL 3H well	80
Figure 4.2 Oxygen to carbon (O/C) ratio versus hydrogen to carbon (H/C) ratio of formulas assigned to molecular ions within MSEEL hierarchical clusters	81
Figure 4.3 Number of iodinated organic ions and their cumulative iodinated ion abundances identified in the MSEEL 3H and 5H wells by date	85

Figure 4.4 Conceptual model of variables and possible impacts on organic iodide cycling at different stages in of hydraulic fracturing.	93
Figure 5.1 Acute toxicity test survival of <i>D. magna</i>	106
Figure 5.2 Change in absorbance following photoirradiation	109
Figure 5.3 Changes in fluorescence following photoirradiation	110
Figure 5.4 PARAFAC component EEM fingerprints for photoirradiation experiments	112
Figure 5.5 Changes in PARAFAC component intensities over photoirradiation experiments	113
Figure 5.6 Van Krevelen diagrams of molecular formulas changing during photoirradiation	116
Figure 6.1 Garrett County, MD streamwater sampling locations	126
Figure 6.2 Van Krevelen diagram of stream water and tracer ions	133
Figure 6.3 4 component PARAFAC model of stream water samples	138
Figure 6.4 Fluorescence spectra of streamwater and hydraulic fracturing fluid samples	139

List of Abbreviations

Abbreviation	Definition
3H	MSEEL hydraulic fracturing well
5H	MSEEL hydraulic fracturing well
AEO	Alcohol ethoxylate
AES	Alcohol ethoxysulfate
BNP	Branched nonylphenol
BOP	Branched octylphenol
BTEX	Benzene, toluene, ethylbenzene, and xylene
CASS	Casselman River watershed
CHO	Compounds containing carbon, hydrogen, and oxygen only
CHOCl	Compounds containing carbon, hydrogen, oxygen and chlorine only
CHON	Compounds containing carbon, hydrogen, oxygen and nitrogen only
CHONS	Compounds containing carbon, hydrogen, oxygen, nitrogen and sulfur only
CHOS	Compounds containing carbon, hydrogen, oxygen and sulfur only
CHOX	Compounds containing carbon, hydrogen, oxygen and one or more halogens
CID	Collision induced dissociation
CL	Compression liquids
DATS	Dialkyltetralin sulfonate
DBE	Double bond equivalent
DBP	Disinfection by-products
DEA	Cocoamide diethanolamine
DEP	Department of Environmental Protection
DIC	Dissolved inorganic carbon
DOC	Dissolved organic carbon
DOM	Dissolved organic matter
DRO	Diesel range organics
E2/E3	Ratio for absorbance wavelengths
EDTA	Ethylenediaminetetraacetic acid
EEM	Excitation and emission matrix fluorescence
EO	Ethoxylate
EPA	Environmental Protection Agency [US]
ESI	Electrospray ionization
FB	Flowback waters
FF	Fracturing fluid

FL	Fractionation liquids
FT-ICR-MS	Fourier transform ion cyclotron resonance mass spectrometry
GC	Gas chromatography
GC-FID	Gas chromatography with flame ionization detection
GC-MS	Gas chromatography with mass spectrometry
GCxGC-TOF-MS	Two dimensional gas chromatography time of flight mass spectrometry
GEOR	Georges Creek watershed
GRO	Gas range organics
H/C	Hydrogen to carbon ratio of a molecular formula
HPLC	High performance liquid chromatography
HS	Homologous series member formula confirmed
HVHF	High-volume hydraulic fracturing
I-DBPs	Iodinated disinfection by-products
IC	Ion chromatography
IC	Isotope pattern confirmed
KMD	Kendrick mass defect
KMD/z*	Homologous series identifier (CH ₂ spacing)
KMD _e /z _e *	Homologous series identifier (C ₂ H ₄ O spacing)
LAS	Linear alkylbenzene sulfonate
LC	Liquid chromatography
LC-TOF-MS	Liquid chromatography time of flight mass spectrometry
LC50	Lethal concentration required to kill 50% of test organism
LNP	Linear nonylphenol
LOP	Linear octylphenol
m/z	mass to charge ratio
MD-DNR	Maryland department of natural resources
MeOH	Methanol
MIP	MSEEL hydraulic fracturing well name
MS	Mass spectrometry
MS-MS	Tandem mass spectrometry
MSEEL	Marcellus Shale Energy and Environment Laboratory
NAPL	Non-aqueous phase liquid
ND	Non-detect
NOM	Natural organic matter
NPEO	Nonylphenol ethoxylate
NPOC	Non-purgeable organic carbon
O/C	Oxygen to carbon ratio of a molecular formula
PAC	Powdered activated carbon
PAHs	Polycyclic aromatic hydrocarbons
PARAFAC	Parallel factor analysis

PCB	Polychlorinated biphenyl
PEG	Polyethylene glycol
PEG-C	Polyethylene glycol carboxylate
PI	Previously identified formula
PPL	Solid phase extraction cartridge with styrene-divinylbenzene polymer modified with a proprietary nonpolar surface
PRUN	Potomac River Upper Northwest Branch watershed
PW	Produced Water
QSU	Quinine sulfate units
SAS	Secondary alkane sulfate
SAVA	Savage River watershed
SPADC	sulfophenyl alkyl dicarboxylic acid
SPE	Solid phase extraction
SR	Slope ratio of absorbance
SRFA	Suwannee River Fulvic Acids
STAC	Sulfotetralin alkyl carboxylic acid
STADC	Sulfotetralin alkyl dicarboxylic acid
SVOC	Semi-volatile organic compound
TBA	Tert-butyl alcohol
TDN	Total dissolved nitrogen
TDS	Total dissolved solids
US	Unsupported but plausible formula assignment
UV	Ultraviolet light
VOC	Volatile organic compound
YOUG	Youghiogheny River watershed

Chapter 1

Introduction

1.1 Unconventional Resources

Large quantities of oil and gas are stored in low permeability formations such as shales and coalbeds and are considered unconventional resources due to the challenge associated with extracting these oil and gas resources. Conventional oil and natural gas wells are drilled in permeable geologic formations such as sandstones and oil and gas naturally flow to the surface through the drilled well (Figure 1.1). Hydraulic fracturing uses high pressure fluids to cause fracturing in a geological formation, which allows for the release of trapped oil and gas from low permeability formations. Hydraulic fracturing is typically used in parallel with horizontal drilling to maximize the amount of surface area being hydraulically fractured and the output of oil and gas (U.S. EPA, 2016).

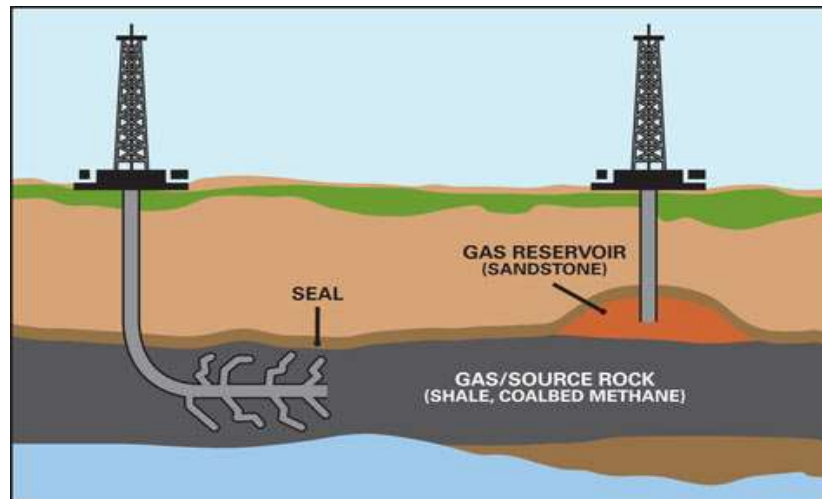


Figure 1.1 Comparison of unconventional well using hydraulic fracturing and horizontal drilling (left) and conventional well drilled in a gas reservoir (right) (Image from Lee, 2015).

The combination of advancements in hydraulic fracturing and horizontal drilling technologies, considered high volume hydraulic fracturing (HVHF), stimulated a rush in the development of unconventional oil and gas resources in the US in the early 2000s. Nearly all newly drilled wells use hydraulic fracturing technology and US domestic energy production has been increasingly dominated by unconventional sources including shale gas and coalbed methane. Shale formations and mixed formations such as shale-limestone are found in most central US states, many of which are actively being drilled (Figure 1.2). The Marcellus shale is the dominant gas producing shale, while the Utica, Eagle Ford, Haynesville, and Permian are also key gas producing formations in the US (U.S. EIA, 2015a).

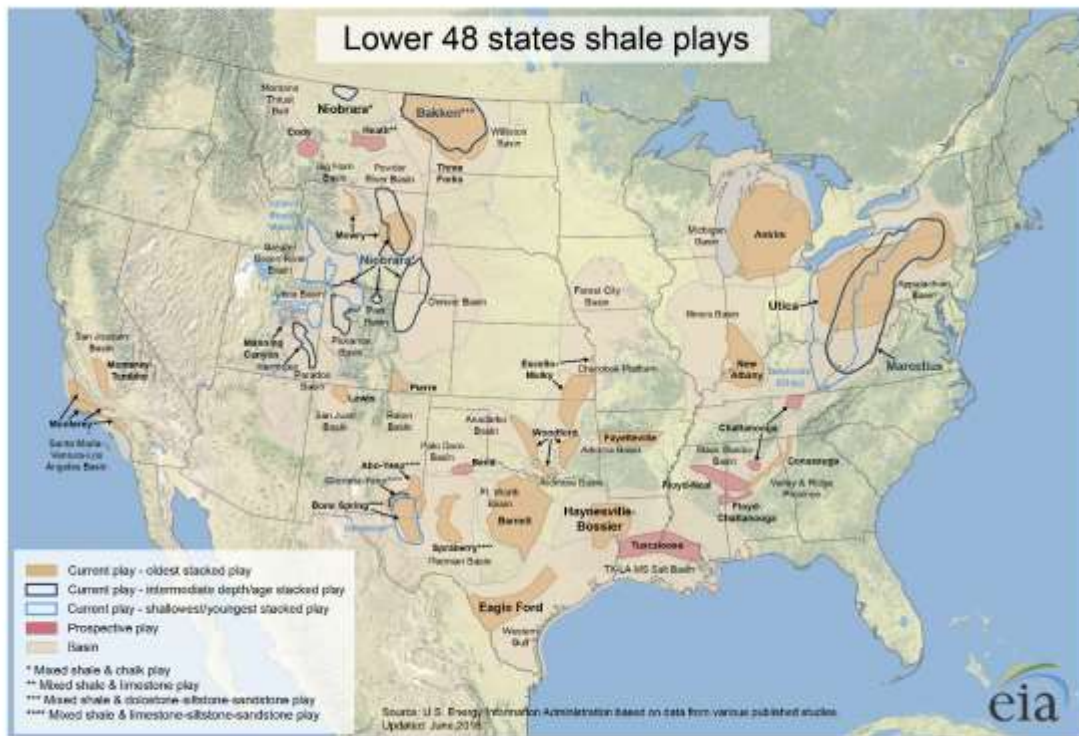


Figure 1.2 Shale plays in the lower 48 states (U.S. EIA, 2016).

1.2 Environmental Policy

Hydraulic fracturing technology has been surrounded by concerns about environmental impacts, particularly regarding drinking water resources. In 1997, the US Court of Appeals ruled that EPA was legally required to regulate HVHF under the underground injection control program of the Safe Drinking Water Act (*No. 95-6501*, 1997) (Figure 1.3). After a 2004 EPA report concluded that hydraulic fracturing posed a limited threat to drinking waters (*US EPA, 2004*), the Energy Policy Act of 2005 exempted hydraulic fracturing fluids from following the Safe Drinking Water Act (*Energy Policy Act of 2005, 2005*). Exemption meant that companies were no longer required to disclose the chemicals used in hydraulic fracturing, and this exemption is still in place at the federal level. Following the implementation of this policy, the rate of new wells being drilled increased rapidly, as did the oil and gas production. Rapid increases in well drilling without public information on the chemicals used resulted in fear and concern about water quality as millions of gallons of unknown and potentially hazardous fluids were used to hydraulically fracture thousands of wells in the US. A second, more comprehensive study of the impacts of HVHF on drinking water resources by the US Environmental Protection Agency was proposed to address these concerns and released in 2016 (U.S. EPA, 2016). This report identified the most likely routes of contamination of drinking water resources from hydraulic fracturing activities as spills during wastewater management, injection in to faulty wells which directly connect the well to groundwater resources, inadequate treatment and discharge to surface waters, and storage and disposal of wastewaters in unlined pits. Because of these policies, accessibility for independent scientists and researchers to lists of chemicals used and actual hydraulic

fracturing fluids and wastewaters has been a challenge. As a result, scientific understanding of the content of these fluids and their environmental stability, mobility, and toxicity has moved slowly. In 2011, the FracFocus online database (fracfocus.org) was launched to provide the public with information on the chemicals used in hydraulic fracturing. An example hydraulic fracturing fluid from FracFocus is given in Table 1.1. These reports of disclosed chemical have been an excellent resource for researchers in understanding the chemicals used, volumes, frequency of use, and informing further studies (Kekacs et al., 2015; Rogers et al., 2015; Yost et al., 2016).

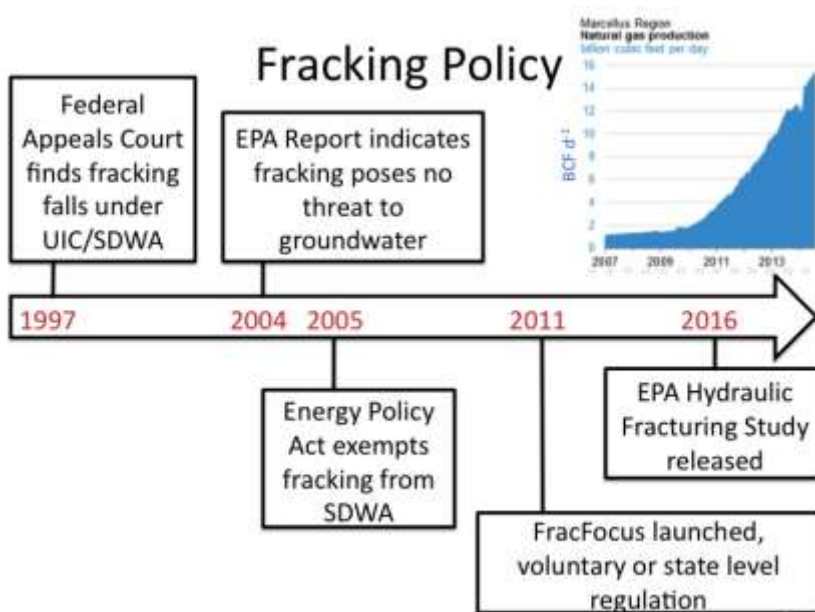


Figure 1.3 Key policy issues and regulatory reports associated with hydraulic fracturing activities. Marcellus shale natural gas production (billion cubic feet per day) is shown over the 2007 – 2015 time frame (U.S. EIA, 2015b).

1.3 Hydraulic Fracturing Fluid and Wastewater Life Cycle

During HVHF, large volumes of waters are used for a number of processes on site including well drilling, hydraulic fracturing, and gas processing and transmission (Figure

1.4) (Jiang et al., 2014). Hydraulic fracturing fluids make up the largest proportion of water usage, and these volumes range from 2,600 – 21,000 m³ (Jiang et al., 2014).

Median water usage varies by geologic formation, with the Woodford, Haynesville, and

Table 1.1 Example hydraulic fracturing fluid components and disclosed ingredients (fracfocus.org).

Component	Disclosed Ingredients
Carrier	Water
Proppant	Sand
Acid	Hydrochloric acid
Fe Control	Citric acid
Corrosion Inhibitor	Ethylene glycol, dimethyl formamide, 2-butoxyethanol, isopropanol, octanol, proprietary mixture
Friction Reducer	Petroleum distillate, alcohol ethoxylated C12-C16, sodium chloride, ammonium chloride
Surfactant	Ethoxylated alcohol, aromatic hydrocarbon mixture, naphthalene isopropanol, citrus terpenes
Biocide	Glutaraldehyde, ethanol, quaternary ammonium chloride
Cross Linker	Ethylene glycol, boric acid, ethanolamine
Gelling Agent	Petroleum distillate, proprietary polymer
Clay Stabilizer	Proprietary non-hazardous salt
Breaker	Ammonium persulfate
pH Adjustor	Potassium carbonate, potassium hydroxide

Fayetteville formations having the highest median use, between 19,400 and 23,700 m³ (Kondash and Vengosh, 2015). These hydraulic fracturing fluids are injected under high pressure and the well undergoes a shut-in period (under pressure) that allows necessary infrastructure for the next step to be laid. The length of well shut-in can influence the volume of fluid returning to the surface, as can the formation pressure, fracture conductivity, and the scale of fractures (e.g., multiple stages and fracture clusters) (Niazhen et al., 2015). After the pressure is released, fluid returns to surface, and is initially termed flowback, made up of injected additives and water derived from the

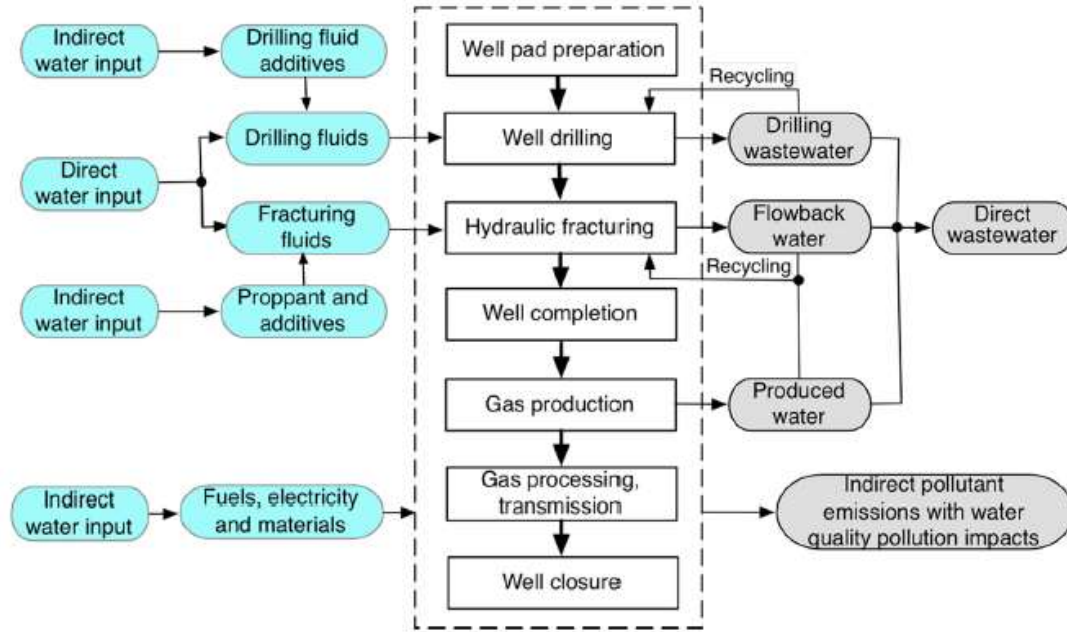


Figure 1.4 Life cycle processes associated with water in a Marcellus shale gas well (from Jiang et al., 2014). Shale gas well process (white boxes), inputs (blue boxes), outputs (grey boxes).

formation. The well continues to produce water over the lifetime of the well, termed produced water (U.S. EPA, 2016). The flowback period is generally considered completed within the first few weeks, associated with a period when the fluid characteristics become more like the formation waters (Engle and Rowan, 2014; Kim et al., 2016; Oetjen et al., 2018; Rosenblum et al., 2017b). Differentiation between fluid types using a number of chemical parameters recently distinguished three unique clusters in a Denver-Julesburg basin well: a flowback stage (day 1-2), a transition stage (days 6-21), and a production period (days 21-87) (Oetjen et al., 2018).

Rates of fluid return to the surface are typically highest in the initial flowback period, with 19-48% of fluid returned within the first 6 months in the major shale plays (Kondash and Vengosh, 2015; Kondash et al., 2017a). Water production decreases over time, and also increases in total dissolved solids, a major challenge for water treatment and reuse (Kondash et al., 2017a). The volumes of water produced over the first 6-10

years of operation can be similar to the injection volume (e.g., Barnett shale) or much higher (e.g., Niobrara shale, 5-fold higher) (Kondash and Vengosh, 2015). These wastewaters are managed differently by region, depending on the fluid characteristics and available management options (U.S. EPA, 2016; Veil, 2015). In Pennsylvania, Marcellus shale gas wastewater is increasingly reused for additional hydraulic fracturing activities (~85% of wastewaters 2011) (Lutz et al., 2013; Maloney and Yoxtheimer, 2012; Rahm et al., 2013; Veil, 2015). Injection for enhanced oil recovery or disposal are also dominant produced water management techniques, with up to 90% sent for disposal by deep well injection in Ohio (U.S. EPA, 2016; Veil, 2015). However, deep well injection has been associated with earthquakes, particularly when injected at high rates (Kim, 2013; Weingarten et al., 2015).

1.4 Dissertation Framework

Hydraulic fracturing fluids and wastewaters have been analyzed using a number of techniques with the bulk of studies focusing on inorganic compounds with established analytical methods (Ferrer and Thurman, 2015a). The number of studies on organic compounds are limited (Luek and Gonsior, 2017), and questions driving this dissertation included understanding not only what specific compounds are injected, but also how these fluids are transformed following injection and the new characteristics of fluids returning to the surface. Ultrahigh resolution mass spectrometry was used as the main tool for characterizing the organic compound pool and potential transformation products not understood *a priori*. This dissertation is written as a series of discrete papers as chapters, two of which have been peer-reviewed and published. The topic of organic compounds present in hydraulic fracturing fluids and wastewaters is introduced in

Chapter 2 as a review paper published in *Water Research*, followed by four research chapters. Chapter 3 focuses on halogenated organic compounds identified in hydraulic fracturing wastewaters from multiple sites, and is published in *Environmental Science and Technology*. Chapter 4 uses ultrahigh resolution mass spectrometry to track changes in the organic composition in two experimental Marcellus shale gas production wells over time. Chapter 5 describes the photochemical fate and toxicological impacts of an organic extract of these Marcellus shale gas wastewater fluids. Finally, Chapter 6 compares the identified common organic compounds found in these fluids to natural streamwaters to identify potential environmental tracers, and final thoughts and conclusions are given in Chapter 7.

Chapter 2

Organic Compounds in Hydraulic Fracturing Fluids and Wastewaters: A Review

Luek, J.L., Gonsior, M. 2017. *A Review of Organic Compounds in Hydraulic Fracturing Fluids and Wastewaters*. *Water Research* 123, 536-548.

DOI:10.1016/j.watres.2017.07.012

© Elsevier

Contribution: All data analysis, text and figures

Abstract

High volume hydraulic fracturing (HVHF) of shale to stimulate the release of natural gas produces a large quantity of wastewater in the form of flowback fluids and produced water. These wastewaters are highly variable in their composition and contain a mixture of fracturing fluid additives, geogenic inorganic and organic substances, and transformation products. The qualitative and quantitative analyses of organic compounds identified in HVHF fluids, flowback fluids, and produced waters are reviewed here to communicate knowledge gaps that exist in the composition of HVHF wastewaters. In general, analyses of organic compounds have focused on those amenable to gas chromatography, focusing on volatile and semi-volatile compounds oil and gas compounds. Studies of more polar and non-volatile organic compounds have been limited by a lack of knowledge of what compounds may be present as well as quantitative methods and standards available for analyzing these complex mixtures. Liquid chromatography paired with high-resolution mass spectrometry has been used to investigate a number of additives and will be a key tool to further research on transformation products that are increasingly solubilized through physical, chemical, and biological processes *in situ* and during environmental contamination events. Diverse

treatments have been tested and applied to HVHF wastewaters but limited information has been published on the quantitative removal and transformation of individual organic compounds. This review focuses on recently published information on organic compounds identified in flowback fluids and produced waters from HVHF.

2.1 Introduction

Shale gas extraction via high volume hydraulic fracturing (HVHF) in the U.S. has resulted in the use of 116 billion liters of fluids annually from 2012-2014 and yielded similar volumes of flowback and produced waters (Kondash and Vengosh, 2015). These fluids contain a complex mixture of inorganic and organic compounds used as additives (Elsner and Hoelzer, 2016; Stringfellow et al., 2014) as well as compounds extracted from the shale itself including salts, metals, radionuclides, oil and gas compounds, and natural organic matter (NOM) (Abualfaraj et al., 2014; Chapman et al., 2012; Engle and Rowan, 2014). Understanding these complex fluid mixtures is essential for understanding efficacy of additives, fluid treatment options for reuse in future HVHF jobs or discharge, and threats to the natural environment and human exposure.

The identification and quantification of individual organic compounds among the complex mixture of additives, oil and gas compounds, NOM, and transformation products requires diverse sample preparation and analytical techniques (Ferrer and Thurman, 2015a). Mass spectral techniques provide data of variable confidence ranging from having only the exact masses of interest to having confirmed structures by reference standards (Schymanski et al., 2014a). Gas chromatography paired with mass spectrometry has been traditionally used to identify hydrophobic oil and gas

hydrocarbons found in produced waters (Ferrer and Thurman, 2015a; Maguire-Boyle and Barron, 2014; Orem et al., 2014; Strong et al., 2013), and can be used to quantify many of the compounds in HVHF fluids and wastewaters of known toxicity (Elliott et al., 2017). Liquid chromatography paired with mass spectrometry has been shown to be useful in identifying many of the more hydrophilic organic compounds used in HVHF additives such as ethoxylated surfactants (Ferrer and Thurman, 2015a, 2015b; Getzinger et al., 2015; Hoelzer et al., 2016), but further method development requires overcoming analytical barriers such as the complex high salinity matrix. Analytical methods for describing unknown shale extracts and transformation products will require higher resolution techniques such as two dimensional gas chromatography with time of flight mass spectrometry (GC×GC-TOF-MS) (Hoelzer et al., 2016), liquid chromatography with time of flight mass spectrometry (LC-TOF-MS) (Ferrer and Thurman, 2015b; Thurman et al., 2014), and Fourier transform ion cyclotron resonance mass spectrometry (FT-ICR-MS), each requiring laborious data analysis and interpretation. Time of flight mass spectrometry can provide sufficiently high resolution that exact masses can be combined with GC or LC to determine unknown molecular formulas and structures with relatively high confidence in the absence of standards, especially when combined with fragmentation spectra (Ferrer and Thurman, 2015b; Marshall and Hendrickson, 2008; Thurman et al., 2014). Ultrahigh resolution FT-ICR-MS allows for direct determination of the assigned molecular formula based on the exact mass alone but provides no direct details on molecular structure (Marshall and Hendrickson, 2008) unless paired with MS-MS techniques. However, large numbers of possible isomers at higher masses make this approach challenging, but this challenge might be partially overcome by using LC.

Organic compounds observed in these fluids have been characterized by their mobility, persistence, toxicity, and frequency of use to understand the level of concern for human exposure via groundwater (Rogers et al., 2015). However, the combination of multiple organic compounds, inorganic compounds, and multiple phases complicates modeling the behavior of these organic compounds in the natural environment. Experimental and field studies are needed to address questions of mobility, persistence, and toxicity of HVHF fluid additives, geogenic organic compounds, and potential transformation products.

A number of studies have worked to identify analytical methods and quantify organic compounds in HVHF fluids, flowback fluids, and produced waters, and describe how these compounds are transformed within diverse environments. However, these studies have yet to be synthesized to provide a holistic perspective on the processes controlling organic compounds within these fluids. This review aims to synthesize existing literature on organic compounds quantitatively and qualitatively identified in HVHF fluids, flowback fluids and produced waters. Additionally, this review focuses on the distribution of HVHF associated organic compounds during environmental contamination and their use as tracers of contamination, the removal efficiencies of specific organic compounds during wastewater treatment, and makes recommendations for future research.

2.2 Hydraulic Fracturing Fluid Additives

The majority of organic additives included in HVHF fluid have been described by class and their frequency of use (Elsner and Hoelzer, 2016; Rogers et al., 2015).

Additionally, lists of additives are publicly available through the website FracFocus (fracfocus.org) and are summarized in the EPA hydraulic fracturing study report (U.S. EPA, 2016). Organic compounds are used at every stage in the HVHF process: 1) mixing of the base fluid including solvent and surfactants, 2) as cross linkers and breakers, 3) clay stabilizers, 4) corrosion, scale, and 5) biofouling inhibitors (Elsner and Hoelzer, 2016; Stringfellow et al., 2014). Alcohols are the dominant organic class used in a number of functions including as solvents (methanol, isopropanol, ethanol), surfactants (ethylene glycol, ethoxylated alcohols and phenols) and corrosion inhibitors (propargyl alcohol) (Elsner and Hoelzer, 2016). Polymers are also used in a large number of processes including as gelling agents, friction reducers, proppant coatings, corrosion and scale inhibitors (Elsner and Hoelzer, 2016). Many synthetic polymers and biopolymers are readily biodegraded, although their monomers may be of environmental concern (Elsner and Hoelzer, 2016; Stringfellow et al., 2014). Hydrocarbons, as light and heavy petroleum distillate mixtures and individual compounds (naphthalene, tetradecane, limonene), are an additional dominant class of additives, used primarily as solvents (Elsner and Hoelzer, 2016).

Of the remaining additives, some are specifically added to be reactive. For example, strong oxidants are used as biocides (infrequently) (Kahrilas et al., 2015) and as breakers (77% of surveyed well disclosure lists) (Elsner and Hoelzer, 2016).

Glutaraldehyde and dibromonitrilopropionamide are the dominant biocides used (27% and 24%, respectively) and behave by reacting with specific functional groups (thiol, amino, sulfhydryl) and destroying protein function (Kahrilas et al., 2015; Maillard, 2002). Breakers are used to “break” polymers and reduce surface tension of the fluid, allowing

flowback fluids to return to the surface. These breakers and biocides may react not only with their targets, but also on the other organic compounds present as additives or from geogenic sources and result in unknown transformation products (Hoelzer et al., 2016; Luek et al., 2017; Maguire-Boyle and Barron, 2014).

2.3 Flowback and Produced Waters

Specific organic compounds have been analyzed both qualitatively and quantitatively in more than 238 flowback (early fluids, first few weeks of production) and produced water (fluids over lifetime of well) samples from hydraulically fractured shale gas wells in published literature (Table 2.1, Figure 2.1). These analyses have focused on both oil and gas related compounds (e.g., hydrocarbons, benzene, toluene, ethylbenzene and xylene [BTEX]), small organic acids related to microbial degradation, and other additives. Confidence in identification of organic compounds is variable, with some compounds identified quantitatively using standards while others rely on spectral libraries or match of exact mass due to a lack of standards and standardized methods (Schymanski et al., 2014a). The use of quantitative techniques (^q), standards (^s), or spectral libraries (^l) is indicated in Table 2.1 by publication and technique.

Seventy percent of the samples analyzed for organic compounds have been collected from the Marcellus shale basin, which makes up ~37% of unconventional natural gas production but less than 0.01% of oil production (*Drilling Productivity Report*, 2017). Gas chromatography has been used extensively in these studies for volatile and semi-volatile organic compound (VOC, SVOC) analyses (Table 2.1). Ion chromatography (IC) has also been used to analyze small organic acids (Akob et al., 2015; Lester et al., 2013). High resolution LC-TOF-MS has been used to investigate

specific additives, focusing mostly on samples from Weld County, Colorado in the Denver-Julesberg basin (Ferrer and Thurman, 2015b; Rosenblum et al., 2016; Thurman et al., 2014). Organic analyses have also been performed on samples collected from the Barnett shale (Maguire-Boyle and Barron, 2014; Thurman et al., 2014), the Wolfcamp and Cline shales in the Permian basin (Khan et al., 2016), New Albany shale (Orem et al., 2014), an unknown formation in Texas (Thacker et al., 2015), a single sample from each of the Eagle Ford, Fayetteville, Burket, and unspecified formations in Pennsylvania, Nevada, and Louisiana.

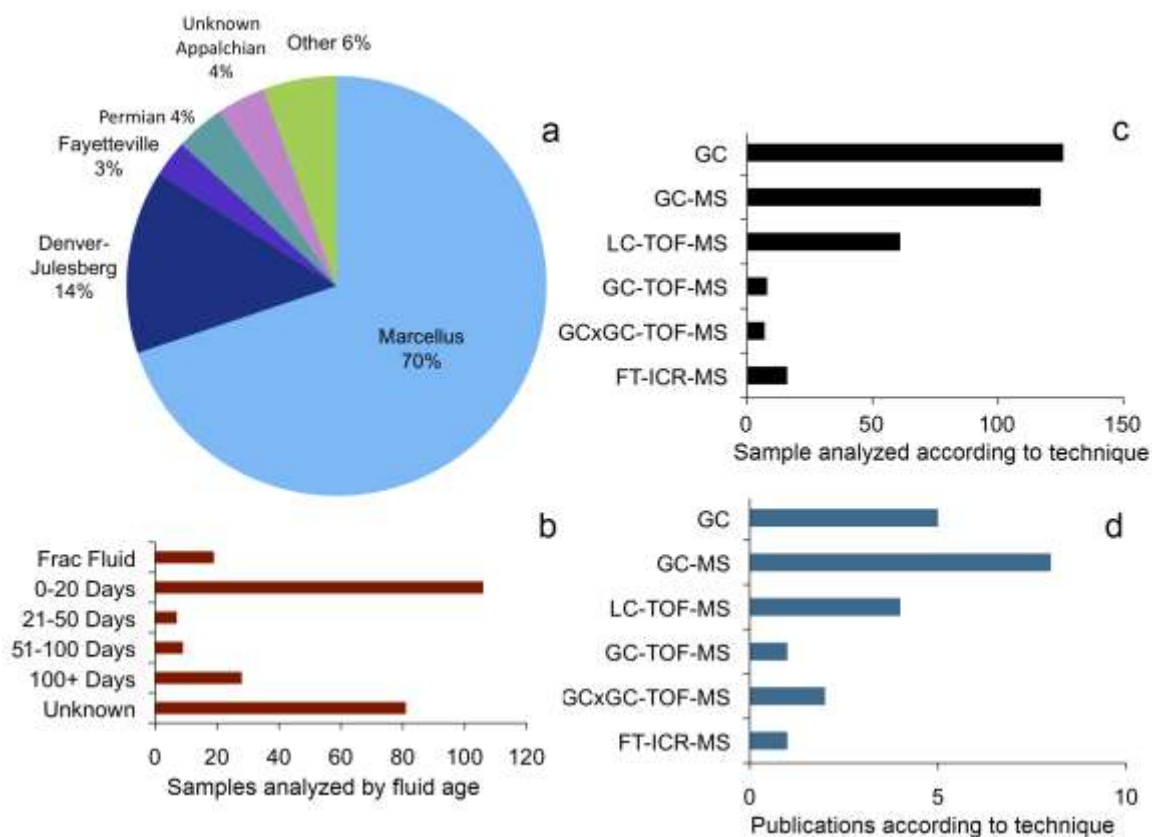


Figure 2.1 Summary of flowback and produced water samples analyzed to date for organic compounds in 18 studies given in Table 2.1. a) by basin b) fluid age c) analytical technique and d) number of publications by analytical technique.

2.3.1 Organic Additives

A number of known and suspect additives have been identified in flowback and produced waters, although not all studies had access to the corresponding list of additives or the HVHF fluid alone prior to injection (Cluff et al., 2014; Hayes, 2009; Hoelzer et al., 2016; Lester et al., 2015; Orem et al., 2014; Rosenblum et al., 2016; Strong et al., 2013; Thacker et al., 2015; Wolford, 2011). Quantitative analyses for known organic

Table 2.1 Published reports and peer-reviewed literature analyzing organic compounds in shale gas flowback and produced waters. ^qquantitative; ^scompared to standards; ^lcompared to spectral library [^]sample origins not precisely specified and up to 5 may overlap with samples reported by (Lester et al., 2015; Rosenblum et al., 2016) *MBA, methyl blue active substances (for anionic surfactants).

Basin/Shale Gas Formation (state) [#]	Fluid Type (time of sampling)	Analytical Method for Organic Compound Identification (targeted classes)	Number of Samples	Source
Marcellus (PA), Burket (PA)	Produced (5 months - 38 months)	GC-MS (VOCs ^{q,s} , IC (organic acids)	13	(Akob et al., 2015)
Marcellus (PA)	Flowback and Produced	GC (alkenes, alkanes, acetate ^l), LC-TOF-MS (ethoxylated surfactants)	31	(Cluff et al., 2014)
Denver-Julesberg (CO)	Flowback and Produced	LC-TOF-MS (gels, surfactants, biocides ^s)	22 [^]	(Ferrer and Thurman, 2015b)
Marcellus (PA, WV)	Flowback (Day 1, 5, 14) Produced (Day 90)	GC-MS (VOCs, SVOCs, pesticides ^{q,s}) GC-ECD (PCBs ^{q,s}) GC-FID (ethylene glycol ^{q,s})	78	(Hayes, 2009)
Fayetteville (AR)	Flowback (Week 0-3) Produced (Week 50)	GC-FID (VOCs ^{q,s}), GC-MS (SVOCs), GCxGC-FID and GCxGC-TOF-MS (SVOCs)	6	(Hoelzer et al., 2016)
Permian-Wolfcamp, Cline (TX)	Produced (Day 130-441)	GCxGC-TOF-MS (VOCs ^{q,s,l} , SVOCs ^{q,s,l})	8	(Khan et al., 2016)
Marcellus (WV), Denver-Julesberg (CO), Utica (OH), ND, PA, WV	Flowback, Produced, Compression liquids	FT-ICR-MS (dissolved ionizable (ESI-) organics)	16	(Luek et al., 2017)
Denver-Julesberg (CO)	Flowback composite (unknown timing)	IC (acetic acid ^q), GC-MS (VOC, SVOC ^{q,s}) LC-TOF-MS (trace organic chemicals)	1	(Lester et al., 2015)
Marcellus (PA)	Flowback	HPLC (organic acids ^q)	3	(Murali Mohan et al., 2013b)

Marcellus (PA), Eagle Ford (TX), Barnett (NM)	Produced (unknown)	GC-MS (aliphatic, aromatic, resin, asphaltenes, halogenated ^l)	3	(Maguire-Boyle and Barron, 2014)
Marcellus (PA) New Albany (IN, KY)	Flowback and Produced (time series)	GC-MS (PAHs, , aromatic amines, phenols, heterocyclic and other aromatic & aliphatic compounds, phthalates, fatty acids ^{q,s,l}), HPLC (volatile fatty acids ^q)	(>14)	(Orem et al., 2014)
Denver-Julesberg (CO)	Produced (Unknown)	LC-TOF-MS (polyethylene glycols), GC-FID (total petroleum hydrocarbons)	4	(Rosenblum et al., 2016)
Marcellus (Greene County, PA)	Produced water (18 months)	GCxGC-TOF-MS (aliphatic, cycloaliphatic, and aromatic compounds, and PAHs)	1	(Strong et al., 2013)
Unknown (TX)	Unknown	GC-MS (VOCs ^{q,l} , SVOCs), LCMS-IT-TOF (surfactant), IC (organic acids ^q)	3	(Thacker et al., 2015)
Denver-Julesberg (CO), Barnett (TX), PA, NV, LA	Flowback and Produced	LC-TOF-MS (ethoxylated surfactants ^s)	12 [^]	(Thurman et al., 2014)
Marcellus (PA)	Flowback, Produced and Flowback/Produced Mixture	GC-FID (acetic acid, ethylene glycol, 1,2-propanediol ^{q,s}) HPLC (citric acid ^{q,s})	10	(Wolford, 2011)
Marcellus (WV)	Flowback (Day 0, 7, 14, 35)	Unreported, listed as EPA certified labs	13	(Ziemkiewicz, 2013)
Marcellus (WV)	Flowback	GC-MS (VOCs ^{q,s}) GC-FID (petroleum hydrocarbons ^{q,s}) MBA* (surfactants ^{q,s})	13	(Ziemkiewicz and He, 2015)

additives are still limited by a lack of standards and standard methods and many compounds can only be putatively identified. Several surfactants/dispersants have been identified including ethoxylated alcohols (Cluff et al., 2014; Lester et al., 2015; Thurman et al., 2014), ethoxylated phenols (Orem et al., 2014), glycols (Hayes, 2009; Orem et al., 2014; Robert Wolford, 2011; Rosenblum et al., 2016), alkyl amines (Thacker et al., 2015), cocamide compounds (Ferrer and Thurman, 2015b; Thacker et al., 2015), 2-butoxyethanol (Thacker et al., 2015), and bulk anionic surfactants (as methyl blue active substances) (Ziemkiewicz and He, 2015). Of these surfactants, only ethylene glycol and propylene glycol were reported quantitatively (Hayes, 2009; Wolford, 2011). The

biocides alkyl dimethyl benzyl ammonium chloride, glutaraldehyde, and hexahydro-1,3,5-trimethyl-1,3,5-triazine-2-thione have been detected but only the latter was above quantitation limits (Ferrer and Thurman, 2015b; Orem et al., 2014). The triazine biocide was initially detected in flowback at very high levels (1.5 mg L^{-1}) but returned to very low levels ($10 \text{ } \mu\text{g L}^{-1}$) within one week of well operation (Orem et al., 2014). Phthalates have been identified in several flowback and produced water samples (Hayes, 2009; Hoelzer et al., 2016; Lester et al., 2015; Maguire-Boyle and Barron, 2014; Orem et al., 2014). In quantitative analyses of phthalates, di-n-octyl-phthalate peaked in Marcellus shale early flowback ($5600 \text{ } \mu\text{g L}^{-1}$) and rapidly declined (Orem et al., 2014), but no clear pattern was observed in nineteen Marcellus shale well time series for diethyl phthalate, di-n-butyl phthalate, di-n-octyl-phthalate, or bis-(2-ethylhexyl) phthalate (Hayes, 2009).

Citric acid, used for iron control, was reported in Marcellus flowback samples at high concentrations (9, 53, and 70 mg L^{-1}) but was not identified in any produced water samples within the same study (Wolford, 2011). 2,2,4-trimethyl-1,3,-pentanediol (solvent) and tridecane (fuel component) were also traced in a Marcellus shale well across flowback and produced waters, and while both peaked around the second day of flowback, both remained above $200 \text{ } \mu\text{g L}^{-1}$ in produced waters (Orem et al., 2014). The gelling agent guar gum was analyzed for but neither detected nor quantified in twenty-two Denver-Julesberg flowback and produced water samples (Ferrer and Thurman, 2015b). Bisphenol F and 2-butoxy ethanol were reported in a Texas produced water sample (Thacker et al., 2015), and a number of other additives have been reported qualitatively in several shale plays including a dioctadecyl ester of phosphate (lubricant),

and some fluorinated organic compounds (possible flowpath tracers) (Hoelzer et al., 2016; Maguire-Boyle and Barron, 2014).

2.3.2 Geogenic organic compounds from additives and/or shale

Ultrahigh resolution mass spectrometry has been used to qualitatively identify more than 30,000 organic compounds in shale oil.^{20,22} Although shale gas is more aged than shale oil and likely contains fewer organic compounds, interactions of the fracturing fluid with shale likely extracts a very large number of geogenic organic compounds from both oil and gas producing wells. Combined with a number of petrogenic additives such as petroleum distillates (hydrocarbon mixture such as naphtha), kerosene, BTEX, mixed alkanes, and naphthalenes, many geogenic compounds may be present in any given flowback fluid or produced water. Indeed, more than a thousand geogenic organic compounds have been identified in flowback and produced waters using GC-FID, GC-MS, and GCxGC-TOF-MS (Hoelzer et al., 2016; Maguire-Boyle and Barron, 2014; Orem et al., 2014; Strong et al., 2013), but only twenty four of these compounds have been reported quantitatively above the limit of detection in the peer reviewed literature (Akob et al., 2015; Lester et al., 2015; Ziemkiewicz and He, 2015; Ziemkiewicz, 2013). Reported concentrations of these quantifiable organic compounds are given in Appendix 1, including data from two non-peer reviewed sources (Hayes, 2009; Wolford, 2011). Dissolved methane as well as other light gases including ethane, propane, and butane will not be discussed here as they are by default present in productive wells. Overall, extractable hydrocarbons decreased in concentration during flowback and were lowest in produced water in a large number of analyzed samples (Orem et al., 2014). In broad spectrum reports of organic compounds in flowback and produced waters using various

types of gas chromatography, aliphatic compounds were the dominant class identified (Hoelzer et al., 2016; Maguire-Boyle and Barron, 2014; Orem et al., 2014; Strong et al., 2013). Out of 986 compounds tentatively identified using GCxGC-TOF-MS in a Marcellus shale produced water, 61% of the identified compounds were aliphatic, and 24% were cycloaliphatic (Strong et al., 2013). Aromatic compounds represented 13% of the remaining compounds. PAHs accounted for 2% in this Marcellus shale produced water, and a substantial number of aromatic compounds and PAHs were also identified by other broad spectrum reports of organic compounds (Hoelzer et al., 2016; Maguire-Boyle and Barron, 2014; Orem et al., 2014). A new analytical technique has been developed for quantification of PAHs and other SVOCs in HVHF wastewater pairing solid-phase extraction with GC-MS (Regnery et al., 2016).

BTEX compounds were both the most frequently analyzed organic compounds in flowback and produced water and the most frequently detected organic compounds above detection limits (Figure 2.2). In the Marcellus shale, BTEX concentrations were highest in flowback over the first 90 days, but were detectable at low concentrations in produced waters even several years after the initial HVHF event. Toluene, ethylbenzene, and xylene concentrations in flowback were up to two orders of magnitude lower than benzene quantified concurrently. Fayetteville, Burket, and Denver-Julesberg samples were only analyzed in early flowback and had similar levels to the Marcellus shale (Akob et al., 2016; Hoelzer et al., 2016; Lester et al., 2015). In the Permian basin, produced water after 130-441 days of operation had consistently high levels of benzene, toluene, and ethylbenzene, of hundreds of mg L^{-1} , while xylenes concentration was three orders of magnitude lower, similar to Marcellus flowback (Khan et al., 2016). High BTEX

concentrations found in the Permian could be associated with oil production compared to the generally dry Marcellus shale gas. A clear distinction was made in a side by side comparison of BTEX in a dry and a wet Marcellus shale gas; wet gas concentrations were two orders of magnitude higher for all ions than dry gas, peaking in wet gas seven days after HVHF (benzene = 375 $\mu\text{g L}^{-1}$, toluene = 2,100 $\mu\text{g L}^{-1}$, xylenes (m,p) = 2,400 $\mu\text{g L}^{-1}$) [ethylbenzene not reported] (Ziemkiewicz, 2013).

Aromatic compounds including polycyclic aromatic hydrocarbons have been quantitatively reported in a number of studies. Phenol, 2-methylphenol, 3&4-methylphenol, 2,4 dimethylphenol, 2-methylnaphthalene, phenanthrene, and pyrene were all quantified in a composite Denver-Julesberg basin flowback sample (Lester et al., 2015) and in Marcellus shale flowback and produced waters (Hayes, 2009). 1,2,4-trimethylbenzene and isopropylbenzene were quantified in Fayetteville flowback fluids and Marcellus shale flowback and produced waters (Hoelzer et al., 2016). New Albany shale produced waters also frequently contained alkyl naphthalenes, phenanthrenes, and pyrene (Orem et al., 2014). Alkylated benzenes and alkylated naphthalenes were identified but not quantified in Barnett and Marcellus shales (Maguire-Boyle and Barron, 2014). Methyl phenol and dimethylphenol were detected in much higher concentrations in a composite flowback sample from the Denver-Julesberg basin than PAHs (150-830 $\mu\text{g L}^{-1}$ vs. <10 $\mu\text{g L}^{-1}$) (Lester et al., 2015), but similar concentration ranges of both the phenolic and PAH compounds were observed in the Marcellus (Hayes, 2009). A number of oxygen containing resins/asphaltenes were identified in Marcellus, Barnett and Eagle Ford shale produced waters (Maguire-Boyle and Barron, 2014).

Polychlorinated biphenyls (PCBs) and pesticides were analyzed for the Hayes report (Hayes, 2009) in nineteen wells over the first ninety days after HVHF, but were only detected sporadically in low concentrations and the report concluded that testing for these compounds in future wastewater analyses was unnecessary. These compounds have not been specifically targeted in any other study, and no evidence has been provided for a potential source for these compounds in fracturing additives.

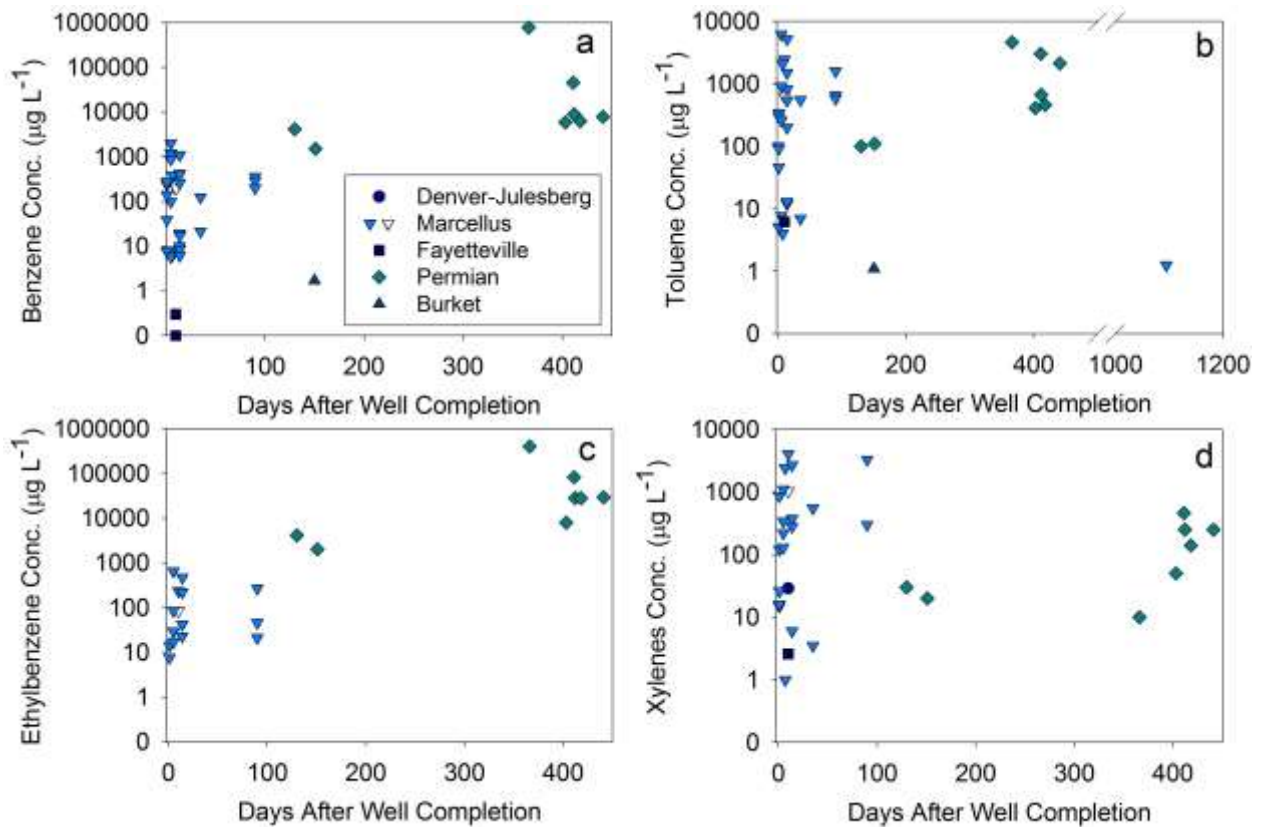


Figure 2.2 Concentrations (log scale) of benzene (a), toluene (b), ethylbenzene (c), and xylene (d) in flowback and produced water samples by days after HVHF well completion from literature. Open triangles indicate mean of 13 Marcellus samples (Ziemkiewicz and He, 2015), colored triangles represent individual data points. Fayetteville samples are shown on day 10 for comparison but were collected within the first three weeks (Hoelzer et al., 2016). Note: benzene and ethylbenzene are given on a different scale than toluene and xylenes.

2.3.3 Transformation products of organic constituents

Transformations in HVHF fluids of organic compounds may occur through physico-chemical or biological processes. Indeed, specific additives are designed to chemically transform and “break” polymers in the fracturing fluid to reduce surface tension before flowback begins (Stringfellow et al., 2014). Despite the use of biocides, high bacterial cell counts have been identified both in the injected fluids and in flowback and produced waters (Cluff et al., 2014; Mohan et al., 2014; Murali Mohan et al., 2013a). Hence, a combination of physical, chemical and biologically mediated reactions ultimately drive the transformation of organic compounds in these fluids (Elsner and Hoelzer, 2016; Hoelzer et al., 2016).

A number of small organic acids are produced through microbial transformation under the anaerobic conditions frequently observed in HVHF wastewater via fermentation (Müller, 2008). Small organic acids were analyzed in a handful of studies, although not all report quantitative results. Acetate was measured in seven studies (Figure 2.3), formate in three (Akob et al., 2015; Strong et al., 2013; Thacker et al., 2015), and citrate (Wolford, 2011), lactate, propionate, butyrate, and pyruvate (Akob et al., 2015) were each analyzed in one study. Acetate, propionate, and butyrate were measured in the Hayes dataset with high method detection limits (10mg L^{-1}) but are not included due to data qualifiers associated with the reported values (i.e., outside of calibration range) (Hayes, 2009). Acetate and other organic acids are likely produced during the anaerobic degradation of additives and potentially geogenic substances as hydrocarbons are degraded to acetate under anaerobic conditions (Callbeck et al., 2013). Indeed, fermentative classes of bacteria capable of producing organic acids were identified in

flowback samples where acetate was identified (Cluff et al., 2014; Murali Mohan et al., 2013b). Acetate concentrations were highest in flowback samples, presumably due to the high concentrations of degradable organic additives such as ethoxylates, guar gum, and glycols. The highest concentration of acetate observed (1600 mg L^{-1}) was in a composite flowback sample, and was three times higher than the next highest sample and an order of magnitude higher than most flowback samples (Lester et al., 2015). Aeration of flowback fluid resulted in acetate decreasing below detection limits, which is not surprising as fermentation would no longer be occurring

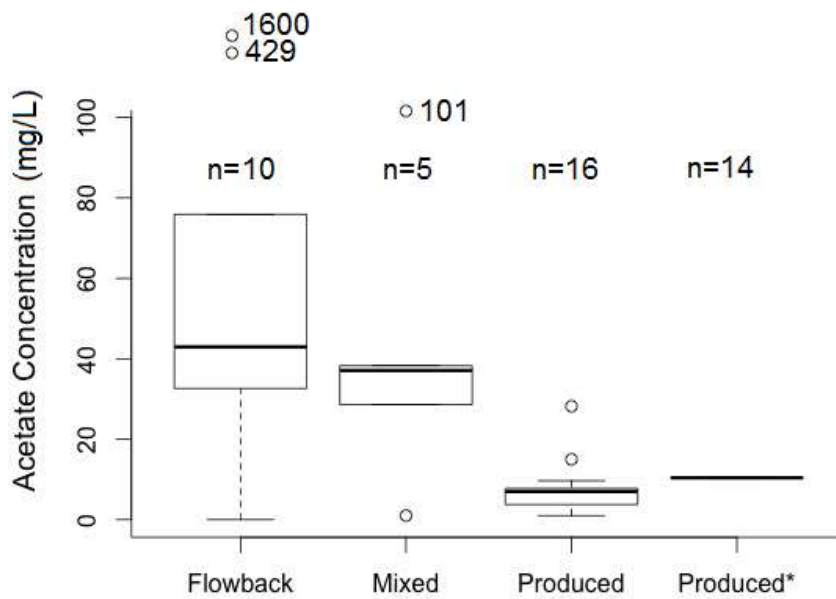


Figure 2.3. Boxplot of acetate/acetic acid concentrations in quantified samples reported in literature. Box gives median and 25th and 75th percentiles, whisker represent 90th percentile, and individual points show outliers. Acetate values below detection for one produced and two HVHF wastewater samples were not included in the box plot (Strong et al., 2013; Thacker et al., 2015). Mixed is a combination of flowback and produced water (Wolford, 2011). Produced* represents mean of 14 samples reported by (Orem et al., 2014).

and any acetate previously produced would likely be readily mineralized *in situ* under aerobic conditions (Murali Mohan et al., 2013b). Produced water samples contained much lower acetate concentrations. In 14 Marcellus shale produced water samples (Figure 2.3, Produced*), the mean acetate concentration was 10.6 mg L^{-1} , but the range was not reported (Orem et al., 2014). In 16 other produced water samples, the mean acetate concentration was 7.0 mg L^{-1} . Formate was not detected in two of the three studies in which it was analyzed, and in those where it was not detected acetate was also absent (Strong et al., 2013; Thacker et al., 2015). Butyrate was not detected in any of the 13 produced water samples it was analyzed in, but propionate, lactate, formate, and pyruvate were detected in produced water samples at low levels ($<4 \text{ mg L}^{-1}$ each) and acetate in slightly higher concentrations (mean 5.8 mg L^{-1}). These are indications for continued bacterial activity as these are highly labile compounds (Akob et al., 2015).

Acetone in flowback may originate from its use as an additive, may be a transformation product via anaerobic fermentation via pyruvate (Rosenfeld and Simon, 1950), or may be associated with both sources. Acetone concentrations were highly variable in flowback samples (most not detected, median $90 \text{ } \mu\text{g L}^{-1}$ in positive detections, mean of $1,060 \text{ } \mu\text{g L}^{-1}$ in $n=37$ positive detections) and acetone was not measured in any samples after 90 days (Figure 2.4). The highest observed concentration was measured in a composite flowback sample ($16,000 \text{ } \mu\text{g L}^{-1}$) (Lester et al., 2015), and several other flowback samples had acetone concentrations ranging from $10^2 - 10^3 \text{ } \mu\text{g L}^{-1}$ (Hayes, 2009). Interestingly, in at least one supply water sample (used for mixing to make HVHF fluid), acetone concentrations were even higher than in flowback (Hayes, 2009), suggesting that this supply water was likely a recycled fluid that contained high levels of

acetone as an additive or degradable organic additives that underwent fermentation to form acetone. In a simulated bioreactor “spill” of HVHF fluids, acetone was produced as a degradation product (Kekacs et al., 2015).

19% of the 404 identified organic compounds in Fayetteville shale flowback fluid and produced waters using GCxGC-TOF-MS were suspected to be formed through subsurface reactions (Hoelzer et al., 2016). Many of these compounds included carbonyl groups (Hoelzer et al., 2016) that may indicate degradation of geopolymers or hydrolysis products of delayed-release acids used as breakers (Hoelzer et al., 2016; Orem et al.,

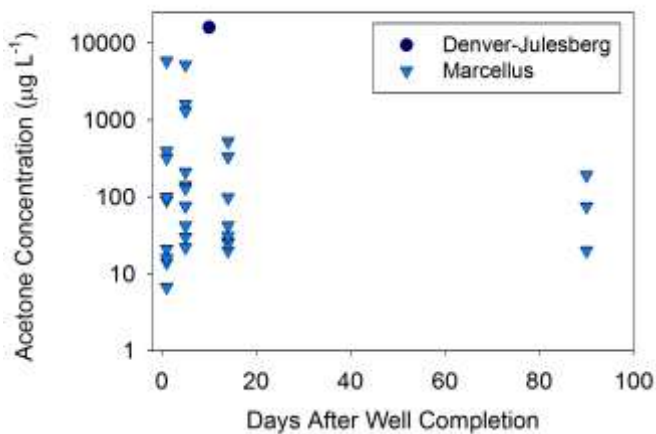


Figure 2.4 Acetone concentrations in flowback and produced water to 90 days compiled from literature values. Acetone analyses were not performed on samples collected more than 90 days after HVHF well completion.

2014, 2010). In Marcellus shale produced waters, 2,2,4-trimethyl-1,3-pentanediol was identified at high concentrations (130 - 500 µg L⁻¹) in flowback and remained at those concentrations in the produced waters even 234 days after HVHF (Orem et al., 2014).

This compound has not been identified as an additive previously, but a related compound, 2,2,4-trimethyl-1,3-pentanediol monoisobutyrate, has been used industrially as a solvent and may potentially be related to the source of this derivative (Orem et al., 2014). A

direct transformation product of the known additive azobis, (isobutyronitrile) tetramethylsuccinonitrile was identified by GCxGC-TOF-MS in Fayetteville shale produced waters (Hoelzer et al., 2016). Dimerization and trimerization of the frequently used biocide glutaraldehyde under the variable salinity, temperature, and pressure conditions reflecting a shale gas well has been tested under laboratory conditions (Kahrilas et al., 2016), but has not been observed in flowback and produced waters (Ferrer and Thurman, 2015b). Additionally, hydroxylated phenols identified in flowback fluids are likely degradation products of alkylphenol ethoxylate additives (Hoelzer et al., 2016).

A number of studies have putatively identified halogenated organic compounds in flowback and produced waters that are much more diverse than the limited number of known halogenated additives (Table 2.2). Perfluorinated organic compounds identified in the Eagle Ford shale produced waters were suggested to be tracers used for reservoir mapping (Maguire-Boyle and Barron, 2014). Methylene chloride is the only explicitly disclosed halogenated organic compound identified in flowback and produced waters, but four additional halogenated organic compounds (chloromethyl propanoate, chloromethyl pentanoate, chloromethyl hexanoate, chloromethyl octanoate) identified by Hoelzer and colleagues are suspected HVHF additives (Hoelzer et al., 2016). Four studies have identified a number of additional halogenated organic compounds that are likely transformation products and several potential mechanisms for the formation of these compounds are hypothesized (Hayes, 2009; Hoelzer et al., 2016; Luek et al., 2017; Maguire-Boyle and Barron, 2014). Maguire-Boyle and Barron (2014) identified the corresponding non-halogenated aliphatic compound for each halogenated compound and

suggested that the halide salts or free halogens created during oxidative treatments could cause the observed halogenation (Maguire-Boyle and Barron, 2014). Similarly, Hoelzer and colleagues indicated radicalic substitution, nucleophilic substitution, and electrophilic addition in the presence of halides and free halogen species as the proposed halogenation mechanisms (Hoelzer et al., 2016). In streambed sediments downstream of a deep well injection facility, several halogenated organic compounds including 1,54-dibromotetrapentacontane were identified (Orem et al., 2017).

Table 2.2 Halogenated organic compounds identified in flowback and produced waters. *Italicized* compounds are explicit and suspect fracturing fluid additives. Note: Compounds identified in Hayes (2009) rely on EPA methods with quantification using reference standards; Hoelzer et al., (2016) and Maguire-Boyle and Barron (2014) match ions using spectral libraries and report confidence in assignment in their supplemental materials. Halogenated chemical formulas in Luek et al., (2017) not included due to lack of structural information.

Compound	Molecular Formula	Method	Source
Chloromethane	CH ₃ Cl	GC/MS EPA Method SW846 8260B	Hayes 2009
<i>Dichloromethane</i>	<i>CH₂Cl₂</i>	<i>GC/MS EPA Method SW846 8260B</i>	<i>Hayes 2009</i>
<i>Dichloromethane</i>	<i>CH₂Cl₂</i>	<i>GCxGC-TOF-MS</i>	<i>Hoelzer et al., 2016</i>
<i>Dichloromethane</i>	<i>CH₂Cl₂</i>	<i>GC/MS</i>	<i>Maguire-Boyle and Barron 2014</i>
Trichloromethane	CHCl ₃	GC/MS	Maguire-Boyle and Barron 2014
Tetrachloroethene	C ₂ Cl ₄	GC/MS EPA Method SW846 8260B	Hayes 2009
1,1-dichloroethane	C ₂ H ₄ Cl ₂	GC/MS	Maguire-Boyle and Barron 2014
1,1'-oxybis[1,1]-dichloromethane	C ₂ H ₄ Cl ₂ O	GC/MS	Maguire-Boyle and Barron 2014
<i>Chloromethyl propanoate</i>	<i>C₄H₇ClO₂</i>	<i>GCxGC-TOF-MS</i>	<i>Hoelzer et al., 2016</i>
bis(2-chloroethyl) ether	C ₄ H ₈ Cl ₂ O	GC/MS EPA Method SW846 8260B	Hayes 2009
1-chloro-5-iodo-pentane	C ₅ H ₁₀ ClI	GCxGC-TOF-MS	Hoelzer et al., 2016
1,1-dimethyl-3-chloropropanol	C ₅ H ₁₁ ClO	GCxGC-TOF-MS	Hoelzer et al., 2016
Hexachlorobenzene	C ₆ Cl ₆	GC/MS EPA Method SW846 8270C	Hayes 2009
2-(chloromethyl) tetrahydropyran	C ₆ H ₁₁ ClO	GCxGC-TOF-MS	Hoelzer et al., 2016
2-chlorocyclohexanol	C ₆ H ₁₁ ClO	GCxGC-TOF-MS	Hoelzer et al., 2016

<i>Chloromethyl pentanoate</i>	$C_6H_{11}ClO_2$	<i>GCxGC-TOF-MS</i>	<i>Hoelzer et al., 2016</i>
1-chloro-3,3-dimethyl-butane	$C_6H_{13}Cl$	GCxGC-TOF-MS	Hoelzer et al., 2016
1,2,3-trichlorobenzene	$C_6H_3Cl_3$	GC/MS EPA Method SW846 8260B	Hayes 2009
1,2,4-trichlorobenzene	$C_6H_3Cl_4$	GC/MS EPA Method SW846 8260B	Hayes 2009
1,4-dichlorobenzene	$C_6H_4Cl_2$	GC/MS EPA Method 624	Hoelzer et al., 2016
2,6-dichlorophenol	$C_6H_4Cl_2O$	GC/MS EPA Method SW846 8270C	Hayes 2009
2,4-dichloro-5-oxo-2-hexenedioic acid	$C_6H_4Cl_2O_5$	GC/MS	Maguire-Boyle and Barron 2014
Dichlorophenol	C_6H_4ClO	GC/MS EPA Method SW846 8260B	Hayes 2009
2,2-dichloro-3,6-dimethyl-1-Oxa-2-silacyclohexa-3,5-diene	$C_6H_8Cl_2OSi$	GC/MS	Maguire-Boyle and Barron 2014
3-chloro-1,1,2,2-tetramethyl-cyclopropane	$C_7H_{13}Cl$	GCxGC-TOF-MS	Hoelzer et al., 2016
<i>Chloromethyl hexanoate</i>	$C_7H_{14}ClO_2$	<i>GCxGC-TOF-MS</i>	<i>Hoelzer et al., 2016</i>
<i>Chloromethyl octanoate</i>	$C_9H_{17}ClO_2$	<i>GCxGC-TOF-MS</i>	<i>Hoelzer et al., 2016</i>
1-chlorohexadecane	$C_{16}H_{33}Cl$	GC/MS	Maguire-Boyle and Barron 2014
1-chlorooctadecane	$C_{18}H_{37}Cl$	GC/MS	Maguire-Boyle and Barron 2014
Trichlorodocosylsilane	$C_{22}H_{45}Cl_3Si$	GC/MS	Maguire-Boyle and Barron 2014
1-chloroheptacosane	$C_{27}H_{55}Cl$	GC/MS	Maguire-Boyle and Barron 2014
Bromomethane	CH_3Br	GC/MS EPA Method SW846 8260B	Hayes 2009
Tribromomethane	$CHBr_3$	GC/MS EPA Method SW846 8260B	Hayes 2009
2-bromo-hexane	$C_6H_{13}Br$	GCxGC-TOF-MS	Hoelzer et al., 2016
1-bromo-2-methyl-cyclohexane	$C_7H_{13}Br$	GCxGC-TOF-MS	Hoelzer et al., 2016
4-bromoheptane	$C_7H_{15}Br$	GCxGC-TOF-MS	Hoelzer et al., 2016
2-piperidinone, N-[4-bromo-n-butyl]	$C_9H_{16}BrNO$	GCxGC-TOF-MS	Hoelzer et al., 2016
2-bromo-tricyclo[3.3.1.1(3,7)]decane	$C_{10}H_{15}Br$	GCxGC-TOF-MS	Hoelzer et al., 2016
3-bromo-cyclodecene	$C_{10}H_{17}Br$	GCxGC-TOF-MS	Hoelzer et al., 2016
4,5-dibromo-, (R*,R*)-decane	$C_{10}H_{20}Br_2$	GCxGC-TOF-MS	Hoelzer et al., 2016
1,12-dibromododecane	$C_{12}H_{24}Br_2$	GC/MS	Maguire-Boyle and Barron 2014
14-bromo-1-tetradecene	$C_{14}H_{27}Br$	GC/MS	Maguire-Boyle and Barron 2014
1-bromopentadecane	$C_{15}H_{31}Br$	GC/MS	Maguire-Boyle and Barron 2014
7-bromomethyl-pentadec-7-ene	$C_{16}H_{31}Br$	GCxGC-TOF-MS	Hoelzer et al., 2016
1-bromohexadecane	$C_{16}H_{33}Br$	GC/MS	Maguire-Boyle and Barron 2014
1-bromooctadecane	$C_{18}H_{37}Br$	GC/MS	Maguire-Boyle and Barron 2014

1,54-dibromotetrapentacontane	C ₅₄ H ₁₀₈ Br ₂	GC/MS	Maguire-Boyle and Barron 2014
3-iodo-propanoic acid,	C ₃ H ₅ IO ₂	GCxGC-TOF-MS	Hoelzer et al., 2016
2-iodo-3-methyl-butane	C ₅ H ₁₁ I	GCxGC-TOF-MS	Hoelzer et al., 2016
5-iodopentan-2-one	C ₅ H ₉ IO	GCxGC-TOF-MS	Hoelzer et al., 2016
1-iodo-nonane	C ₉ H ₁₉ I	GCxGC-TOF-MS	Hoelzer et al., 2016
1-iodo-2-methylundecane	C ₁₂ H ₂₅ I	GCxGC-TOF-MS	Hoelzer et al., 2016
1-iodo-2-methylundecane	C ₁₂ H ₂₅ I	GC/MS	Maguire-Boyle and Barron 2014
1-iodo-tetradecane	C ₁₄ H ₂₉ I	GCxGC-TOF-MS	Hoelzer et al., 2016
Bromodichloromethane	CHBrCl ₂	GCxGC-TOF-MS	Hoelzer et al., 2016
1,3-dioxolane, 2-(3-bromo-5,5,5-trichloro-2,2-dimethylpentyl)	C ₁₀ H ₁₆ BrCl ₃ O ₂	GCxGC-TOF-MS	Hoelzer et al., 2016
1-bromo-11-iodoundecane	C ₁₁ H ₂₂ BrI	GC/MS	Maguire-Boyle and Barron 2014

2.4 Environmental Contamination

2.4.1 Contamination Events

In the peer-reviewed literature, specific organic compounds have been identified in surface water, sediments, and groundwater and have been linked to recent HVHF activities (Cozzarelli et al., 2017; DiGiulio and Jackson, 2016a; Drollette et al., 2015; Gross et al., 2013; Hildenbrand et al., 2016, 2015; Kassotis et al., 2014; Llewellyn et al., 2015; Orem et al., 2017). These suspected contamination events were documented in the Bakken, Powder River Basin, Marcellus, Permian, Barnett, and Denver-Julesberg basins, and next to a deep well injection facility in West Virginia. The EPA has also published five “retrospective case studies” investigating the impacts of HVHF on drinking water sources in five different locations between 2011-2013 (U.S. EPA, 2015a, 2015b, 2015c, 2015d, 2015e). Organic analyses have focused on additives and oil and gas related compounds; inorganic tracers of HVHF including anions and metals have also been analyzed in these samples to understand the potential contamination events.

The only large volume surface spill of HVHF wastewaters (11.4 million liters) extensively analyzed for organic compounds and published in the literature occurred in

Blacktail Creek in North Dakota (Bakken formation) in January of 2015. Streamwater and stream bed sediment samples were collected in February and June of 2015 for a large number of organic and inorganic chemical analyses, biological, and toxicological analyses (Cozzarelli et al., 2017). SVOCs including 1,3,5-trimethylbenzene, 1,2,3,4-tetramethylbenzene, and 1-methylnaphthalene were quantified in unfiltered water samples in a location of an oily sheen downstream from the spill location. However, these compounds were absent from filtered water samples, suggesting that many of these organic compounds might have been particle-bound. Trace SVOCs were identified in streambed sediment below reporting limits, but the authors suggested that the spill pathway over 10s of meters of soil could have resulted in substantial sorption of hydrophobic organic compounds to soil prior to the spill entering the stream (Cozzarelli et al., 2017). Surface contamination of streamwaters and streambed sediments were also investigated outside of a deep well injection facility in West Virginia to determine if the large volumes of HVHF wastewater transported and unloaded on site resulted in contamination of the nearby environment (Akob et al., 2016; Orem et al., 2017). Extensive organic chemical analyses were performed targeting oil and gas compounds, known HVHF chemical additives, disinfection by-products, and additional SVOCs including halogenated compounds (Orem et al., 2017). In streamwater, only tetra-hydrothiophene 1,1-dioxide, a compound used for cleaning natural gas, was consistently identified downstream of the facility. In sediments, a complex mixture of organic compounds was identified which included a number of halogenated organic compounds (trifluoroacetate/alkanes and halogenated alkanes), some of which have been identified previously in HVHF fluids (Maguire-Boyle and Barron, 2014) and wastewaters while

others are of unknown origin. Although the results are complex and indicate possible broader contamination in the region upstream of the facility, the distribution of organic compounds combined with inorganic analyses (Akob et al., 2016) indicated clear environmental contamination from the HVHF wastewater disposal facility.

The largest groundwater investigation to investigate the impacts of HVHF were performed using private and public groundwater wells from aquifers overlying the Permian (n=42 wells, multiple time points) and Barnett basins (n=550 wells, n=100 wells) (Fontenot et al., 2013; Hildenbrand et al., 2016, 2015). Samples in both basins were analyzed using GC-MS and headspace-gas chromatography (HS-GC) for a number of organic compounds identified in HVHF fluid as well as others associated with oil and gas development. BTEX compounds, chlorinated solvents (dichloromethane, chloroform), and low molecular weight alcohols were detected in a number of Barnett region samples, with only toluene and methanol distributions indicative of surface spills (Hildenbrand et al., 2015). Ethanol was found alongside high bromide concentrations, found in high concentrations in HVHF wastewater (Hildenbrand et al., 2015). Permian basin groundwater wells were sampled at four time points, during which unconventional oil and gas development increased significantly (Hildenbrand et al., 2016). Following the initial time point, ethanol and dichloromethane elevated significantly at an additional time point, and a number of other organic compounds associated with oil and gas development and degradation (isopropyl alcohol, propargyl alcohol, acetaldehyde, cyclohexane, toluene, xylene, ethylbenzene) that were not present in the initial sampling campaign were identified (Hildenbrand et al., 2016). The authors ultimately concluded

that their findings indicated the transient nature of potential contamination events in developed areas (Hildenbrand et al., 2016).

In northeastern Pennsylvania, groundwater samples were collected from private residential wells (9-231 m depth) and analyzed for GC-amenable compounds (Drollette et al., 2015). Gas related organic compounds were detected in 9 of 59 wells and diesel related organic compounds were detected in 23 of 41 wells in highly variable concentrations (Drollette et al., 2015). BTEX compounds were identified in 6 samples at trace levels below EPA drinking water maximum contaminant level recommendations (Drollette et al., 2015). The highest concentrations of observed organic compounds were identified within 1 km of a shale gas well as well as in close proximity to a well that caused an environmental health and safety violation (e.g., failure to properly store, transport, process or dispose of residual waste). Based on geochemical fingerprinting tools, the authors concluded that the groundwater contamination was likely due to surface spills associated with HVHF activities rather than via subsurface contamination. Additionally, a disclosed additive, bis(2-ethylhexyl) phthalate, was identified in the same two samples with the highest diesel related organic compounds concentrations. Foaming was also observed in three residential drinking water wells in northern Pennsylvania located in close proximity to HVHF wells (Llewellyn et al., 2015). Commercial laboratories were unable to detect any compounds during this known contamination event other than methane that exceeded regulatory drinking water standards and recommendations, but 2-butoxyethanol was identified in the foaming waters using GCxGC-qTOF-MS. 2-butoxyethanol is an ingredient in the Airfoam HD additive frequently used during HVHF (Llewellyn et al., 2015).

In Weld County, CO, 218 groundwater samples were analyzed for BTEX following 77 industry reported spills of oil or produced waters. Following remediation at several sites, benzene remained above the maximum contaminant limit for groundwater in 59% of sites, and above these levels outside of the remediation area in 37% of sites (Gross et al., 2013). In Garfield County, CO, groundwater samples were collected in a high density shale gas drilling region and analyzed for the endocrine disruption capacity (EDC) of the solid phase extracts [known to extract many known endocrine disruptors] of these fluids (Kassotis et al., 2014). In 39 samples, 89% of samples exhibited estrogenic activity, 41% anti-estrogenic, 12% androgenic, and 46% anti-androgenic activity; significantly higher than nearby drilling sparse control sites. These high EDC activities were suspected to be related to groundwater contamination due to HVHF activities from any of the more than 100 known EDCs found in HVHF additives (Kassotis et al., 2014).

Following complaints of residents, the EPA investigated groundwater contamination in Pavilion, WY suspected to be associated with the HVHF of shallow gas wells through the installation of several shallow and deep groundwater monitoring wells (DiGiulio and Jackson, 2016a; DiGiulio et al., 2011). Multiple phases of monitoring were performed beginning with existing residential and municipal wells, followed by shallow monitoring wells, and finally by two explicitly drilled deep monitoring wells (235 m, 295 m) (DiGiulio et al., 2011). Shallow wells had high levels of BTEX, diesel and gas related compounds, and other hydrocarbons, but ultimately were suspected of contamination by the use of surface unlined pits where fluids including diesel used for gas extraction were stored and likely solute transport mechanisms (DiGiulio and Jackson, 2016a). However, organic compounds identified in deep groundwater monitoring wells were different than

those identified in surface wells and a number of known synthetic organic compounds used for HVHF were identified (DiGiulio and Jackson, 2016a; DiGiulio et al., 2011). These included isopropanol (biocide, surfactant, breakers, foaming agents), nonylphenol and octylphenol (surfactants), diethylene glycol, triethylene glycol, tetraethylene glycol (solvent, foaming agent), 2-butoxyethanol (foaming agent, gel-based frac fluid), and a suspected degradation product of possible undisclosed additives, tert-butyl alcohol (DiGiulio and Jackson, 2016a; DiGiulio et al., 2011). Aromatic solvent, diesel oil, heavy aromatic petroleum naphtha, toluene, xylene and petroleum raffinates (material remaining following extraction of specific petroleum products) were reported as fracturing fluid additives in the nearby well, and a number of compounds reflecting these additives were identified in the monitoring wells including BTEX, trimethylbenzenes, naphthalenes, and phenols (DiGiulio and Jackson, 2016a; DiGiulio et al., 2011). Diesel and gas related organic compounds (DRO and GRO) in 23 of 28 nearby domestic well samples correlated with reports of foul odors (DiGiulio et al., 2011). Phthalates, acetone, 2-butanone, and 3-methyl-2-pentanone, benzoic acid, and other small organic acids were also identified in the groundwater samples.

In the EPA retrospective case studies (U.S. EPA, 2015a, 2015b, 2015c, 2015d, 2015e) a suite of organic compounds including VOCs, SVOCs, and diesel and gas range organic compounds (DRO and GRO) were analyzed in groundwater and surface water samples based on complaints of changes in water quality. In the Northeastern PA and Southwestern PA case studies (Marcellus shale), low level and sporadic detections of organic compounds including phthalates, toluene, benzene, 1,2,3-trimethylbenzene, 1,2,4-trimethylbenzene, chloroform, acetone, phenol, 2-butoxyethanol, and phthalates as

well as DRO and GRO were suspected laboratory and field contaminants and inconsistent with contamination due to hydraulic fracturing activities due to a lack of other potential indicators such as chloride, total dissolved solids, barium, or strontium (U.S. EPA, 2015a, 2015d). Similarly, detections of these compounds as well as xylene in the Killdeer aquifer were presumed to be laboratory contaminants with the exception of tert-butyl alcohol (TBA) at two groundwater sites. At these sites, along the groundwater flowpath from a documented well blowout, TBA was elevated ($975 \mu\text{g L}^{-1}$) and had a documented HVHF fluid source. TBA as well as chloride decreased over the four time points, consistent with the movement of a contaminant plume through the wells (U.S. EPA, 2015b). Acetate and formate, indicators of hydrocarbon degradation, were detected in 31% of wells and 10% of wells, respectively, in the sampled groundwaters (U.S. EPA, 2015b). In Wise County, TX (Barnett Shale), VOCs were detected, including tert-butyl alcohol, methyl tert-butyl ether, ethyl tert-butyl ether, tert-amyl methyl ether, m+p-xylene, o-xylene, 1,2,4-trimethylbenzene, and benzene; however, the sources of the compounds was considered unidentified because there were not repeated detections and no glycol ethers indicative of hydraulic fracturing (U.S. EPA, 2015e). In the Raton Basin, CO, (coal bed methane) a large number of organic chemicals were detected, representing possible HVHF fluid additives, as well potential natural sources (U.S. EPA, 2015c). VOCs such as BTEX detected in this study were interpreted to originate from water-rock interactions or enhanced solubilization due to the solvent-like properties of the injection fluid (U.S. EPA, 2015c). Again, TBA was detected in some sites at high levels (maximum $1,310 \mu\text{g L}^{-1}$), but the observation was interpreted as not necessarily representing contamination from a HVHF fluid event because neither TBA or its parent

compounds were disclosed, and sufficient spatial data or adequate pre-HVHF controls did not exist (U.S. EPA, 2015c).

These studies and their critics bring up common issues in interpreting environmental data and associating the observations with a specific contamination source. First, in nearly all scenarios, relatively few baseline data exist for sampling locations as all extensive studies have been completed in response to perceived threats or changes. Baseline data for organic compounds are rarer than for inorganic ions and are completely absent for specific tracers that may be strong indicators of a HVHF source. Reference sites in the same geologic region are sometimes used as a control variable, but these are also susceptible to contamination from past events, especially considering shale gas regions are co-located in conventional oil and gas regions that have been drilled for longer time periods. Unfortunately, baseline data cannot retroactively be collected and this will continue to be a critical issue in interpreting data. A second common critique is of the observations of some compounds associated with HVHF, but an absence of others associated with HVHF (Connor et al., 2016; McHugh et al., 2016, 2014). Fontenot, Meik and colleagues responded in describing the role changing pH and redox conditions plays on dissolved metal concentrations (Fontenot et al., 2014; Meik et al., 2016). DiGiulio and Jackson responded by explaining that heterogeneity in itself is indicative of anthropogenic impact if groundwater samples are obtained from the same formation (DiGiulio and Jackson, 2016b). Previous research has shown the differences in groundwater transport of contaminants based on the strength of their interaction with the geologic formation and soils, as reactive or nonreactive solutes (Brusseau, 1994; Burr et al., 1994; Mackay et al., 1986). Nonreactive solutes such as chloride will be transported

faster than reactive organic compounds associated with HVHF fluids which may be retarded through interactions with the geologic formations and organic carbon present in these formations (Allen-King et al., 2002; Mackay et al., 1986).

2.4.2 Simulated bioreactor “spills”

Two published studies have simulated spills of HVHF fluids at the bench scale under aerobic conditions. In each of these studies, a synthetic mixture of HVHF fluid additives was mixed with natural microbial communities and the organic additives quantified over 7-180 days. In an aerobic solution inoculated with an activated sludge microbial community, the overall dissolved organic carbon (DOC) content decreased by 52% in 6.5 days in freshwater and a 20 g L⁻¹ saline solution. At higher salinities (40 g L⁻¹ and 60 g L⁻¹), DOC did not change significantly over the same time period. Acetone, a degradation product, increased by two orders of magnitude, and volatile additives such as naphthalene and benzene were rapidly decreased in concentration, likely due to volatilization (Kekacs et al., 2015). In the second study, varying combinations of fracturing fluid additives were mixed with agricultural soil and the *in situ* microbial community and their changes tracked to understand co-contaminant interactions over 180 days (McLaughlin et al., 2016). The presence of glutaraldehyde biocide impeded the degradation of polyethylene glycol surfactants, and high salt levels also severely inhibited their degradation. Polyacrylamide was not degraded over the duration of the experiment, but did react with the biocide glutaraldehyde (McLaughlin et al., 2016).

2.5 Flowback and Produced Water Treatment

High total dissolved solids (TDS) create a significant challenge for the treatment of flowback and produced waters (Gregory et al., 2011; Kondash et al., 2017b), hence wastewaters are frequently sent to Class II disposal wells (U.S. EPA, 2016). TDS varies by basin and increases over the lifetime of the well (Kondash et al., 2017b); high levels of TDS limit direct reuse due to scaling problems and reduced effectiveness of friction reducers (Gregory et al., 2011; Kamel and Shah, 2009). The fate of the treated effluent determines the type and amount of treatment required. The treatment for reuse in HVHF requires a different level of treatment (e.g., precipitation of scaling cations, disinfection, (Lester et al., 2015)) than other beneficial reuses or discharge to the environment (Estrada and Bhamidimarri, 2016; Gregory et al., 2011). High TDS formation produced waters, such as the Bakken or Marcellus, cannot be directly reused and TDS must be first reduced either by using dilution or treatment, which is in contrast to formations such as the Niobrara or Eagle Ford, that have much lower TDS (Kondash et al., 2017b).

The wide variety of treatment methods used for flowback and produced waters have been reviewed previously (Drewes et al., 2009; Estrada and Bhamidimarri, 2016; Fakhru'l-Razi et al., 2009; Gregory et al., 2011; U.S. EPA, 2016). Traditional oil and gas centralized waste treatment and municipal treatment facilities (no longer in use) have not been shown to sufficiently remove key contaminants from HVHF wastewaters prior to discharging to streams (Ferrar et al., 2013; Getzinger et al., 2015; Warner et al., 2013). Thermal distillation and crystallization technologies efficiently remove TDS but may be energy intensive (Gregory et al., 2011; Jang et al., 2017; Shaffer et al., 2013). Membrane technologies such as reverse osmosis, forward osmosis, and nanofiltration are prone to

clogging and fouling and are more effective when combined with pre-treatment technologies such as coagulation/flocculation, filtration, or dissolved air flotation (Coday et al., 2014; Estrada and Bhamidimarri, 2016; Riley et al., 2016; Shaffer et al., 2013). High concentrated wastes may be disposed of or potentially used as industrial feedstocks for salt products (Estrada and Bhamidimarri, 2016; Gregory et al., 2011).

Few individual organic compounds have been tracked through industrial treatment facilities, although any given treatment train could neglect a number of organic compounds, additives, and transformation products. The effectiveness of a given treatment method on organic compounds is frequently reported only for regulated hydrocarbons such as total oil and grease (Drewes et al., 2009), or other bulk measurements including dissolved organic carbon (DOC), chemical oxygen demand and 3D excitation-emission matrix fluorescence (Hickenbottom et al., 2013; Lobo et al., 2016; Riley et al., 2016).

Bench-scale experiments have examined the removal efficiencies of a number of organic compounds frequently found in HVHF wastewaters. Guar gum, a common HVHF additive likely to foul membranes, was effectively removed biologically (~90%) at low TDS using an activated sludge mixture (Lester et al., 2014). In a different synthetic HVHF wastewater, forward osmosis rejected >99.9% of oil while acetic acid rejection was much lower at only 82% (23 °C) and 74% (60 °C) (Zhang et al., 2014). More hydrophobic compounds, including alkanes and polycyclic aromatic hydrocarbons, were removed with 90-99% efficiency using forward osmosis (Bell et al., 2017). Powdered activated carbon (PAC) combined with coagulants were tested for removal efficiency of total petroleum hydrocarbons and polyethylene glycols from actual HVHF flowback and

produced waters. PAC was shown to be effective at high doses (750 mg L⁻¹, 1,000 mg L⁻¹ PAC) for polyethylene glycol removal in all cases and in three out of four wastewaters for total petroleum hydrocarbons (Rosenblum et al., 2016). However, these specific classes represented only a fraction of the DOC, and much of the DOC was not removed (52-90%) using PAC (Rosenblum et al., 2016).

2.6 Considerations and Future Research

Reviewing and synthesizing the literature on HVHF organic compounds remains challenging due to inconsistencies in reporting information such as age of fluids and sampling techniques (storage conditions, head-space free, etc.). Building on the suggested reporting parameters listed by Bibby and colleagues ((Bibby et al., 2013): (1) shale play/formation (2) fracturing/stimulation approach (3) well age (4) water quality (bulk parameters, inorganics), we suggest reporting additional information helpful in interpreting organic analyses: (5) Sample location (well, separator, collection tank) (6) Sampling information (bottle type, head-space free, storage conditions and duration).

Gas chromatography paired with mass spectrometry has been the most frequently used technique for organic compound analysis of HVHF fluids and wastewaters. GC and GC-MS have a large number of standardized methods for VOCs and SVOCs including oil and gas compounds in HVHF fluids. Continued research on these compounds is critical in understanding basin to basin variability, differences in HVHF techniques, and quantifying many known toxic compounds (Elliott et al., 2017). Quantification using standard methods is essential for tracking the distribution of HVHF fluids and wastewaters when they accidentally enter the environment.

The Marcellus shale region is the dominant location of HVHF fluid samples analyzed for organic compounds, followed by the Denver-Julesberg basin. Although the Marcellus is the dominant shale gas producer, oil is not co-produced in this formation (U.S. EIA, 2017a), indicating a lower complexity background organic carbon pool compared to a shale oil (Bae et al., 2010). Analysis of the Denver-Julesberg, Permian, and other co-producing gas and oil basins will inevitably differ in their distribution of geogenic organic compounds compared to gas-only basins. Future research should work to diversify basin coverage across gas, oil, and co-producing basins to understand the variability in geogenic signatures and diversity of HVHF fluid systems. Treatment goals and techniques also vary by basin and further investigation into the removal rates of specific organic compounds of interest is needed across treatment schemes developed across all basins (i.e., halogenated organic compounds, BTEX, hazardous chemicals).

DOC concentrations compared to concentrations of specific organic compounds show that a large portion of the organic carbon pool remains uncharacterized. Additional research needs to build on recent progress developing new analytical methods that can overcome the extremely complex high salinity matrix for known additives and identified transformation products in these fluids, particularly using LC-MS techniques. Continued research using alternative extraction methods and high-resolution non-targeted techniques will allow for the investigation of the diverse transformation products in HVHF fluids and wastewaters during treatment as well as environmental contamination events. New standards must be made available for known additives, geogenic organic compounds, and newly identified transformation products to further progress in this field and gain a broad understanding of the fate of organic compounds in HVHF.

2.7 Conclusions

Organic compounds are used as HVHF fluid additives and a number of these have been detected in these flowback and produced waters. Geogenic compounds and transformation products from biotic and abiotic processes have also been identified in these wastewaters. BTEX, acetate, and acetone are the most frequently analyzed and detected organic compounds, and VOC and SVOCs are commonly analyzed. However, non-targeted techniques have highlighted the diversity of organic compounds that may be present in a given fluid for which new standards and analytical methods need to be developed. Organic chemical additives have been used in combination with inorganic chemical tracers to infer and track environmental contamination events. Further analytical development will benefit these investigations, allowing quantitative comparisons of new organic chemical tracers highly specific to HVHF to be made against background levels.

Chapter 3

Halogenated organic compounds identified in hydraulic fracturing wastewaters using ultrahigh resolution mass spectrometry

Luek, J.L., Schmitt-Kopplin, P., Mouser, P., Richardson, S.D., Petty, W.T., Gonsior, M. 2017. Halogenated organics identified in produced waters using ultrahigh resolution mass spectrometry. Environmental Science & Technology 51, 5377-5385.

DOI: 10.1021/acs.est.6b06213

© American Chemical Society

Contribution: Experiment conception, data collection, analysis and interpretation, all text, and all figures and tables except Figure 3.1 and SI Table S4/Appendix A2.4.

Abstract

Large volumes of water return to the surface following hydraulic fracturing of deep shale formations to retrieve oil and natural gas. Current understanding of the specific organic constituents in these hydraulic fracturing wastewaters is limited to hydrocarbons and a fraction of known chemical additives. In this study, we analyzed hydraulic fracturing wastewater samples using ultrahigh resolution Fourier transform ion cyclotron resonance mass spectrometry (FT-ICR-MS) as a non-targeted technique to assign unambiguous molecular formulas to singly charged molecular ions. Halogenated molecular formulas were identified and confirmed using isotopic simulation and MS-MS fragmentation spectra. The abundance of halogenated organic compounds in flowback fluids rather than older produced wastewaters suggested that the observed molecular ions might have been related to hydraulic fracturing additives and related subsurface reactions, such as through the reaction of shale-extracted chloride, bromide, and iodide with strong oxidant additives (e.g., hypochlorite, persulfate, hydrogen peroxide) and subsequently with diverse dissolved organic matter. Some molecular ions matched the exact masses of known disinfection by-products including diiodoacetic acid, dibromobenzoic acid, and

diiodobenzoic acid. The identified halogenated organic compounds, particularly iodinated organic molecules, are absent from inland natural systems and these compounds could therefore play an important role as environmental tracers. A suite of organic chemical tracers are needed to complement inorganic tracers which are transported at variable rates in the subsurface.

3.1 Introduction

The combination of hydraulic fracturing and horizontal drilling to extract unconventional oil and gas has become a key energy source in the United States and globally (U.S. EIA, 2016b). Chemical additives are mixed with large volumes of water ($>10^7$ L for many shale formations) and injected into the well to hydraulically fracture the formation (Kondash and Vengosh, 2015). A fraction of the injected water, as well as water from the formation itself, returns to the surface in the form of flowback and produced waters, with 19-48% of fluid returned within the first 6 months (Kondash and Vengosh, 2015; Kondash et al., 2017a; Nicot and Scanlon, 2012). This wastewater is known to contain a complex mixture of injected chemical additives and naturally occurring shale-extracted inorganic and organic constituents (Akob et al., 2015; Engle and Rowan, 2014; Ferrer and Thurman, 2015b; Maguire-Boyle and Barron, 2014; Orem et al., 2014).

The majority of the initial flowback water (first 2-4 weeks) is often reused in hydraulic fracturing fluids (89-95% of cases in the Marcellus region) (Jiang et al., 2014), but produced water (released through the lifetime of the well) is less frequently recycled due to high TDS. Produced water is highly saline and contains substantial levels of naturally occurring radioactive material (Chapman et al., 2012; Haluszczak et al., 2013)

and a diverse pool of dissolved organic matter (DOM). The complexity and the highly variable nature of flowback and produced waters make treatment challenging (Gregory et al., 2011) and deep well injection has therefore been the dominant waste management pathway in many regions (e.g., Ohio, 90%) (Mauter and Palmer, 2014; Veil, 2015). However, the growing evidence that deep well injection of these wastewaters is linked to increased seismicity (Keranen et al., 2013; Kim, 2013; Weingarten et al., 2015) suggests that future best practices will support wastewater treatment options and reuse (Estrada and Bhamidimarri, 2016; Gregory et al., 2011). For example, in Pennsylvania where deep well injection is expensive due to transportation costs to take it out of state, more than 85% of flowback waters are being reused for hydraulic fracturing operations (Lutz et al., 2013; Maloney and Yoxtheimer, 2012; Rahm et al., 2013; Veil, 2015).

Nearly 10^{12} L of these wastewaters have been produced since the early 2000s (Kondash and Vengosh, 2015), which underlines the tremendous challenge of wastewater treatment. In order to design efficient treatment methods, it is critical to further investigate and understand the complexity of DOM in flowback and produced waters, whose removal during treatment has been scarcely addressed (Hickenbottom et al., 2013; Lobo et al., 2016; Riley et al., 2016; Rosenblum et al., 2016). Characterization of the complex DOM can also provide insightful information about the processes occurring within the well, such as identifying transformation products and the lability of additives (Ferrer and Thurman, 2015b; Hoelzer et al., 2016; Orem et al., 2014).

Current research on hydraulic fracturing wastewaters has been heavily biased towards inorganic components, radioactivity, and known chemical additives (Barbot et al., 2013; Bibby et al., 2013; Chapman et al., 2012; Ferrar et al., 2013; Ferrer and

Thurman, 2015a; Haluszczak et al., 2013; Lester et al., 2015; Llewellyn et al., 2015; Osborn et al., 2011; Thurman et al., 2014; Warner et al., 2012a). The complex organic components present in additives, as well as extracted DOM from the shale formation itself, are analytically challenging due to their complexity, a lack of standards, and the difficult high salinity matrix. Non-targeted two-dimensional gas chromatography paired with high resolution mass spectrometry has been shown to be a powerful tool to identify many geogenic compounds, suspected additives, as well as potential transformation products (Hoelzer et al., 2016; Strong et al., 2013). However, compounds in hydraulic fracturing wastewater that are not amenable to gas chromatography remain largely uncharacterized. Further investigation in to non-volatile compounds using liquid chromatography (Getzinger et al., 2015) and broad spectrum, non-targeted ultrahigh resolution approaches are needed to begin to deconvolute this complex mixture.

Ultrahigh resolution Fourier transform ion cyclotron resonance mass spectrometry (FT-ICR-MS) has been previously used to identify more than 30,000 chemical components in shale oil (Bae et al., 2010), and researchers have used targeted gas chromatography to identify additives and shale-extracted hydrocarbons ranging in size from methane to asphaltene in hydraulic fracturing wastewaters (Gross et al., 2013; Jackson et al., 2013; Maguire-Boyle and Barron, 2014; Orem et al., 2014; Parker et al., 2014). FT-ICR-MS has been previously used to look at the complex mixture that makes up natural DOM (Hertkorn et al., 2008), as well as unique halogenated organic compounds formed during disinfection of drinking and ship ballast waters (Gonsior et al., 2015; Lavonen et al., 2013). Paired with solid-phase extraction (SPE) to concentrate DOM and remove salts (Dittmar et al., 2008), FT-ICR-MS is capable of identifying the exact mass of ionizable

mesophilic to hydrophobic organic molecular ions that can then be assigned to a precise molecular formula (Hertkorn et al., 2008).

During the hydraulic fracturing process, the added fluid undergoes internal reactions between chemical additives and external reactions with the shale and microbes present in the well (Cluff et al., 2014; Daly et al., 2016; Hoelzer et al., 2016; Kahrilas et al., 2016; Maguire-Boyle and Barron, 2014; Murali Mohan et al., 2013b). The use of strong oxidants, including hypochlorite and persulfate (Kahrilas et al., 2015; Stringfellow et al., 2014), in the presence of the shale-derived dissolved halides (chloride, bromide, iodide) (Dahm et al., 2011; Haluszczak et al., 2013; Harkness et al., 2015) may result in the formation of reactive halogen species which can subsequently interact with the diverse organic compounds present as additives and of geogenic origin (Hoelzer et al., 2016; Maguire-Boyle and Barron, 2014). During fluid storage, the *in situ* microbial community and added biocides may further alter this pool of organics (Murali Mohan et al., 2013b). Indeed, a handful of halogenated organic molecules have been identified previously in hydraulic fracturing wastewaters (Hoelzer et al., 2016; Maguire-Boyle and Barron, 2014).

SPE paired with FT-ICR-MS has been used previously to successfully identify diverse halogenated disinfection by-products formed during drinking water and ballast water treatments (Gonsior et al., 2015, 2014; Lavonen et al., 2013). The goal of this study was to use FT-ICR-MS to determine the diversity of halogenated organic compounds present in these hydraulic fracturing wastewaters.

3.2 Materials and Methods

3.2.1 Sample Collection and Extraction

Sixteen hydraulic fracturing wastewater samples were obtained from North Dakota, Colorado, Ohio, West Virginia, and Pennsylvania including both flowback (n=7, FB), produced waters (n=2, PW), natural gas compression liquids wastewater (n=6, CL), and natural gas liquid fractionation liquids wastewater (n=1, FL). Additional information about sampling, sample storage, and conductivity is provided in Table A2.1. Exact well locations were only known for 3 sites and FracFocus reports were obtained for the five FB samples (FB3-7) from these 3 sites. Unfiltered samples were stored at 4 °C prior to extraction and analysis. Samples were filtered through pre-combusted 0.7 µm glass fiber filters (Whatman GF/F, 47mm). High purity hydrochloric acid was added to 200 mL samples (except FB3 - 10mL) to adjust to pH 2 to maximize extraction efficiency onto SPE cartridges due to the protonation of organic acids. Agilent Bond Elut PPL SPE cartridges (1g, 3mL) were activated with pure methanol (Chromasolv, LC-MS grade, Sigma Aldrich) and rinsed with 0.1% formic acid water (Chromasolv, Sigma Aldrich). Samples were then gravity-fed (~5-10 mL min⁻¹) to the SPE cartridges. After extraction, the SPE cartridge exterior was rinsed with Milli-Q water and the resin was rinsed with 200mL dilute HCl and then 30mL 0.1% formic acid water to remove remaining sample solution and salts. The SPE cartridges were dried under vacuum and then eluted with 10 mL of pure methanol and stored at -20° C.

Salts present in the methanolic extracts can produce halide adduct formation during negative electrospray ionization, and have even been used to assist in the ionization of poorly ionizing compounds like sugars (Boutegrabet et al., 2012). Although

the original methods to remove seawater salts state that only 3 cartridge volume rinses are necessary to sufficiently remove oceanic salt concentrations (Dittmar et al., 2008), cartridges were rinsed with at least 10 cartridge volumes of 0.1% formic acid water in this study to make sure that complete salt removal was achieved. Similar extraction and rinsing methods have been used previously to efficiently desalt samples prior to FT-ICR-MS analysis to identify new halogenated disinfection by-products (Gonsior et al., 2015; Lavonen et al., 2013; Wang et al., 2016). Using this conservative approach we thus minimize the potential formation of salt adducts that can form during the electrospray ionization and therefore expect that the halogen containing formulas correspond to organohalogens.

3.2.2 Solid Phase Extraction Recoveries

Filtered samples were analyzed for the dissolved organic carbon (DOC) content of filtered wastewater and dried and reconstituted methanolic extracts (Table A2.2). Small volume filtered samples for DOC analysis were frozen and stored prior to analysis using a total organic carbon analyzer (Shimadzu TOC-V). Briefly, thawed samples were diluted then automatically acidified (5% HCl addition) and purged using carbon-free air for 2.5 minutes to remove dissolved inorganic carbon (DIC). Organic carbon was quantified as non-purgeable DOC using potassium hydrogen phthalate standards. Duplicate injections were averaged (CV <5%, best 2 of 3) to obtain the final reported value. Caveats associated with low extraction efficiencies and recoveries are discussed in Appendix 2.

3.2.3 FT-ICR-MS Analysis

A Bruker Solarix 12 Tesla FT-ICR-MS interfaced with electrospray ionization (ESI) in negative mode was used for sample analyses. At ultrahigh resolution, ESI has been demonstrated to produce mainly singly charged intact molecular ions, and it enables accurate and unambiguous molecular formula assignments (Stenson et al., 2003). Methanol sample extracts were diluted twenty-fold using high purity methanol to optimize instrument signal and to avoid over-saturation of the ion cyclotron resonance ion trap, which could lead to peak splitting and calibration challenges. Diluted sample extracts were introduced to the FT-ICR-MS at a flow rate of 120 $\mu\text{L/hr}$, and spectra were obtained over a mass to charge ratio (m/z) range of 147-1,000 amu. Samples were initially calibrated by arginine clusters and again internally post-calibrated using a set of known sulfonic acids that ionized efficiently under negative mode ESI, along with DOM and isotopically confirmed heteroatom ions (Table A2.3), to obtain a mass accuracy greater than 0.2 ppm. DOM samples calibrated with known DOM m/z peaks were analyzed on the FT-ICR-MS concurrently and were used to cross-validate the calibrations where only a few calibrants were detected. Mass resolution of greater than 400,000 at m/z 400 was always observed. The m/z ions with a signal to noise ratio less than 10 were removed from the mass list prior to export from the Bruker software.

A non-targeted approach was first used to probe the FT-ICR-MS spectra for all DOM including halogenated organic ions (Figure A2.1). After halogenated organic ions were identified, a semi-targeted approach was used to better understand the observed ions and determine if they matched known compounds. To this end, all m/z ions were compared to a list of 384 halogenated disinfection by-product (DBP) ions (259 exact

masses due to multiple isomers of some DBP ions) (Figure 3.1, Table A2.4). Not all known DBPs, however, would be extracted and/or ionized using the methods applied in this study. Highly polar and volatile DBPs would not be extracted using this process, and some nonpolar compounds would also not be ionized in negative electrospray mode due to a lack of readily deprotonated functional groups. Although many DBPs would not be identified through the SPE and FT-ICR-MS approaches used, this technique is advantageous as it allows for the identification of a diverse array of halogenated organic compounds and complements existing studies using GC-based approaches (Drollette et al., 2015; Maguire-Boyle and Barron, 2014).

Formulas were assigned within 0.3 ppm error of the actual masses with a maximum possible elemental assignment $H_{\infty}C_{60}O_{30}N_3S_2P_2Cl_3Br_3I_3$. Formula assignments were reduced by removing formulas that did not pass the nitrogen rule (F.W. McLafferty and F. Turecek, 1993), those with negative double bond equivalency, an oxygen to carbon ratio (O/C) greater than one, and molecular ions greater than 700 m/z due to increasing likelihood of formula mis-assignment at high m/z . To prevent ambiguous or false assignments, the assigned formulas were filtered conservatively by first identifying all formulas with less than two heteroatoms and then removing ions in this subset assigned to more than one formula. The number of unambiguous formula assignments with two or fewer total heteroatoms (N, S, P, X) ranged from 15-49% of the total m/z peaks (Table A2.5, Figures A2.2-A2.4). The m/z ions containing Cl and Br in more than one sample were individually checked for the presence and intensity of the isotopologues ^{37}Cl and ^{81}Br in the FT-ICR-MS spectra, respectively. Methanol instrument blanks,

laboratory blanks, and field blanks were checked to confirm the absence of the identified halogenated organics for both methods.

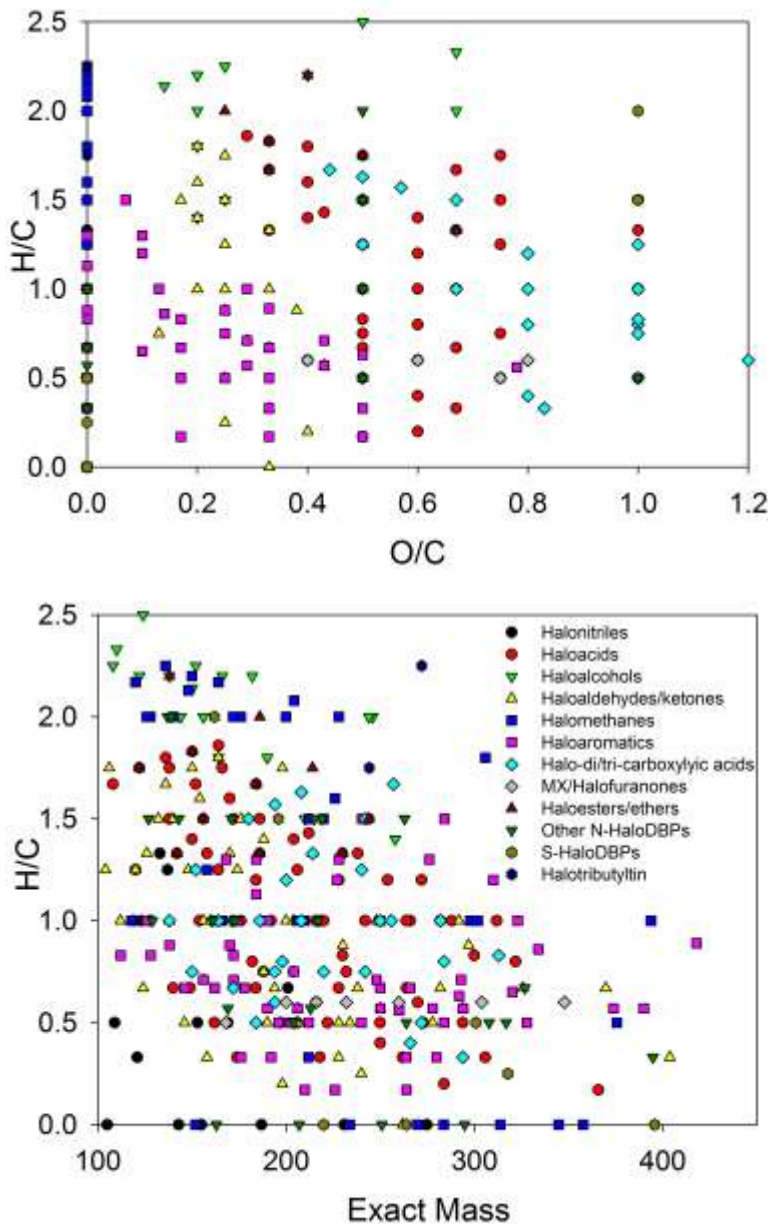


Figure 3.1 Oxygen to carbon (O/C) versus hydrogen to carbon (H/C) ratios (Van Krevelen (van Krevelen, 1950)) (top) and mass to charge ratio (m/z) versus H/C ratios (bottom) of 259 known halogenated disinfection by-products by class (Table A2.4). Not all formulas shown are extracted or ionizable using the methods employed in this study. Note: H/C values below 0.5 are possible because of substitution of H by halogens in the chemical formula.

3.2.3 Orbitrap MS-MS analysis

MS-MS analyses were performed on a subset of samples (FB1, FB2, FB3) that contained high intensity ions assigned an iodinated formula to investigate the presence of iodinated organic compounds. This was undertaken due to the monoisotopic nature of iodine and hence difficulties using only isotopic pattern simulation for confirmation. Fragmentation was performed using a Thermo LTQ Orbitrap XL mass spectrometer with negative mode ESI. High-intensity m/z ions with an iodinated formula assignment were fragmented within a m/z window of 1 Da using the MSⁿ capability of the Thermo LTQ Orbitrap XL MS and ultrahigh purity helium (AirGas) as a collision gas. The collision-induced dissociation was varied and a final value of 30 eV was selected to allow for high dissociation of the parent m/z peak to maximize the iodine m/z peak at 126.9045. More than 40 high intensity molecular formulas containing one or two iodine atoms were evaluated and the iodine fragment was observed in all MS-MS spectra.

3.3 Results and Discussion

At a signal to noise ratio of 10:1, the number of m/z ions ranged from 2271 to 9206 for individual mass spectra (Table A2.5). The unassigned m/z ions may represent the secondary isotopic m/z ions, heteroatoms other than those containing N, S, P, and X (halogens), or other formulas for which multiple assignments were identified for a single exact mass and hence confidence in an unambiguous formula assignment was low. FT-ICR-MS settings were optimized for natural DOM, and the majority of all observed molecular ions fell between 200 and 500 m/z for all spectra ($69\pm 8\%$, standard deviation). Unlike typical natural DOM samples (Cottrell et al., 2013; Dittmar et al., 2008; Hertkorn

et al., 2008), a number of ions with a large negative mass defect (0.8-0.99) were observed in the samples, particularly in FB1, FB2, and FB3. Many of these ions were unambiguously assigned to halogenated formulas (Figure 3.2).

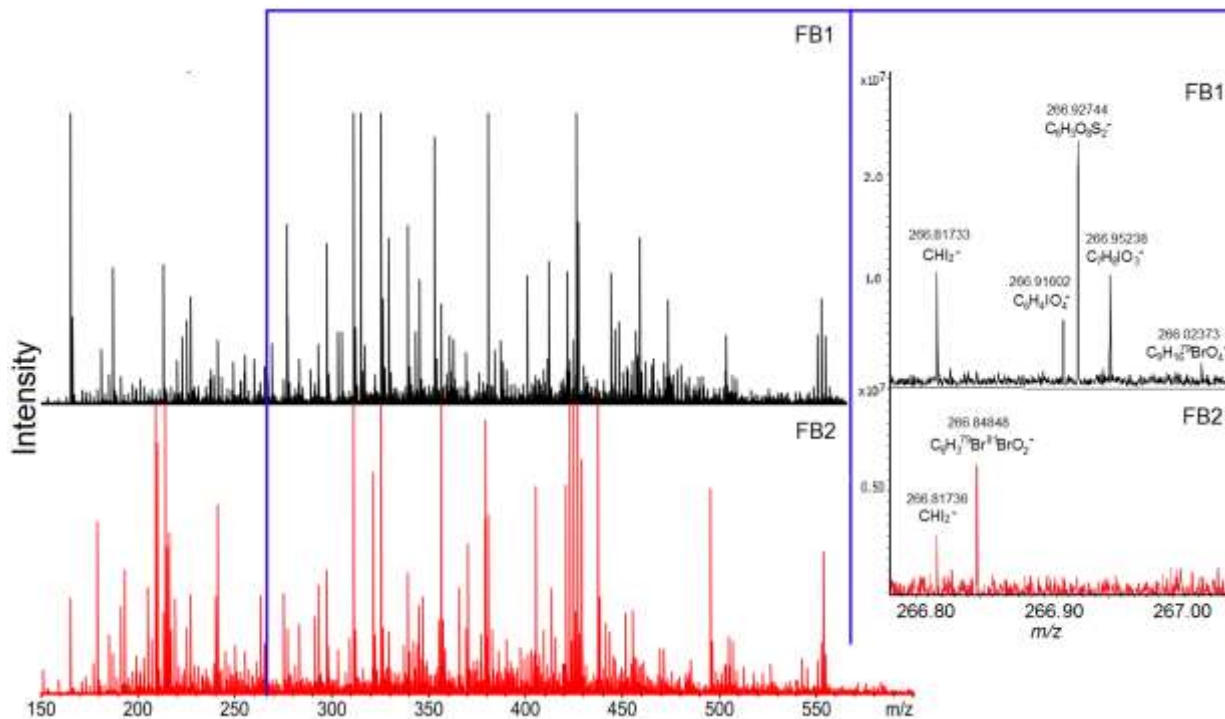


Figure 3.2 Ultrahigh resolution mass spectra of FB1 (top) and FB2 (bottom) flowback water samples showing exact masses and molecular formula assignments between m/z 266.75-267.05.

A list of halogenated formula assignments present in more than one sample were compiled (Table A2.6), with selected molecular ions given in Table 3.1. The reported halogenated ions were absent from methanol blanks and field blanks. These observed m/z ions ranged from small ions with low oxygen to carbon ratios (O/C) (e.g., CH_2^-) to large ions (e.g., $\text{C}_{22}\text{H}_{44}\text{O}_{13}\text{Cl}^-$) and high O/C ratios (e.g., $\text{C}_2\text{HO}_2\text{I}_2^-$), and varying degrees of unsaturation, as shown using van Krevelen diagrams (van Krevelen, 1950) (Figure 3.3). The van Krevelen diagram can be used to show the distribution of assigned molecular formulas and their degree of oxidation and hydrogenation (van Krevelen, 1950). Some

ions were observed with the same number of carbons, hydrogens, and oxygens, but with both Cl and Br analogues ($C_{10}H_{16}O_4Br^-$, $C_{10}H_{16}O_4Cl^-$; $C_{12}H_{22}O_8Cl^-$, $C_{12}H_{22}O_8Br^-$).

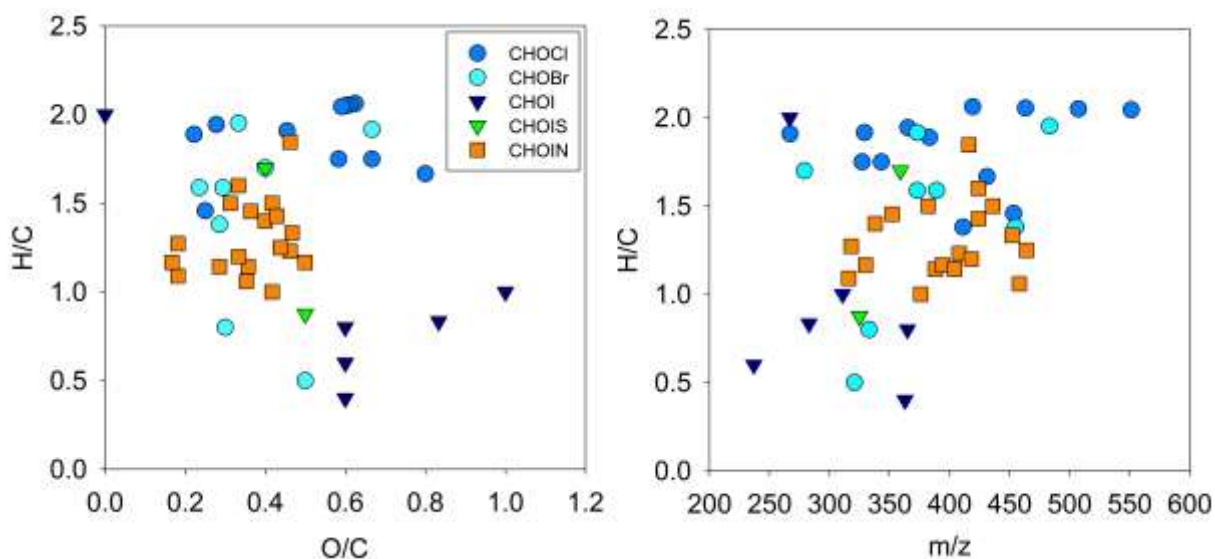


Figure 3.3 Halogenated organic molecular formulae identified in at least two flowback water samples shown as their oxygen to carbon (O/C) versus hydrogen to carbon (H/C) ratios (Van Krevelen (van Krevelen, 1950)) (left) and mass to charge ratio (m/z) versus H/C ratio (right). Exact formulas are given in Table A2.6.

Table 3.1. Selected halogenated organic molecular formulae identified in at least two flowback water samples; remaining ions are given in Table A2.6. # Isotopic simulation comparison given in Figures A2.5 and A2.6.

Exact Mass	Formula	FB1	FB2	FB3	FB4	FB5	FB6	FB7	PW1	PW2	CL1	CL2	CL3	CL4	CL5	CL6	FL2
236.90541	$C_5H_2O_3I^-$	x	x			x	x	x									
266.81731	CHI_2^-		x						x								
310.80714	$C_2HO_2I_2^-$		x						x								
320.84036	$C_8H_3O_4Br_2^-$	x	x	x			x					x					
332.87675 [#]	$C_{10}H_7O_3Br_2^-$	x	x	x													
362.80206	$C_5HO_3I_2^-$	x				x	x										
364.81771	$C_5H_3O_3I_2^-$	x	x														
383.17614 [#]	$C_{18}H_{33}O_4Cl_2^-$		x	x				x									

These halogenated formula assignments were confirmed by comparing the observed spectrum to a simulated isotopic spectrum within the Bruker Daltonics software

to ensure isotope pattern matching. This is a powerful tool due to the fact that not only can the location of possible isotopes be confirmed but also its relative abundance within an approximate maximum error of 10 %. Chlorinated and brominated formula assignments were easily confirmed using this method due to high abundances of their stable isotopologues (^{81}Br : 49.5%; ^{37}Cl : 24.2%) (Figures A2.5, A2.6). Each brominated assigned formula identified in Figure 3.2 was also able to be confirmed using isotopic pattern matching where both the ^{79}Br and ^{81}Br isotope ions could be identified.

For iodinated ions, only the ^{13}C and at times the ^{15}N and ^{34}S peaks could be used for isotopic confirmation due to the monoisotopic nature of stable iodine (i.e., only ^{127}I). Unfortunately many secondary m/z ion peak intensities were below the signal to noise ratio and could not be used to confirm iodinated formula assignments. However, 40 high intensity iodinated m/z ions in FB1 (Table 3.2), FB2, and FB3 had sufficient intensity for isotopic pattern matching, and were then investigated using the Thermo LTQ Orbitrap XL in MS-MS mode to look for the production of an iodide (m/z 126.9045) fragment ion. Fragmentation of iodinated ions, such as iodinated pharmaceuticals, frequently produces a dominant iodine fragment (spectra from MassBank) (Horai et al., 2010), supporting that the presence of this fragment is consistent with the iodinated formula assignments. Three additional pieces of information support that these identified iodinated ions are indeed covalently bound ions rather than adducts. First, several of the identified singly charged m/z ions contain more than one halogen. If one of the halogens was an adduct, this would still require that the remaining halogens are covalently bound in this singly-charged state. Secondly, single iodinated ions present in FB1 were targeted in positive ionization mode using direct injection on the Orbitrap MS. Iodinated adducts are not expected to form in

Table 3.2 Iodinated compounds identified in FB1 with sufficient intensity to be confirmed using isotopic pattern matching and production of a fragment at m/z 126.9045. ^Fragmentation spectra given in supplemental materials (Figure A2.11) *Also identified in positive ionization mode as $[M+H]^+$ or $[M+Na]^+$ ion.

Measured Ionic Exact Mass	Theoretical Ionic Exact Mass	Mass Error (ppm)	Molecular Formula Neutral	Intensity
222.92611	222.92615	-0.166	C ₅ H ₅ IO ₂	7.16 x10 ⁷
236.94177	236.9418	-0.114	C ₆ H ₇ IO ₂	2.57 x10 ⁷
252.93669	252.93671	-0.087	C ₆ H ₇ IO ₃	2.47 x10 ⁷
259.95777	259.95778	-0.043	C ₈ H ₈ INO*	4.75 x10 ⁷
292.93164	292.9317	-0.198	C ₈ H ₇ IO ₄	6.36 x10 ⁷
302.95238^	302.95236	0.059	C ₁₀ H ₉ IO ₃	7.72 x10 ⁷
316.96803^	316.96801	0.056	C ₁₁ H ₁₁ IO ₃	6.24 x10 ⁷
317.96329	317.96326	0.091	C ₁₀ H ₁₀ INO ₃	1.29 x10 ⁷
332.01532	332.0153	0.072	C ₁₂ H ₁₆ INO ₂	4.12 x10 ⁶
332.96294	332.96293	0.039	C ₁₁ H ₁₁ IO ₄	1.70 x10 ⁷
333.99458	333.99456	0.056	C ₁₁ H ₁₄ INO ₃	1.29 x10 ⁷
335.97383	335.97383	0.011	C ₁₀ H ₁₁ INO ₄	1.37 x10 ⁷
337.98949	337.98948	0.041	C ₁₀ H ₁₄ INO ₄ *	1.88 x10 ⁷
340.98916	340.98914	0.052	C ₁₀ H ₁₅ IO ₅	1.66 x10 ⁷
350.02589	350.02586	0.082	C ₁₂ H ₁₈ INO ₃	5.53 x10 ⁶
355.00482	355.00479	0.078	C ₁₁ H ₁₇ IO ₅	9.93 x10 ⁶
386.8596	386.85957	0.077	C ₅ H ₁₀ I ₂ O ₄	6.73 x10 ⁷
388.00514^	388.00513	0.035	C ₁₄ H ₁₆ INO ₄	1.53 x10 ⁷
400.87526^	400.87522	0.099	C ₆ H ₁₂ I ₂ O ₄	1.37 x10 ⁸
473.14064	473.14056	0.017	C ₁₈ H ₃₅ IO ₆ *	1.11 x10 ⁸

positive mode, so the presence of the $[M+H]^+$ and $[M+Na]^+$ of the previously identified ions in positive mode support that these are covalently bound iodinated organic compounds. Three of the high intensity iodinated ions (ESI-) given in Table 3.2 were indeed identified within 3 ppm error (ESI+), despite expected poor ionization (Figure A2.7). Finally, a dilution test was performed on iodinated ions to test if adding sodium iodide resulted in an increase in the iodinated organic ions. An increase in intensity with

iodide addition would indicate a given ion is likely to form an adduct. During this experiment, only two of the ten ions tested were identified as clearly increasing in both raw intensity and intensity relative to a base peak: m/z 259.95778 and m/z 292.9317 (Figure A2.8), indicating these two ions could be adducts. The majority of the peaks did not change substantially in intensity, and many decreased over time. This information provides additional support that many, but not all, of the identified ions are indeed covalently bound halogenated organic compounds rather than adducts.

Only CL5 and FL1 did not contain halogenated ions common with the other samples (Table A2.6). Flowback waters contained significantly more common halogenated m/z ions than the PW, CL, and FL samples combined (Student's t-test, two-tailed, $p=0.03$). FB1, FB2, and FB3 contained the highest number of shared halogenated m/z ions. FB2 had the most halogenated organic compounds, and it was the only FB sample that did not have a large amount of iron precipitate present in the sample. It is probable that inorganic precipitation stripped out organic compounds during the process, possibly explaining this observation. Alternatively, this well could have used different chemical or relative concentrations of these additives resulting in this distribution. Interestingly, there is some overlap between ions between FB5, FB6, and FB7, which shared very similar fracturing fluid additives, while FB4, did not share any halogenated organic compounds with these even though it came from the same well as FB6 (earlier flowback).

From the formula assignments not individually confirmed using secondary methods (Figures A2.3, A2.4), FB samples were similar in their distribution of non-halogenated organic compounds, with CHO ions as the primary class, followed by CHOS

and CHON. CHOX compounds represented between 4 – 13% of the assigned formulas. CHONX compound were also a dominant class, with 2 – 19% of the assigned formulas. FB1 contained the largest number of CHONX compounds, dominated by CHOIN compounds. The distribution of PW and CL assignments were similar, but generally had fewer CHO and more CHON and CHOS formula assignments. The percent of assigned CHOX and CHONX formulas was smaller than in the FB samples, but within these older wastewaters, PW1, PW2, and CL3 had higher values, coincident with higher conductivity (66, 247, and 8 mS cm⁻¹, respectively) than the FL and other CL samples.

A small number of chlorinated and brominated organic compounds have been previously reported in Marcellus, Barnett, and Eagleford produced waters using a targeted GC-MS approach (Maguire-Boyle and Barron, 2014). Recently, thirteen halogenated organic compounds were identified in the Fayetteville shale wastewater using two-dimensional gas chromatography paired with high resolution mass spectrometry, including halogenated benzenes, halogenated pyrans, halogenated alkanes, and halogenated acetones (Hoelzer et al., 2016). However, these exact masses were not identified using our method of SPE paired with FT-ICR-MS; not surprising considering these ions lack easily ionizable functional groups within negative ESI mode while others are outside of the analytical window of the method due to their small masses and volatility. Analysis using an alternative ionization method (e.g., photoionization) and analysis in positive mode expand the range of compounds detected using FT-ICR-MS.

To the best of our knowledge, natural gas compression liquids (CL) and natural gas fractionation liquids (FL) have not been previously investigated in the context of hydraulic fracturing wastewaters. The CL and FL fluids had extremely high DOC, much

higher than produced water samples previously reported, where a decrease in DOC is expected with the age of the well after organic additives are depleted (Cluff et al., 2014). Unlike FB and PW, where the DOM molecules remain in solution, CL liquids are less likely to contain non-volatile components because these fluids are not recovered until gas compression. The CL DOM pool is therefore less likely to contain more polar compounds, potentially including halogenated organics.

Presumably, a large number of possible structural isomers exist for each assigned formula, hence the structures remain unknown and require further investigation to elucidate. However, the molecular structures of two m/z ions could be confidently determined, due to having only one probable structural isomer: CHI_2^- , diiodomethane and $\text{C}_2\text{HO}_2\text{I}_2^-$, diiodoacetic acid. In an attempt to confirm these ions, fragmentation experiments were performed on PW1 and FB2 samples over 500 scans and the intensities of these ions were too low to confirm these structures without separation (Figures A2.9, A2.10).

3.3.1 Origin of Halogenated Organics

There are four plausible sources of halogenated organic compounds identified in hydraulic fracturing wastewater: a) chemical additives b) shale c) biotic reactions occurring within the fluids or d) abiotic reaction occurring within the fluids. The identified halogenated organic molecular ions do not match known chemical additives (“FracFocus,” 2017; Stringfellow et al., 2014; U.S. EPA, 2016). The only known halogenated organic compound used as an additive is dichloromethane (“FracFocus,” 2017; Hoelzer et al., 2016; Maguire-Boyle and Barron, 2014). Additionally, chloromethyl propanoate, chloromethyl pentanoate, chloromethyl hexanoate, chloromethyl octanoate

have also been identified in hydraulic fracturing wastewater as suspect additives (Hoelzer et al., 2016). Fluorinated compounds were also identified, and were suggested to be flowpath tracers (Maguire-Boyle and Barron, 2014). The identified halogenated organic compounds in this study do not match these known additives.

Approximately 5,000 naturally occurring halogenated organic compounds have been identified in the environment from both biotic and abiotic reactions (Gribble, 2010). Halogenated organic molecules are not typically preserved in the fossil record (Peters et al., 2005), hence are unlikely to persist in the sedimentary shale. In our analysis of a Utica shale water extract, we did not identify any of the reported naturally occurring halogenated organic compounds, and suspect that the identified iodinated organics are not present in the shale prior to energy development.

Although biocides are applied to hydraulic fracturing fluids to limit microbial growth (and prevent clogging, hydrogen sulfide production, etc.), a functional microbial community persists in these fluids and wastewaters (Daly et al., 2016; Mouser et al., 2016). The exact masses for diiodoacetic acid and diiodomethane identified in this study can be produced abiotically and biotically in the environment. Diiodomethane has been associated with the marine bacteria *Roseovarius* spp. and both diiodomethane and diiodoacetic acid have been identified in marine algae (Dembitsky, 2006). Indeed, *Roseovarius* spp., iodide-oxidizers, have been identified in hydraulic fracturing wastewater impoundments in multiple inland locations (Murali Mohan et al., 2013b, *see Chapter 4*).

Diiodoacetic acid may also be produced as a DBP, and nine additional ions were identified within the exact mass list of 259 known halogenated DBPs which have been

previously identified using a similar extraction technique and FT-ICR-MS (Pan et al., 2016; Plewa et al., 2004; Postigo et al., 2016) or GC-MS (Smith et al., 2010) (Table A2.7). Two chlorinated formula assignments were previously identified by FT-ICR-MS in a study of chlorination of natural DOM (Zhang et al., 2012). However, the majority of the assigned halogenated formulas in hydraulic fracturing wastewater have not been previously reported, and may reflect new high molecular weight DBPs. FT-ICR-MS has been previously shown to be a useful tool in identifying unknown halogenated DBPs (Gonsior et al., 2015, 2014; Zhang et al., 2012). A DBP-like formation process is likely occurring in the hydraulic fracturing fluids and wastewater, and is a probable abiotic source of the identified halogenated organic compounds. Abiotic transformations via three halogenation reaction mechanisms were also proposed for the formation of the halogenated organic compounds identified in Fayetteville Shale wastewaters (Hoelzer et al., 2016). These three mechanisms, radicalic substitution, nucleophilic substitution, and electrophilic addition, were proposed for the formation of dihalomethanes, halogenated alkanes, and halogenated acetones (Hoelzer et al., 2016), and are well described in organic chemistry. Marine shale contains high levels of chloride, bromide, and iodide (Harkness et al., 2015) that are released during the hydraulic fracturing process and create brine flowback and produced waters. Breakers are used to reduce the viscosity of the fracturing fluid gels after the well has been fracked (Barati and Liang, 2014; Stringfellow et al., 2014; Wang et al., 2012), to allow the fluid to return to the surface. At high temperature and pH conditions, inorganic oxidants such as oxides, peroxides, and persulfates are used as breakers. Persulfates have also been shown to interact with chloride and bromide ions and DOM to form chlorinated and brominated DBPs (Lu et al.,

2015; Xie et al., 2015). When these dissolved halogens are exposed to strong oxidants frequently used as breakers (Barati and Liang, 2014) or disinfectants such as hypochlorite (used in 3% of wells) (Kahrilas et al., 2015) in the well or during wastewater treatment (Harkness et al., 2015; Hladik et al., 2014; Sun et al., 2013), hypobromite and hypiodite or other reactive species are readily formed (Westerhoff et al., 2004). Free halogens have been shown to react with diverse DOM precursors to form complex and variable DBPs (Ding et al., 2013; Gonsior et al., 2014; Lavonen et al., 2013). Chlorine dioxide, used in 8% of wells, has been shown to produce a handful of halogenated DBPs as well, different from those identified during chlorination (Richardson et al., 2003, 2000, 1994). Because hydraulic fracturing wastewater contains diverse organic compounds as well as inorganics (Barbot et al., 2013), it is therefore expected that highly diverse DBPs will be formed under conditions present in hydraulically fractured wells.

Unfortunately, information about the specific biocides and breakers used was only available for 5 of the 16 samples from FracFocus reports. FB3 reports the use of hydrogen peroxide as a breaker, and FB4, FB5, FB6 and FB7 report the use of ammonium persulfate. The use of these strongly oxidizing breakers supported the proposed formation pathway, and the finding of high numbers of halogenated organics in the FB samples rather than the PW, CL, and FL samples supported our hypothesis that many of the halogenated organics were indeed originating from reactions occurring in the early hydraulic fracturing fluid and flowback. $C_5H_2O_3I^-$ was the most frequently detected iodinated compound, while two chlorinated exact masses were the most frequently detected halogenated ions but had been previously identified in a daphnid metabolome study with no clear origin (Taylor et al., 2010). In the only non-FB sample with a known

fluid age, PW1 (5 y), the only halogenated organic compounds were the two ions (diiodomethane and diiodoacetic acid) known to have biotic production pathways.

To test if shale-derived DOM was sufficient to form halogenated DOM in the presence of halide ions, hypochlorite and bromide or iodide were combined with a Utica shale drill cuttings similar to previous chlorination experiments (Wang et al., 2016), and analyzed using the same extraction and FT-ICR-MS analysis methods employed in this study (see methods section in supporting information). Indeed, a number of halogenated organic compounds including known DBPs were formed including three m/z ions that matched known DBPs identified in hydraulic fracturing wastewater samples - diiodoacetic acid, 5,6-diiodo-2-hydroxybenzoic acid, and 4-chloro-2,6,-di-tertbutylphenol (Table A2.8).

3.3.2 *Environmental Relevance*

Using a non-targeted approach, a large number of unique halogenated formulas were assigned to precise, highly resolved molecular ions and confirmed using isotopic pattern matching. This non-target technique allowed for the simultaneous investigation of a large number of potential transformation products outside of the window of compounds expected to be present in hydraulic fracturing wastewaters (hydrocarbons, additives). From here, future targeted analyses can investigate the structure of the identified formulas and hopefully quantify individual compounds. However, the reported ions represented only a fraction of the total halogenated ions that may be present in these samples but were at too low intensity to be confirmed using isotopic pattern matching. More than 800 iodinated formulas were identified in FB1 alone, with 58 containing two iodine atoms. Of these, 95% of the highest intensity ions could be confirmed using

isotopic pattern matching and all produced a fragment at m/z 126.904 representing iodine during MS-MS fragmentation (Table 3.2, Figure A2.11). The stability and toxicity of these diverse halogenated compounds is poorly understood, even less so considering that the structures remain largely unknown. It is known that bacteria associated with iodide cycling have been identified in flowback water impoundments (Murali Mohan et al., 2013b). In a comparison of flowback water samples extracted at four separate time points over eighteen months and stored at 4° C between each extraction, iodinated compounds were consistently extracted and identified in the mass spectra. This suggests that at least some of these compounds are stable under these storage conditions. Further characterization is necessary to describe these compounds and to understand their stability and toxicity. The large numbers of possible iodinated DBPs identified are of particular concern, considering iodinated DBPs have been found to be much more toxic than their chlorinated and brominated counterparts (Plewa et al., 2008; Richardson et al., 2008). Iodinated DBPs have been identified during the treatment of highly saline waters, such as through desalination or saltwater waste treatment (Gong and Zhang, 2015; Kim et al., 2015), as well as in chloraminated drinking waters impacted by saltwater intrusion or connate water (Plewa et al., 2004; Richardson et al., 2008). If these compounds are relatively stable, they may also be suitable tracers for hydraulic fracturing wastewater in the environment due to their unusual composition.

In addition to those DBPs already identified in the flowback and produced waters, disinfection during shale gas wastewater treatment also introduces the potential for new DBP formation (Harkness et al., 2015; Hladik et al., 2014; Sun et al., 2013). As treatment techniques for hydraulic fracturing wastewater advance and the environmental impact of

deep well injection becomes increasingly apparent (Kim, 2013; Weingarten et al., 2015), the potential of this saline wastewater to produce halogenated organic compounds during the disinfection process in wastewater treatment must also be considered (Harkness et al., 2015; Parker et al., 2014).

Chapter 4

Temporal Dynamics of halogenated organic compounds in Marcellus Shale flowback

*Luek, J.L., Harir, M., Schmitt-Kopplin, P., Mouser, P.J., Gonsior, M.
Submitted to Water Research 23 October 2017.*

*Contribution: Experimental design, all sample analysis, data analysis and interpretation
[except 16S rRNA data], and all text and figures.*

Abstract

The Marcellus Shale Energy and Environment Laboratory was established to address a gap in scientific knowledge in hydraulic fracturing technology and its environmental implications. A time series of hydraulic fracturing fluids, flowback fluids, and produced waters was collected from two adjacent Marcellus Shale gas wells for organic composition analyses using ultrahigh resolution mass spectrometry. Hierarchical clustering was used to extract ions specific to different fluid ages and many organohalogen molecular ions were identified in flowback fluids. Iodinated molecular ions identified using exact mass and isotopic pattern (^{13}C) matching were tracked from the injected fluids through flowback fluids and produced waters. Iodinated molecular ions were almost completely absent in hydraulic fracturing fluid prior to injection, but then increased drastically in flowback and remained elevated after nine months. We hypothesize that these trends are driven by dissolved organic matter (DOM) reacting with reactive halide species formed abiotically through oxidizing chemical additives and biotically from iodide-oxidizing bacteria that remain in these fluids several months after hydraulic fracturing. Further investigation of these pathways, particularly biological pathways, and in to the structures, stabilities, and toxicities of these compounds are

important steps moving forward our understanding of the fate and environmental impact of hydraulic fracturing fluids.

4.1 Introduction

Gaining access to samples from unconventional oil and gas wells is an on-going challenge for government, academic, non-governmental organizations, and industry scientists alike. Without regular access to aqueous and solid samples from well sites, progress not directly advantageous to industry is challenging and potentially restricted, which severely limits our understanding of the impacts of these important technologies to the environment and our ability to improve upon them for the betterment of society. Most studies investigating the impacts of hydraulic fracturing on the aquatic environment have focused on tracking known fluid additives or formation-derived constituents (halides, metals, etc.) in samples collected near existing well pads (Drollette et al., 2015; Hildenbrand et al., 2015; Llewellyn et al., 2015). Studies of actual hydraulic fracturing fluids and wastewaters have been particularly limited, with only ~250 samples analyzed for organic constituents [other than light gases] (Akob et al., 2015; Luek and Gonsior, 2017; Orem et al., 2014; Strong et al., 2013) during a period when more than 25,000 individual wells were drilled and hydraulically fractured annually (U.S. EPA, 2016).

In an effort to address the challenge of independent scientific access to wells, a partnership between private industry, academia, and government scientists was developed as the Marcellus Shale Energy and Environment Laboratory (MSEEL). In 2016, the Marcellus Shale produced over 5 trillion cubic feet of recoverable gas in Pennsylvania alone (*PA DEP*, 2016). The goal of this collaboration is “to provide a long-term field site

to develop and validate new knowledge and technology to improve recovery efficiency and minimize environmental implications of unconventional resource development” (mseel.org). In 2015, two Marcellus Shale horizontal wells were drilled and hydraulically fractured in Morgantown, WV with explicit access for researchers throughout the process.

For companies, the correct combination of additives during hydraulic fracturing is important for developing productive gas wells (Barati and Liang, 2014; Stringfellow et al., 2014). Information about additives has become increasingly available for researchers through the FracFocus online database (fracfocus.org), but only a handful of published studies have tracked this mixture once it is diluted with formation waters and transformed by biotic and abiotic reactions (Cluff et al., 2014; Hoelzer et al., 2016; Kahrilas et al., 2016). Time-series analyses of hydraulic fracturing fluid additives and flowback have provided key information about the changes in microbial communities over the early life of a well (Cluff et al., 2014; Murali Mohan et al., 2013a), and in the temporal dynamics of inorganic constituents, additives and bulk properties (Kim et al., 2016; Miller et al., 2013; Rosenblum et al., 2017a; Ziemkiewicz and He, 2015). Targeted analyses of specific contaminants are useful for describing changes in wells and understanding potential toxicity (Hayes, 2009; Orem et al., 2014; Ziemkiewicz and He, 2015), but additional approaches are needed to further understand time-resolved chemical transformations occurring in these fluids (Hoelzer et al., 2016).

Ultrahigh resolution Fourier transform ion cyclotron resonance mass spectrometry (FT-ICR-MS) is widely used to characterize diverse organic matter (Dvorski et al., 2016; Gonsior et al., 2011; Kellerman et al., 2014; Roullier-Gall et al., 2015; Walker et al.,

2014). This non-targeted approach has been used to describe changes in organic chemical composition in natural and engineered systems based on its highly precise exact masses rather than individual standards (Chen et al., 2016; Gonsior et al., 2016; Lavonen et al., 2013; Shakeri Yekta et al., 2012; Sleighter et al., 2014a). Halogenated organic compounds have been recently identified as potential transformation products in shale gas wastewaters (Hoelzer et al., 2016; Luek et al., 2017; Maguire-Boyle and Barron, 2014) and FT-ICR-MS has been shown to be useful for identifying halogenated organic constituents including disinfection by-products (DBPs) (Gonsior et al., 2015; Lavonen et al., 2013; Luek et al., 2017; Xu et al., 2013). Halogenated organic compounds have been hypothesized to be transformation products associated with the use of strong oxidants (Hoelzer et al., 2016; Luek et al., 2017), although iodinated compounds may also be related to iodide-oxidizing bacteria present in hydraulic fracturing wastewaters (Murali Mohan et al., 2013b). FT-ICR-MS paired with solid phase extraction (SPE) (Dittmar et al., 2008) is uniquely suited for describing the temporal dynamics of dissolved organic matter (DOM) found in high salinity shale gas wastewater, particularly for halogenated organic compounds.

Therefore, the aim of this study was to track changes to the organic matter pool over the lifetime of two Marcellus Shale gas wells from the injection of fluids over the first nine months of flowback. Specifically, we combined SPE with FT-ICR-MS and used hierarchical clustering analysis to identify key shifts in the distribution of organic molecules. We further investigated the distribution and evolution of iodinated organic molecules and developed a framework for describing drivers of halogenated organic compounds over the lifetime of a shale gas well.

4.2 Materials and Methods

Hydraulic fracturing fluid prior to injection, flowback fluid, and produced water samples were collected from two adjacent MSEEL hydraulic fracturing wells in Morgantown, WV (Figure A3.1) between November 2015 and September 2016 (Carr, 2017). Dissolved organic compounds were extracted with solid phase extraction cartridges from water samples and analyzed using FT-ICR-MS. Hierarchical clustering analyses were performed on the resulting ions to track temporal dynamics of DOM and were then assigned exact molecular formulas.

4.2.1 Sample Collection

MSEEL wells MIP-3H and MIP-5H (herein referred to as 3H and 5H) were sampled from a gas-fluid separator in autoclaved high-density polyethylene carboys from the separator outlet. Fluid was then transferred in to 1L base-washed low-density polyethylene containers using a peristaltic pump minimizing headspace. Samples were collected approximately daily during the initial week of flowback (December 2015), bi-weekly for the following 3 months (early production water), monthly for 3 months, and then bimonthly (late production water). On certain dates, the 5H well was not producing fluid so no sample was collected. Samples were refrigerated at 4 °C and shipped on ice within two weeks of collection.

4.2.2 Organics extraction

Upon receipt, samples were filtered over a 0.7 µM glass fiber filter (Whatman GF/F) into glass bottles previously baked at 500 °C. Filtered samples were stored frozen prior to dissolved organic carbon (DOC) and total nitrogen (TN) analysis. Filtered samples (200 mL) for SPE were immediately acidified to pH 2 with concentrated

hydrochloric acid and extracted over activated 1g/6mL Bond Elut PPL solid phase extraction cartridges (Dittmar et al., 2008). Loaded cartridges were desalted using a 200 mL dilute hydrochloric acid (pH = 2) rinse followed by a 30 mL 0.1% formic acid solution rinse to avoid any halide ion contamination of the methanolic extract. Cartridges were dried under vacuum and eluted with 10 mL ultrapure methanol. Methanolic extracts were stored at -20 °C prior to FT-ICR-MS analysis.

4.2.3 Dissolved organic carbon and total nitrogen analysis

Frozen filtered samples were thawed, shaken to thoroughly mix samples, and diluted ten fold or more as needed to obtain a concentration between 0.5 – 20 mg L⁻¹ C and 0.25 – 10 mg L⁻¹ N. Diluted samples were acidified externally using 20 µL of concentrated hydrochloric acid then analyzed using a Shimadzu TOC-V CSH total organic carbon/nitrogen analyzer with catalytic combustion at 720°C and nondispersive infrared detection. Samples were quantified using potassium hydrogen phthalate and potassium nitrate standards as non-purgeable organic carbon (NPOC) and total dissolved nitrogen (TDN), respectively. The maximum coefficient of variation was set to 2% with up to five 200µL injections (minimum three). All injections were averaged to calculate NPOC and TDN.

4.2.4 FT-ICR-MS analysis

Methanolic sample extracts were diluted 1:5 in ultrapure methanol and injected at 120 µL hr⁻¹ using a Bruker Solarix 12T FT-ICR-MS with negative mode electrospray ionization located at the Helmholtz Zentrum Munich, Germany. 500 individual scans were averaged for each sample and a post calibration was performed using a list of known dissolved organic matter internal calibrants to obtain a mass accuracy of less than

0.2 ppm (Table A3.1). The obtained full scan mass resolution was better than 400,000 at m/z 400 allowing for precise formula assignments (Hertkorn et al., 2008). All m/z ions identified in the field blank were subtracted prior to further processing. Following the methods of Sleighter et al. (2012), replicate sample mass spectra were compared to confirm that variability across samples was different from variability among extraction replicates (Figure A3.2, A3.3).

Formulas were assigned individual ions between 150 - 600 m/z using in-house software. Formulas were assigned with a maximum value per assignment of $C_{100}H_{\infty}O_{80}N_3S_2Cl_3Br_3I_3$ and a maximum error of 0.2 ppm. Corresponding ^{13}C isotope peaks were searched for within 1 ppm of the assigned formulas. Formulas not passing the nitrogen rule were removed (F.W. McLafferty and F. Turecek, 1993) and remaining assignments were further reduced to remove invalid formulas by removing those with an oxygen to carbon ratio (O/C) greater than one or a negative double bond equivalent (DBE). Additional filtering of assigned formulas identified during the cluster analysis involved removing assignments with more than 3 heteroatoms and preferentially removing duplicate assignments with very low O/C ratios and higher heteroatoms. All assigned formulas matching known compounds, particularly additives, are putatively named as such based on their probable presence in these fluids and likelihood to ionize under the methods used, but have not been confirmed structurally. Halogenated formula assignments were compared to their theoretical isotopic patterns and those ions not matching their theoretical isotope patterns (Figure A3.4) were removed. Ions with insufficient intensity to confirm isotopically were not removed.

Iodinated ions have a large mass defect and therefore easily separate from most other organic formula assignments. Of the observed m/z ions assigned to an iodinated formula, approximately 50% had a duplicate formula assignment containing S and Cl, but were determined false assignments because the distinctive ^{35}Cl to ^{37}Cl isotopic ratios were not observed in the mass spectra. Large volume washing of cartridges reduces the likelihood of iodo-adducts (Luek et al., 2017; Xu et al., 2013) and prior investigations have found that high and ultrahigh resolution electrospray mass spectrometry have confirmed covalently-bound iodine in complex mixtures (Luek et al., 2017; Moulin et al., 2001; Xu et al., 2013).

4.2.5 Hierarchical Cluster Analysis

Hierarchical cluster analysis was performed using Gene Cluster 3.0 and TreeView on log transformed ions. Hierarchical clustering analysis was performed on log transformed and uncentered m/z ions identified in each well using intensities as a) m/z ions common to all samples m/z 150 – 600 (3H, n= 1735; 5H, n= 1021) and b) only m/z ions present in 2 or more samples m/z 150 – 400 (3H, n= 6613; 5H, n=5296). Selected clusters with unique trends during the time series were then assigned formulas.

4.3 Results and Discussion

4.3.1 Dissolved organic carbon and total nitrogen

Dissolved organic carbon (DOC) concentrations were low in the initial hydraulic fracturing fluid (Figure A3.5). After thawing the frozen filtered fracturing fluid samples, a clear “gel” solid was visible, indicating that the gelling agents used (acrylamide, guar gum) were not dissolved and therefore not part of the dissolved phase, complicating the

interpretation of DOC values. DOC and TDN concentrations increased in the flowback and early production waters, and TDN concentrations continued to rise to a maximum of 135 mg L⁻¹ in the 5H well and 112 mg L⁻¹ in the 3H well. DOC concentrations increased over the first 100 days after hydraulic fracturing, and then were highly variable during later sampling periods. DOC peaked at 277 mg L⁻¹ in the 3H well 200 days after hydraulic fracturing. This high variability is likely due to the presence of a non-aqueous phase, making consistent sampling of the dissolved phase challenging. The observed DOC increases are not in agreement with three other Marcellus Shale gas wells, where initial concentrations dropped from 400 mg L⁻¹ to less than 100 mg L⁻¹ forty days after the initial flowback (Cluff et al., 2014). Total organic carbon (TOC) analyses in the Marcellus Shale region have been reported over a range from 23 – 5800 mg L⁻¹ in produced waters, also suggested to be related to miscible oils (Orem et al., 2014). The observed increase in DOC and TDN following hydraulic fracturing may be due to a higher background of DOC/TDN in this region of the Marcellus, while previous observations of decreasing DOC (Cluff et al., 2014) may be due to lower underlying DOC levels in the sampled formation. Overall, DOC concentrations are of limited use, due to the fact that gelling agents and non-aqueous phases unpredictably contribute to DOC, especially when samples are frozen and thawed. This may impact partitioning of other DOM to the dissolved phase, particularly in the gelled injected fluids.

4.3.2 Molecular ions indicative of additives and their degradation products

Ions assigned to formulas containing only carbon, hydrogen and oxygen were the most common constituents of the fluids. The number of CHO molecular ions initially increased between those identified in the fracturing fluid and those in the initial flowback,

then declined over the following nine months. This trend in the diversity of DOM is consistent with the notion of a fracturing fluid DOM pool mixing with a shale-derived DOM pool to create the highest diversity in initial flowback. One of the most consistent high intensity CHO ions in flowback and produced waters, m/z 165.01934 [$C_8H_5O_4^-$] matched the exact mass of phthalic acid. Phthalic acid is not listed as an additive but many phthalates may have been used in the plasticizers used in tubing and storage containers. Phthalates have previously been proposed as tracers of hydraulic fracturing fluids but have received pushback due to their diverse origins and frequent occurrence as a laboratory contaminant (DiGiulio et al., 2011; Hayes, 2009; Orem et al., 2014; U.S. EPA, 2015a, 2015d).

Alcohol ethoxylate additives were used in both wells, listed as the technical mixture C14-15 ethoxylated alcohols (7EO) and as a friction reducer containing a trade secret alcohol ethoxylate mixture. These compounds have low double bond equivalents, making these ions readily distinguishable from most natural DOM ionizable using negative electrospray ionization (Hertkorn et al., 2008). Polypropylene glycols were also used as additives, which have similar properties and have some overlapping formulas with alcohol ethoxylates. The exact masses of known alcohol ethoxylates, alcohol ethoxysulfates, and polypropylene glycols were searched for in all samples (Morales-Cid et al., 2009; Schymanski et al., 2014b). Several alcohol ethoxylate exact masses were identified including those matching octylphenol ethoxylates and nonylphenol ethoxylates, both of known environmental concern (Soares et al., 2008). The putatively assigned octylphenol carboxylate (OP2EC) ion was the most consistently observed alkylphenol group ion, increasing in abundance in flowback but varying in produced water samples.

The two most abundant alcohol ethoxysulfate ions, m/z 369.19525 ($C_{16}H_{33}O_7S^-$) and 325.16904 ($C_{14}H_{29}O_6S^-$), were absent in the fracturing fluids but dominant in flowback and early production water. These compounds may have two possible origins: (1) as part of the trade secret friction reducer (sent down separately and/or not present in the fracturing fluid sample received by our group), or (2) as a sulfonated transformation product of the injected C12 – C14 (7EO) alcohol ethoxylates. Corresponding non-sulfur containing ethoxylate ions were also identified, but are likely ionized less efficiently than their S-containing counterparts, which may explain why they are identified at lower abundances although they could be present at higher concentrations. Polypropylene glycols in the measured mass range were not identified, although this may be due to poor ionization in negative mode [these polyglycols have a stronger ionization in positive mode] (Thurman et al., 2017)].

In addition to disclosed ethoxylated and propoxylated additives, Thurman et al., (2017) also identify a series of polyethylene glycol carboxylate ions in flowback and produced waters from the Wattenberg field (CO, USA), suggesting they are a degradation product or trace impurity of a polyethylene glycol additive. Exact mass $[M-H]^-$ ions matching ethoxylated carboxylates were identified in MSEEL flowback and produced waters. Polyethylene glycol was not a disclosed additive, but the abundance of 7EO and 8EO homologues (putative naming per Thurman et al., 2017) in early flowback suggests that in the MSEEL fracturing fluid, these ions are instead related to the disclosed 7EO alcohol ethoxylate additive (Figure 4.1, Table A3.2). A rapid decline is seen in the highest ethoxymers (EO9, EO10) after the first week of flowback, while the lower ethoxymers also decrease in intensity after the first week but remain above the baseline at

all later dates. These patterns are consistent with what would be expected for an ethoxylate fracturing fluid additive degrading but remaining in low concentrations, consistent with their previous identification in 100 day old produced water (Thurman et al., 2017).

Changes in fluid characteristics can impact extraction efficiencies and abundance and potentially lead to false trends in abundance and intensity plots. The most important variable for most compounds, including ethoxylate carboxylates, is the possible presence of a secondary phase that can concentrate organic compounds and reduce dissolved phase concentrations. Gels and organic solvent additives should decrease over time in a dry gas well, suggesting that many extractable organic compounds should theoretically increase in the dissolved phase and in the observed mass spectra as a secondary phase decreases. However, the opposite trend was observed for ethoxylate carboxylates, suggesting that their observed trends are indeed real as this is plausible and matches timeseries trends of the parent PEGs in flowback (Rosenblum et al., 2017b).

Nitrogen-containing ions were among the most abundant ions identified in hydraulic fracturing fluid samples (e.g., similar ions: $C_{20}H_{41}O_6N_2^-$; $C_{20}H_{41}O_8N_2^-$; $C_{20}H_{39}O_6N_2^-$; $C_{18}H_{37}O_6N_2^-$), but were not identified in any flowback or produced water samples. These ions did not match the formulas of any known additives or even known compounds. Of the disclosed additives, the only large organic nitrogen containing compounds were alkyl (C12-16) dimethylbenzyl ammonium chloride, EDTA, and 2-acrylamido-2-methylpropanesulfonic acid polymer. In flowback and produced waters, one of the consistently high intensity ions contained both nitrogen and sulfur, m/z

431.11629 [C₁₄H₂₇N₂S₂O₉⁻], and was confirmed using three stable isotopic peak matches. However, this formula does not match any known additives or known compounds.

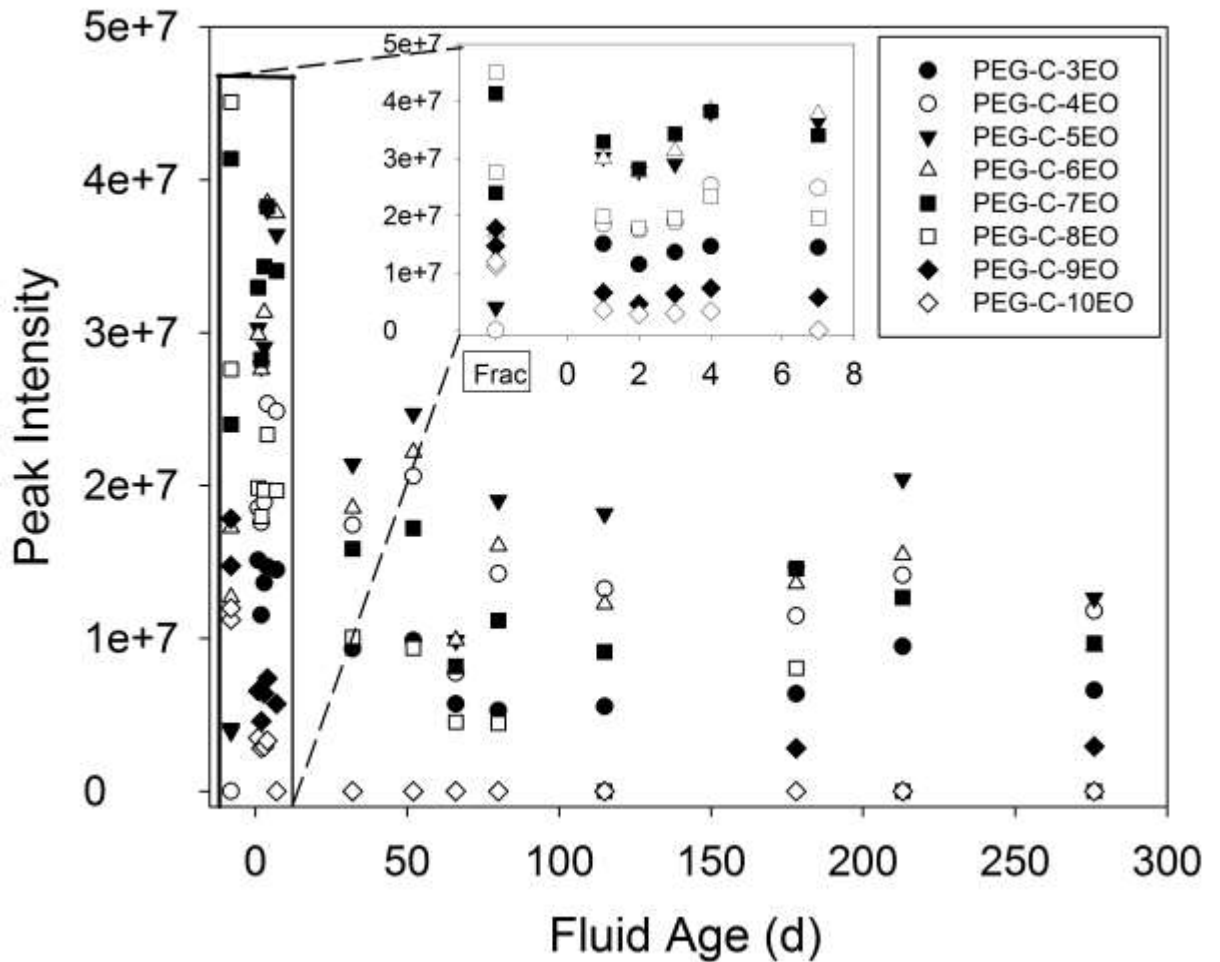


Figure 4.1. Time series of specific ethoxylate carboxylate homologue abundance (as peak intensity) in MSEEL 3H well (naming as per Thurman et al., 2017).

4.3.3 Cluster analysis reveals sulfur and halogenated ions unique to flowback

In the “All Common Ions” clusters (“A” clusters), nearly all ions could be assigned formulas containing carbon, hydrogen, oxygen (CHO) or nitrogen and/or sulfur heteroatoms (CHON, CHOS, CHONS) (Table A3.3, Figure 3.2). This distribution among all common ions was expected as it mirrors natural organic matter and known

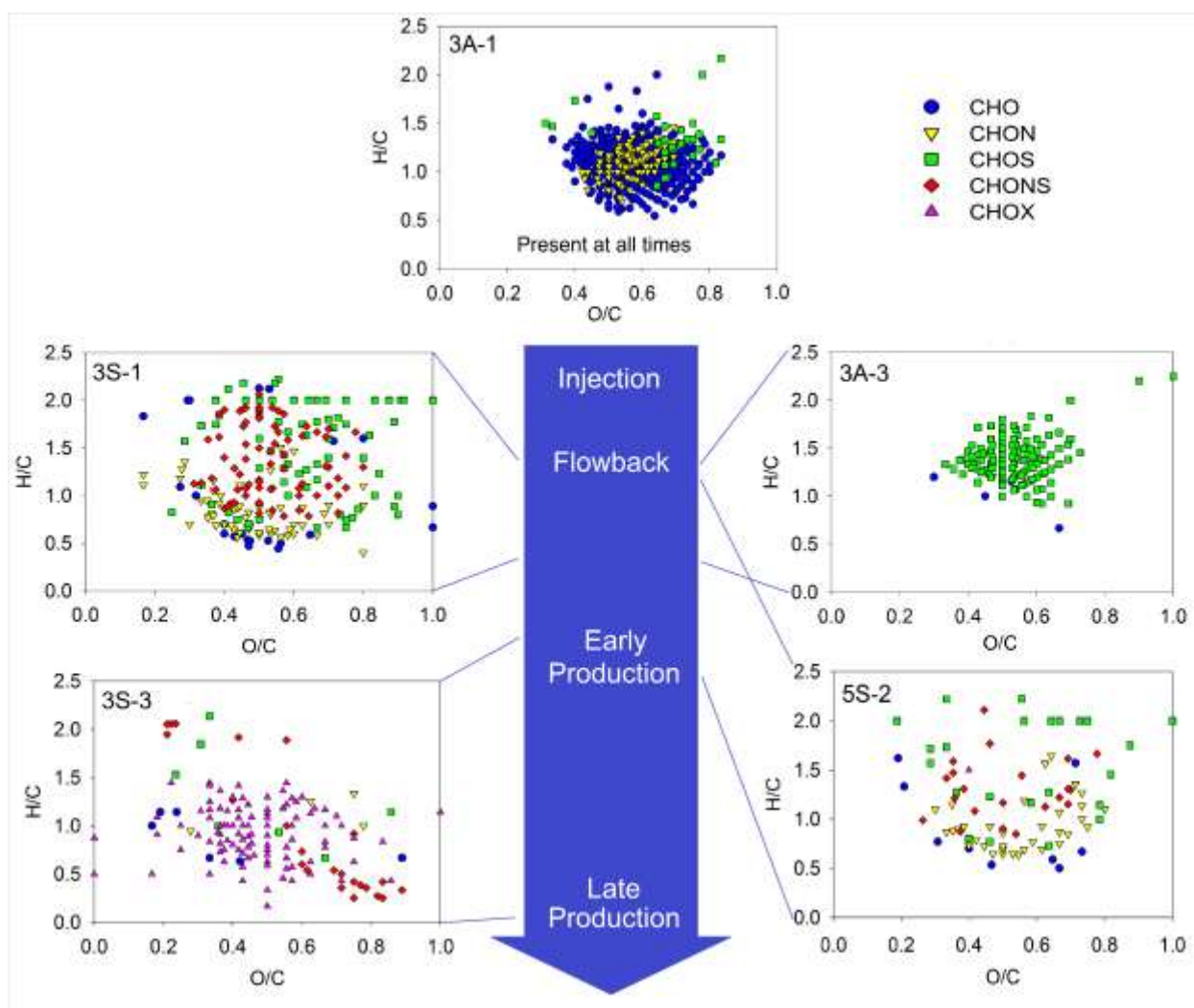


Figure 4.2 Oxygen to carbon (O/C) ratio versus hydrogen to carbon (H/C) ratio of formulas assigned to molecular ions within the hierarchical clusters shown Table A3.3 (van Krevelen, 1950). Additional cluster Van Krevelen diagrams are shown in Figure A3.8.

additives. The largest contrast was seen in ions peaking in flowback and early production water (cluster 3A-3), where nearly all ions were assigned a sulfur-containing formula. A similar sulfur-dominant cluster was not observed in the 5H well. The 3A-3 sulfur cluster may represent transformations, i.e, reactions with sulfide during the month-long well shut-in period or later (Brüchert, 1998; Damsté et al., 1989; Einsiedl et al., 2008; Ferdelman et al., 1991; Werne et al., 2008). Indeed, sulfide production from thiosulfate

by the dominant species in these wells, *Halanaerobium spp.*, has been observed (Booker et al., 2017). Alternatively, this dominance of sulfur-containing ions in flowback and early production waters could also be related to changes in ionization efficiency, as acidic sulfonate groups ionize efficiently in negative mode.

“Ions in 2+ Samples” cluster ions (“S” clusters) were much more diverse than the “All Common Ion” cluster ions (Figure 4.2, Figures A3.6, A3.7), with a large number of heteroatom formula assignments rather than those containing only carbon, hydrogen, and oxygen. These ions were also assigned formulas with a wider variety of oxygen to carbon ratios (O/C) and hydrogen to carbon ratios (H/C). Cluster 3S-3, representing ions present only in early production water (30-115 d), had 155 ions with plausible halogenated formula assignments that could be validated to varying degrees (Table A3.4). Sixty-five of these halogenated formula assignments were supported with secondary and tertiary peaks matching their theoretical stable isotopic spectra (e.g., Figure A3.4). Five iodinated ions had been previously identified in a North Dakota flowback fluid where their assignment was supported with the production of a 126.9045 m/z peak (iodine) during fragmentation (Luek et al., 2017). Of the remaining ions assigned plausible halogenated formulas, many were members of homologous series [separated by CH₂ groups determined using kmd/z^* values (Shakeri Yekta et al., 2012)] where at least one member of the series had been confirmed isotopically. Thirty-eight of the remaining halogenated formula assignments had intensities too low to rely on isotopic pattern matching (particularly iodinated assignments which rely solely on the small ¹³C peak). Interestingly, a matching “halogenated” cluster in the 5H well was not observed, and among all other “Ions in 2+ Samples” clusters, only five plausible halogenated formula

assignments were identified and three confirmed using isotopic pattern matching. All m/z ions identified in these clusters are given in supplemental Table A3.5 regardless of whether or not they could be assigned an exact molecular formula.

4.3.4 Iodinated organic ions high in flowback and produced water

Prior to injection, the 3H and 5H well fracturing fluids were nearly devoid of iodinated ions, with three or fewer identified at relatively low abundances in individual samples (Figure 4.3). Beginning with the first week of flowback, the number of iodinated ions drastically increased, and remained high in all produced water samples out to 276 days. The cumulative abundance of all iodinated ions also followed this trend, with higher intensities but more variability observed in the 3H well. Cumulative intensity trends may be biased by differences in fluid characteristics such as TDS (e.g., decreased solubility at high salinity). Mass spectra for all samples except injected hydraulic fracturing fluid had similar mass spectra and similar maximum intensities, suggesting comparable behavior and limited ion suppression issues within the mass spectrometer for all fluids returned to the surface. It cannot be ruled out, however, that low intensities and numbers of iodinated compounds in injected samples and early flowback were not due to differences in extraction efficiencies or distributions (e.g., dissolved versus sorbed to secondary phase of gel/solvent additives) at early time points relative to late produced waters. However, a timeseries analysis of organic compounds in Marcellus well fluids revealed no clear differences in the extraction efficiency of an organic surrogate standard (p-terphenyl-d14) even in the very distinct hydraulic fracturing fluids and early flowback during a liquid-liquid extraction (Piotrowski et al., 2018). A small volume (20 mL) quality control extraction was performed in August 2016 on all previously collected

samples and showed the same trends over the time series although the small volume extractions had slightly lower numbers of ions and intensities, likely related to either smaller sample volumes or the aging of the fluids prior to extraction (3-7 months storage unfiltered at 4 °C).

Iodinated organic compounds in these fluids are of particular interest for a number of reasons. Iodinated organic compounds are not used as additives, and relatively few iodinated organic compounds occur naturally (Dembitsky, 2006). Secondly, their biological formation is plausible as a result of iodide-oxidizing bacteria, which have been previously identified in flowback (Murali Mohan et al., 2013a). Thirdly, they can be formed as disinfection by-products (DBPs), and I-DBPs have shown higher toxicity than their chlorinated and brominated counterparts (Richardson et al., 2008).

The majority of iodinated ions contained only carbon, hydrogen, oxygen, and one iodine atom, but ten ions contained nitrogen or sulfur (Table 4.1), and six contained two iodine atoms. The observed distribution of O/C and H/C ratios (Figure A3.9) was consistent with the distribution of aromatic, particularly oxygen-rich and phenolic compounds (e.g., fulvic acids) susceptible to reaction with reactive iodine (Moulin et al., 2001). Halogenation of unsaturated compounds, aromatic structures, substituted aromatic structures (i.e., phenols) and natural organic matter can occur rapidly via electrophilic aromatic substitution (Criquet et al., 2015; Westerhoff et al., 2004). A similar O/C and H/C distribution of iodinated DBPs formed during chloramination of drinking water containing iodide, indicating the preferential formation of iodinated compounds from these aromatic precursors (Wang et al., 2016). FT-ICR-MS provides no structural information, but some structures can be inferred based on the limited number of structural

isomers for small compounds and their ability to be extracted and ionize under the experimental conditions. For example, the corresponding neutral formula $C_2H_2O_2I_2$ is expected to be diiodoacetic acid, a known disinfection by-product (DBP) (Plewa et al., 2004) and naturally occurring compound (Dembitsky, 2006). However, most identified ions are large and therefore cannot be structurally determined without further analyses.

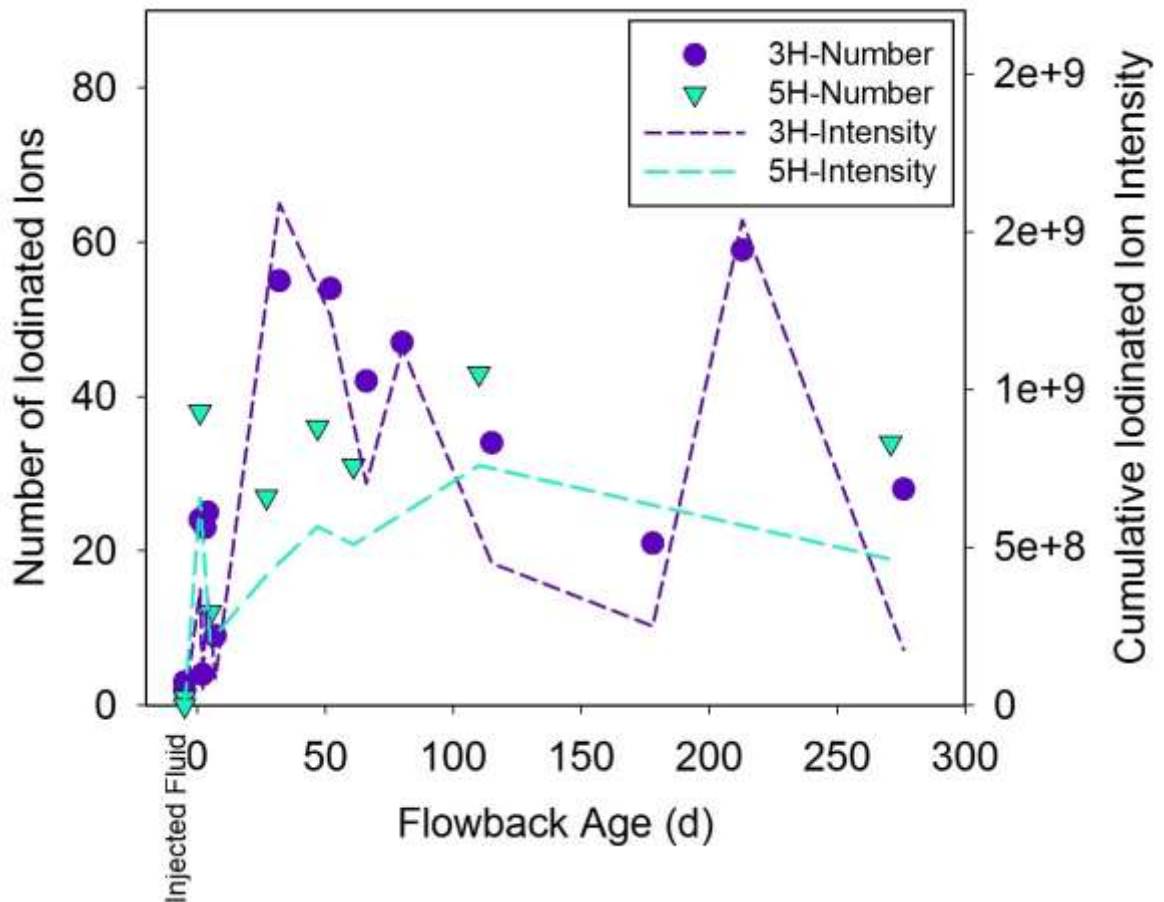


Figure 4.3 Number of iodinated organic ions and their cumulative iodinated ion abundances identified in the MSEEL 3H and 5H wells by date.

Table 4.1 Iodinated molecular formulas supported with ^{13}C peak. ^PPreviously identified in fracturing fluid (Luek et al., 2017a); ^SExact masses also identified in stream water DOM unrelated to hydraulic fracturing.

Measured Mass	No. Times identified	H	C	O	N	S	I
236.9054 ^P	31	2	5	3	0	0	1
276.9367 ^S	39	6	8	3	0	0	1
282.9473	16	8	7	4	0	0	1
292.8952	8	2	7	5	0	0	1
292.9316 ^P	31	6	8	4	0	0	1
305.9633	13	9	9	3	1	0	1
306.9109	29	4	8	5	0	0	1
306.9473 ^S	33	8	9	4	0	0	1
308.9266	38	6	8	5	0	0	1
310.8072 ^P	21	1	2	2	0	0	2
312.9943	3	14	9	4	0	0	1
320.963	37	10	10	4	0	0	1
322.8072	13	1	3	2	0	0	2
322.9422	34	8	9	5	0	0	1
322.9786	25	12	10	4	0	0	1
327.0099 ^S	42	16	10	4	0	0	1
334.9422 ^S	32	8	10	5	0	0	1
334.9786	21	12	11	4	0	0	1
336.9579	35	10	10	5	0	0	1
338.9194	19	8	9	4	0	1	1
338.9735	30	12	10	5	0	0	1
339.0099	2	16	11	4	0	0	1
342.9143	20	8	8	5	0	1	1
343.0048	16	16	10	5	0	0	1
345.0205	14	18	10	5	0	0	1
350.9372	33	8	10	6	0	0	1
350.9735	26	12	11	5	0	0	1
351.0099	3	16	12	4	0	0	1
352.9528	26	10	10	6	0	0	1
352.9892	28	14	11	5	0	0	1
353.0984	5	26	14	2	0	0	1
355.0048 ^P	15	16	11	5	0	0	1
355.0412	19	20	12	4	0	0	1
357.0205	14	18	11	5	0	0	1
359.0838	2	24	11	3	2	0	1
364.9528 ^S	24	10	11	6	0	0	1

367.0049	7	16	12	5	0	0	1
369.0205	6	18	12	5	0	0	1
370.0521	3	21	12	4	1	0	1
371.0361	6	20	12	5	0	0	1
373.0518	5	22	12	5	0	0	1
376.9528 ^S	31	10	12	6	0	0	1
376.9891	17	14	13	5	0	0	1
378.9684 ^S	28	12	12	6	0	0	1
379.0048	11	16	13	5	0	0	1
381.0205	11	18	13	5	0	0	1
383.0361	4	20	13	5	0	0	1
383.0725	3	24	14	4	0	0	1
385.0517	2	22	13	5	0	0	1
387.031	4	20	12	6	0	0	1
392.9476 ^S	21	10	12	7	0	0	1
397.0154	14	18	13	6	0	0	1
397.0881	1	26	15	4	0	0	1
399.0311 ^S	8	20	13	6	0	0	1
401.0467	2	22	13	6	0	0	1
402.8334	15	5	8	3	0	0	2
404.00	16	15	14	5	1	0	1
406.9633 ^S	23	12	13	7	0	0	1
420.8076	6	3	7	5	0	0	2
421.0153	9	18	15	6	0	0	1
423.031	10	20	15	6	0	0	1
423.0673	8	24	16	5	0	0	1
425.0467	12	22	15	6	0	0	1
427.026	8	20	14	7	0	0	1
427.0623	7	24	15	6	0	0	1
428.7796	21	3	5	5	0	1	2
433.1206	21	30	14	5	2	0	1

4.3.5 Origin of halogenated organics

Four sources have been proposed for the origin of halogenated organic molecules in flowback fluids: a) chemical additives in the hydraulic fracturing fluid b) leached shale molecules c) biotic reactions between additives and/or shale compounds and d) abiotic reactions between additives and/or shale compounds (Hoelzer et al., 2016; Luek et al., 2017; Maguire-Boyle and Barron, 2014). The specific additives reported for MSEEL

wells on the FracFocus database (fracfocus.org) do not contain iodinated organic compounds or other halogenated organic molecules. Moreover, nearly all halogenated organic compounds were absent from hydraulic fracturing fluid analyses (prior to injection and subsequent addition of an oxidizing breaker). These two observations suggest the identified halogenated organic molecules are leached from the shale or formed through abiotic or biotic reactions as the well matures.

Naturally occurring biogenic halogenated organic compounds do exist (Gribble, 2010), but the number of known iodinated compounds are particularly limited, with just over 110 compounds identified in the published literature (Dembitsky, 2006). To this end, the Marcellus shale could contain halogenated organic compounds derived from ancient biogenic processes that were not remineralized during diagenesis and slowly leached from the shale as the wells matured. On the other hand, many biogenic halogenated formula, such as methyl halides and halogenated phenols can be microbially degraded (Gribble, 2010), and may not persist in the environment, suggesting their biogenic sourcing would be unlikely, although this possible source is poorly characterized. We searched all samples for the exact masses of all known biogenic iodinated organic compounds (Dembitsky, 2006) and identified four. Two of the four were supported with their ^{13}C peak, iodotyrosine (m/z 305.96326) and iodophloroglucinol (m/z 376.95276, also identified in fracturing fluid prior to injection), while the other two exact masses were unsupported by their ^{13}C peak- diiodomethane (m/z 266.81732) and diiodoacetic acid (m/z 310.80717) due to their low intensity.

In addition to their possible sourcing as natural biogenic products, diiodomethane and diiodoacetic acid can also be formed as disinfection by-products (DBPs). These two

compounds were not the only putative DBPs identified in this dataset; several other exact masses also matched known DBPs, two of which were identified in a previous study from a fracturing fluid sample prior to its injection [chlorooctanedioic acid and haloaldehyde] (Luek et al., 2017). DBPs detected only in flowback and produced waters included halogenated acetic acids, iodomethylbutenedioic acid, and several halogenated aromatic structures (halogenated benzaldehydes, benzoic acids, phenols, and benzoquinones). Organohalogens can be formed when oxidizing chemicals such as chloramines and persulfates react with halides to form reactive halogen species, which subsequently react with DOM and xenobiotic compounds (Gong and Zhang, 2015; Plewa et al., 2004; Postigo et al., 2016; Wang et al., 2016; Xie et al., 2015). Of the identified iodinated molecular formulas (Table 3.1), all but 7 had their non-iodinated counterparts (replacing I with H) present in MSEEL samples and these were consistently abundant intensities ($>10^8$). Ammonium persulfate (listed as diammonium peroxodisulphate on FracFocus), a strong oxidizing agent, was used in both the 3H and 5H wells, but was applied at a concentration 75 times higher in the 3H well than the 5H (fracfocus.org). Despite concentration differences in ammonium persulfate use, a large number of iodinated, brominated, and chlorinated molecular formulas were identified in both wells and had similar chronological dynamics. Persulfate oxidation has been used for *in situ* chemical oxidation, relying on the activation of persulfate (via heat, UV light, ultrasound, or an electron) to form two sulfate radicals (Matzek and Carter, 2016). High temperatures found in the Marcellus Shale at depth and many potential electron donors (e.g., transition metals, additives) could easily activate the added persulfate. The resulting sulfate radicals are highly reactive, and can propagate a number of diverse reactions beyond their

intended role of breaking polymers. Persulfate oxidation can form reactive halogens including iodine, hypoiodite, radical iodine, and others that ultimately react with organic compounds including NOM and phenols (Lu et al., 2015; Wang et al., 2017).

Interestingly, reactive iodine species involved in these halogenation reactions can also be formed through natural processes without the external addition of oxidant additives, through abiotic reactions with NOM (Li et al., 2012) and oxidation of iodide to reactive iodine by biotically produced hydrogen peroxide and organic acids (Steinberg et al., 2008).

Bacteria known to oxidize iodide have been identified in hydraulic fracturing wastewaters (Amachi et al., 2005; Murali Mohan et al., 2013a), and may be an additional source of reactive iodine. These bacteria are capable of converting inorganic iodide to reactive iodine that can subsequently react with DOM along the same pathways as abiotically-produced reactive iodine. Although biocides are employed to limit bacterial growth, diverse and active communities are found in these fluids downhole (Cluff et al., 2014; Daly et al., 2016; Mouser et al., 2016; Murali Mohan et al., 2013a), and hydraulic fracturing increases the shale poresize, removing this physical limitation for microbial life in the deep shales (Mouser et al., 2016). The extended period over which iodinated formulas were observed supports a bacterially-derived source of reactive iodine. If the source of reactive iodine [i.e., diammonium peroxidosulphate] was solely derived from the initial fluid injection, a peak in halogenated organic molecules would be expected in flowback, but would likely decline rapidly as activated persulfate is removed through alternative rapid reactions or as fluid flows to the surface. The observed peak in the number of iodinated ions nine months after initial flowback, rather than in flowback,

supports an additional alternative source of iodinated ions not associated with the fluid additives. We searched for taxa phylogenetically associated to known iodide-oxidizing bacteria in 16S rRNA data from MSEEL samples. Taxa closely related to uncultured *Roseovarius spp.* were observed in MSEEL 3H drilling muds (2-4%) as well as flowback and early produced fluids (from 2 through 119 days) from both the 3H and 5H wells (<1%) (Figure A3.10) (unpublished data from Kelly Wrighton, methods- Cluff et al., 2014; Daly et al., 2016). Some *Roseovarius spp.* are capable of iodide oxidation in conjunction with production of iodinated organic compounds, including methyl halides (Amachi et al., 2005; Fuse et al., 2003). This reaction requires iodide, an oxidant (e.g., peroxide), and appropriate genes (i.e. halide peroxidases) that are poorly characterized in bacteria. As mineral iodides and oxidants (e.g. persulfate) are present in this system, these data suggest the potential exists for biotic production of iodinated organic compounds in conjunction with abiotic reactions in this system, albeit by low abundance microbial community members. However, hydraulic fracturing wells become rapidly dominated by anaerobic bacteria, suggesting these aerobic bacteria may only be important early prior to the well fluids becoming anoxic (Mouser et al., 2016).

4.3.6 Conceptual Model

The high diversity of halogenated molecular formulas and their presence in multiple clusters identified at different fluid ages indicate that there may be multiple processes involved resulting in their observed dynamics. Our results suggest that halogenated organic compounds observed in the MSEEL wells may be formed when DOM interacts with reactive halogens produced abiotically by activated persulfate and biotically by iodide-oxidizing bacteria. In addition to these controls observed in the

MSEEL wells, many other factors could influence the presence and dynamics of iodinated organic compounds in any given hydraulic fracturing fluid or wastewater (Figure 4.4).

The hydraulic fracturing fluid source waters and the chemicals added can impact the observed dynamics. Source waters used in the MSEEL wells came from fresh river water and were likely treated with a biocide to minimize bacterial input. The low levels of freshwater iodide as well as bromide and chloride would minimize the production of halogenated DBPs in the source water and fracturing fluid mixture if an oxidizing chemical biocide was used (i.e., chlorine). However, if recycled flowback is used as source water, high levels of halides could result in halogenated DBPs in injected fluids, if specific disinfectants are used.

Following well shut in and subsequent breaking of the fluid, the added chemicals can rapidly react with halides to form reactive halogen species and subsequently react with DOM. The DOM pool at this point consists of both additives, shale-derived compounds, and transformation products (Hoelzer et al., 2016), and this diverse DOM precursor pool will establish the possible halogenated products. As time passes, the amount of highly reactive breaker available to form reactive halogen species will decrease, and the fluid flow to the surface will become increasingly dominated by formation waters (Kondash et al., 2017a). If an active iodide-oxidizing microbial community continues to thrive in the well, they may continue to produce reactive iodine species from the shale-supplied iodide and a continuous supply of iodinated organic compounds will be observed in fluid returning to the surface. Finally, the ultimate fate of

fluids returning to the surface may be treatment, where dissolved inorganic halides may react with oxidants and DOM to produced halogenated DBPs (Hladik et al., 2014).

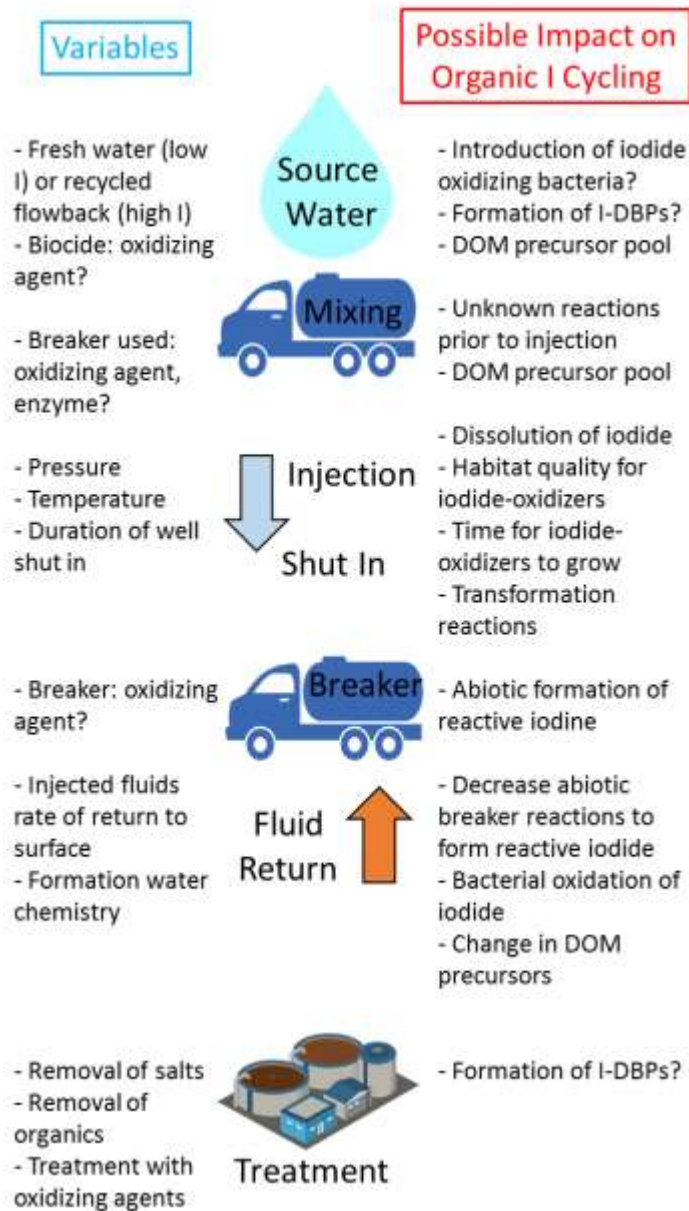


Figure 4.4 Conceptual model of variables and possible impacts on organic iodide cycling at different stages in of hydraulic fracturing. Images courtesy of the Integration and Application Network, University of Maryland Center for Environmental Science (ian.umces.edu/symbols/).

4.4 Conclusions

Iodinated organic ions were tracked through the first nine months of operation of two Marcellus Shale gas wells using FT-ICR-MS and revealed a steep increase in the number of ions assigned iodinated organic molecular formulas during the initial flowback period. The number and intensity of iodinated organic ions remained elevated in produced waters 276 days later. Hierarchical clustering analysis revealed a large number of brominated and chlorinated ions that were unique to fluids returning to the surface of the 3H well 1-4 months after the initial flowback and a handful of halogenated ions in the 5H well that were present prior to injection and decreased over the following nine months. Although the appearance and disappearance of ions in FT-ICR-MS spectra does not necessarily indicate the formation and removal of compounds when ion suppression issues are considered, these results suggest that these ions are likely the result of transformation reactions rather than compounds existing *a priori* in the fluids or the shale. Based on the observed temporal dynamics, we hypothesize that biotic and abiotic oxidation of halides subsequently reacting with diverse DOM contributes to the observed organohalogen temporal dynamics. However, a number of additional factors may also influence whether halogenated organic compounds are present in hydraulic fracturing fluids, flowback fluids, or produced waters, as described in our conceptual model.

The Marcellus Shale Energy and Environment Laboratory has allowed for careful study of the temporal dynamics of injected hydraulic fracturing fluids as they return to the surface as flowback and produced waters using a non-targeted approach. Analysis using FT-ICR-MS allows for the investigation of compounds not determined *a priori*, broadening our understanding of the physical, biological and chemical changes occurring

in a hydraulic fracturing well, including an expansion of the known organohalogens identified in flowback and produced water beyond those amenable to analysis with gas chromatography (Hoelzer et al., 2016; Maguire-Boyle and Barron, 2014). Tracking changes in the organic composition of fluids can help us to better understand the fundamental changes occurring in hydraulic fracturing fluids, but also address more applied questions of the life span and interactions of a given additive, flowback reuse, and produced water treatment engineering.

Chapter 5

Environmental fate and toxicity of organic compounds present in shale gas wastewaters

Luek, J.L., Mitchelmore, C., Mouser, P.J., Harir, M., Schmitt-Kopplin, P., Gonsior, M.

Contribution: Experimental design, all sample analysis, data analysis and interpretation, and all text and figures.

Abstract

Shale gas extraction using hydraulic fracturing techniques creates large volumes of wastewater. These wastewaters are managed through a variety of techniques but their use, treatment, storage, and disposal carry risks for environmental contamination. Although some questions about the environmental fate have been investigated including sorption, transport, and biotic degradation pathways, our understanding still remains limited, particularly with questions of photochemical fate and toxicological impacts. We used solid-phase extracted material of water-soluble organic compounds in three shale gas flowback fluids and produced water mixtures to investigate a) acute and chronic toxicity to *Daphnia magna* and *Ceriodaphnia dubia* species, respectively, and b) the photochemical fate of organic compounds during 20 hr solar-simulated irradiation experiments. Absorbance and fluorescence spectroscopy and ultrahigh resolution mass spectrometry were used to investigate changes in the optical properties of the fluids and their detailed chemical composition, respectively. Preliminary acute toxicity tests on *D. magna* revealed no significant differences in survival between the controls and redissolved shale gas wastewater organic extracts [6.25% to 100% of original pre-extraction concentration]. Solar-simulated irradiation experiments resulted in modest decreases in absorbance and fluorescence, with spectral shifts resembling natural organic

matter in all but the earliest flowback fluid. Solar-simulated irradiation resulted in an increase in compounds with higher oxygen content, and a decrease in chlorinated compounds, potentially indicating photodehalogenation. Focusing on the fate of shale gas waste fluids with similar environmental mobility can help us to understand the fate of specific fractions as they enter the environment.

5.1 Introduction

Shale gas has become a dominant source of energy, accounting for nearly all new production in recent years (*U.S. EIA*, 2017b). With the implementation of hydraulic fracturing technologies in the Marcellus shale, gas production has increased over the last decade to nearly 20,000 million cubic feet per day (*U.S. EIA*, 2017b). Hydraulic fracturing requires large volumes of water to stimulate low permeability geological formations such as shale and release natural gas (Kondash and Vengosh, 2015; Nicot and Scanlon, 2012). Fluid volume varies based on the well characteristics including well depth and length, and can range from 1-25 million liters per hydraulic fracturing job (Kondash and Vengosh, 2015). After pressure is released, the injected fluids and connate fluids return to the surface alongside natural gas for the lifetime of the well (Kondash and Vengosh, 2015; Nicot and Scanlon, 2012). A Marcellus shale gas well requires 16 million liters of hydraulic fracturing fluids on average, with around 5 million liters of fluid returning to the surface (Kondash and Vengosh, 2015); much of the early flowback fluid is reused on the next hydraulic fracturing job (Jiang et al., 2014). These fluids contain a complex mixture of the chemicals originating from the shale formation, fluid additives, and *in situ* reactions (Hoelzer et al., 2016; Luek and Gonsior, 2017; Vengosh et al.,

2017). The injected and returning fluids can potentially impact the environment in a number of different ways (U.S. EPA, 2016; Vengosh et al., 2014; Vidic et al., 2013), including spills to surface waters and groundwaters (Cozzarelli et al., 2017; Gross et al., 2013; Rozell and Reaven, 2012).

Documented spills of hydraulic fracturing fluids, flowback fluids, and produced waters have been fairly evenly distributed across soil, groundwater, and surface water (U.S. EPA, 2016). However, the high variability and complexity of the injected fluids makes tracking these fluids in the environment challenging and subject to debate (U.S. EPA, 2016). Biological, chemical, and physical transformations will control the fate and toxicity of these fluids as they move through the environment during a spill (Cluff et al., 2014; Cozzarelli et al., 2017; Kahrilas et al., 2016; Murali Mohan et al., 2013a; Strong et al., 2013).

Although a number of individual chemicals identified in additives and connate fluids are known to be of environmental and human health concern based on their toxicity, frequency of use and potential for aquatic transport (Abdullah et al., 2017; Yost et al., 2016), studies on the toxicity of actual injected fluids or fluids returned to the surface have been limited to date. Acute toxicity was observed in zebrafish embryos exposed to flowback waters, as well as induction of the cytochrome P450 1A pathway for aryl hydrocarbons in both zebrafish embryos and juvenile rainbow trout (He et al., 2017a, 2017b), indicative of exposure. During a spill of oil and gas wastewater in Blacktail Creek, North Dakota, detailed investigations of both inorganic and organic chemicals revealed the complexity of their fate, particularly the roles of sorption and volatilization of organic compounds (Cozzarelli et al., 2017). Although sediment may sorb additives

and many potentially toxic compounds (e.g., PAHs), growth and survival toxicity testing performed on amphipods using field-collected sediments (Blacktail Creek) were not significantly different than control sites (Cozzarelli et al., 2017). Six months after the Blacktail Creek spill, significant larval fathead minnow toxicity (97.5% mortality) was observed 7.2 km downstream and attributed to high ammonium (Cozzarelli et al., 2017).

Photochemical degradation may play a key role in the fate of spilled hydraulic fracturing fluids and wastewaters, through both direct and indirect degradation pathways (Schwarzenbach et al., 2003). Although produced waters have been shown to absorb and fluoresce (Dahm et al., 2013; Freedman et al., 2017), the photochemical fate of hydraulic fracturing fluids and wastewaters has not been previously investigated. Oil has been shown repeatedly to degrade under solar irradiation, forming products with high oxygen content, increased aqueous solubility, and increased toxicity (King et al., 2014; Radović et al., 2014; Ray et al., 2014). Many hydraulic fracturing fluid additives may not necessarily be directly photodegraded by sunlight, but the presence of natural organic matter such as humic substances may allow for indirect photodegradation via reactive oxygen species (Cooper et al., 1988; Schwarzenbach et al., 2003). Additionally, understanding the role of photoirradiation is important for developing treatment systems, particularly those relying on light energy (Lester et al., 2015).

Organic compounds present in hydraulic fracturing fluids and wastewaters have been investigated using a variety of extraction techniques and analytical methods (Ferrer and Thurman, 2015a). Analyses of targeted fractions of organic components may be particularly useful when parsing out the environmental behavior and sources of toxicity in these fluids (Rosenblum et al., 2017b). The volatile organic fraction has been the most

consistently sampled (Hoelzer et al., 2016; Luek and Gonsior, 2017; Orem et al., 2014), while the non-volatile and water soluble component needs more analytical development (Ferrer and Thurman, 2015b; Thurman et al., 2014). Without understanding the toxicity of these fluids and the impact of solar irradiation on the stability of organic compounds in shale gas wastewaters, important pathways explaining the environmental fate of these fluids may be missed.

This study therefore focused on the solid phase extractable nonpolar to mesophilic organic compounds in shale gas wastewaters and their environmental behavior. Solar-simulated irradiation experiments were performed to track how solid-phase extracted organic compounds in shale gas wastewaters are impacted by sunlight. Fluorescence spectroscopy and ultrahigh resolution mass spectrometry were used to describe changes over 20 hr irradiation experiments. Acute and chronic standard EPA whole effluent toxicity tests of the solid phase extracted organic compounds were also performed on *D. magna* and *C. dubia*.

5.2 Materials and Methods

5.2.1 Sample collection and extraction

Shale gas wastewaters were collected from two adjacent wells in Monongalia County, WV [US] at multiple time points during the first nine months of well operation. Fluid samples were stored cold and then shipped on ice within one week of collection. Upon receipt, 200 mL samples were filtered using 0.7 μm GFF filters and extracted using Bond Elut PPL solid phase extraction cartridges as described previously (Luek et al., 2017). Loaded cartridges were dried under N_2 gas and eluted with methanol to obtain the

non-volatile mesophilic to nonpolar organic fraction. Experiments were performed after evaporating methanol solvent under ultrahigh purity N₂ gas, reconstituting the dried extract in water and sonicating the mixture for 5 minutes.

5.2.2 Dissolved organic carbon (DOC) analysis

DOC was measured on a Shimadzu TOC-V CSH as non-purgeable organic carbon using catalytic combustion and nondispersive infrared detection. Quantification was performed using hydrogen phthalate standards and percent recovery during extraction was calculated by dividing the DOC concentration of the re-dissolved sample by the DOC concentration of the original filtered sample. DOC recoveries ranged from 4% to 17%, clearly missing a large fraction of polar and volatile organic compounds, but exposure concentrations were approximately 5 mg L⁻¹ DOC.

5.2.3 Toxicology experiments

Acute and chronic exposure experiments were performed on *D. magna* and *C. dubia* (Table 5.1) using certified algal and YTC feedstocks [chronic only] and daphnids obtained from Aquatic BioSystems, Inc. Experiments were performed by modifying EPA whole effluent toxicity method guidelines for freshwater invertebrates (EPA Methods 2021 and 1002, (*US EPA*, 2002a, *US EPA*, 2002b)), using solid phase extracted shale gas wastewater as “effluent” to understand the toxicity as a spill is diluted in the environment. This method was selected because Marcellus shale gas wastewaters have high total dissolved solids (up to 250 g L⁻¹) (Kondash et al., 2017b), lethal to freshwater organisms. Sufficient dilution of total dissolved solids to remove acute toxicity from salt alone (<4 g L⁻¹) (Schuytema et al., 1997) would also substantially dilute the organic fraction of interest. Therefore, solid phase extracts of mesophilic to nonpolar dissolved

organic compounds were investigated to determine if this fraction alone was lethal. Differing groundwater transport rates of non-reactive constituents (e.g., chloride) and the more reactive organic constituents (e.g., halogenated organic compounds) (Burr et al., 1994; Mackay et al., 1986) could result in organisms being exposed to only some constituents at a given time following a spill, hence the interest in focusing on the organic constituent alone.

The original 200 mL shale gas wastewater samples were solid phase extracted and eluted in 10 mL methanol, then evaporated and reconstituted in 200 mL moderately hard synthetic water to return to the original pre-extraction volume (100% reconstituted “effluent”). Treatments for all tests included a 100% reconstituted “effluent”, 50%, 25%, 12.5%, and 6.25% dilutions, a negative control (0%), and a potassium chloride positive control series. Four replicates of 5 daphnids in 25mL fluid were used for each acute test treatment and ten replicates of one adult daphnid in 15mL fluid were used for each chronic test treatment. Standard water quality measurements (temperature, dissolved oxygen, pH, conductivity) were performed on each treatment fluid prior to the experiment and daily with static renewal during the chronic test (Table A4.1-4.5). Free chlorine in the negative controls and reconstituted “effluent” was less than or equal to the method detection limit in all samples (0.02 mg L^{-1}). Data analysis was performed using an excel spreadsheet managed by the EPA Office of Wastewater Management based on EPA Methods 2021 and 1002.

Table 5.1 Toxicity tests performed on daphnid species.

Toxicity Test	Species	Well ID	Fluid Age (d)
Acute (48 hr)	<i>Daphnia magna</i>	3H+5H	1-4
Acute (48 hr)	<i>Daphnia magna</i>	3H+5H	115-120
Chronic (8 d)	<i>Ceriodaphnia dubia</i>	3H+5H	1-9

5.2.4 Photoirradiation experiments

Six 20 hr photoirradiation experiments were performed using solid phase extracts reconstituted in MilliQ water (Table 5.2). Reconstituted samples were loaded in to a solar simulator irradiation system with semi-continuous flowthrough absorbance and fluorescence excitation emission matrix measurements (Timko et al., 2015a). The solar simulator irradiation system has been described previously in detail (Timko et al., 2015a) It consists of a 1,000 W Xe arc lamp with a 1.5 air mass filter (AM 1.5) to match the direct and diffuse solar spectrum at the Earth surface at a zenith angle of 48.2 °, and an intensity of 850 W m⁻². The irradiation cell consists of a custom-built circular flow cell, 2mm wide by 1mm deep, with a surface area of 101 cm², and is temperature controlled at 25 °C. This system is directly connected to an Aqualog spectrofluorometer (Horiba Jobin Yvon Instruments) and sample fluid continuously circulates between the irradiation flowcell and the spectrofluorometer. Actinometry measurements (*p*-nitroanisole/pyridine) indicated that the light intensity measured at the irradiation cell is approximately 76% of the measured irradiation (850 W m²), equivalent to the fraction of fluid in the flowcell versus the tubing and spectrophotometer at any given time (Timko et al., 2015a).

Absorbance and fluorescence measurements were performed every 20 minutes over

excitation/absorbance and emission wavelengths of 600 – 230 nm in 3 nm steps, and emission wavelengths of 211 - 617 in 3.27 nm increments using an integration time of 0.4 s. Corrections for Rayleigh scattering, Raman scattering, and inner filter effects were performed using the Aqualog software and converted to quinine sulfate units (QSU) using a 1 ppm quinine sulfate standard (Starna). Additionally, baseline drift in the absorbance spectra was corrected by subtracting the recorded absorbance at 600nm from the absorbance spectra (Timko et al., 2015a). Additional data processing was performed in Matlab ®. Photoirradiation fluorescent spectra were analyzed statistically with parallel factor analysis (PARAFAC) using the N-way toolbox (Murphy et al., 2013; Stedmon and Bro, 2008). A four-component model was selected to adequately explain the data and was split-half validated following previously described guidelines (Murphy et al., 2013).

Table 5.2. Photoirradiation experiments sample information, DOC concentrations, and absorbance changes. E2/E3 ratio and slope ratio (SR) as per Helms et al., 2008 and Peuravuori and Pihlaja, 1997. *Error in absorbance measurements, excluded from absorbance/fluorescence analyses.

Well ID	Fluid Age (d)	DOC Recovery	Reconstituted DOC (mg L ⁻¹)	% loss in a ₂₅₄	% loss in a ₃₀₀	E2/E3 T ₀	E2/E3 T ₂₀	SR T ₀	SR T ₂₀
3H	3	4%	9.3	9%	20%	14.2	22.3	0.95	1.03
3H	66	4%	3.5	4%	19%	13.8	23.7	0.83	0.87
3H*	276	12%	11	NA	NA	NA	NA	NA	NA
5H	4	5%	9.9	6%	17%	20.1	26	0.73	1.15
5H	61	9%	5.8	8%	18%	17	26	1.1	1.02
5H	271	17%	10.2	4%	11%	28	31.5	0.95	1.26

5.2.6 Mass spectrometry

Reconstituted solid-phase extracts from before and after the photoirradiation experiments were extracted using small volume (200 mg/2mL elution) Bond Elut PPL cartridges. Methanolic extracts were directly analyzed using a Thermo Solarix 12 Tesla Fourier Transform Ion Cyclotron Resonance Mass Spectrometer (FT-ICR-MS) with electrospray ionization in negative mode located at the Helmholtz Center for Environmental Health in Munich, Germany as described previously (Luek et al., 2017). Briefly, individual sample spectra were calibrated using arginine clusters and again post-calibrated using known m/z ions to obtain a mass accuracy of less than 0.2 ppm and ions identified in a field blank were subtracted from the spectra. Formulas were assigned using in-house software (maximum $C_{100}H_{\infty}O_{80}N_3S_2Cl_3Br_3I_3$) to ions between m/z 125 and 600 and invalid formulas were removed by eliminating formula assignments with an oxygen to carbon ratio greater than 1 and/or a negative double bond equivalency. Halogenated formula assignments were investigated using isotopic pattern matching (Luek et al., 2017).

5.3 Results and Discussion

5.3.1 Daphnid toxicity tests

Survival of *D. magna* over a 48-hour exposure period revealed no differences in survival as a function of fracturing fluid exposure/concentration (Figure 5.1) tested using the Dunnett test (log transformed data). The lowest observed effect concentration (LOEC) and the 50% lethal concentration (LC50) were both greater than the highest concentration, >100% of effluent. Survival fractions ranged from 0.85 to 1.0 for negative

controls and all treatments during both acute tests. During the 8-day chronic exposure of *C. dubia* to the 1-week old flowback fluid, the number of young per treatment was determined and not significantly different between control and treatments based on the Dunnet test (IC25 >100% of effluent). However, the minimum number of control young (15 per adult) was not met, so results are inconclusive. Complete results for acute and chronic tests are reported in Tables A4.6-4.8.

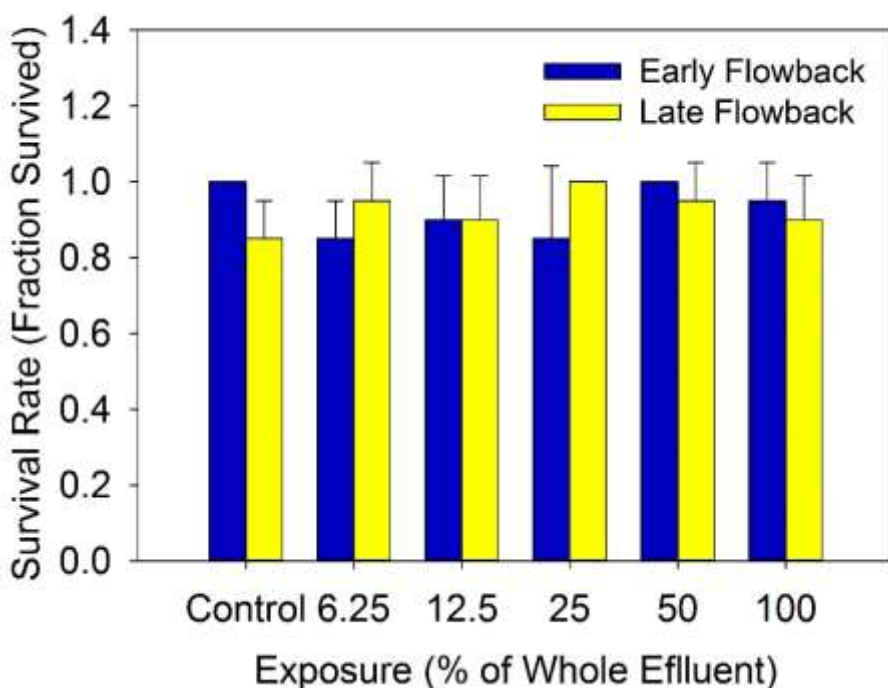


Figure 5.1 Acute toxicity test survival rate (fraction survived per replicate) of *D. magna* over 48 hours when exposed to two different flowback fluids. 4 replicates per concentration, n=5 per replicate.

Field or laboratory testing of shale gas wastewater toxicity has not been performed on daphnid species. Toxicity tests performed with flowback fluids (high salinity) on zebrafish embryos as well as juvenile rainbow trout revealed substantial toxicity, with embryo LC50 values more than a 25 fold dilution (of initial 243,000 mg/L TDS) (He et al., 2017a, 2017b). Interestingly, removal of organic compounds (and likely

heavy metals) using activated carbon resulted in lower toxicity than the untreated fraction in the earliest exposed embryos, suggesting PAHs and other sorbed organic compounds contribute to toxicity (He et al., 2017a). Pathways for juvenile rainbow trout toxicity included induction of the aryl hydrocarbon receptor and endocrine disruption activity (He et al., 2017b). Following the Blacktail Creek produced water spill, increased endocrine disruption activity was observed although specific tests on fathead minnows and amphipods did not identify toxicity related to organic compounds (Cozzarelli et al., 2017).

Although solid phase extraction of organic compounds has been used successfully to extract PAHs in hydraulic fracturing fluids with reversed phase cartridges (C18) (Regnery et al., 2016), it is unlikely that the methanol elution solvent is as efficient as the hexane/acetone mixture used during the C18 extraction method. Compared to these prior whole fluid/high salinity exposure experiments, the daphnid toxicity tests only looked at a small fraction (4-17% of DOC) of the possible toxicants present in hydraulic fracturing fluid, having eliminated inorganic, polar, and volatile chemicals. The observed lack of toxicity to daphnids could be attributed to a) insufficient concentrations of toxic compounds such as PAHs in the raw fluid b) sorption to particles, poor extraction efficiency, or volatilization of toxic compounds such as PAHs during drying or c) differences in species. Analysis of the remaining organic fraction (83-96% of DOC) toxicity, separate from salinity and metals, would provide further insight in to the possible sources and fate of toxic organic compounds present in these fluids. Separation techniques including membrane options should be tested to improve extraction of the highly polar organic fraction without the brine matrix.

5.3.2 Decrease in absorbance and spectral slopes during photoirradiation

Absorbance increased at the lowest UV wavelengths (230-240nm), but decreased at higher wavelengths (Figure 5.2). At wavelengths above 450nm, no changes were observed. The largest increases at these low wavelengths were observed in the oldest wastewater sample, 5H-271d (Figures A4.1, A4.2). After 20 hours of irradiation, absorbance at 254nm and 300nm decreased in all samples (Table 5.1), decreasing more at 300nm (11-20%) than at 254nm (4-9%). Ratios in absorbance at different wavelengths can indicate changes in molecular weight in natural aquatic systems, and were calculated as E2/E3 ratios (a_{254}/a_{365}) and as spectral slope ratios ($SR, S_{270-295}/S_{350-400}$) (Helms et al., 2008; Peuravuori and Pihlaja, 1997). E2/E3 ratios and slope ratios increased during photoirradiation, and although these experiments include potential additives in addition to natural DOM, these shifts in absorbance support a decrease in molecular weight, as expected when photoirradiation acts to break chemical bonds (Helms et al., 2014; Timko et al., 2015a, 2015b).

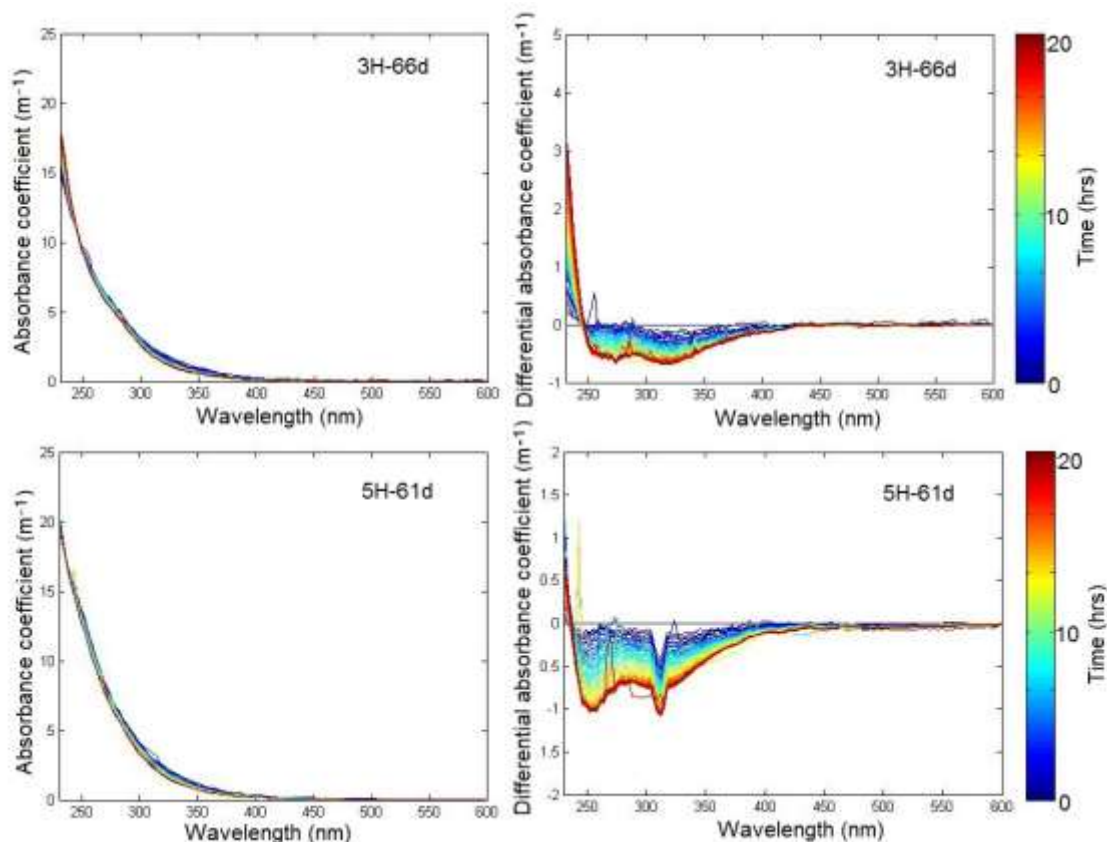


Figure 5.2 Change in absorbance of two month old shale gas wastewaters from 3H and 5H wells. Individual lines represent spectral scans taken every 20 minutes.

5.3.3 Dominant fluorescence changes during photoirradiation mimic NOM behavior

20hr photoirradiation experiments caused decreases in fluorescence in similar regions for all samples, regardless of fluid age. A maximum loss of 25% occurred in the low UV area (ex<300nm, em300-500nm) (Figure 5.3a-c). Fluorescence signal degradation occurred at three dominant regions, with maximum fluorescence changes at longer emission wavelengths (ex250/em400-475; ex300-350/em400-450), as well as at shorter emission wavelengths (ex250-300, em325-375) consistent with protein-like fluorescence (Coble, 1996). Similar degradation losses have also been observed in photoirradiation of open ocean waters and Suwannee River Fulvic Acids (SRFA) (Timko et al., 2015a, 2015b). The magnitude of fluorescence loss observed in this study was

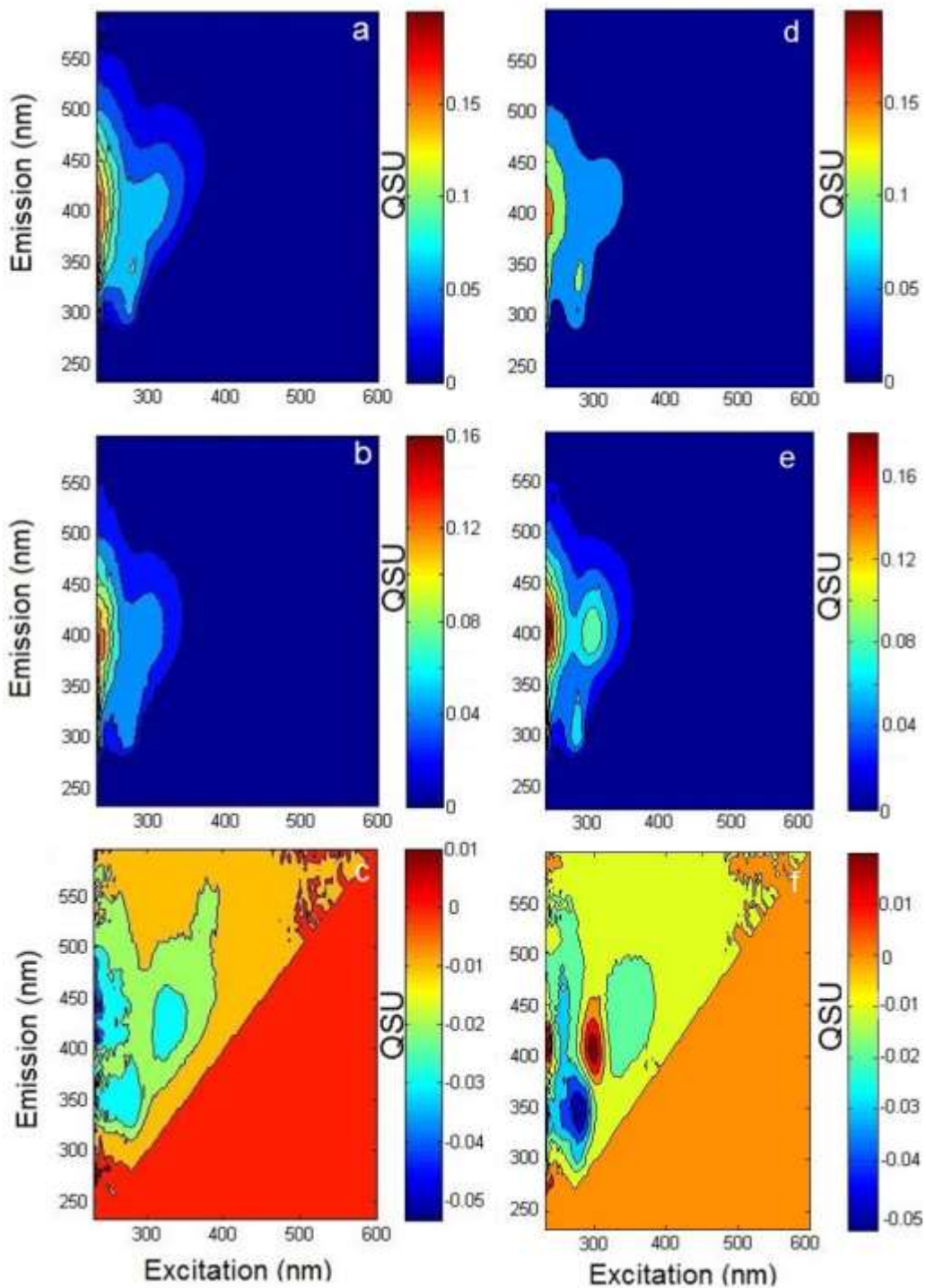


Figure 5.3 Fluorescence EEM of 5H-271d (a-c) and 3H-3d (d-f) before 20hr photoirradiation (a,d), after photoirradiation (b,e) and differential (c,f).

similar to that observed in SRFA over a 20 hr photoirradiation (pH 4). Although fluorescence may have many sources in these complex samples, these data suggest that

the extracted and reconstituted solid-phase extracted material likely obtain their dominant fluorescence signals from natural organic matter compounds rather than specific additives. The earliest flowback sample, however, diverged from this, increasing in two regions (ex300/em375-450 and ex<250/em400-450) during irradiation (Figure 5.3d-f). Early flowback would contain the highest fraction of chemical additives, likely resulting in the observed divergence from changes consistent with NOM.

The only published shale gas wastewater fluorescence data analyzed Piceance basin late production filtered water (rather than an organic extract of produced water), and was dominated by peaks associated with fluorescent hydrocarbons and protein-like fluorescence (Freedman et al., 2017). Comparatively, light fluorescent hydrocarbons were likely removed during the sample extraction and drying processes used in this study, reducing this potential signal. During treatment using biologically active filtration of Piceance produced water, both signals decreased substantially (Freedman et al., 2017). Bacterial communities are active in hydraulic fracturing waste fluids (Cluff et al., 2014; Mouser et al., 2016; Murali Mohan et al., 2013a), and fluorescence markers (e.g., fluorescent amino acids) suggest fluorescence peaks in this low UV region could be attributed to bacterial activity. The dominant fluorescence spectra observed in most samples likely originates from injected fluid source water and Marcellus shale NOM, efficiently extracted during solid phase extraction. The most likely chemical additive source of fluorescence, hydrotreated light petroleum distillates (containing naphthenes, alkylbenzenes, etc.), made up 25% of the friction reducer used in both wells. The unique fluorescence and degradation spectra during irradiation of the early 3H well flowback water (3H-3d) could be related to the petroleum distillates used, but it is unclear why

evidence of fluorescent additives were not seen in the 5H well early flowback (5H-4d) as petroleum distillates were both used in presumably similar amounts.

A four-component PARAFAC model was applied to the data to obtain a quantitative statistical measure of fluorescence during photoirradiation (Figure 5.4). Three and five component PARAFAC models were also built but could not be validated. The obtained components resemble DOM spectra, consistent with “humic-like” materials (FMax1, 2, 4) and bacterial activity (Fmax3) (Fellman et al., 2010), although many other compounds may fluoresce in these regions, including oil and degraded oil (Zhou et al., 2013).

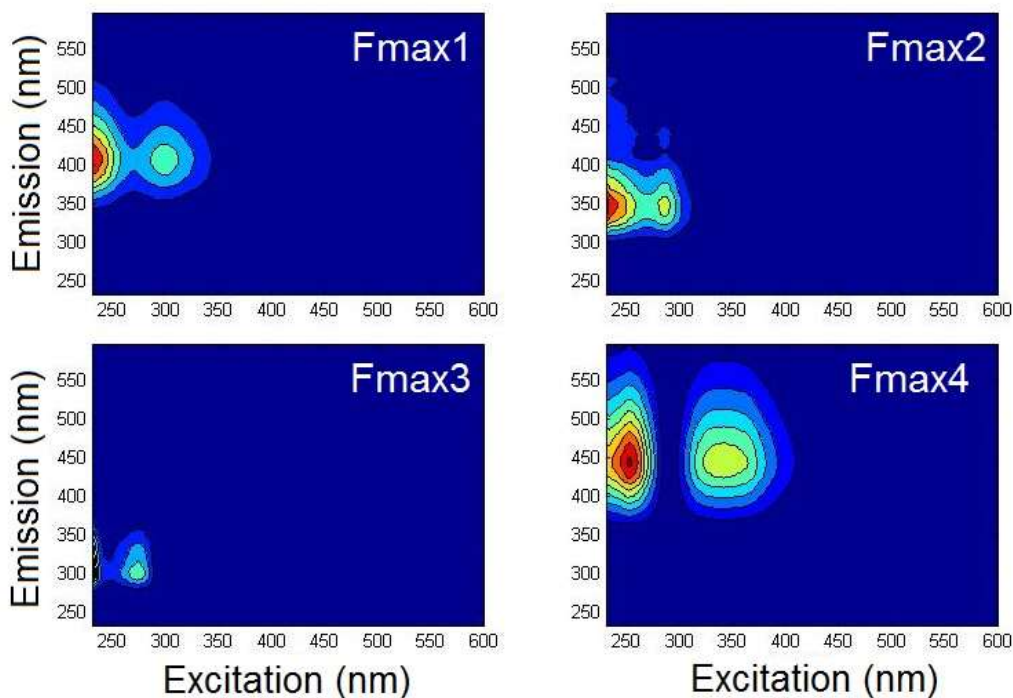


Figure 5.4 PARAFAC component EEM fingerprints of all photoirradiation experiments modeled together.

All fluorescent PARAFAC components decreased or remained stable during photoirradiation, except for Fmax1 in the 3H-3d fluid sample (Figure 5.5). Again, this highlights the probable influence of additives on early flowback fluid fluorescence.

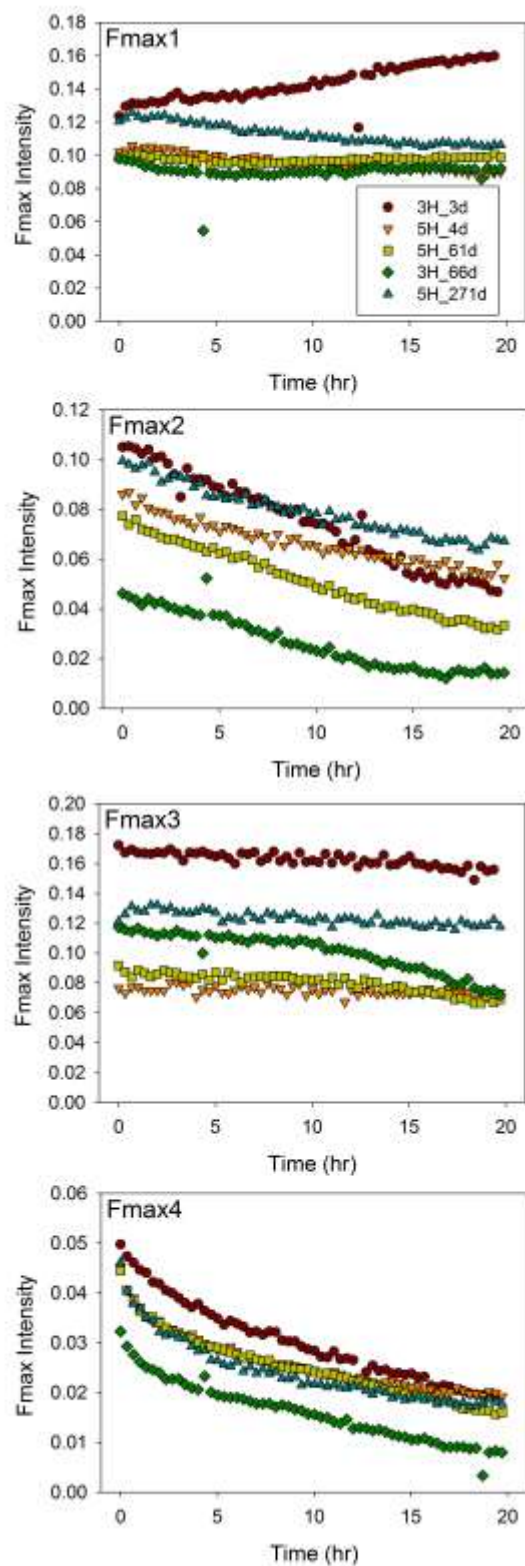


Figure 5.5 Changes in PARAFAC component intensities over 20hr photoirradiation for five photoirradiation experiments.

Interestingly, although the 5H-4d fluid sample was of similar age, 5H-4d Fmax1 behaved more similarly to all other samples than 3H-3d. This disparity may reflect the slightly different fracturing fluid additives used in the two wells. Fmax2 and Fmax4 each consistently decreased during photoirradiation, while Fmax3 remained relatively stable or decreased only slightly (3H-66d). Because there was some variability in the slope shape of individual Fmax values, a linear regression was applied to determine changes in all fluorescent components to allow for comparison across experiments (Table A4.9). Fmax2 was fit using a single exponential decay model (Eq. 1) and Fmax4 curves were better fit using a double exponential decay function (Table A4.10, Figure A4.3), as described previously for DOM degradation (Eq. 2),

$$\text{Equation 1} \quad F_t = F_1 e^{-k_1 t} + F_2$$

$$\text{Equation 2} \quad F_t = F_1 e^{-k_1 t} + F_2 e^{-k_2 t} + F_3$$

where fluorescence (F) at time t is equal to the combined degradation rates of k_1 , k_2 , and k_3 , which may represent photo labile, photo semi-labile, and photo refractory organic matter fractions (Timko et al., 2015a).

For Fmax2 and Fmax4, the components that consistently decreased in all samples, the largest decreases and therefore fastest rates were observed in 3H-3d. 5H Fmax4 fluorescence behaved similarly at all fluid ages, although 3H_66d was dominated by k_2 rather than k_1 (Table A4.10). This suggested that 3H_66d did not contain as much highly photo labile fluorescent material (k_1) in the Fmax4 region and therefore behaved more as semi-photolabile material (k_2). Fmax3 remained constant in most samples but decreased rapidly after 10 h photoirradiation in 3H-66d. Although inorganics and additional DOM are removed during extraction which can influence degradation pathways and rates, these

data show the variability in fluorescence behavior during photoirradiation of hydraulic fracturing wastewaters, highlighting the DOM variability across fluid ages and their resulting optical properties.

5.3.4 Photoirradiation results in increased molecular oxygen content

Only a small fraction of molecular ions consistently overlapped across all fluid samples. Although m/z ion intensities do not represent true changes in concentration, ions with consistent behavior can be identified and used to help understand how these fluids may be changing (Chen et al., 2016; Herzsprung et al., 2012; Kellerman et al., 2014; Sleighter et al., 2014b). A subset of ions found to be substantially and consistently increasing ($n=60$) or decreasing ($n=107$) during photoirradiation experiments were identified as those ions changing by greater than 50% in at least one experiment and changing in the same direction in any other samples containing the same ions. Molecular formulas assigned to these ions can be summarized using their saturation (H/C), oxidation (O/C), and size (m/z) using Van Krevelen diagrams (van Krevelen, 1950) (Figure 5.6, Tables A4.11, A4.12).

A one-sided Student's t -test ($\alpha=0.05$) was applied to CHO/N/S ions in increasing versus decreasing ion groups to determine if the oxygen to carbon ratios and double bond equivalents were significantly different, as has been observed during the solar irradiation of oils (Ray et al., 2014; Vaughan et al., 2016). Indeed, increasing ions had significantly higher oxygen to carbon ratios than ions decreasing during photoirradiation ($p=0.015$). An increase in oxygen to carbon ratio suggests that photoirradiation resulted in increased oxygenation via hydroxylation and/or carboxylation. A decrease in solution pH was also

observed during the 20 hour photoirradiation, supporting the formation of more acidic moieties.

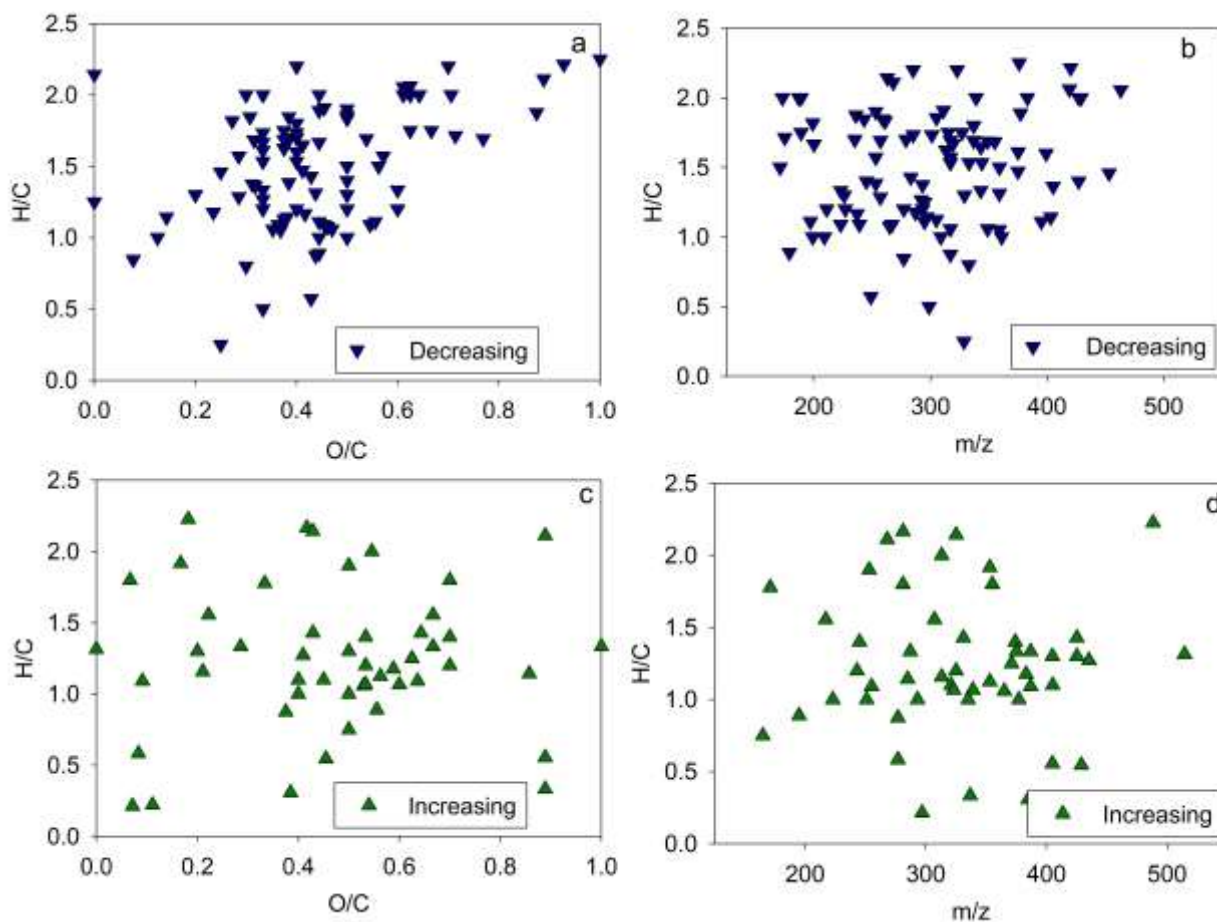


Figure 5.6 Assigned molecular formulas identified to be decreasing (a,b) or increasing (c,d) in intensity by >50% after 20hr photoirradiation shown as their oxygen to carbon ratio versus hydrogen to carbon ratio (a,c) and mass to charge ratio (m/z) versus hydrogen to carbon ratios (b,d). Formulas with inconsistent directional behavior across experiments were excluded.

Hydrogen to carbon ratios were also significantly lower for the increasing ions than the decreasing ions (1.32[inc] vs 1.49[dec], $p=0.010$), with a corresponding significant change in double bond equivalent (5.94[inc] vs 4.66[dec], $p=0.011$). This is consistent with previous research demonstrating an increase in the number of condensed aromatic compounds identified following the photoirradiation of natural organic matter

(Chen et al., 2014). These results could be interpreted as an increase in the number of condensed aromatics, but this is unlikely as photoirradiation applies energy to break bonds and no viable pathway is known to photochemically form condensed aromatic compounds. A more likely explanation is that these results indicate the addition of carboxyl and hydroxyl groups to highly condensed molecules, pulling existing highly condensed aromatic molecules into the analytical window due to much enhanced ionization efficiency. This explanation is reasonable because condensed aromatic compounds are highly susceptible to reactive oxygen species (Miller and Olejnik, 2001).

A handful of halogenated ions were identified in the ion groups consistently increasing or decreasing in intensity. All organohalogen ions were compared to their predicted stable isotopic patterns to provide additional support for their identification. Chlorinated, brominated, and iodinated formulas were assigned, but only the chlorinated ions and one iodinated ion were supported with their secondary stable isotopes. Nine chlorinated ions were identified as decreasing, while only one chlorinated ion increased. Although three of the four iodinated ions found to be increasing had insufficient intensity to be confirmed using their ^{13}C isotopic peak, all had been identified and isotopically confirmed previously (*see Chapter 4*). The iodide ion (m/z 126.9045) was identified in all samples and increased during all photoirradiation experiments, one of only three ions to behave as such.

The observed changes in halogenated ions during photoirradiation are therefore somewhat conflicting, as increasing iodide intensity and decreasing chlorinated ion intensity suggest photodehalogenation, but the increase in iodinated organic compounds does not support photodehalogenation. Photohalogenation of phenols, salicylic acid, and

dissolved organic matter has been observed in seawaters and brackish waters, likely through the photo-induced formation of reactive halogenated species (Calza et al., 2008; Hao et al., 2017; Tamtam and Chiron, 2012). A larger scale photoirradiation system using larger volumes/higher concentrations of fracturing fluids and specific targeted analyses are needed to address the dynamics of photodehalogenation or potentially photohalogenation in these shale gas fluids.

5.4 Conclusions

Hydraulic fracturing fluid wastewaters are highly complex, and deconvoluting this mixture and potential divergent fates requires investigating various fractions of these fluids. This study targeted dissolved mesophilic to nonpolar organic compounds found in a Marcellus shale gas flowback and produced waters to understand the photochemical fate and toxicity of this specific fraction. Fluorescent material was found in this fraction, and was substantially degraded during solar irradiation. The observed fluorescence spectra and its behavior during solar irradiation indicated that this fraction resembled natural organic matter in most samples, excluding one early flowback sample. Solar irradiation may directly degrade chemical of concern in these fluids, with dehalogenation of particular interest, and indirect photodegradation through reactions with DOM material (Cooper et al., 1988) may also result in further degradation. No acute or chronic effects were observed on daphnid species in the low volatility mesophilic to nonpolar organic fraction, representing 4-17% of DOC. Due to the complexities of hydraulic fracturing fluids, investigating subsets of these fluids with similar environmental mobility can

further our understanding of the fate of these fluids and can be useful in targeting remediation efforts following a spill.

Chapter 6

Organic matter fingerprinting techniques for identification of stream contamination
arising from hydraulic fracturing activities

Luek, J.L., Heyes, A., Harir, M., Schmitt-Kopplin, M., Gonsior, M.

Contributions: Contribution: Experimental design [except stream sampling sites/frequency], all sample analysis, data analysis and interpretation, and all text and figures.

Abstract

Drilling and hydraulic fracturing of unconventional oil and gas resources involves the use, transport, and disposal of large volumes of fracturing fluids and wastewaters. During any of these processes, fluids may accidentally be released and enter surface waters and groundwater. Stream water samples were collected from 19 streams in Garrett County, Maryland (US) over four years, a region where no hydraulic fracturing is occurring, and analyzed for dissolved organic matter (DOM) using ultrahigh resolution electrospray ionization Fourier transform ion cyclotron resonance mass spectrometry (FT-ICR-MS) and excitation emission matrix (EEM) fluorescence spectroscopy. Stream water DOM data were then compared to thirty-eight hydraulic fracturing fluid and wastewater samples to identify molecular ions and fluorescence signals absent from natural waters but present in hydraulic fracturing wastewaters to determine possible organic chemical tracers of contamination plumes. Hydraulic fracturing wastewater fluorescence fingerprints were not unique from stream water DOM, suggesting EEM fluorescence is not a good tracer of hydraulic fracturing contamination in streams. However, a number of exact m/z ions and unambiguously assigned molecular formulas were identified in hydraulic fracturing fluids and wastewaters but absent from stream

water samples, indicating these compounds may be suitable tracers. Non-targeted mass spectrometry techniques provide a powerful approach to determine if a stream has been contaminated from hydraulic fracturing activities.

6.1 Introduction

Hydraulic fracturing requires the use, transport, and disposal of large volumes of hydraulic fracturing fluids. Large volumes of water, ranging from 1.3×10^6 L (Niobrara shale formation) and 23.8×10^6 L (Woodford shale formation) are mixed with additives on site prior to injection, and large volumes of flowback and produced waters return to the surface following hydraulic fracturing (Kondash and Vengosh, 2015; Kondash et al., 2017a; Nicot and Scanlon, 2012; Rahm et al., 2013). Flowback and produced waters are also stored onsite for recycling and reused as injection fluids (Shaffer et al., 2013). Due to limited options for the reuse of formation-derived high salinity samples, these wastewaters are frequently transported long distances for centralized waste treatment or deep well injection disposal (Gilmore et al., 2014; Gregory et al., 2011; Kondash et al., 2017a; Rahm et al., 2013).

Risk assessments indicate that human error is the primary cause of environmental contamination events from hydraulic fracturing activities, and occurs most frequently during transit or storage (Patterson et al., 2017; Soeder et al., 2014). Frequently used tracers such as chloride, bromide, methane and its isotopes and trace metals have a diversity of natural sources and the absence of baseline data has resulted in challenging data interpretation and criticism. A number of previous studies have used different tracers to support their argument that surface and groundwaters have been contaminated from

hydraulic fracturing activities (Darrah et al., 2014; DiGiulio and Jackson, 2016a; Drollette et al., 2015; Hildenbrand et al., 2016; S. G. Osborn et al., 2011; Warner et al., 2012b). However, these studies have been frequently challenged, with common critiques including a) the inability to prove that the identified tracers were absent prior to the advent of drilling and b) heterogeneity of tracer data (Connor et al., 2016; McHugh et al., 2016, 2014; Saba and Orzechowski, 2011; Schon, 2011). Better inorganic tracers are also being developed, such as the ratio of lithium and boron isotopes (Cozzarelli et al., 2017; Warner et al., 2014). Additionally, inorganic and organic chemical tracers are transported at rates in the subsurface (Allen-King et al., 2002; Brusseau, 1994; Burr et al., 1994; Mackay et al., 1986), so organic chemical tracers are needed understanding the full contamination plume after the non-reactive tracer pulse (e.g., chloride) has moved through the sampling site. Our collective inability to constantly monitor groundwater and surface waters for all possible chemical tracers nationwide creates a challenge for understanding when and where hydraulic fracturing contaminants enter the aquatic environment. FT-ICR-MS can be used to identify unique organic chemical tracer ions that can be further developed with targeted techniques.

Hydraulic fracturing chemical additives are mixed with freshwater or recycled waters on site, and the mixed fracturing fluids are highly chemically diverse, exhibiting a range of chemical properties and toxicities (fracfocus.org; Stringfellow et al., 2014; Yost et al., 2016). Chemical additives used in hydraulic fracturing fluids are frequently company-specific and vary as a function of geological characteristics at the drilling site such as depth and temperature (fracfocus.org; Stringfellow et al., 2014). Quantitative methods for a limited number of known organic additives have been developed, but only

a few of these compounds have been detected in actual samples (Ferrer and Thurman, 2015b; Orem et al., 2014; Thacker et al., 2015). Additionally, many organic additives are members of complex homologous series for which obtaining standards for individual compounds is challenging (Thurman et al., 2014). Flowback fluids and produced waters are also variable in their composition and are poorly characterized, particularly the organic fraction (Luek and Gonsior, 2017). Due to the diverse and largely undescribed makeup of hydraulic fracturing wastewaters, ubiquitous and reliable organic chemical tracers of these fluids have yet to be developed.

Hence, the use of background monitoring is essential for understanding potential future environmental impacts. To this end, the Maryland Department of Natural Resources and colleagues underwent environmental monitoring of streams in Garrett County, MD, USA from 2013 – 2016, a region overlying the Marcellus shale but currently not being used for hydraulic fracturing, to collect baseline measurements prior to the possible advent of hydraulic fracturing in this region. A diversity of measurements including conductivity, anion and cation concentrations, trace metal concentrations, bulk methane and methane isotope concentrations, polycyclic aromatic hydrocarbon quantification, and mercury levels were performed (MD-DNR, 2017).

Solid-phase extraction of DOM paired with Fourier transform ion cyclotron resonance mass spectrometry (FT-ICR-MS) has been used to understand the diverse DOM composition of natural and engineered systems, and is particularly advantageous when complex systems are undergoing transformations that are not well understood *a priori* (Gonsior et al., 2014, 2011b, 2009; Herzsprung et al., 2010; Roullier-Gall et al., 2015; Shakeri Yekta et al., 2012). A non-targeted FT-ICR-MS approach was therefore

used to characterize these fluids and Western Maryland stream dissolved organic matter (DOM) in detail. By comparing the organic molecular ions identified in the FT-ICR-MS spectra from baseline stream water to those identified in hydraulic fracturing fluids and wastewaters, a discrete list of m/z ions unique to hydraulic fracturing fluids and wastewaters could be identified. A subset of these m/z ions, based on their abundance and frequency, were proposed as suitable tracers of hydraulic fracturing activities potentially contaminating stream waters. Fluorescence provides a highly sensitive yet rapid analysis of DOM, so fluorescent fingerprints were also investigated to see if fluorescent tracers could be developed.

6.2 Materials and Methods

Stream water samples were collected seasonally between April 2013 – May 2016 in Garrett County, MD, USA and hydraulic fracturing fluids and wastewaters from the Appalachian basin (Marcellus, Utica) were collected and solid phase extracted to desalt and concentrate DOM. Extracts were analyzed using FT-ICR-MS and excitation emission matrix (EEM) fluorescence spectroscopy. Stream water DOM data were then directly compared to hydraulic fracturing fluids and wastewaters to identify organic matter fingerprints specific to hydraulic fracturing fluids that may be useful in tracing hydraulic fracturing contaminants.

6.2.1 Sampling

Sampling sites in Garrett County, Maryland (US) were selected by Maryland Department of Natural Resources (MD-DNR) to represent a range of 1st-4th order streams draining multiple watersheds with varying land use (Figure 6.1, Table A5.1). No

hydraulic fracturing is occurring in Maryland, so sites represent background conditions in the Appalachian region. Six sites were collected seasonally and an additional 13 sites were collected annually under baseflow conditions. 1L clean glass containers were baked at 500 °C for 5 hrs and used to collect 1 L whole water samples that were processed within 24 hours. Fluorescence samples were immediately filtered using 0.2 µm Whatman PTFE type syringe filters, stored in clean 40 mL amber glass vials, refrigerated and analyzed within one week. Regional hydraulic fracturing flowback and produced water samples were obtained from two adjacent wells at the Marcellus Shale Energy and Environment Laboratory (Morgantown, WV [US]) (Carr, 2017) and from eleven additional locations in Pennsylvania, Ohio, and West Virginia (n=38) (Table A5.2). Hydraulic fracturing samples were extracted in smaller volumes (200 mL) due to expected high DOC content.

6.2.2 Solid Phase Extraction

Stream water and hydraulic fracturing fluid and wastewater samples were filtered using 0.7 µm Whatman GF/F filters and acidified to a pH of 2 using formic acid or hydrochloric acid. Acidified samples were then extracted over activated Bond Elut PPL cartridges (1 g, 6 mL, Agilent) using gravity at a rate of 5-10 mL min⁻¹ to extract nonpolar to mesophilic DOM (Dittmar et al., 2008). Cartridges were rinsed with dilute hydrochloric acid and formic acid to remove salts, dried under vacuum, and eluted with 10 mL of ultrapure methanol. Methanol extracts were stored at -20° C until analysis.

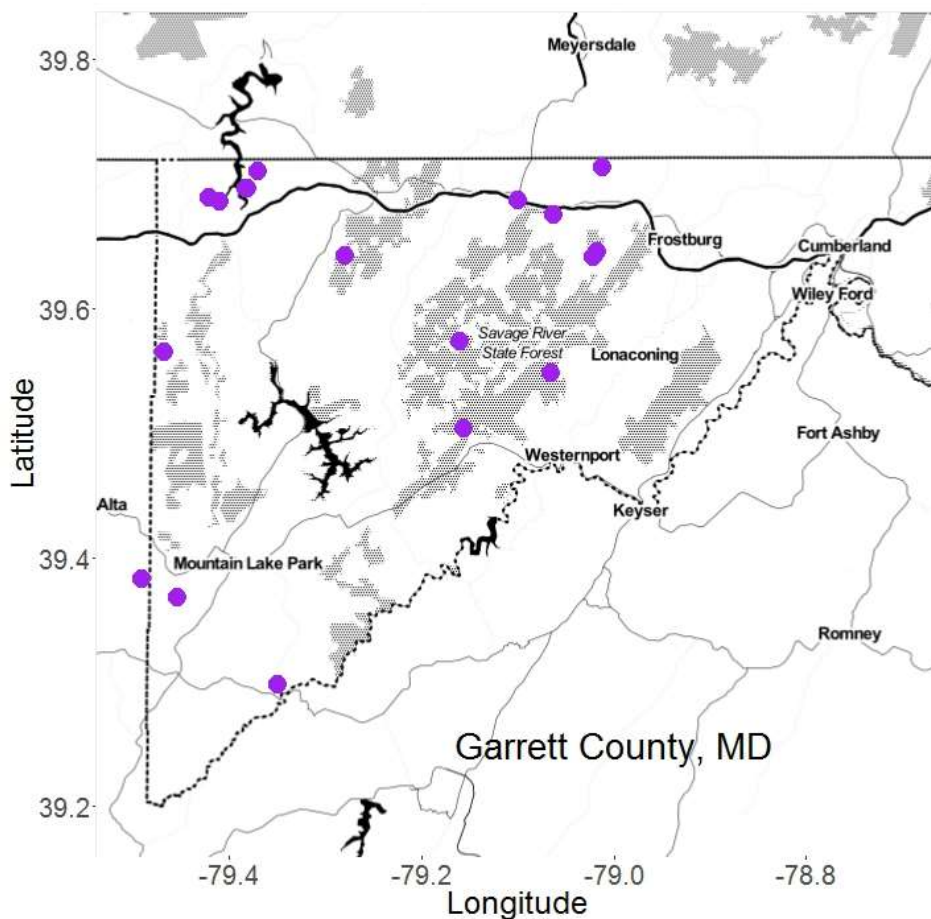


Figure 6.1. Garrett County, MD stream water sampling locations.

6.2.3 FT-ICR-MS Analysis

Methanolic extracts were diluted to optimize signal and analyzed using a 12 Tesla electrospray ionization FT-ICR-MS in negative ionization mode with a mass accuracy better than 0.2 ppm and a mass resolution of 400,000 at m/z 400 at the Helmholtz Center for Environmental Health in Munich, Germany. Calibration was first performed using arginine clusters and individual samples were then post-calibrated using known m/z ions. A signal to noise ratio of 1:7 was selected for the stream water samples using Bruker software after comparing multiple samples and attempting to minimize false signal selection. A more conservative ratio of 1:10 was used for the hydraulic fracturing

samples. Exact molecular formula assignments for precisely measured mass peaks were assigned based on established procedures described in numerous previous publications within a mass error window of 0.2 ppm (Gonsior et al., 2015, 2014; Koch et al., 2007). Molecular formula assignments were confirmed using isotopic pattern simulations using Bruker Daltonics software. Exact masses and formula assignments were also compared to a list of known surfactants compiled from the literature (Morales-Cid et al., 2009; Schymanski et al., 2014b) and a list of theoretical alcohol ethoxylate combinations based on industrial mixtures.

6.2.4 Identifying Non-Targeted Organic Chemical Tracers

A list of all m/z ions identified in four years of stream water baseline monitoring was compiled, and this list was used to determine if a given ion identified in fracturing fluid or wastewater was absent from the background stream waters. 28,306 individual m/z ions were identified in at least one of the 38 hydraulic fracturing fluid and wastewater samples and absent from all stream water samples. Two methods were used to produce a more concise list of m/z ions that may be suitable as organic chemical tracers. No tracer ions were present in more than 90% of samples, so frequently identified ions were selected as those m/z ions present in two-thirds of the 38 total hydraulic fracturing fluid and wastewater samples. Second, a set of highly abundant m/z ions (total ion count $>10^9$, $\sim 500\times$ above baseline) present in at least two samples were selected, and all selected ions were actually identified in 6 or more samples. Seventy-seven m/z ions were selected based on at least one of these two criteria, with several m/z ions both highly abundant and frequently identified. Forty-five of these m/z ions could then be assigned to unambiguous molecular formulas as discussed above. Each identified formula was then

confirmed using isotopic pattern matching in a hydraulic fracturing fluid or wastewater sample where it was present at high intensity. Higher molecular weight m/z ions were less frequently unambiguously assigned formulas due to the higher number of plausible atomic combinations and increased difficulty using the isotopic pattern matching than lower m/z ions due to their lower abundances.

6.2.5 Fluorescence Analysis

Methanolic sample extracts of both streamwaters and hydraulic fracturing fluids and wastewaters were dried under ultrahigh purity nitrogen gas and re-dissolved in ultrapure MilliQ water, removing ionic strength effects on fluorescence. Fluorescence spectra were collected using a Horiba Jobin Yvon Aqualog fluorescence spectrometer. Samples were measured over an excitation range of 230 – 600 nm at 3nm intervals and emission range of 210 – 617 nm at 3.27 nm intervals, corrected for inner filtering and Raleigh scattering, then normalized to a STARNA 1 ppm quinine sulfate standard using the Aqualog software. Parallel factor analysis (PARAFAC) modeling was applied to the stream water fluorescence dataset using the drEEM N-way toolbox in Matlab (Murphy et al., 2013; Stedmon et al., 2003).

6.3 Results and Discussion

6.3.1 Tracer ions contain high double bond equivalency

The identified tracer ions ranged from m/z 199-621, with more ions unambiguously assigned at lower masses than higher masses (Tables 6.1, 6.2). Three high abundance tracer ions had large negative mass defects, m/z 418.84133, 450.8674, and 542.80323, but could not be unambiguously assigned to a formula. Although the mass

assignments for these were ambiguous, large negative mass defects suggest the presence of one or more heavy atoms (e.g., iodine) under the assumption that all ions are singly charged. The remaining ions generally had highly positive mass defects relative to their mass, indicating a large number of hydrogen ions and saturated bonds. The mean hydrogen to carbon ratio (H/C) of all non-target tracer ions was 1.94, much higher than typically observed in stream water samples (Figure 6.2).

Of the forty-five unambiguously assigned molecular formulas, the majority contained carbon, hydrogen, and oxygen (CHO, n=17), or sulfur (CHOS, n=14) or chlorine heteroatoms (CHOCl, n=8). Indeed, double bond equivalents (DBE) calculated for these groups were consistently low, with an average DBE of 1.9 for CHO ions and 0.5 for CHOS ions. These are much lower than observed in stream water DOM and lower than what has been observed in riverine systems (Bae et al., 2011; Gonsior et al., 2016). For example, a stream water sample had an average DBE of 11.9 for CHO and 1.9 for CHOS compounds. The chlorine-containing tracers also had a low average DBE (1.75) and a high H/C ratio (2.0).

6.3.2 Organic tracers may be related to ethoxylated surfactants

The highly saturated CHO and CHOS tracer ions exhibit a range of oxygen to carbon ratios. The identified tracer compounds overlap substantially with known surfactants on a Van Krevelen diagram, particularly ethoxylates and glycols. Ethoxylated and propoxylated compounds are frequently used as hydraulic fracturing fluid additives (fracfocus.org), generally listed as mixtures rather than individual compounds. Alcohol ethoxylate mixtures were listed in all three FracFocus reports linked to fracturing fluid samples. Industrial mixtures of ethoxylates are generally complex mixtures, with

Table 6.1 Tracer ions unambiguously assigned molecular formulas and their molecular characteristics. DBE-double bond equivalent, COS- carbon oxidation state, KMD-Kendrick mass defect, KMD/z*-methyl spacing (CH₂) homologous series identifier (Shakeri Yekta et al., 2012), KMD_e/z_e*- ethoxylate spacing (C₂H₄O) homologous series identifier. n=38 samples.

Theoretical Exact Mass (<i>m/z</i>) of Assigned Formula	Error of Assigned Formula (ppm)	Tracer Selection	Isotopically Confirmed Neutral Formula	Number of Sample Detections	D B E	O/C	H/C	COS	KMD /z*	KMD _e /z _e *
235.07426	-0.127	frequency	C10H17O4Cl	31	3	0.40	1.70	-0.90	0.091	-0.0021
237.11661	-0.094	frequency	C10H22O4S	34	0	0.40	2.20	-1.40	0.010	-0.0007
241.05401	-0.166	frequency	C11H14O4S	28	5	0.36	1.27	-0.55	0.021	-0.0038
251.11363	-0.08	frequency	C10H20O7	31	1	0.70	2.00	-0.60	0.012	-0.0024
253.08483	-0.155	frequency	C10H19O5Cl	29	2	0.50	1.90	-0.90	0.016	-0.0059
259.1551	0.012	frequency	C13H24O5	30	2	0.38	1.85	-1.08	0.021	0.0019
261.13436	0.007	frequency	C12H22O6	37	2	0.50	1.83	-0.83	0.038	-0.0072
267.10048	-0.079	frequency	C11H21O5Cl	35	2	0.45	1.91	-1.00	0.016	-0.0013
273.06497	-0.024	frequency	C8H18O8S	28	0	1.00	2.25	-0.25	0.039	-0.0027
277.12928	0.002	frequency	C12H22O7	36	2	0.58	1.83	-0.67	0.087	-0.0010
279.02375	0.012	frequency	C10H17O4Br	28	3	0.40	1.70	-0.90	0.020	-0.0048
283.19148	0.024	frequency	C16H28O4	32	3	0.25	1.75	-1.25	0.012	0.0012
289.16566	0.053	frequency	C14H26O6	33	2	0.43	1.86	-1.00	0.038	0.0000
291.14493	0.063	frequency	C13H24O7	33	2	0.54	1.85	-0.77	0.087	-0.0014
293.12419	0.023	frequency	C12H22O8	28	2	0.67	1.83	-0.50	0.014	-0.0031
305.16058	0.006	frequency	C14H26O7	33	2	0.50	1.86	-0.86	0.087	-0.0072
313.13265	0.019	both	C12H26O7S	32	0	0.58	2.17	-1.00	0.026	-0.0012
319.17623	0.034	frequency	C15H28O7	32	2	0.47	1.87	-0.93	0.087	-0.0002
320.22312	-0.106	abundance	C19H31O3N	6	5	0.16	1.63	-1.32	0.128	0.0013
321.15549	0.012	frequency	C14H26O8	30	2	0.57	1.86	-0.71	0.014	-0.0010
331.11652	0.031	frequency	C12H25O8Cl	30	1	0.67	2.08	-0.75	0.062	-0.0037
331.21261	0.011	frequency	C17H32O6	27	2	0.35	1.88	-1.18	0.038	0.0011
339.11192	-0.037	frequency	C13H24O8S	27	2	0.62	1.85	-0.62	0.026	-0.0069
341.16395	0.147	both	C14H30O7S	33	0	0.50	2.14	-1.14	0.026	-0.0032

357.15887	0.032	both	C14H30O8S	32	0	0.57	2.14	-1.00	0.039	-0.0012
372.20278	0.08	frequency	C18H31O7N	28	4	0.39	1.72	-0.94	0.041	-0.0005
373.22318	-0.051	frequency	C19H34O7	30	3	0.37	1.79	-1.05	0.047	0.0003
375.14274	-0.001	frequency	C14H29O9Cl	31	1	0.64	2.07	-0.79	0.135	-0.0037
376.2624	0.01	abundance	C20H40O3N Cl	6	2	0.15	2.00	-1.70	0.152	0.0024
379.23374	0.059	frequency	C18H36O8	30	1	0.44	2.00	-1.11	0.015	0.0009
385.19017	-0.01	both	C16H34O8S	29	0	0.50	2.13	-1.13	0.039	-0.0033
391.19736	-0.082	frequency	C18H32O9	28	3	0.50	1.78	-0.78	0.017	-0.0072
401.18508	-0.015	both	C16H34O9S	32	0	0.56	2.13	-1.00	0.064	-0.0012
402.27805	0.038	abundance	C22H42O3N Cl	5	3	0.14	1.91	-1.64	0.055	0.0012
404.2937	-0.1	abundance	C22H44O3N Cl	7	2	0.14	2.00	-1.73	0.152	0.0017
414.3225	-0.146	abundance	C23H45O5N	6	2	0.22	1.96	-1.52	0.027	0.0033
419.16895	0.029	both	C16H33O10 Cl	32	1	0.63	2.06	-0.81	0.021	-0.0037
429.19775	-0.077	frequency	C17H34O12	31	1	0.71	2.00	-0.59	0.069	-0.0051
429.21638	-0.106	both	C18H38O9S	29	0	0.50	2.11	-1.11	0.064	-0.0033
431.20534	-0.032	abundance	C18H37O9Cl	8	1	0.50	2.06	-1.06	0.135	-0.0056
436.28353	-0.098	abundance	C22H44O5N Cl	7	2	0.23	2.00	-1.55	0.018	0.0101
463.19517	-0.003	abundance	C18H37O11 Cl	26	1	0.61	2.06	-0.83	0.026	-0.0037
473.22397	-0.163	frequency	C19H38O13	31	1	0.68	2.00	-0.63	0.149	-0.0051
489.23751	-0.068	abundance	C20H42O11 S	24	0	0.55	2.10	-1.00	0.022	-0.0012
517.26881	0.133	abundance	C22H46O11 S	12	0	0.50	2.09	-1.09	0.022	-0.0032
533.26373	0.11	abundance	C22H46O12 S	10	0	0.55	2.09	-1.00	0.027	-0.0012
561.29503	0.044	abundance	C24H50O12 S	10	0	0.50	2.08	-1.08	0.027	-0.0032

Table 6.2 Unassigned tracer ions identified and their molecular characteristics. KMD/z^* -methyl spacing (CH_2) homologous series identifier (Shakeri Yekta et al., 2012), KMD -Kendrick mass defect, KMD_e/z_e^* - ethoxylate spacing (C_2H_4O) homologous series identified. Italicized KMD/z^* and KMD_e/z_e^* values indicate these values matching tracer ions given in Table 6.1, suggesting these ions may be members of homologous series assigned molecular formulas above. n=38 samples.

Exact Mass (<i>m/z</i>)	Tracer Selection	Number of Sample Detections	KMD/z^*	KMD_e/z_e^*
378.27806	abundance	4	0.011	0.0035
241.18089	frequency	29	0.008	0.0020
559.3408144	abundance	7	<i>0.020</i>	<i>0.0012</i>
471.288264	abundance	5	0.058	<i>0.0012</i>
199.13393	frequency	30	0.008	<i>0.0011</i>
377.2180772	frequency	30	0.014	<i>0.0000</i>
487.2831891	abundance	7	0.127	<i>0.0000</i>
275.1500067	frequency	31	<i>0.038</i>	<i>-0.0002</i>
363.2024346	frequency	29	<i>0.014</i>	<i>-0.0002</i>
548.307724	abundance	6	<i>0.027</i>	<i>-0.0005</i>
546.303256	abundance	8	0.023	-0.0006
415.2256883	abundance	14	0.058	-0.0006
589.326355	abundance	4	<i>0.027</i>	<i>-0.0007</i>
272.1139728	frequency	27	<i>0.026</i>	<i>-0.0012</i>
445.2112462	both	30	0.140	<i>-0.0012</i>
457.2323735	abundance	2	0.068	<i>-0.0013</i>
621.31273	abundance	5	<i>0.047</i>	<i>-0.0013</i>
335.1711321	frequency	31	<i>0.014</i>	<i>-0.0014</i>
296.1503668	frequency	27	<i>0.016</i>	-0.0018
209.08526	frequency	28	<i>0.010</i>	<i>-0.0033</i>
473.2425454	abundance	23	0.140	<i>-0.0033</i>
517.2501183	frequency	31	0.023	<i>-0.0051</i>
349.1868023	frequency	34	<i>0.014</i>	-0.0072
465.1129185	abundance	6	0.040	-0.0087
450.8675022	abundance	5	0.063	-0.0123
430.132288	abundance	22	0.114	-0.0130
477.172562	frequency	27	0.030	-0.0175
542.803167	abundance	5	0.398	-0.0183
418.8412954	abundance	5	0.044	-0.0201
479.1285248	abundance	4	0.040	-0.0375

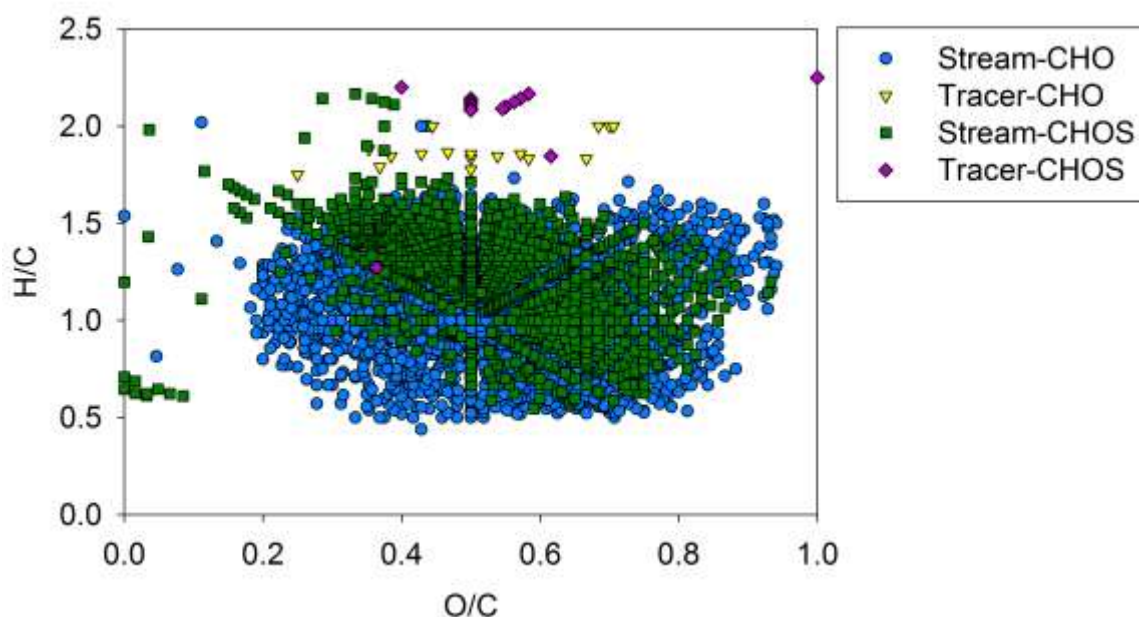


Figure 6.2 Van Krevelen diagram showing oxygen to carbon ratio versus hydrogen to carbon ratio of stream water and tracer ions assigned to molecular formulas containing carbon, hydrogen, oxygen, and sulfur.

compounds related by ethoxylate spacing (Thurman et al., 2014). Indeed, 12 of the 14 identified CHOS tracers (all DBE=0) were related to one or more CHOS tracers by ethoxylate spacing, as members of homologous series. Homologous series were described using Kendrick mass defect (KMD) (Hughey et al., 2001) and z-score values (z^*) (Stenson et al., 2003). The KMD value can be divided by the parameter z score (z^*) (Stenson et al., 2003) for compounds with the same subset of elements to look at homologous series separated by CH_2 groups (Shakeri Yekta et al., 2012). Similarly, the KMD can be calculated on the basis of ethoxylate, KMD_e , (Thurman et al., 2014) and this value can be divided by z^* that is also calculated on the basis of ethoxylate, z_e^* , as shown in Equation 1. This will provide a unique identifier for each set of molecules related to one another based on the precise ethoxylate distance.

$$\text{Equation 1. } \text{KMD}_e / z_e^* = [(\text{neutral mass} * 44) / (44.0262147 - \text{nominal mass})] / [(\text{modulus}(\text{nominal mass}/44)) - 44]$$

Several unconfirmed formula ions were also found to be members of the same homologous series as confirmed CHO and CHOS tracer ions (having the same KMD_e / z_e^* value), indicating that these ions are likely higher molecular weight homologues.

Sulfonated alcohol ethoxylates are common surfactants, and like many other sulfonated surfactants, these compounds are likely efficiently ionized and would readily be seen above a DOM background (Gonsior et al., 2011b). Sulfur-containing alcohol ethoxylates were not explicitly listed on the obtained FracFocus reports, but their consistency across samples suggests that the identified ions were likely additives rather than transformation products. Alternatively, transformation via sulfurization of organic matter is possible under the well conditions, potentially occurring when sulfide reacts with DOM to produce sulfur-containing organic compounds (Brüchert, 1998; Damsté et al., 1989; Einsiedl et al., 2008; Ferdelman et al., 1991; Werne et al., 2008). Indeed, sulfide production from thiosulfate has been observed by the dominant *Halanaerobium* spp. extracted from hydraulic fracturing wells, indicating a sulfide source within these wells (Booker et al., 2017).

Within the list of 28,306 m/z ions unique to hydraulic fracturing fluids and wastewaters, 108 ions matched known surfactant exact masses but were not quantified against known standards (Morales-Cid et al., 2009; Schymanski et al., 2014b) (Table A5.3). Ethoxylated surfactants were the most prevalent surfactant exact masses identified, including a number belonging to homologous series of ethoxylated surfactants

include polyethylene glycols, alcohol ethoxylates, alcohol ethoxysulfates, nonylphenol ethoxylates. However, none of these identified surfactant ions were members of the 77 selected non-target tracers based on their high frequency or high abundance. The sulfur-containing tracer ions may, however, be co-products of known surfactants but not listed on prior surfactant lists (Morales-Cid et al., 2009; Schymanski et al., 2014b). Indeed, fragmentation spectra of a sulfur-containing tracer ion (m/z 313.13265) generated a HSO_4^- fragment indicative of a sulfonate group the dominant fragment observed in alcohol ethoxysulfate fragmentation spectra (Fernández-Ramos et al., 2014) (Figure A5.1a). The chlorinated tracer ion (m/z 419.16895) produced a fragment representing the loss of the exact mass of an ethoxylate, previously used for confirming ethoxylate surfactants (Thurman et al., 2014) (Figure A5.1b). The identified CHO tracer compounds, many of which are also members of homologous series with ethoxylate spacing, could be degradation products of surfactants, and their high abundances could either be indicative of increased ionization efficiency following transformation (i.e., addition of carboxylic acid groups) or the build up of surfactant degradation products in the environment.

The majority of the identified chlorinated tracer ions also had low double bond equivalents and were members of homologous series. Four confirmed chlorinated tracers were homologues separated by $\text{C}_2\text{H}_4\text{O}$, three sets of two chlorinated tracers were homologues separated by CH_2 , but no unconfirmed tracers matched homologous series identifiers of assigned formulas. Halogenated transformation products have previously been identified in hydraulic fracturing wastewaters, produced through several possible halogenation mechanisms (Hoelzer et al., 2016; Luek et al., 2017; Orem et al., 2014). The common use of a number of ethoxylated surfactants and a probable formation pathway

indicates that chlorination of ethoxylated surfactants could have resulted in the observed low double bond equivalency chlorinated ions.

6.3.3 Hydraulic fracturing wastewater fluorescence overlaps with natural fluorescence

Fluorescence across streams was highly similar and four statistical PARAFAC components could be used to describe more than 99% of the variability across samples (Figure 6.3, Figure A5.2). These identified components are among the most consistently described components in natural and engineered aquatic ecosystems (Ishii and Boyer, 2012), and have been previously described in a coastal plain watershed of Maryland as well (Hosen et al., 2014). Component 1 (C1) matches the frequently described “humic-like” component (Coble, 2007) and had >95% similarity matches with 16 different PARAFAC models in the OpenFluor database describing aquatic DOM (Figure A5.3) (Murphy et al., 2014). It should be noted here that other chromophores that are not related to humic substances fluoresce in this region. This component is generally considered to be the dominant terrestrial precursor and strongly resistant to both biodegradation and photodegradation (Ishii and Boyer, 2012; Timko et al., 2015a). Components C2, C3, and C4 also matched a number of modeled components reported in the OpenFluor database (>95% similarity), 13, 18, and 7 different models, respectively (Figure A5.4-A5.6) (Ishii and Boyer, 2012).

More so than changes in the actual fluorescence spectra, variability in overall fluorescence intensity was observed across watersheds and seasons. Fluorescence intensity differed across watersheds, with the highest median intensity observed in the Casselman River (CASS) watershed, a watershed sampled only in 1st order streams. The lowest median abundance was observed in the Georges Creek (GEOR) watershed, which

also contained only 1st order streams. This variability is expected due to different land use—the GEOR watershed is highly forested, while the CASS watershed is more anthropogenically influenced, flowing adjacent to a golf course. The distribution of fluorescence intensity of individual components varied similarly to total fluorescence intensity (Figure A5.7). The lowest fluorescence was observed in January and increased over the following months, peaking in August and September (Figure A5.8). This trend also held true within each individual site (Figure A5.9).

The highly consistent nature of fluorescence, well described using the 4-component PARAFAC model, can be compared to the fluorescence of hydraulic fracturing fluids and wastewater extracts (Figure 6.4). Solid phase extracts of hydraulic fracturing fluids and wastewaters revealed fluorescent signals similar to stream water systems. However, the intensity of the given peaks in these samples varied somewhat from stream water, with peaks near Component 4 (Ex250-325nm, Em300-350nm) frequently the dominant feature in the hydraulic fracturing wastewater spectra (Figure 6.4b,c). The only sample with a peak clearly outside of the modeled stream water fluorescent components was a hydraulic fracturing fluid sample extract prior to injection, with a narrow peak at Ex310-330nm and Em330-350nm (Figure 6.4d). Although few differences were observed between solid phase extracts from stream water and hydraulic fracturing wastewater fluorescence spectra, whole water hydraulic fracturing wastewaters have been previously shown to contain higher intensity fluorescence (Dahm et al., 2013; Freedman et al., 2017). Excitation emission matrix fluorescence cannot provide clear evidence of a hydraulic fracturing fluid or wastewater spill due to the overlap in fluorescence with naturally occurring systems. However, its low cost and rapid response

may be useful in some instances to show that change has occurred in the system, signaling further analyses are needed.

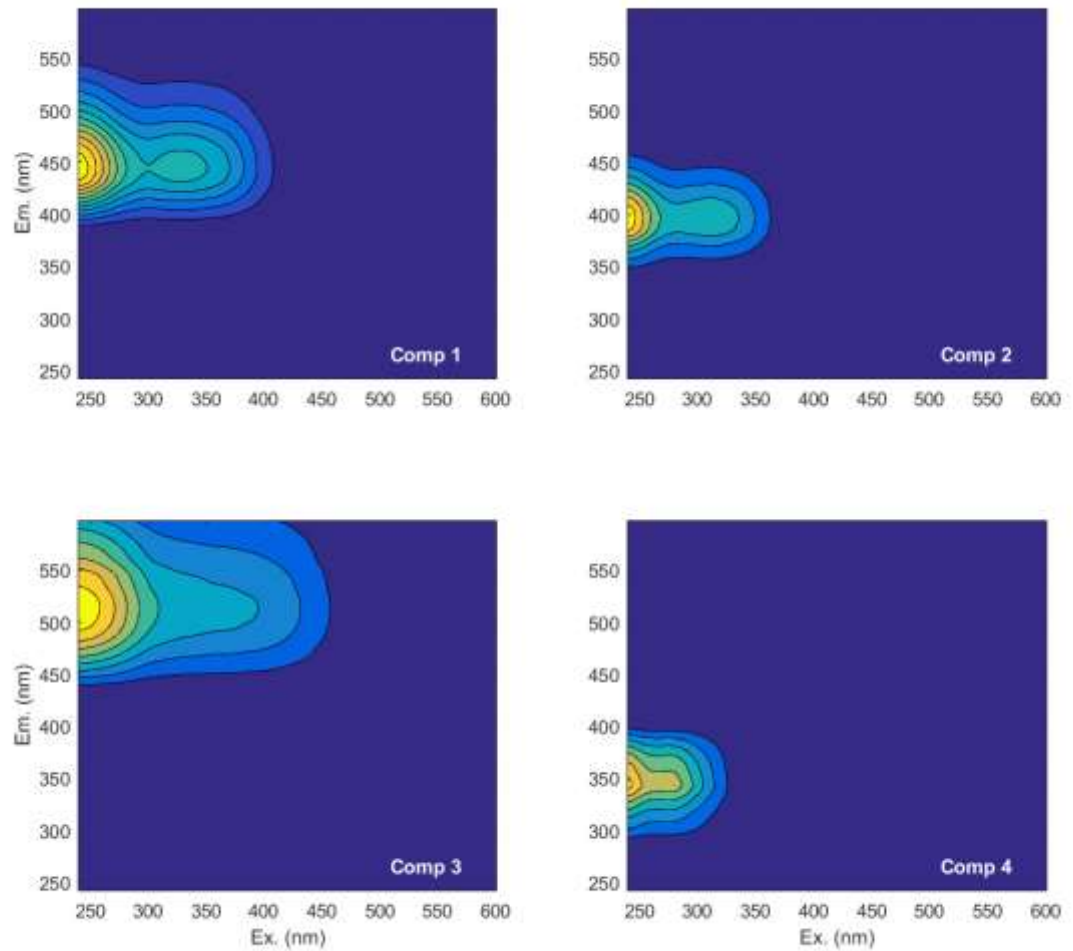


Figure 6.3 4-Component PARAFAC fluorescence model of Western Maryland sample extracts.

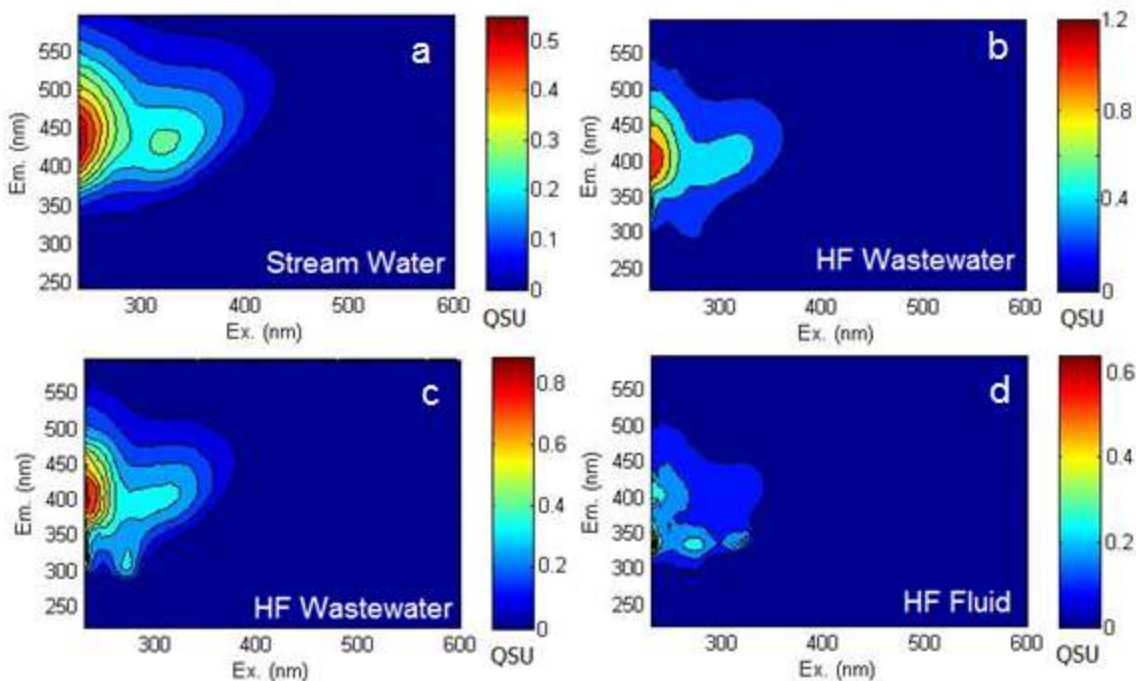


Figure 6.4 Fluorescence spectra of a) stream water sample b) hydraulic fracturing wastewater 1 c) hydraulic fracturing wastewater 2 and d) hydraulic fracturing fluid extracts. [Scale on panel a is divided by 5 to account for differences in extraction volume for direct comparison (1000 mL stream water, 200 mL hydraulic fracturing fluid and wastewaters)]

6.3.4 Feasible new tracer development

Existing tracers of hydraulic fracturing contamination have received strong pushback citing a number of other potential sources for the compounds used as evidence of groundwater and surface water contamination (Connor et al., 2016; McHugh et al., 2016, 2014). Although many inorganic tracers have been proposed, organic tracers need to be developed due the observed differences in transit time of reactive solutes such as organic contaminants in groundwater versus non-reactive solutes such as chloride (Allen-King et al., 2002; Brusseau, 1994; Burr et al., 1994; Mackay et al., 1986). For example, this was observed in the Killdeer North Dakota fracturing blowout, where groundwater contaminant plume resulted in an initial pulse of chloride followed later by a pulse of the

known additive tert-butyl alcohol (U.S. EPA, 2015b). The use of a broad spectrum of inorganic and organic chemical tracers is needed to best understand and track environmental contamination during an accidental release of hydraulic fracturing fluids or wastewaters.

Sulfur and chlorine containing organic chemical tracers were identified as potential tracers of hydraulic fracturing fluids and wastewaters. These tracers were identified based on their high abundance and frequency, and their high ionization efficiency indicates that these may indeed be highly sensitive tracers. However, mixing experiments combining hydraulic fracturing wastewaters and stream waters are needed to identify at what dilution factor these tracers could still be identifiable. The absence of the identified tracer ions from stream waters over four years and multiple seasons suggests that existing anthropogenic influences do not supply these ions to the streams of Western Maryland, and may be applicable more broadly in the Appalachian region. If these ions are indeed absent in most environments, tracers may be useful even when no background data exists. One caveat, being that many of the identified tracer ions are likely related to the use of alcohol ethoxylates, these ions will not be useful tracers for a given well if alcohol ethoxylates were not used. However, other surfactants, such as alkylbenzene sulfonates and their transformation products, may be used and could also be useful tracers. Sampling of a larger number of wells in the Appalachian region and beyond would provide a broader spectrum of possible tracers.

The use of the identified compounds as tracers of environmental contamination from hydraulic fracturing activities hinges on two additional and currently unexplored factors. First, many of the identified tracer ions have similar molecular formulas to

alcohol ethoxylates, but direct infusion FT-ICR-MS does not provide structural information. Analysis using fragmentation techniques is needed to further determine if these ions are indeed structurally similar to known alcohol ethoxylate surfactants. Once structure is confirmed, standards and quantitative methods can be developed. Secondly, although these ions were identified in hydraulic fracturing fluids and wastewaters, their stability and mobility in the environment remains unknown. Their identification in diverse fluids of many ages, some of which were stored for substantial lengths of time prior to extraction or analysis (samples PA-A,B,C,D,E; WV-C,D,E, see Appendix 5), suggests they are indeed relatively stable, and are somewhat mobile as they were identified in the dissolved phase rather than the particulate phase. However, stability under warm conditions, sunlight exposure, or in groundwater environments is not yet understood.

6.4 Conclusions

Fluorescence data revealed a high similarity between the regions of fluorescence stream water and hydraulic fracturing wastewater extracts, indicating that natural occurring fluorescence could easily mask a contamination event. However, the ease and low cost of analysis for excitation emission matrix fluorescence suggests it may be a useful tool as part of stream water monitoring, with changes in fluorescence signaling further analysis. A number of organic molecular ions that could be suitable tracers of hydraulic fracturing fluids and wastewaters were identified in this study using a non-targeted approach. Individual tracers or in combination with known additives (Ferrer and Thurman, 2015b) and inorganic tracers (Osborn et al., 2011; Warner et al., 2014, 2012b)

may be used to develop a comprehensive view of the fate and risk of aquatic contamination during a hydraulic fracturing fluid or wastewater spill.

Chapter 7

Summary and Conclusions

When this dissertation research began in 2013, peer reviewed scientific research on the chemistry of hydraulic fracturing fluids and wastewater was scarce. Particularly lacking were studies of the organic compounds present in hydraulic fracturing fluids and the fate of these fluids. With this in mind, I developed a series of studies presented in Chapters 2 – 5 to address these questions using a non-targeted analytical approach. Since the start of this dissertation, the field has moved forward substantially, but many questions remain partially answered and numerous additional questions need still to be addressed.

In Chapter 2, I reviewed the state of the science of organic compounds in hydraulic fracturing fluids and wastewaters through early 2017. Over the past decade, increased regulation at the state level and databases like FracFocus have made information about the chemicals being used in these fluids increasingly accessible to scientists and the public. At least 238 individual hydraulic fracturing flowback fluids and produced water samples have been analyzed in the last decade, with the majority of samples originating from the Marcellus shale region. Moving forward, essential research in the organic characterization of hydraulic fracturing fluids is needed to describe the diverse biological, chemical, and physical transformations occurring when chemical additives are combined with shale formations at high temperature and pressure. There is still a clear need for better access for independent scientists to hydraulic fracturing wells, as a list of ingredients does not tell the full story. Analytical methodology for key

components of hydraulic fracturing fluids and their known degradation products are still needed to be able to quantify the observed changes.

The use of non-targeted techniques to investigate hydraulic fracturing wastewaters has been particularly useful in the identification of transformation products (Hoelzer et al., 2016; Strong et al., 2013). To date, we are the only group to apply ultrahigh resolution mass spectrometry to hydraulic fracturing fluids and wastewaters. I was able to use this technique to identify halogenated organic compounds in flowback fluid samples (Chapter 3). A consistent critique of identifying halogenated organic compounds using FT-ICR-MS remains the possibility of falsely identifying adducted halogens as covalently bound halogens; however, I worked towards solving this problem in Chapter 3 and have found that our results converged with findings of other researchers using very different techniques (Hoelzer et al., 2016; Maguire-Boyle and Barron, 2014; Orem et al., 2014). We identified a number of chlorinated, brominated, and iodinated organic compounds in flowback fluids, some of which matched the exact masses of known disinfection byproducts including diiodoacetic acid, dibromobenzoic acid, and diiodobenzoic acid. Because iodinated organic compounds are generally absent in freshwater systems, we propose the use of these compounds as potential chemical tracers of environmental contamination during accidental spill events.

In Chapter 3, I analyzed a wide variety of samples but did not have key pieces of information about fluid age, fracturing fluid ingredients, or before/after snapshots to infer the source of halogenated organics. I was fortunate to become involved in the Marcellus Shale Energy and Environmental Laboratory (MSEEL), a large collaborative research project associated with the drilling of two hydraulic fracturing wells in Morgantown,

WV. Through MSEEL, I was able to gain access to fluids prior to injection and at many time points as the fluids returned to the surface over nine months (Chapter 4). Although not included in this dissertation, I will continue to obtain fluids through December of 2017, two years after initial flowback. This fluid time series allowed me to carefully track organic matter and investigate our hypotheses on the proposed source of halogenated organic compounds in hydraulic fracturing fluids. A side-by-side comparison of the two wells drilled with different fluids resulted in remarkably similar trends in iodinated organic compounds, although the strong oxidizing compound, ammonium persulfate, was used at 75-fold differences in concentration. The longterm identification of iodinated compounds ultimately may have both abiotic and biotic sources.

I used desalted organic extract samples from MSEEL flowback and produced waters to investigate questions about environmental fate (Chapter 5). Using solar irradiation experiments, we were able to identify key shifts in the optical properties of these fluids using fluorescence spectroscopy and PARAFAC modeling. The chemical composition of the fluids shifted towards the production of compounds with higher oxygen content following irradiation. Exposure of these organic extracts revealed no acute or chronic toxicity to the freshwater invertebrate daphnids. Examining the fate of this narrowed pool of organic compounds allowed us to understand how a particular subset of these fluids with similar mobility can impact organisms and also how it is altered in the environment.

Hydraulic fracturing fluid additives and oil and gas compounds have been used to infer environmental contamination from hydraulic fracturing fluids, but are frequently cast as insufficient evidence. In Chapter 6, I use FT-ICR-MS and fluorescence

spectroscopy to characterize dissolved organic compounds in a region that currently does not have hydraulic fracturing to establish a baseline. I collected and analyzed baseline-monitoring data on streamwaters in advance of the potential opening of hydraulic fracturing in Maryland through collaborations with a large team of aquatic geochemists and Maryland Department of Natural Resources biological stream survey. However, hydraulic fracturing was formally banned in the state of Maryland in April of 2017, so I compared this streamwater dataset to hydraulic fracturing fluids, flowback fluids, and produced water samples to identify organic compounds unique to hydraulic fracturing fluids and absent from four years of streamwater baseline data. A number of ions unique to hydraulic fracturing fluids and wastewaters were identified, and those consistently identified in fluid samples at high intensities were selected as proposed chemical tracers in the event of an environmental contamination event. In addition to halogenated organic compounds identified in previous chapters, surfactants and transformation products potentially related to surfactants were identified as potential tracers.

In this dissertation, I worked to address a number of questions about organic compounds in hydraulic fracturing fluids and wastewater. I used ultrahigh resolution mass spectrometry to answer these questions alongside other methods including fluorescence spectroscopy and total organic carbon analysis. In addition to addressing the questions posed in each chapter, the extraction and sample storage method combined with a non-targeted analytical approach will allow for future researchers to use the collected data to investigate not only the compounds described in this project but also any other compounds amenable to these techniques.

This research raised a number of new questions that were not addressed in this work. The first, and perhaps most important question raised, is one of analytical methodology. In this work, I used the Bond Elut PPL reversed phase cartridges to extract organic compounds from fracturing fluids in order to target compounds amenable to negative mode electrospray ionization using FT-ICR-MS. These methods were selected to track compounds not amenable to gas chromatography, the most common method used to analyze hydraulic fracturing fluids and wastewaters, and specifically two compound classes: halogenated organic compounds and surfactants. A non-targeted FT-ICR-MS method was selected to not only identify these two classes of interest, but to also identify other compounds not selected *a priori*, such as transformation products. In natural freshwater and marine systems, PPL cartridges can have high recoveries of dissolved organic carbon (60+%) (Dittmar et al., 2008; Li et al., 2016). However, the recovery of dissolved organic carbon from hydraulic fracturing fluids and wastewater on PPL cartridges was low for hydraulic fracturing fluids and wastewaters, particularly for oily samples. The extraction technique targets non-polar to mesophilic compounds, missing polar organic compounds by default and removing highly volatile compounds during the drying step of the extraction process. Although high resolution liquid chromatography-mass spectrometry has been used to begin addressing these questions for polar organic compounds, ideally, a desalting method that retains highly polar compounds would be extremely useful to further investigate a broader pool of organic constituents using ultrahigh resolution mass spectrometry and gain a better understanding of the transformation processes that occur over the lifetime of a well. An extraction process that includes the missing polar organic compounds is needed not only because FT-ICR-MS

analyses cannot be performed on salty samples, but also because subsets of these fluids are needed to ask questions about their specific environmental stability, behavior, and toxicity.

A second key question raised by this study is on the stability of the halogenated organic compounds identified in Chapters 3 and 4 and tracers discussed in Chapter 6. We investigated photochemical stability of the fluorescence and described bulk changes, but a number of other key questions about their stability under varying conditions remain unanswered, and may require more quantitative techniques to address. Targeted degradation experiments are needed to gain more detailed understanding of what changes may occur under varying spill scenarios (i.e., surface water spill versus groundwater spill).

Looking ahead, we will continue investigating fluids from the MSEEL site to identify continued changes over the lifetime of the well. Additionally, we will combine the non-targeted FT-ICR-MS data with bacterial genomics data to start investigating questions about microbial capabilities such as whether or not halogenation or dehalogenation genes are present in the fluids, and at what times. As other researchers begin publishing additional chemical data from the MSEEL fluids, we will start to gain a deeper understanding of the significant changes that occur in hydraulic fracturing fluids, both for these specific wells and more broadly to other wells applying similar techniques.

This dissertation focuses on a narrow sliver of potential water quality issues associated with organic compounds in hydraulic fracturing fluid. A number of other important questions have been raised about the impacts of hydraulic fracturing fluids on water resources, many of which are described in the recent EPA report (U.S. EPA, 2016).

These issues include water scarcity, spill and risk, hazardous chemicals and their hydrological mobility, and wastewater management. Combined with information about air quality, health and socio-economic impacts, and induced seismicity, each piece is needed to develop a holistic understanding of the impacts of hydraulic fracturing technologies.

Appendix 1

Table A1.1 Compilation of quantitative detections of organics reported in multiple literature (Akob et al., 2015; Getzinger et al., 2015; Hayes, 2009; Lester et al., 2015; Murali Mohan et al., 2013b; Wolford, 2011; Ziemkiewicz, 2013) *Summary statistics exclude acetate average reported in (Orem et al., 2014) and all averages given in (Ziemkiewicz and He, 2015).

Compound	Number of Quantitative Detections	Mean ($\mu\text{g L}^{-1}$)	Median ($\mu\text{g L}^{-1}$)	Maximum ($\mu\text{g L}^{-1}$)
1,2 propanediol	3	11	9.18	14.7
1,2,4 trimethylbenzene	3	31	26.8	66
chlorobenzene	8	101	40	350
2-4 dimethylphenol	2	204	NA	790
2-butanone	3	88	17	240
2-methylnaphthalene	9	32	3.7	120
2-methylphenol	3	59	15	150
3&4 methylphenol	9	28	12	170
acetate*	30	89	12.3	1600
acetone	31	1061	90	16000
benzene	41	21149	200	778510
bis (2-ethylhexyl) phthalate	11	103	29	870
cumene (isopropylbenzene)	2	30	49.3	90
ethylbenzene	22	26488	245	399840
phenanthrene	6	12.7	9.75	29
phenol	12	78	10.5	830
pyrene	3	12.6	13	24
toluene	37	934	300	6200
xylenes (total)	31	451	130	330

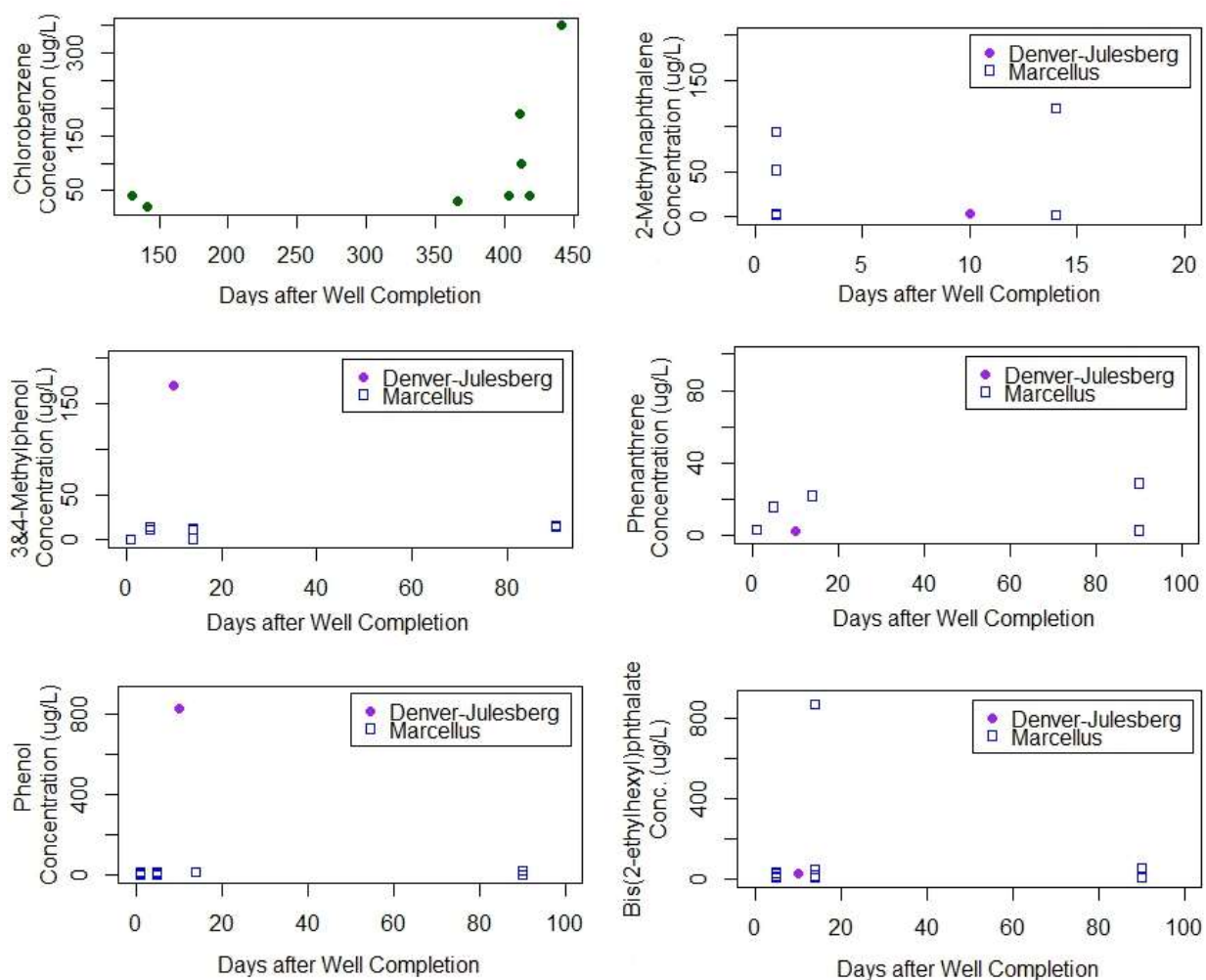


Figure A1.1 Distribution of organic compound concentrations by fluid age and basin. Sources: chlorobenzene (Khan et al., 2016), all others (Hayes, 2009; Lester et al., 2015).

Appendix 2

Table A2.1 Information on sampling location, basin, age, appearance, and sampling and storage conditions. *FB4 and FB6 were collected from the same well 6 weeks apart. ^FB5 and FB7 were collected from the same well 6 weeks apart.

Sample ID	Sample Location	Basin/Formation	Approximate Age	Sampling Comments	Sample Appearance	Storage Comments
FB1	ND	(Bakken)	Initial Flowback (2-3 weeks)	provided in LDPE container	iron precipitate	stored >9 months refrigerated
FB2	CO	(Denver-Julesberg)	Initial Flowback (2-3 weeks)	provided in LDPE container	clear, slightly soapy	stored >9 months refrigerated
FB3	OH	Utica	Recycled flowback	sampled in LDPE container cleaned by authors, no headspace	iron precipitate	analyzed within 1 week of sampling
FB4	WV*	Marcellus	Initial Flowback (<1 week)	sampled in LDPE container cleaned by authors, no headspace	iron precipitate	analyzed within 1 month of sampling
FB5	WV^	Marcellus	Initial Flowback (<1 week)	sampled in LDPE container cleaned by authors, no headspace	iron precipitate	analyzed within 1 month of sampling
FB6	WV*	Marcellus	6 weeks	sampled in LDPE container cleaned by authors, no headspace	iron precipitate	analyzed within 1 week of sampling
FB7	WV^	Marcellus	6 weeks	sampled in LDPE container cleaned by authors, no headspace	iron precipitate	analyzed within 1 week of sampling
PW1	WV	Marcellus	>5 yrs	collected in solvent rinsed clean glass, no head space	iron precipitate	analyzed within 1 week of sampling
PW2	PA	(Appalachian)	From natural gas	collected in HDPE containers	relatively clear, some	stored 3 months refrigerated

			processing plant	from provider, no headspace	iron precipitate	
CL1	PA	(Appalachian)	From natural gas compressor station	collected in HDPE containers from provider, no headspace	water and oil phase, purple tint in oil phase	stored 3 months refrigerated
CL2	PA	(Appalachian)	From natural gas compressor station	collected in HDPE containers from provider, no headspace	water and oil phase	stored 3 months refrigerated
CL3	PA	(Appalachian)	From natural gas compressor station	collected in HDPE containers from provider, no headspace	iron precipitate	stored 3 months refrigerated
CL4	PA	(Appalachian)	From natural gas compressor station	collected in HDPE containers from provider, no headspace	very viscous, clear	stored 3 months refrigerated
CL5	PA	(Appalachian)	From natural gas compressor station	collected in HDPE containers from provider, no headspace	viscous, sudsy, mostly clear	stored 3 months refrigerated
CL6	WV	(Appalachian)	From natural gas compressor station	collected in HDPE containers from provider, no headspace	very dark oily layer and water	stored 3 months refrigerated
FL1	WV	(Appalachian)	From natural gas liquids fractionation plant	collected in HDPE containers from provider, no headspace	water and oil phase	stored 3 months refrigerated

Table A2.2 DOC (0.7 μm filtered non-purgeable organic carbon) and conductivity analyses. DOC Recovery corresponds to the solid phase extracted methanol extract dried down and reconstituted in MilliQ and calculated as concentration relative to original sample volume. FB- Flowback Fluid, PW-Produced Water, CL-Compression Liquid, FL-Fractionation Liquid. #Sample unavailable for conductivity measurement but TDS was reported as 303 mg L^{-1} .

Sample ID	DOC Concentration (mg L^{-1})	DOC recovered MeOH (mg L^{-1})	% Recovery	Conductivity (mS cm^{-1})
FB1	97	4	4.2	N/A#
FB2	35	4.1	12	277
FB3	49	10	21	168
FB4	510	9.1	1.8	42
FB5	110	11	9.9	53
FB6	48	7.8	16	90
FB7	47	7.9	17	77
PW1	68	3.3	4.9	66
PW2	40000	27	0.1	247
CL1	5100	30	0.6	0.3
CL2	12000	55	0.5	0.7
CL3	6400	23	0.4	8.0
CL4	49000	74	0.2	0.3
CL5	160000	61	0.04	0.6
CL6	210000	160	0.1	0.3
FL1	12	5.9	48	0.3

Discussion on DOC concentrations/recoveries

DOC concentrations in the samples were highly variable, ranging from 12 to 210,000 mg C L⁻¹, and were higher in the produced water samples than flowback water samples. The amount of non-volatile DOC present in the methanol extracts were determined by evaporating the methanolic extract, re-dissolving the samples in MilliQ water, and followed by the determination of DOC concentrations as described above. The calculated concentration of DOC recovered in the dried down methanol extract ranged between 3.3 and 156 mg C L⁻¹. Recoveries were highly variable and ranged from 0.04% for a sample with a non-aqueous phase liquid (NAPL) to 48% for the sample with lowest initial DOC concentrations. The obvious reason for such high variability was the presence of non-water soluble petroleum-based hydrocarbons, that were lost during extraction and hence the presence of the NAPL resulted in poor recoveries over the bulk 200 mL volume extracted. Highly volatile compounds potentially present in the methanol would also be lost due to the drying down of the methanolic extract prior to re-dissolution as well as sparging during the DOC analysis, suggesting that the DOC analyzed in the methanol extract on the FT-ICR-MS might have been higher than reflected in recoveries. It is suggested that future extractions should first separate the NAPL component prior to SPE and DOC analyses.

Table A2.3 Calibration list for FT-ICR-MS. *Italicized compounds were used as the primary calibrants for FB1, FB2, and FB3.*

Molecular Formula	Exact Mass	Charge
<i>C₁₇H₂₇O₃S</i>	<i>311.16864</i>	<i>1-</i>
<i>C₁₈H₃₉O₃S</i>	<i>325.18429</i>	<i>1-</i>
<i>C₁₉H₃₁O₃S</i>	<i>339.19994</i>	<i>1-</i>
<i>C₁₆H₂₅O₃S</i>	<i>297.15299</i>	<i>1-</i>
<i>C₆H₃Br₄S</i>	<i>424.667445</i>	<i>1-</i>
<i>C₆H₃Br₄S</i>	<i>422.669494</i>	<i>1-</i>
<i>C₆H₃Br₄S</i>	<i>426.665397</i>	<i>1-</i>
<i>C₈H₅O₄</i>	<i>165.019332</i>	<i>1-</i>
C ₂₇ H ₂₅ O ₃	277.180918	1-
C ₁₀ H ₁₉ O ₆	235.118712	1-
C ₁₆ H ₁₉ O ₅	291.123797	1-
C ₁₉ H ₂₅ O ₇	365.160577	1-
C ₂₁ H ₂₉ O ₈	409.186791	1-
C ₂₅ H ₃₅ O ₁₀	495.223571	1-
C ₂₉ H ₄₃ O ₁₁	567.281086	1-
C ₃₂ H ₄₅ O ₁₁	605.296736	1-
C ₁₆ H ₂₅ O ₈	345.155491	1-
C ₂₂ H ₂₅ O ₁₁	465.140235	1-
C ₂₂ H ₂₇ O ₁₀	451.160971	1-
C ₁₁ H ₁₃ O ₆	241.071762	1-
C ₁₅ H ₂₁ O ₆	297.134362	1-
C ₁₈ H ₃₇ O ₈ S	413.221259	1-
C ₁₂ H ₂₅ O ₅ S	281.142818	1-
C ₂₂ H ₄₅ O ₁₀ S	501.273892	1-
C ₂₀ H ₄₁ O ₉ S	457.247677	1-
C ₁₀ H ₁₁ O ₅ S	243.033268	1-
C ₁₂ H ₂₅ O ₇ S	313.132647	1-
C ₉ H ₇ Br ₂ O ₂	304.881828	1-
C ₂₀ H ₄₁ ClNO ₃	378.278045	1-
C ₂₂ H ₄₃ ClNO ₃	404.293696	1-
C ₂₃ H ₄₄ NO ₅	414.322497	1-
C ₂₂ H ₄₃ BrNO ₃	448.24318	1-

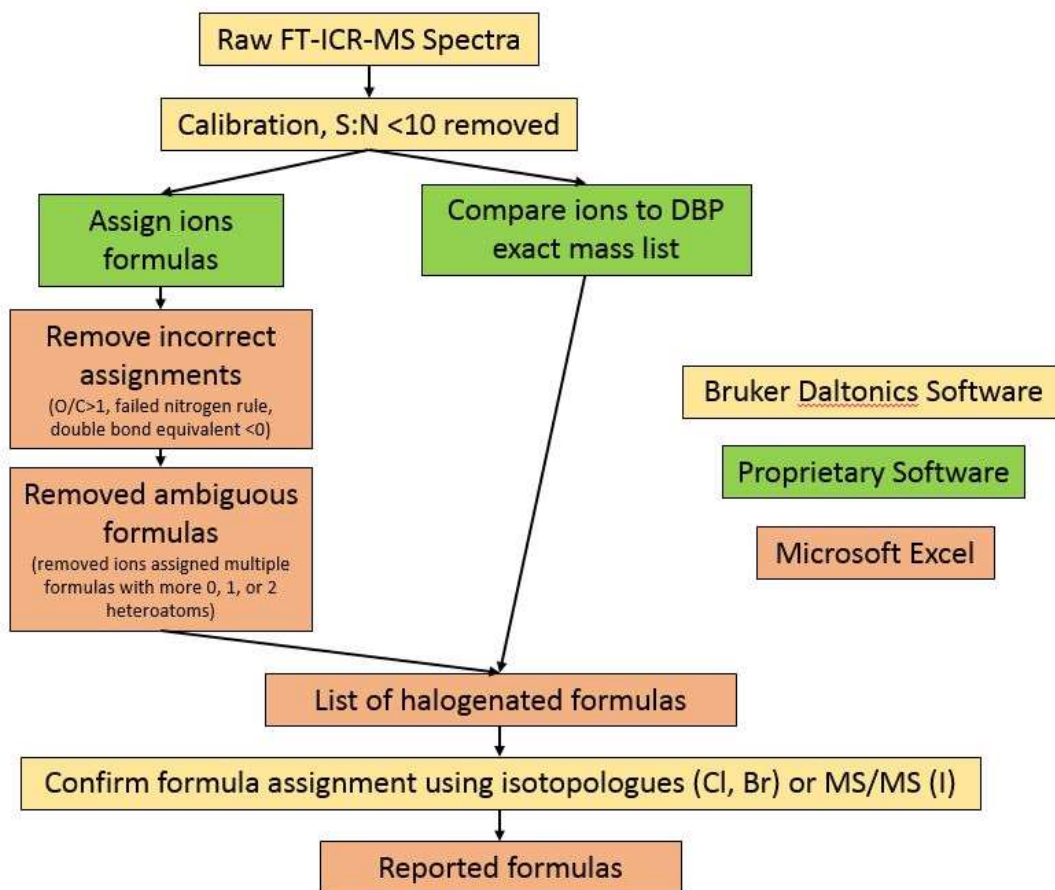


Figure A2.1 Schematic describing data processing of FT-ICR-MS spectra using a non-targeted (left) and semi-targeted approach (right).

Table A2.4 All known disinfection by-products including both halogenated and non-halogenated formulas. Only halogenated formulas greater than the FT-ICR-MS 147 *m/z* cutoff were investigated in this study but all are included here for completeness.

Due to table length, this table can be accessed in the supplemental materials on the American Chemical Society Website:

<http://pubs.acs.org/doi/abs/10.1021/acs.est.6b06213>

Table A2.5 Produced water (PW) and flowback water (FB) sample information. *, ^ Represent same sampling well, respectively, sampled on two dates six weeks apart. ⁺Formulas assigned represent filtered data with 0-2 total heteroatoms that have a single unambiguous formula assignment.

New Sample ID	Sample Location	Peaks <700 Da	Peaks Assigned Formulas⁺	% of Total Peaks Assigned Formulas⁺
FB1	ND	4573	2226	49
FB2	CO	7000	3596	51
FB3	OH	4927	2153	44
FB4	WV*	4690	1035	22
FB5	WV^	4269	660	15
FB6	WV*	4016	632	16
FB7	WV^	4552	919	20
PW1	WV	2856	606	21
PW2	PA	3344	1170	35
CL1	PA	4214	1221	29
CL2	PA	6698	2859	43
CL3	PA	2271	810	36
CL4	PA	9206	4019	44
CL5	PA	5910	1131	19
CL6	WV	6683	3113	47
FL1	WV	4569	2098	46

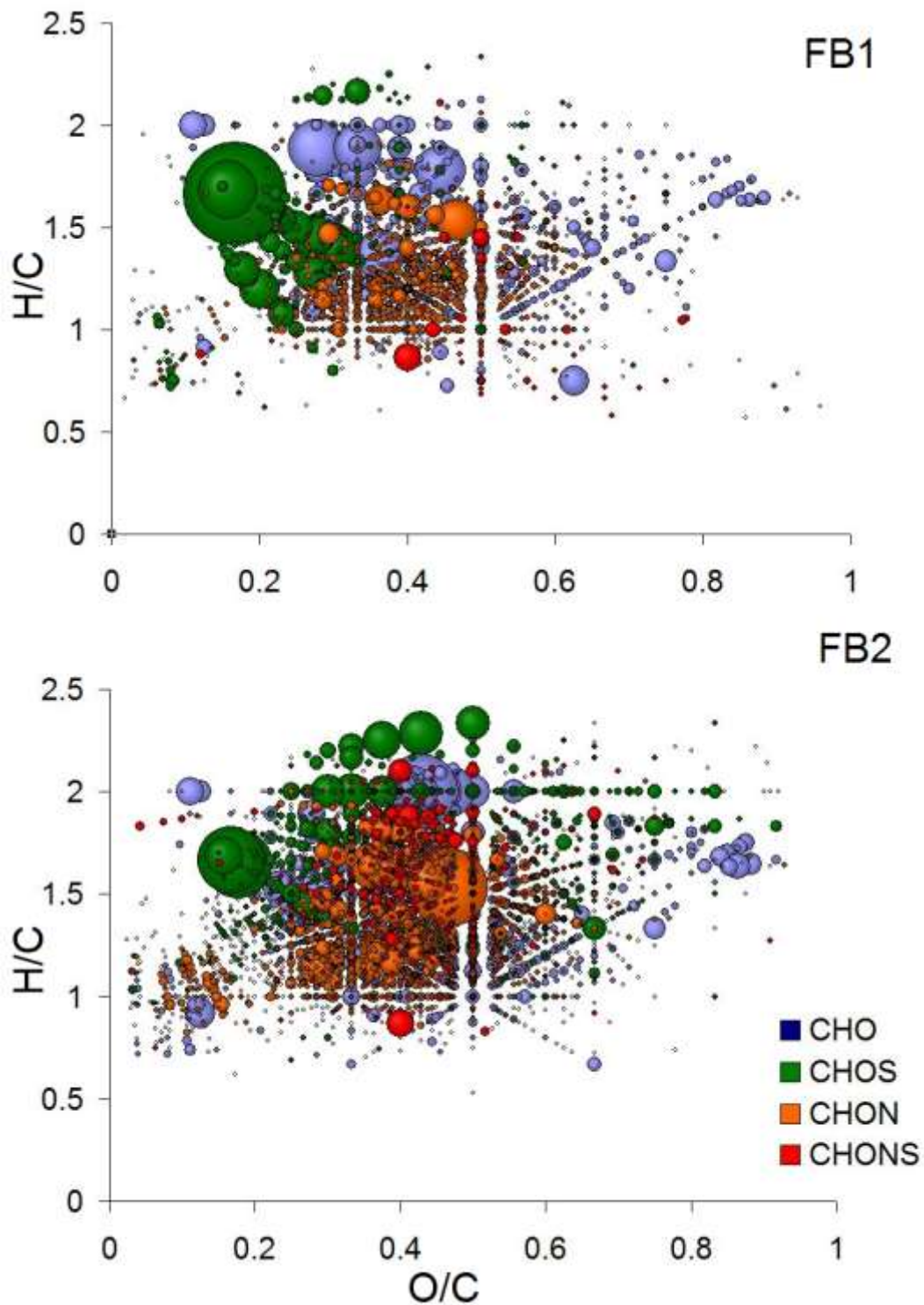


Figure A2.2 Oxygen to carbon ratio (O/C) versus hydrogen to carbon ratio (H/C) (Van Krevelen) of formulas assigned CHO (blue), CHON (orange), CHOS (green), and CHONS (red) for FB1 (top) and FB2 (bottom). Bubble size indicates relative intensity of assigned formula.

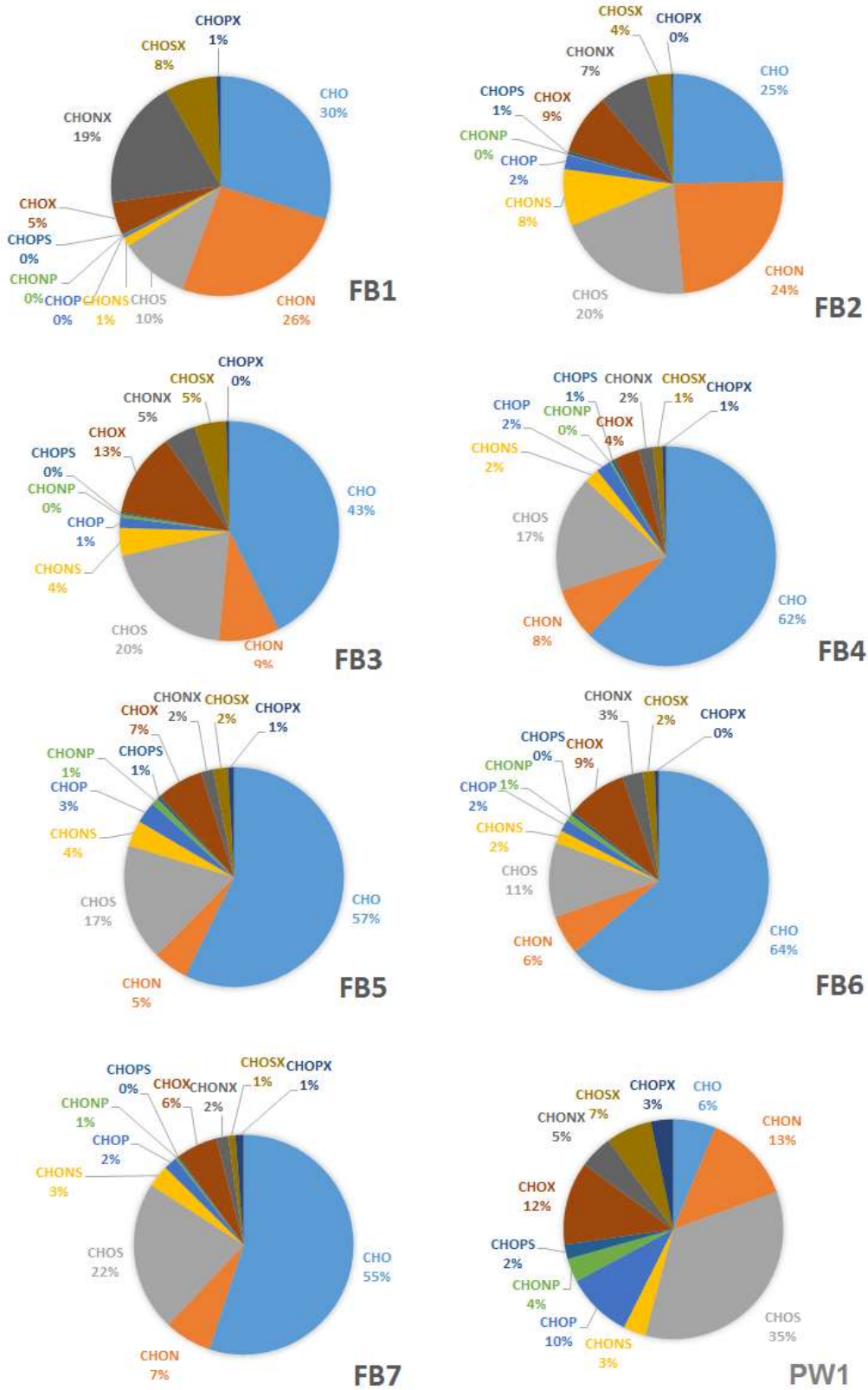


Figure A2.3 Distribution of formula assignments in FB1-FB7, PW1.

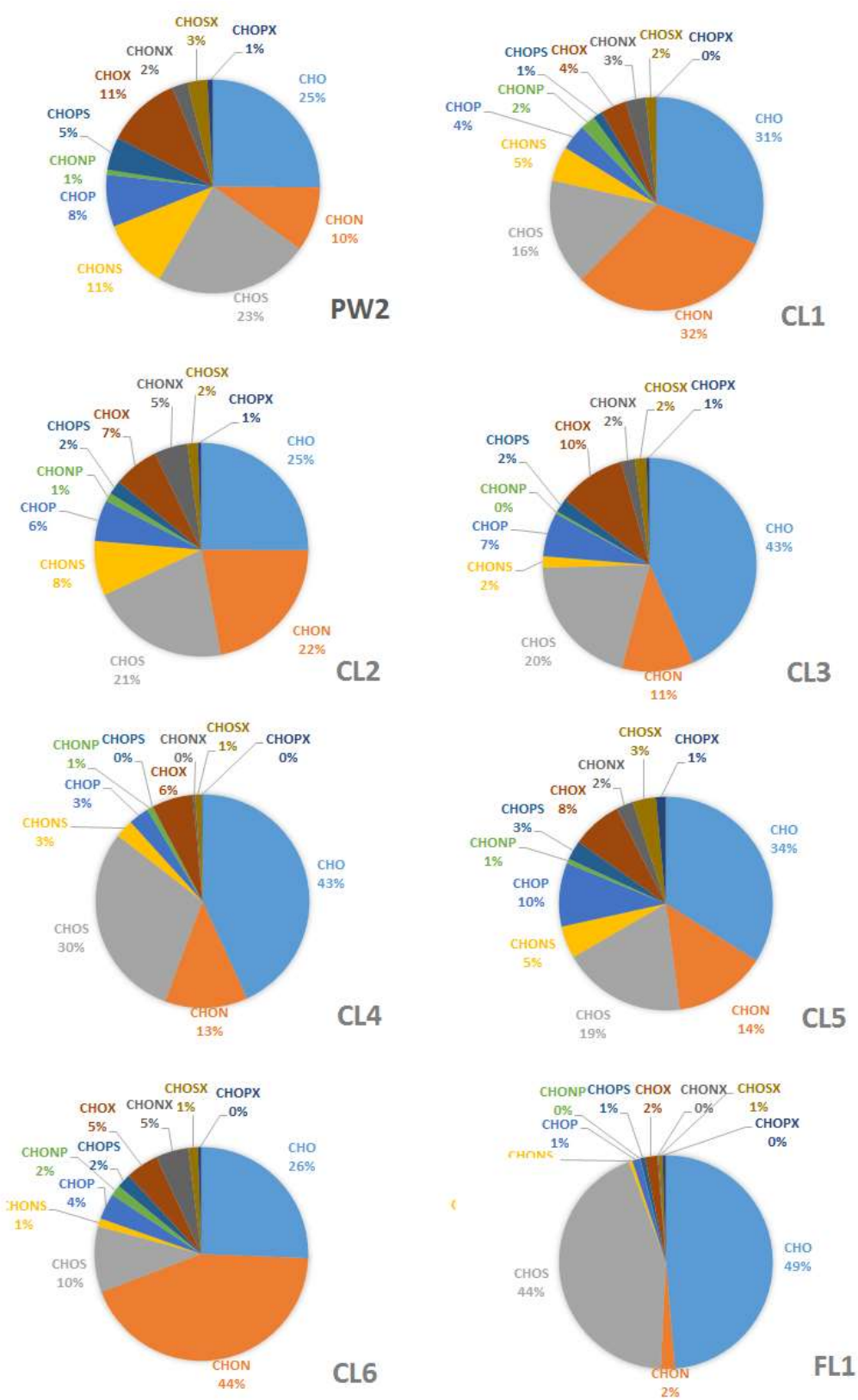


Figure A2.4 Distribution of formula assignments in PW2, CL1-6, and FL1.

Table A2.6 Halogenated organic molecular formulas identified in at least two flowback water samples [#] Isotopic simulation comparison given in supplemental materials; *Exact mass identified in (Taylor et al., 2010); ^ Exact mass identified in identified in (Zhang et al., 2012)

Formula	FB1	FB2	FB3	FB4	FB5	FB6	FB7	PW1	PW2	CL1	CL2	CL3	CL4	CL5	CL6	FL2
C ₅ H ₂ O ₃ I ⁻	x	x			x	x	x									
CHI ₂ ⁻		x						x								
C ₁₁ H ₂₀ O ₅ Cl ⁻		x	x	x	x	x	x			x			x			
C ₁₀ H ₁₆ O ₄ Br ⁻			x	x												
C ₆ H ₄ O ₅ I ⁻	x		x													
C ₂ HO ₂ I ₂ ⁻			x					x								
C ₁₁ H ₁₁ O ₂ NI ⁻	x	x														
C ₁₁ H ₁₃ O ₂ NI ⁻	x	x														
C ₈ H ₃ O ₄ Br ₂ ⁻	x		x			x										
C ₈ H ₆ O ₄ SI ⁻		x	x													
C ₁₂ H ₂₀ O ₈ Cl ⁻		x	x			x										
C ₁₂ H ₂₂ O ₈ Cl ⁻	x	x	x													
C ₁₂ H ₁₃ O ₂ NI ⁻	x	x														
C ₁₀ H ₇ O ₃ Br ₂ ⁻	x	x	x													
C ₁₀ H ₁₃ O ₄ NI ⁻		x	x													
C ₁₁ H ₁₅ O ₄ NI ⁻	x	x														
C ₁₀ H ₁₆ O ₄ NI ⁻			x	x												
C ₅ HO ₃ I ₂ ⁻	x				x	x										
C ₅ H ₃ O ₃ I ₂ ⁻	x	x														
C ₁₈ H ₃₄ O ₅ Cl ⁻	x	x	x			x	x					x			x	
C ₁₂ H ₂₂ O ₈ Br ⁻	x	x	x													
C ₁₇ H ₂₆ O ₄ Br ⁻	x	x							x						x	
C ₁₂ H ₁₁ O ₅ NI ⁻	x	x														
C ₁₂ H ₁₇ O ₅ NI ⁻	x	x														
C ₁₈ H ₃₃ O ₄ Cl ₂ ⁻		x	x				x									
C ₁₄ H ₁₅ O ₄ NI ⁻	x	x														
C ₁₇ H ₂₆ O ₅ Br ⁻	x	x								x	x					
C ₁₂ H ₁₃ O ₆ NI ⁻	x	x														
C ₁₄ H ₁₅ O ₅ NI ⁻	x	x														
C ₁₃ H ₁₅ O ₆ NI ⁻	x	x														
C ₂₁ H ₂₈ O ₆ Cl ⁻		x	x													
C ₁₃ H ₂₃ O ₆ NI ⁻		x	x													
C ₁₅ H ₁₇ O ₅ NI ⁻	x	x														
C ₁₆ H ₃₂ O ₁₀ Cl ⁻			x			x	x		x							
C ₁₄ H ₁₉ O ₆ NI ⁻		x	x													

$C_{15}H_{23}O_5NI^-$		x	x													
$C_{15}H_{24}O_{12}Cl^-$		x	x													
$C_{16}H_{23}O_5NI^-$		x	x													
$C_{15}H_{19}O_7NI^-$		x	x													
$C_{24}H_{34}O_6Cl^-$			x			x	x									
$C_{21}H_{28}O_6Br^-$	x	x	x									x				
$C_{17}H_{17}O_6NI^-$	x	x														
$C_{18}H_{36}O_{11}Cl^-$		x	x			x										
$C_{16}H_{19}O_7NI^-$		x	x													
$C_{21}H_{40}O_7Br^-$	x						x									
$C_{20}H_{40}O_{12}Cl^-$			x	x		x										
$C_{22}H_{44}O_{13}Cl^-$			x			x										

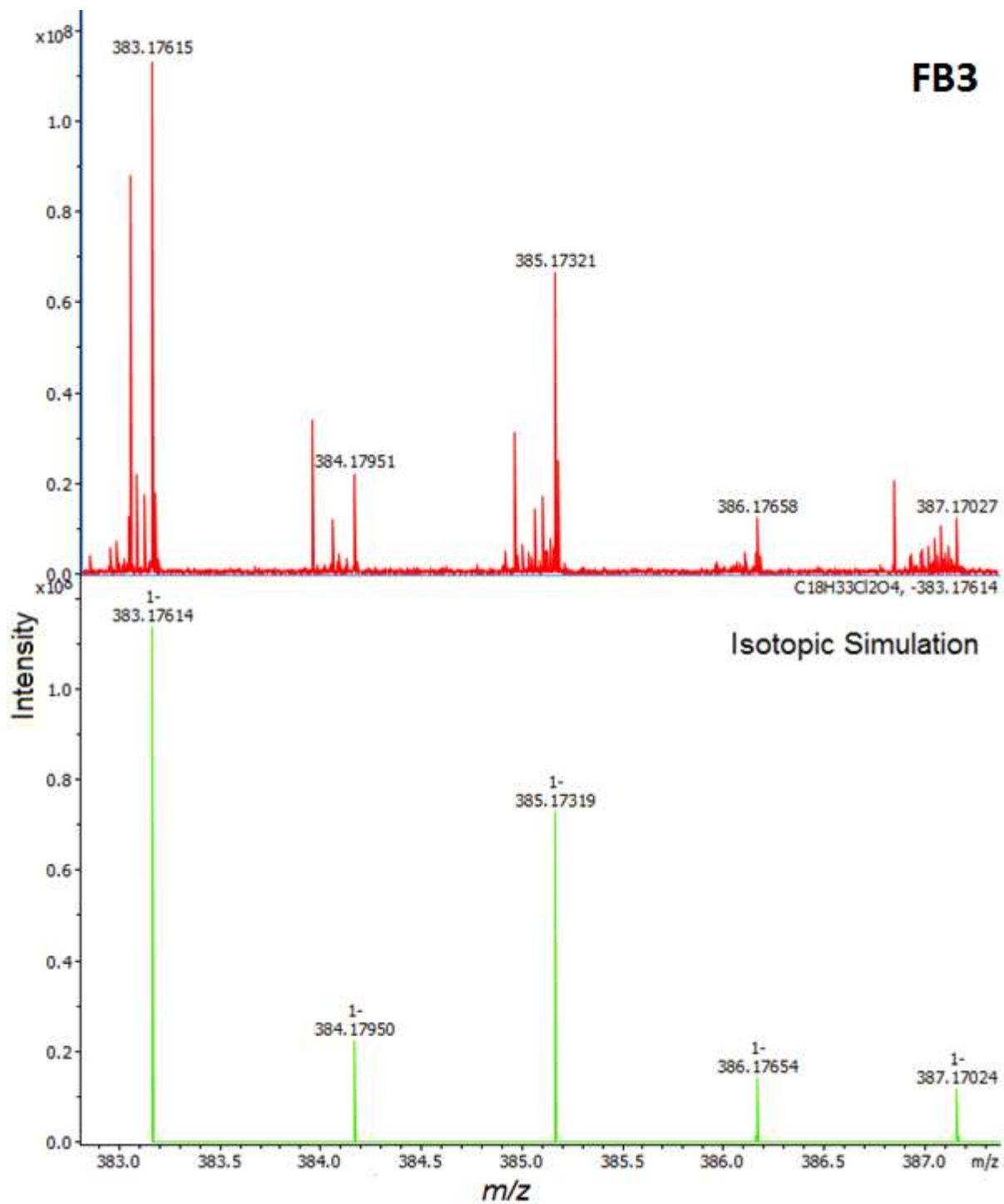


Figure A2.5 Ultrahigh resolution mass spectra of FB3 between m/z 383 – 387 (top); isotopic simulation spectra of proposed chlorinated formula assignment $C_{18}H_{33}Cl_2O_4^-$ (bottom).

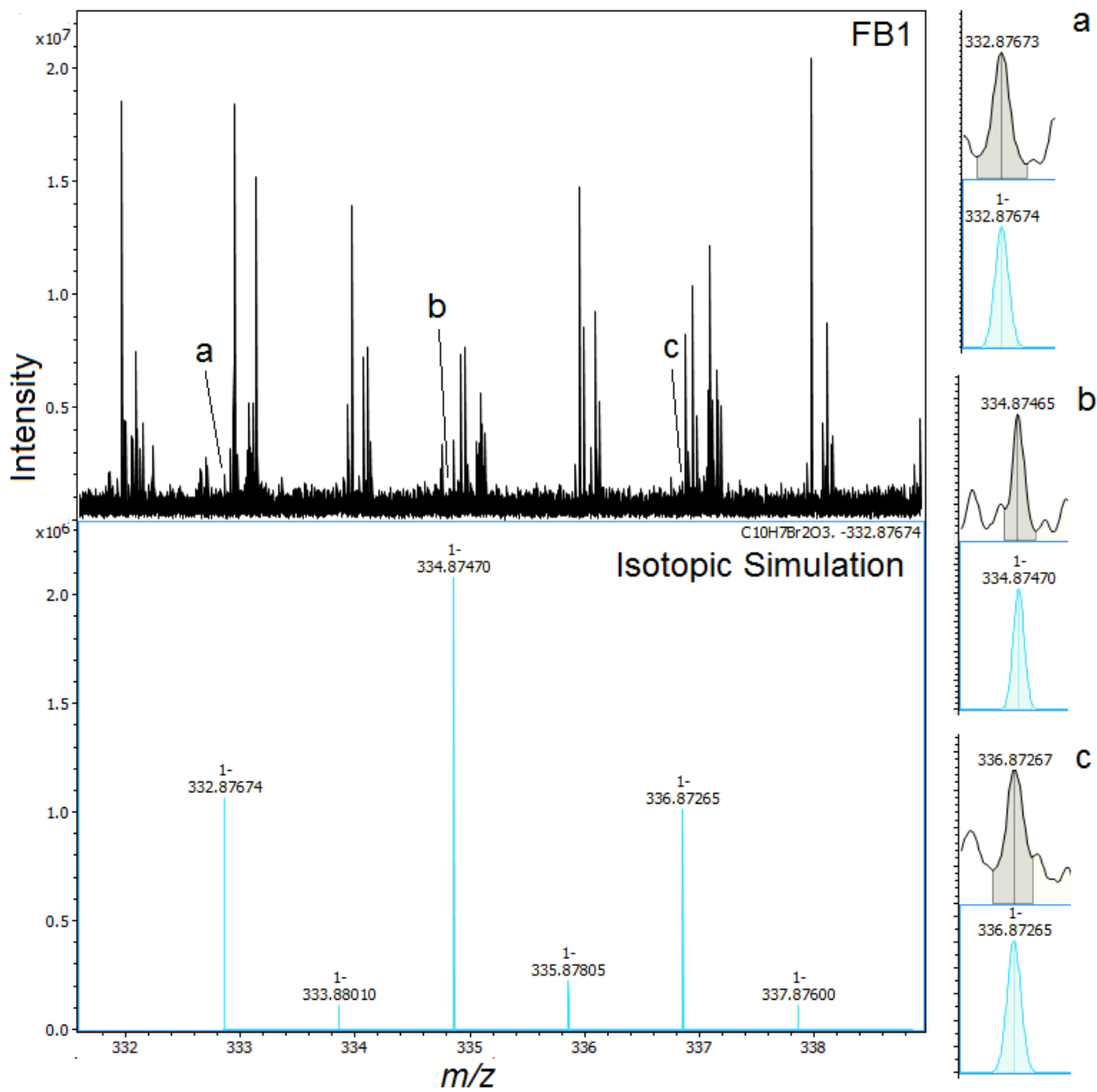


Figure A2.6 Ultrahigh resolution mass spectra of FB1 between m/z 332 – 339; with isotopic simulation spectra of proposed brominated formula assignment $C_{10}H_7Br_2O_3^-$ zooming in on isotopic peaks a) $C_{10}H_7^{79}Br^{79}BrO_3^-$ b) $C_{10}H_7^{79}Br^{81}BrO_3^-$ and c) $C_{10}H_7^{81}Br^{81}BrO_3^-$

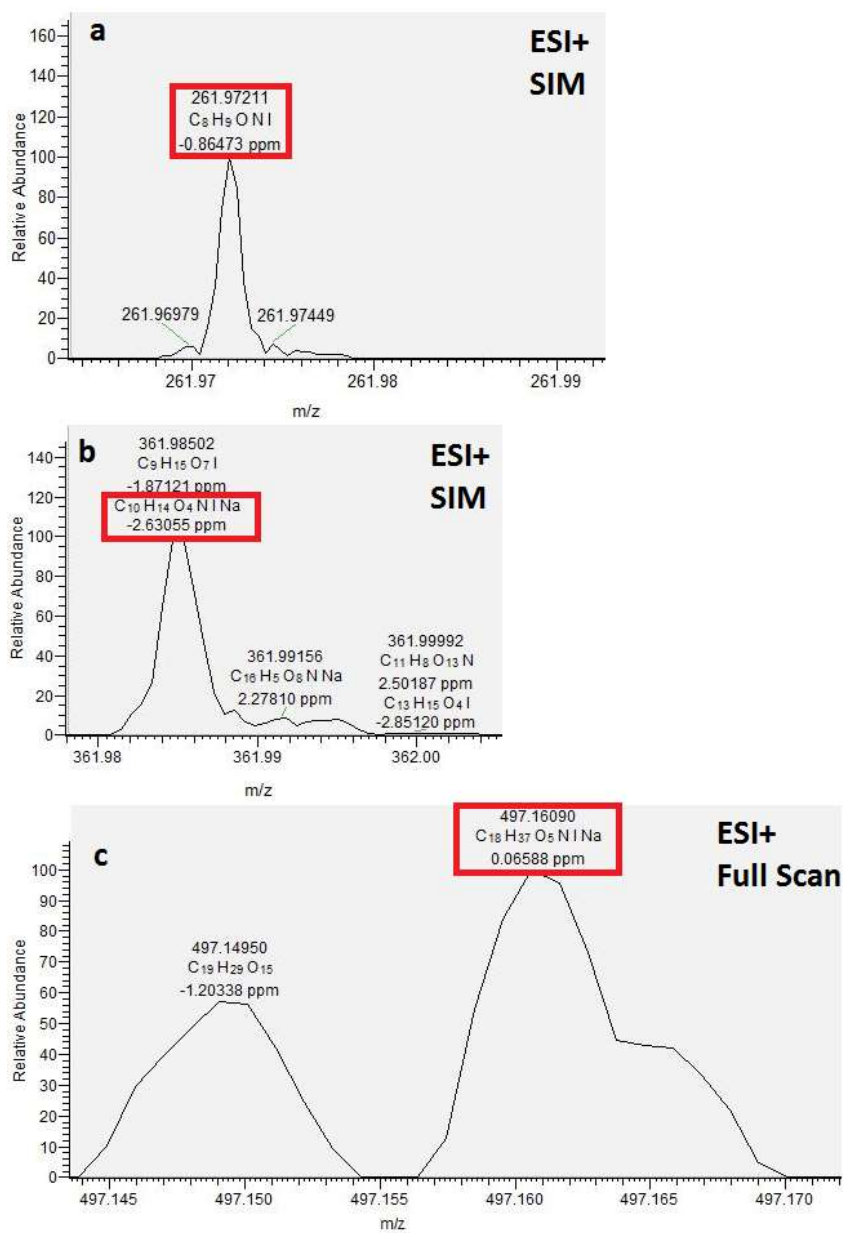


Figure A2.7 Mass spectra of ESI+ $[M+H]^+$ and $[M+Na]^+$ ions matching those identified in ESI- in Table 2.2.

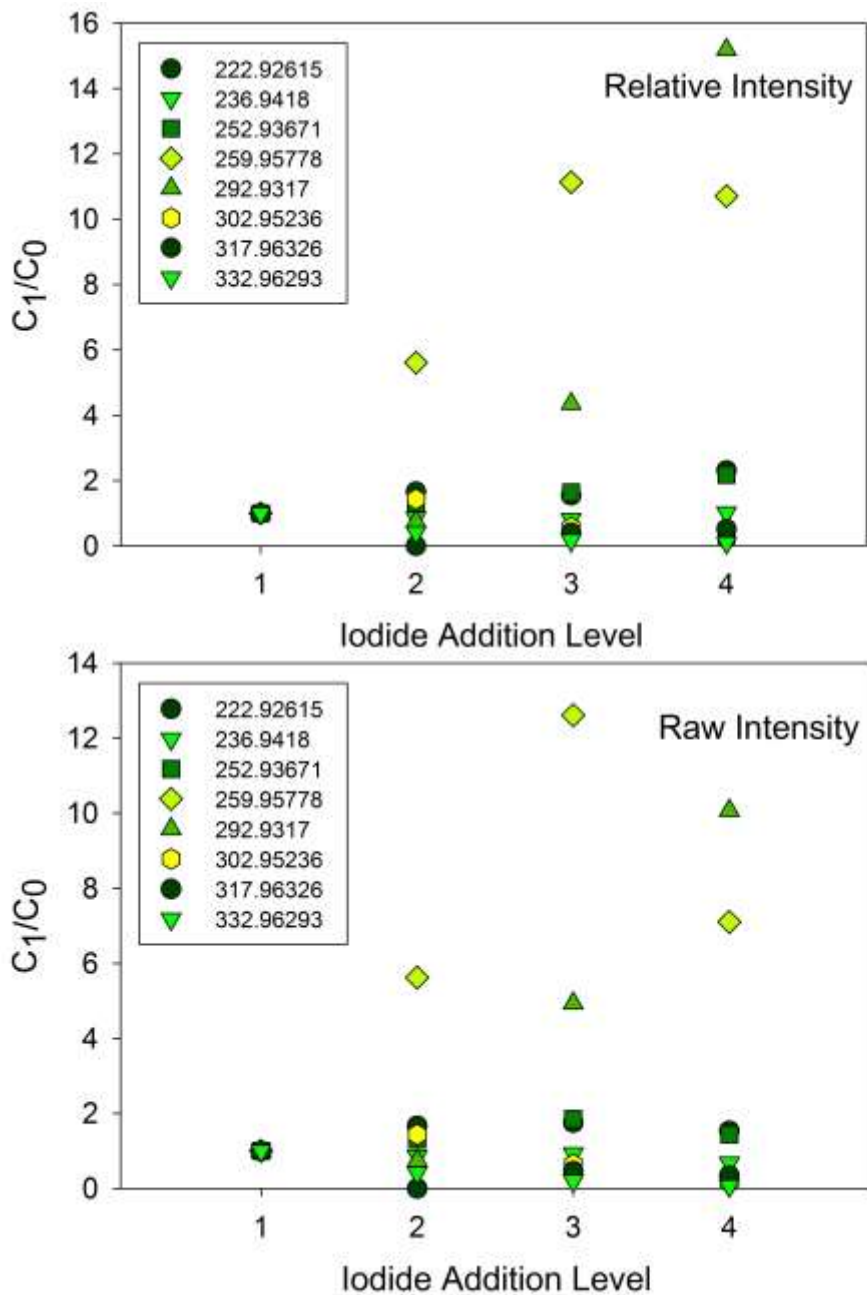


Figure A2.8 Change in iodinated ion peak intensity (Orbitrap FT-MS 100,000 resolution) relative to initial intensity (C_1/C_0) as iodide is added the methanolic extract (FB1). Data is presented as relative intensity (top) and raw intensity (bottom). Iodide addition levels are: Level 1- no addition, Level 2- 0.5 μM I⁻, Level 3- 40 μM I⁻, Level 4- 1.3 mM I⁻

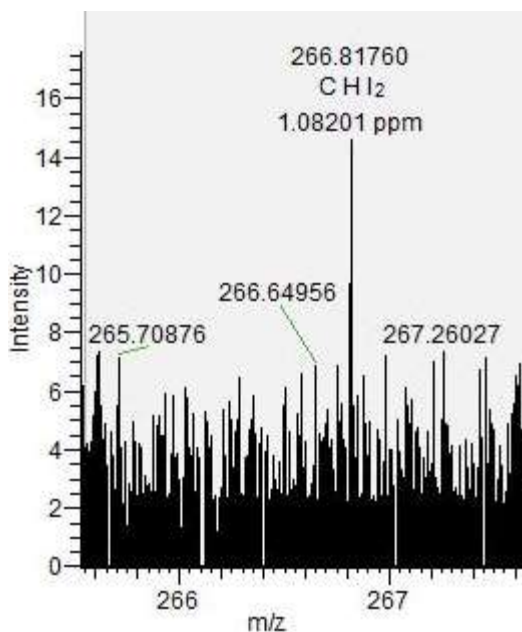


Figure A2.9 Parent peak in fragmentation spectra (CID10, 500 scans) of CHI_2^- ion in PW2 and ppm deviation of formula assignment from theoretical exact mass. No fragments were present above the baseline.

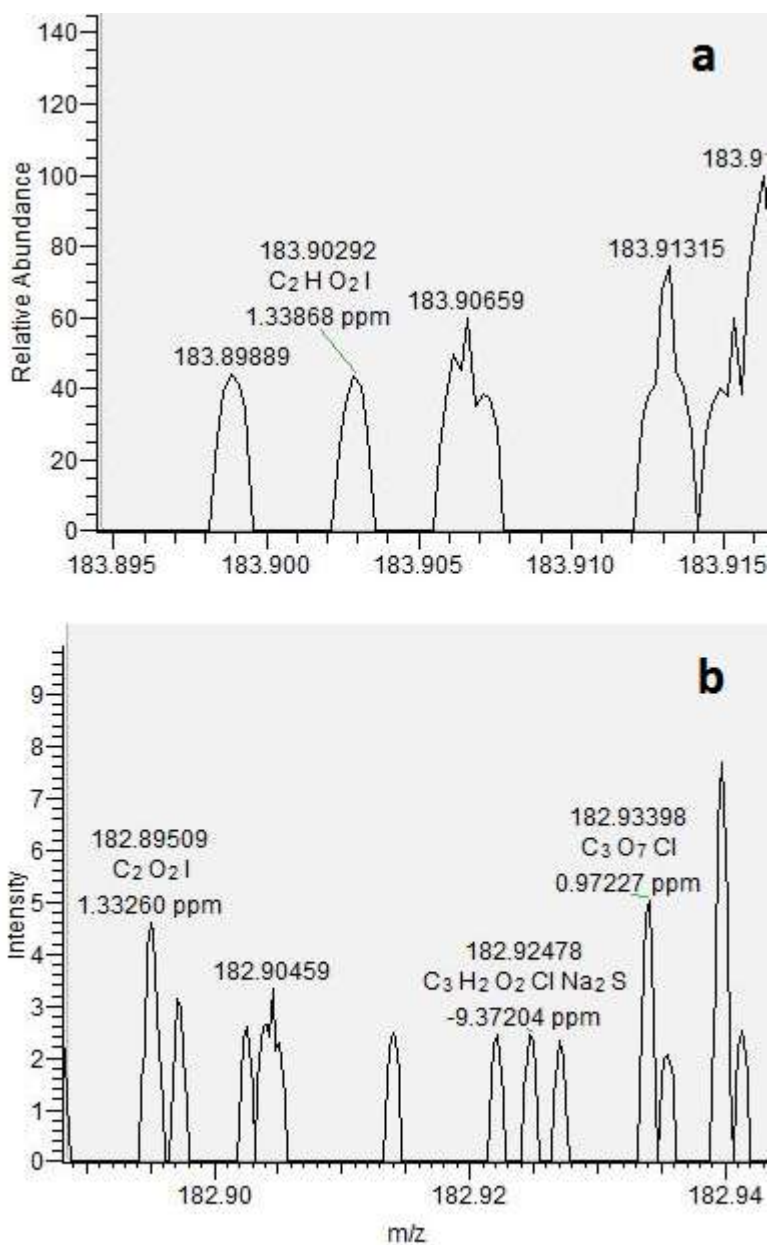


Figure A2.10 Results of fragmentation experiment (CID10, 500 scans) of $C_2HO_2I_2^-$ ion in PW2 and ppm deviation of formula assignment from theoretical exact mass for a) $C_2HO_2I^-$ b) $C_2O_2I^-$. Both fragments are essentially part of the baseline but have the expected ppm error for the instrument in this mass range at the time of the experiment. Parent and I peaks were not distinguishable from the baseline.

Table A2.7 Halogenated disinfection by-products identified in hydraulic fracturing wastewater samples within 0.3 ppm from the list of 384 known halogenated disinfection by-products found in **Table A2.5** above m/z 147. There are many structural isomers so these 259 exact masses were searched for within the samples. *Additional known DBP isomers at the same exact mass: 3-Bromo-5-chloro-2-hydroxybenzoic acid, 3-Bromo-5-chloro-4-hydroxybenzoic acid, +Additional known DBP isomers at the same exact mass: 3,5-Dibromo-2-hydroxybenzoic acid, 3,5-Dibromo-4-hydroxybenzoic acid. a. Exact mass/error given for CL1; CL3 error (0.148 ppm) b. Exact mass/error given for FB1; CL1 error = 0.064 ppm; CL3 error = 0.013 ppm c. Exact mass/error given for PW1; FB1 error = 0.018 ppm; FB2 error = 0.274 ppm.

Measured Ionic Exact Mass	Theoretical Ionic Exact Mass	Mass Error (ppm)	Neutral Formula	Possible Disinfection By-Product	Sample IDed	Intensity
207.04292	207.4296	-0.204	C ₈ H ₁₃ ClO ₄	2-Chlorooctanedioic acid	FB1	2.10E+06
218.87149	218.87153	-0.16	C ₂ H ₂ ClO ₂	Chloriodoacetic acid	FB1	1.03E+07
239.12081	239.1208	-0.039	C ₁₄ H ₂₁ ClO	4-Chloro-2,6-di-tert-butylphenol	PW1	7.46E+06
240.9003	240.90033	-0.112	C ₄ H ₃ IO ₄	Iodobutenedioic acid	FB1	1.75E+06
248.89597	248.896	0.06	C ₇ H ₄ BrClO ₃	3-Bromo-5-chloro-4-hydroxybenzaldehyde*	CL1, CL3 ^a	2.42E+06
262.83495	262.83488	0.274	C ₆ H ₂ Br ₂ O ₂	2,6-Dibromo-(1,4)-benzoquinone	FB7	1.86E+06
276.85061	276.8505	0.274	C ₇ H ₄ Br ₂ O ₂	Dibromobenzoic acid	CL1, CL3, FB1 ^b	2.34E+06
290.91597	290.91598	-0.024	C ₈ H ₅ IO ₄	3-Iodophthalic acid	FB1	3.73E+06
292.84551	292.84545	0.208	C ₇ H ₄ Br ₂ O ₃	3,5-Dibromo-2-hydroxybenzoic acid ⁺	CL3	2.31E+06
310.80717	310.80714	0.096	C ₂ H ₂ I ₂ O ₂	Diiodoacetic acid	FB1, FB2, PW1 ^c	8.09E+06
388.81773	388.81771	0.064	C ₇ H ₄ I ₂ O ₃	5,6-Diiodo-2-hydroxybenzoic acid	FB1	1.52E+07

Methods for Shale Precursor Experiment

The potential for shale-derived organic compounds to act as precursors for disinfection-byproduct formation was investigated by reacting shale drill cuttings with reactive halogens. The specific additives used in hydraulic fracturing wells from which samples were obtained are unknown. Therefore, sodium hypochlorite, a known biocide used in hydraulic fracturing wells (Kahrilas et al., 2015) was selected as the oxidant for these experiments as these results can also be used to understand potential impacts of chlorination during treatment of shale-derived wastewaters. Shale drill cuttings were obtained from the Utica shale and stored cold (4° C) prior to analysis.

Drill cuttings were homogenized using a mortar and pestle and 25 g samples were combined with 500 mL Milli-Q water in eight 1L cleaned glass bottles and placed in the dark on a shaker table at 75 rpm for 24 hours. 500 mL slurries were filtered using 0.7 µm filters (Whatman GF/F, 47mm), then NaBr, or NaI (Sigma Aldrich, >99% and >99.5% purity), at concentrations consistent with flowback and produced waters (250 mg L⁻¹ Br⁻ and 25 mg L⁻¹ I⁻), were added to duplicate samples. 85 µL aliquots of concentrated sodium hypochlorite (13% active chlorine, Acros Organics) were added to the six of the eight filtrate samples containing no salts, NaBr and NaI. As controls, no salts or sodium hypochlorite were added to two 500 mL filtrate samples, and two 500 mL containers of Milli-Q water only was combined with 85 µL of 13% sodium hypochlorite solution to create a 20 mg L⁻¹ solution.

Free chlorine was measured spectrophotometrically immediately using EPA Method 8021 with a Hach Autoanalyzer. After one hour, the free chlorine remaining was measured and was 0.01±0.01 mg L⁻¹ for the chlorinated and brominated waters, and 0.195 mg L⁻¹ for the iodinated waters. Samples were acidified to pH 2 using concentrated formic acid and were solid phase extracted as described previously. Controls of MilliQ water only, MilliQ water and sodium hypochlorite, and shale drill cuttings only were simultaneously extracted. All samples were analyzed by FT-ICR-MS and processed as described for main text.

Appendix 3

MARCELLUS SHALE PRODUCTION &
MSEEL SCIENCE WELLS

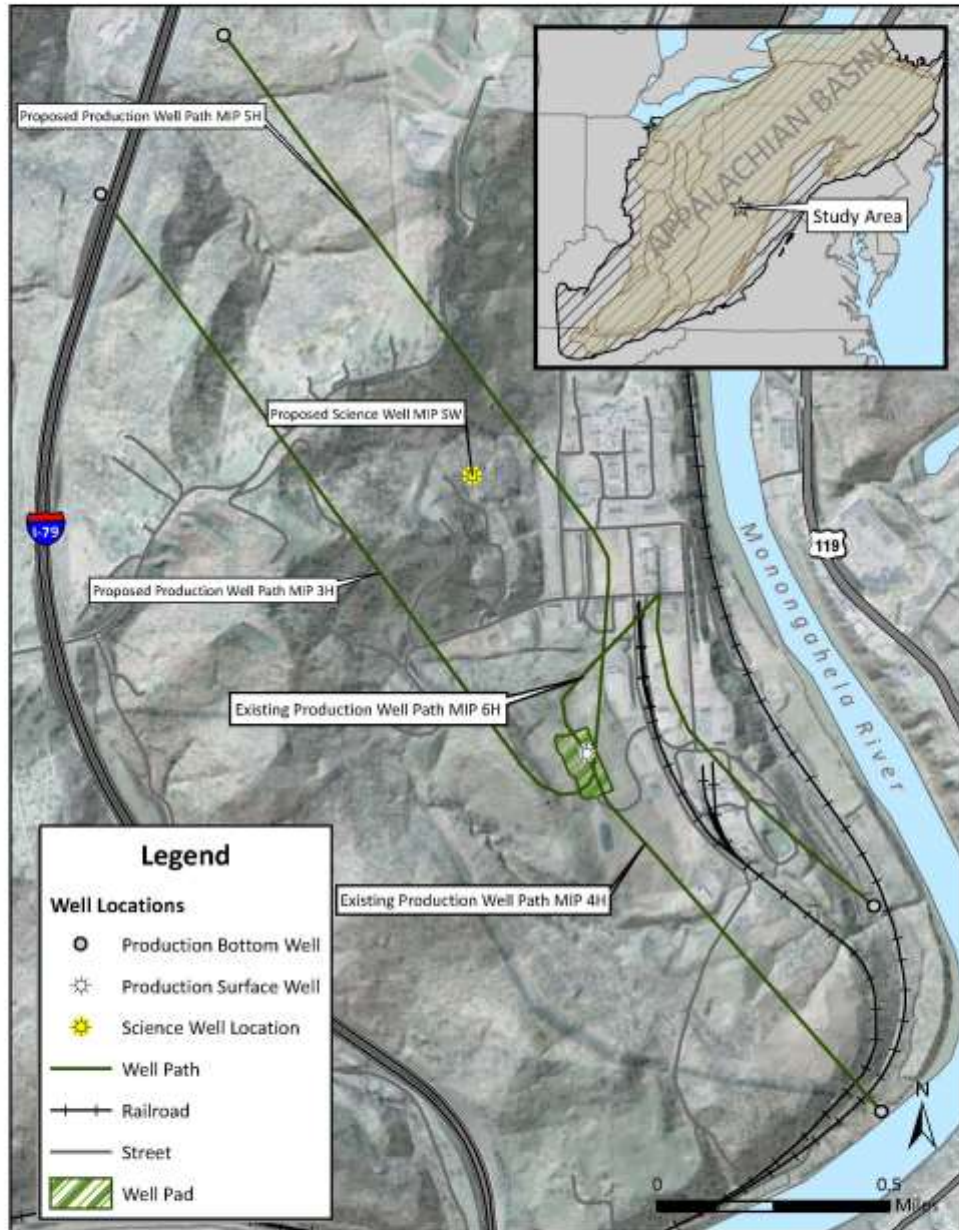


Figure A3.1 MSEEL 3H and 5H well locations; 4H and 6H wells were in existence prior to drilling and hydraulic fracturing 3H and 5H.

Table A3.1 FT-ICR-MS Calibration List

Formula	Exact Mass	Charge
H15C12O6	255.087414	1-
H17C13O6	269.103064	1-
H15C13O7	283.082329	1-
H17C14O7	297.097979	1-
H19C15O7	311.113629	1-
H21C16O7	325.129279	1-
H19C16O8	339.108544	1-
H21C17O8	353.124194	1-
H23C18O8	367.139844	1-
H21C18O9	381.119109	1-
H23C19O9	395.134759	1-
H21C19O10	409.114024	1-
H23C20O10	423.129674	1-
H23C21O10	435.129674	1-
H25C22O10	449.145324	1-
H27C23O10	463.160974	1-
H25C23O11	477.140239	1-
H27C24O11	491.155889	1-
C22H27O13	499.14571	1-
C24H31O12	511.1821	1-
C24H27O13	523.14571	1-
C24H29O13	525.16136	1-
C25H31O13	539.17701	1-
C25H29O14	553.156279	1-
C26H31O14	567.17193	1-
C28H35O14	595.20323	1-
C28H33O15	609.182494	1-
C28H35O15	611.198144	1-
C29H35O15	623.19814	1-
C28H23O18	647.088988	1-
C31H37O16	665.208709	1-
C32H39O16	679.22436	1-
C34H43O16	707.255659	1-
C41H51O19	847.303003	1-

Reproducibility

Following the methods of Sleighter et al., (2012) replicate sample mass spectra were compared to confirm that variability across samples was different from variability among extraction replicates. The intensities of mutual m/z ions within replicate samples collected in June 2016 (Day 179) were plotted against one another and compared to these same overlapping m/z ions present in different sampling months (**Figure A3.2, A3.3**). For the intensity and log intensities of the replicate samples, the linear regression r^2 values were 0.95 and 0.89, respectively, and the log scale more closely followed the $y=x$ line than the raw intensities. In a comparison of the day 179 sample to samples collected on day 116, 214, and 277 a strong linear regression was not observed ($r^2 = 0.07, 0.13, \text{ and } 0.05$, respectively). Hierarchical clustering of m/z ions common to each well (de Hoon et al., 2004) revealed clustering fell according to sampling date; each sample was most similar to the sample collected just prior and just after.

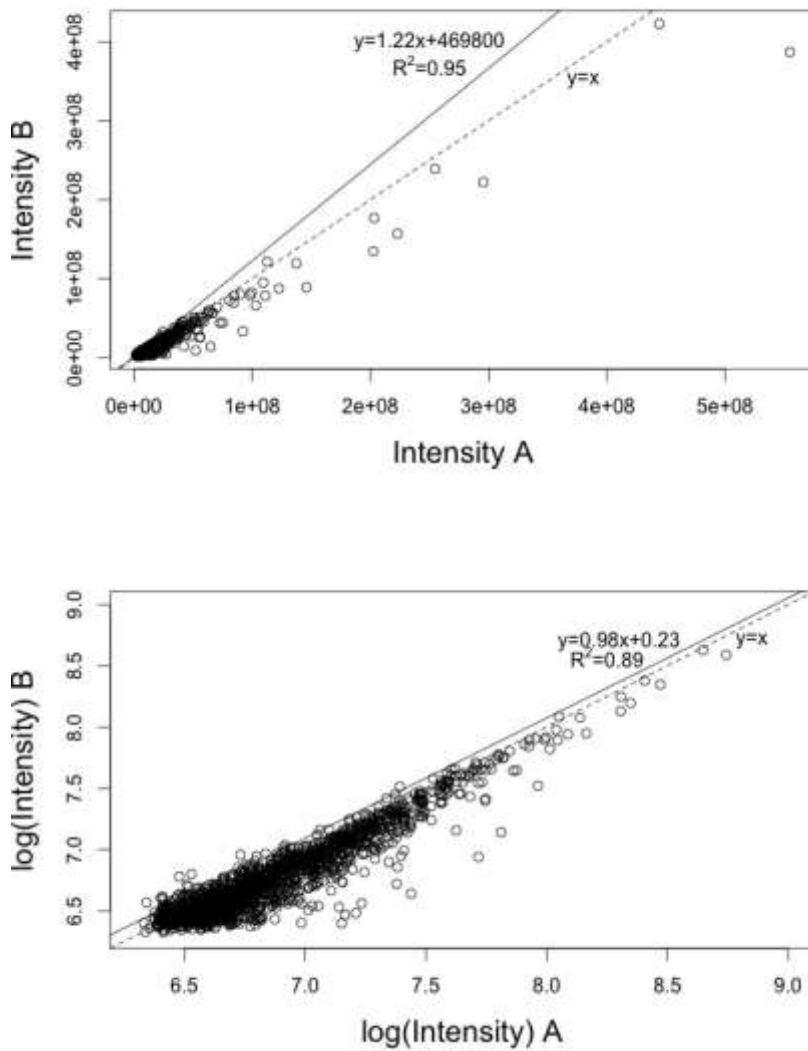


Figure A3.2 Comparison of June 2016 (day 179) duplicate reproducibility showing overlapping ion intensities for duplicate A and duplicate B. Intensity (top), $\log(\text{Intensity})$ (bottom).

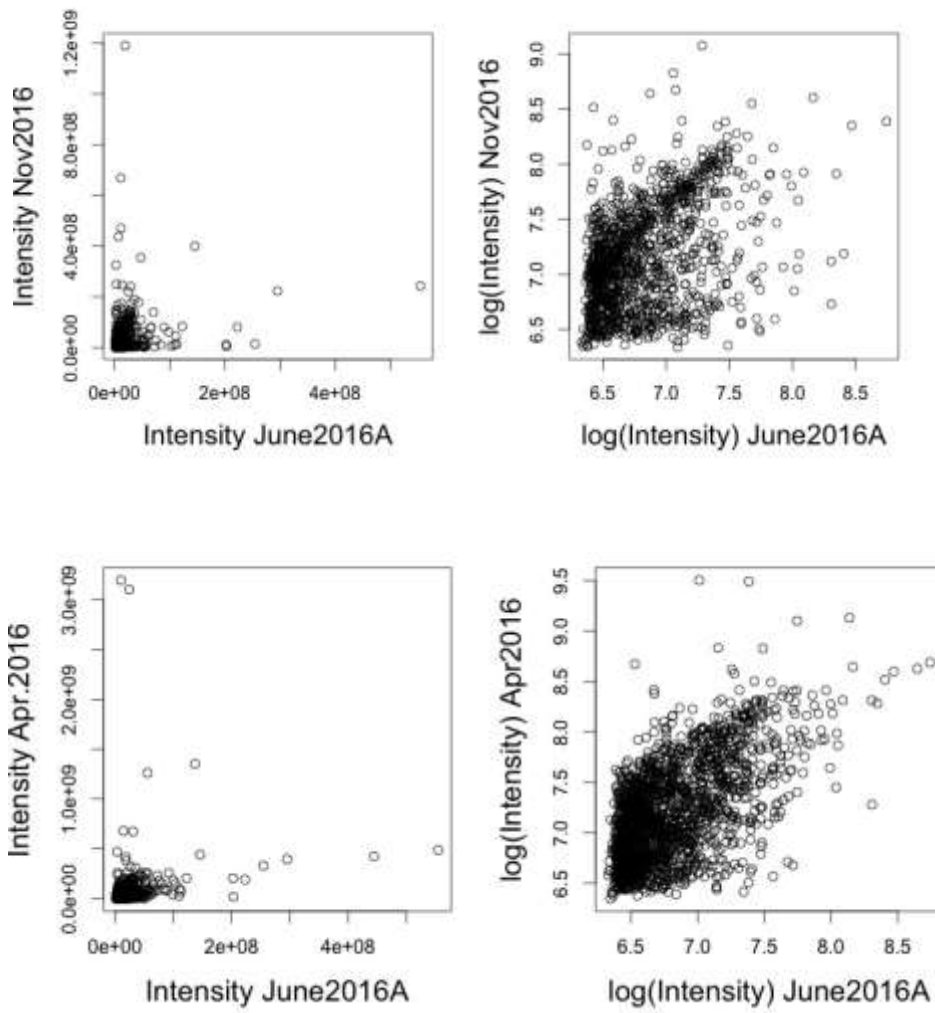


Figure A3.3. Comparison of ion intensities of mutual ions in June (day 179) sample with July (day 214) and April (day 116) samples.

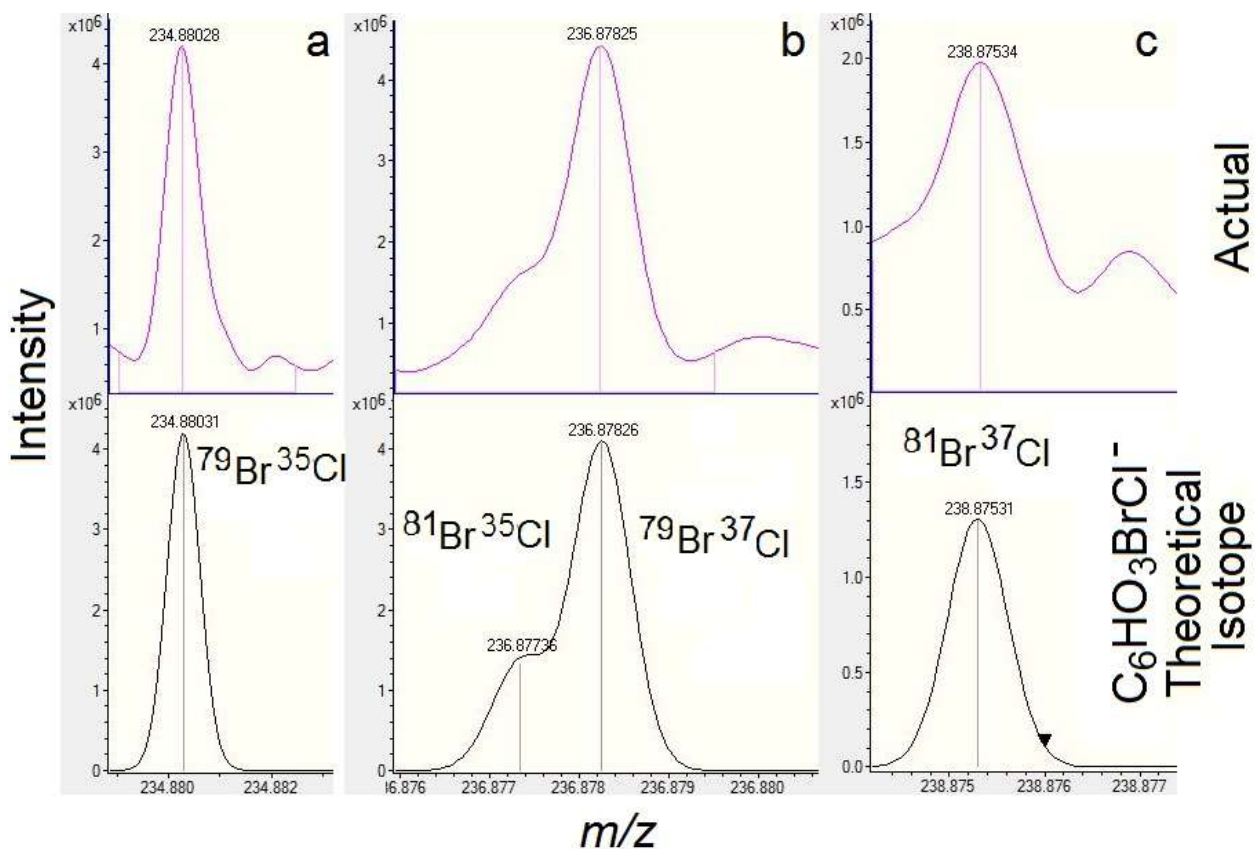


Figure A3.4. Isotopic confirmation of 3H flowback sample (top panels) with respect to theoretical isotopic pattern (bottom panels) for a) $C_6HO_3^{79}Br^{35}Cl^-$ b) $C_6HO_3^{79}Br^{37}Cl^-$ and $C_6HO_3^{81}Br^{35}Cl^-$ c) $C_6HO_3^{81}Br^{37}Cl^-$

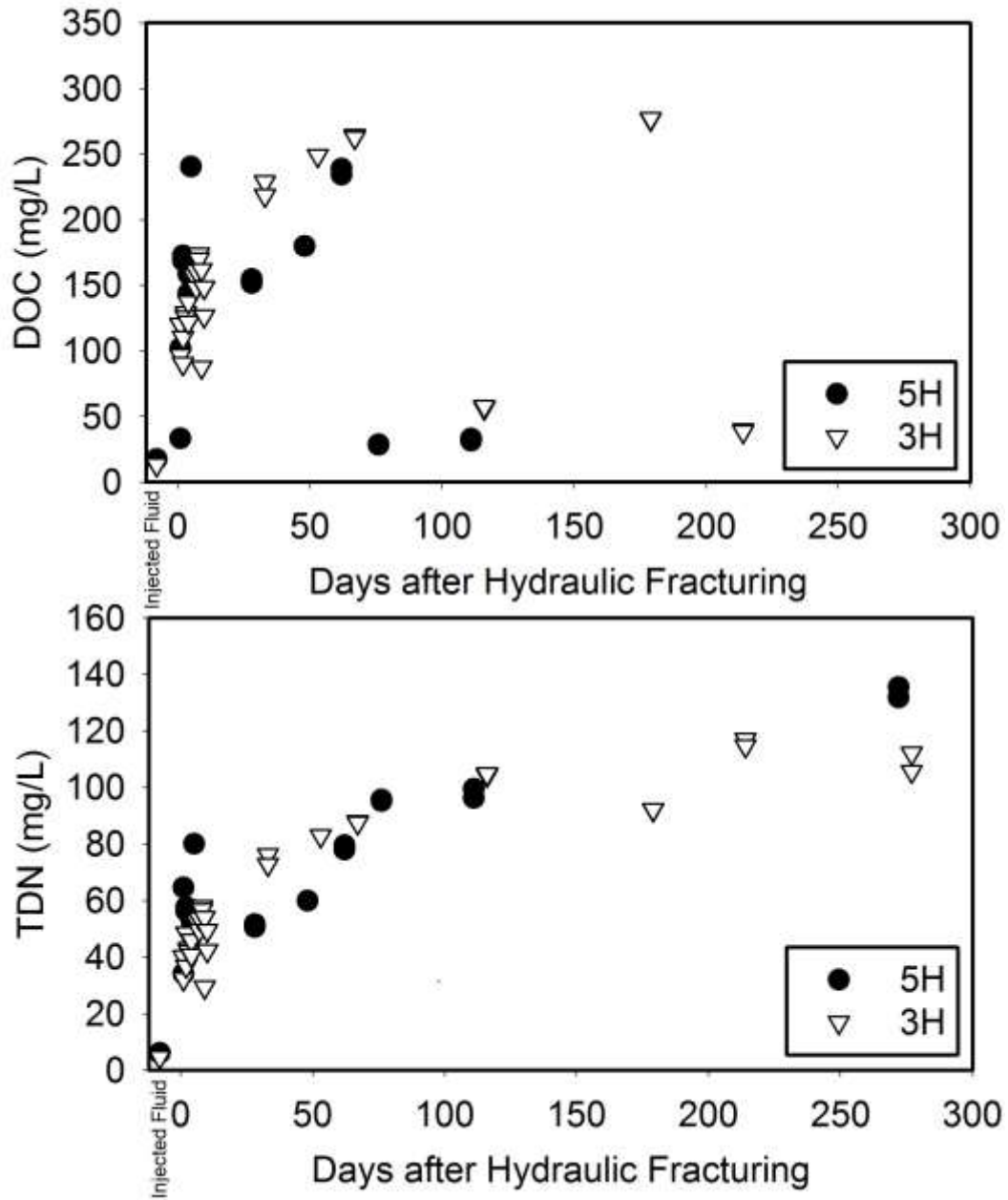


Figure A3.5 Dissolved organic carbon (top) and total nitrogen (bottom) in two adjacent well fluids over first 300 days of return flow, duplicates shown individually.

Table A3.2 Exact masses identified matching ethoxylated carboxylate compounds identified in Wattenberg field produced waters (Thurman et al., 2017). ^Putative identification terminology, polyethylene glycol carboxylate (PEG-C) with number of ethoxymers (EO#) from Thurman et al., 2017.

Measured Mass (<i>m/z</i>)	Putative Ionic Formula [M-H]⁻	Putative identification[^]	Exact Mass (<i>m/z</i>)	Measured Mass Error (ppm)
207.08738	C8H15O6-	PEG-C-EO3	207.08741	0.14
251.11359	C10H19O7-	PEG-C-EO4	251.11363	0.16
295.13985	C12H23O8-	PEG-C-EO5	295.13984	0
339.16608	C14H27O9-	PEG-C-EO6	339.16606	0.06
383.19227	C16H31O10-	PEG-C-EO7	383.19227	0
427.21846	C18H35O11-	PEG-C-EO8	427.21849	0.07
471.2447	C20H39O12-	PEG-C-EO9	471.2447	0.06
515.27085	C22H43O13-	PEG-C-EO10	515.27092	0.14

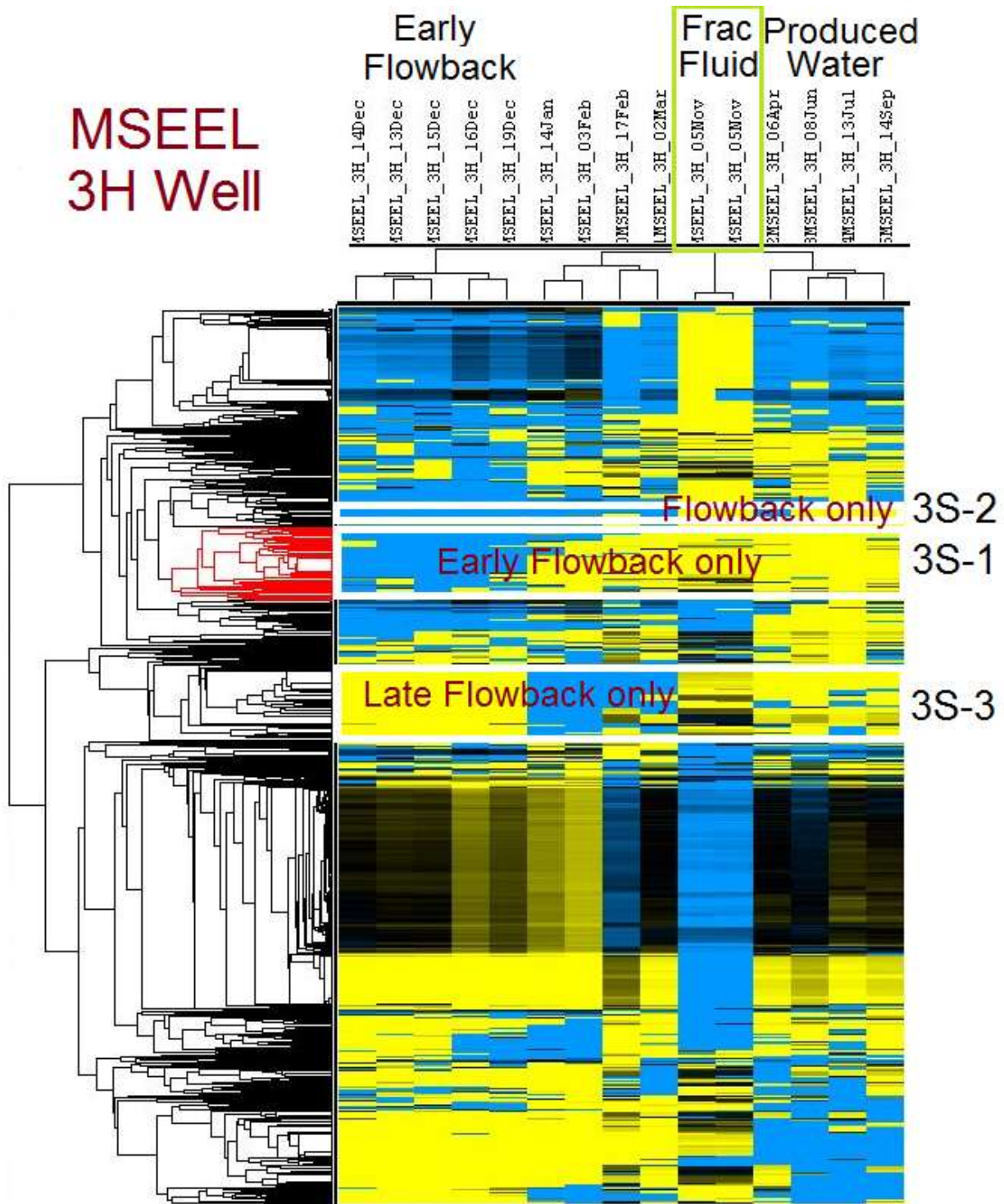


Figure A3.6 Hierarchical clustering of 3H m/z ions present in 2 or more samples with three clusters highlighted; blue (positive/present), yellow (negative/absent).

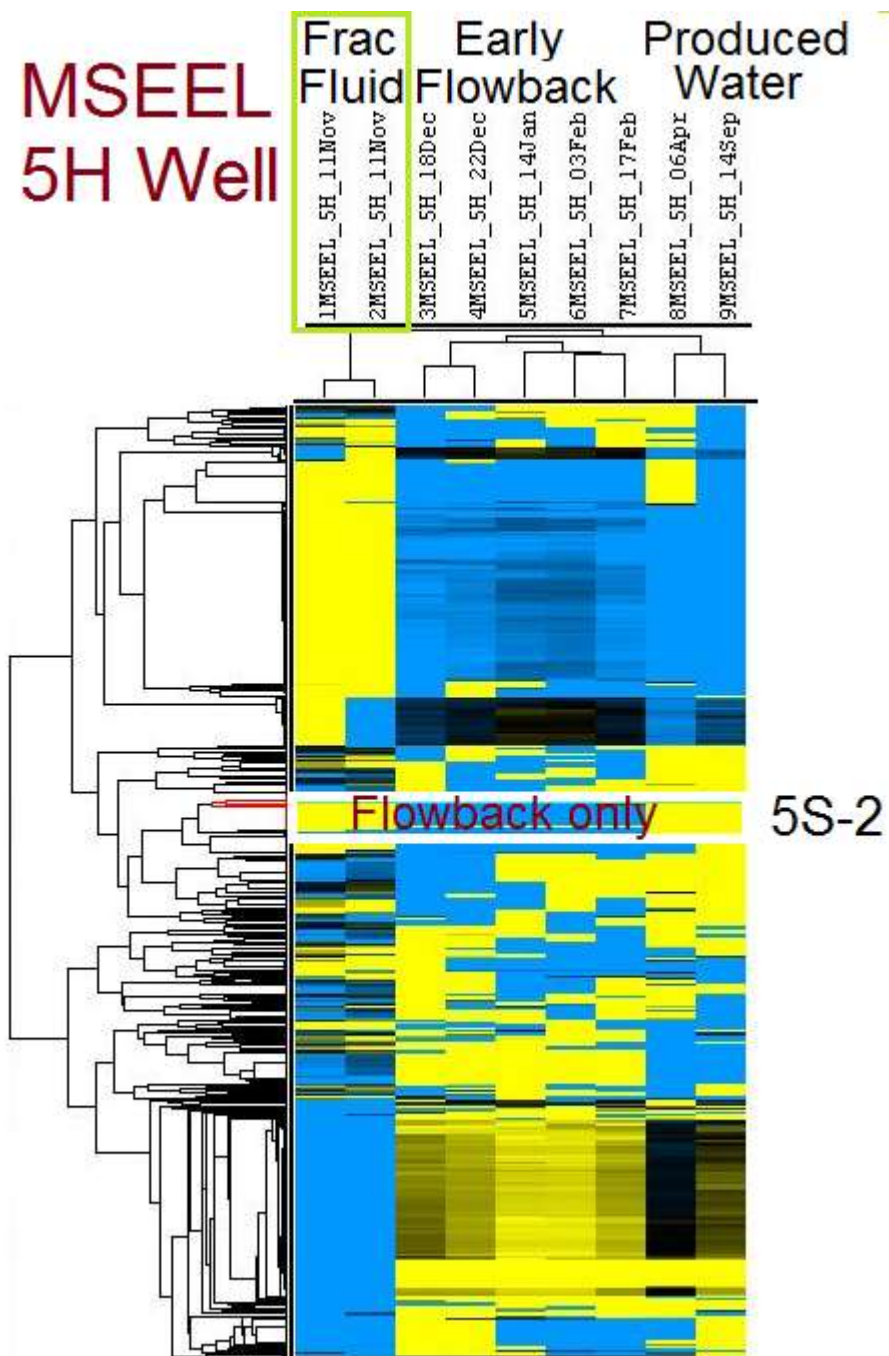


Figure A3.7 Hierarchical clustering of 5H m/z ions present in 2 or more samples with “flowback only” cluster highlighted; blue (positive/present), yellow (negative/absent).

Table A3.3 Specific ion clusters changing over time or unique to flowback and early produced waters and key observations on formula assignments.

	Cluster Group	Well	Number of Ions in Cluster	Cluster	Key observations
3A-1	All Common Ions	3H	585	High in fracturing fluid, decreasing over time	Mostly CHO, many CHON, CHOS
5A-1	All Common Ions	5H	252	High in fracturing fluid, decreasing over time	Isotopically confirmed chlorinated (8) and brominated (2) formula assignments
3A-2	All Common Ions	3H	254	Low in fracturing fluid, increasing over time	Mostly CHO, many CHON, CHOS
5A-2	All Common Ions	5H	479	Low in fracturing fluid, increasing over time	Mostly CHO, some CHON, no CHOS
3A-3	All Common Ions	3H	232	Peaking in only in flowback and early production water	Dominated by sulfur- containing formula
3S-1	Ions in 2+ Samples	3H	535	Only present in flowback and early production water	Few CHO compounds, many CHONS
3S-2	Ions in 2+ Samples	3H	130	Present only in flowback and production water	Few CHO compounds, many CHONS
5S-2	Ions in 2+ Samples	5H	188	Present only in flowback and early production water	Similar numbers of CHO, CHON, CHOS, and CHONS
3S-3	Ions in 2+ Samples	3H	437	Present only in production waters	Dominated by halogenated formulas (155 assigned)

Table A 3.4 Formulas assigned to exact masses $[M-H]^-$ from **Table A3.5** by ion cluster and shown in **Figure 3.2** and **Figure A3.8**. Confidence in formula assignment is given within each cluster. Confidence in formula assignment: IC: isotope pattern confirmed; PI: Previously identified in flowback fluid [isotope and MS-MS confirmation] (Luek et al., 2017); IC-PI-HS: isotope pattern confirmed, previously identified, and member of homologous series PI-HS: previously identified and member of homologous series; HS-IC: member of a homologous series where one or more member was isotopically confirmed in this study; HS: member of a homologous series; US: unsupported but plausible formula assignment.

Confidence in Formula Assignment	Exact Mass Measured	Theoretical Exact Mass	Error (ppm)	H (ionic)	C	O	N	S	Cl	Br	I	kmd/z*	O/C	H/C
<i>3S-3 (3H- Production Waters Only)</i>														
IC	206.96209	206.96213	-0.182	5	7	3	0	0	2	0	0	0.1315	0.429	0.857
IC	217.02727	217.02731	-0.194	10	9	4	0	0	1	0	0	0.0348	0.444	1.222
IC	234.88028	234.88031	-0.128	1	6	3	0	0	1	1	0	0.1880	0.500	0.333
IC	235.03785	235.03788	-0.124	12	9	5	0	0	1	0	0	0.1090	0.556	1.444
IC	244.98582	244.98584	-0.111	6	9	6	0	0	1	0	0	0.0470	0.667	0.778
IC	248.89593	248.89596	-0.131	3	7	3	0	0	1	1	0	0.1880	0.429	0.571
IC	250.91156	250.91161	-0.186	5	7	3	0	0	1	1	0	0.0259	0.429	0.857
IC	254.86205	254.86207	-0.09	2	6	2	0	0	2	1	0	0.0416	0.333	0.500
IC	258.92473	258.92476	-0.114	4	8	5	0	0	0	1	0	0.0597	0.625	0.625
IC	258.96115	258.96115	0.011	8	9	4	0	0	0	1	0	0.0537	0.444	1.000
IC	260.904	260.90403	-0.094	2	7	6	0	0	0	1	0	0.0953	0.857	0.429
IC	262.91159	262.91161	-0.076	5	8	3	0	0	1	1	0	0.1880	0.375	0.750
IC	264.89085	264.89088	-0.085	3	7	4	0	0	1	1	0	0.0285	0.571	0.571
IC	264.92726	264.92726	0.018	7	8	3	0	0	1	1	0	0.0259	0.375	1.000
IC	272.94039	272.94041	-0.09	6	9	5	0	0	0	1	0	0.0597	0.556	0.778
IC	274.91965	274.91968	-0.091	4	8	6	0	0	0	1	0	0.0953	0.750	0.625
IC	278.90654	278.90653	0.036	5	8	4	0	0	1	1	0	0.0285	0.500	0.750

IC	282.85695	282.85699	-0.146	2	7	3	0	0	2	1	0	0.0453	0.429	0.429
IC	282.86645	282.86644	0.053	1	6	3	0	0	1	0	1	0.0443	0.500	0.333
IC	282.94727	282.94728	-0.015	8	7	4	0	0	0	0	1	0.0363	0.571	1.286
IC	282.96116	282.96115	0.037	8	11	4	0	0	0	1	0	0.0349	0.364	0.818
IC	284.87263	284.87264	-0.02	4	7	3	0	0	2	1	0	0.0549	0.429	0.714
IC	284.94038	284.94041	-0.095	6	10	5	0	0	0	1	0	0.0465	0.500	0.700
IC	284.97681	284.9768	0.045	10	11	4	0	0	0	1	0	0.0419	0.364	1.000
IC	286.95606	286.95606	-0.007	8	10	5	0	0	0	1	0	0.0597	0.500	0.900
IC	288.93534	288.93533	0.045	6	9	6	0	0	0	1	0	0.0953	0.667	0.778
IC	290.86621	290.86618	0.092	5	8	2	0	0	0	2	0	0.2260	0.250	0.750
IC	292.88184	292.88183	0.034	7	8	2	0	0	0	2	0	0.0314	0.250	1.000
IC	292.8858	292.88579	0.023	3	8	5	0	0	1	1	0	0.0311	0.625	0.500
IC	292.89524	292.89524	-0.001	2	7	5	0	0	0	0	1	0.0304	0.714	0.429
IC	292.92217	292.92218	-0.017	7	9	4	0	0	1	1	0	0.0285	0.444	0.889
IC	294.94729	294.94728	0.048	8	8	4	0	0	0	0	1	0.0313	0.500	1.125
IC	294.98368	294.98366	0.06	12	9	3	0	0	0	0	1	0.0283	0.333	1.444
IC	295.94117	295.94114	0.086	7	7	7	1	0	0	1	0	0.0348	1.000	1.143
IC	296.92656	296.92654	0.054	6	7	5	0	0	0	0	1	0.0399	0.714	1.000
IC	298.81155	298.81156	-0.021	2	6	2	0	0	1	2	0	0.0645	0.333	0.500
IC	298.95602	298.95606	-0.128	8	11	5	0	0	0	1	0	0.0465	0.455	0.818
IC	300.82719	300.82721	-0.068	4	6	2	0	0	1	2	0	0.0838	0.333	0.833
IC	303.02772	303.02771	0.053	12	12	7	0	0	1	0	0	0.0760	0.583	1.083
IC	306.86112	306.8611	0.092	5	8	3	0	0	0	2	0	0.0339	0.375	0.750
IC	306.90147	306.90144	0.089	5	9	5	0	0	1	1	0	0.0311	0.556	0.667
IC	310.77123	310.77121	0.071	2	6	0	0	0	0	3	0	0.0570	0.000	0.500
IC	316.92221	316.92218	0.1	7	11	4	0	0	1	1	0	0.1065	0.364	0.727
IC	320.91711	320.91709	0.072	7	10	5	0	0	1	1	0	0.0311	0.500	0.800

IC	322.93276	322.93274	0.061	9	10	5	0	0	1	1	0	0.0352	0.500	1.000
IC	322.9786	322.97858	0.08	12	10	4	0	0	0	0	1	0.0313	0.400	1.300
IC	324.92149	324.92146	0.114	6	8	6	0	0	0	0	1	0.0435	0.750	0.875
IC	326.76616	326.76613	0.105	2	6	1	0	0	0	3	0	0.0741	0.167	0.500
IC	328.82218	328.82212	0.167	4	7	3	0	0	1	2	0	0.0898	0.429	0.714
IC	328.89879	328.89885	-0.198	8	9	4	0	0	2	1	0	0.0770	0.444	1.000
IC	330.83783	330.83777	0.178	6	7	3	0	0	1	2	0	0.1313	0.429	1.000
IC	330.91449	330.9145	-0.04	10	9	4	0	0	2	1	0	0.1123	0.444	1.222
IC	332.91315	332.91313	0.067	11	11	2	0	0	0	2	0	0.2260	0.182	1.091
IC	334.85606	334.85601	0.142	5	9	4	0	0	0	2	0	0.0366	0.444	0.667
IC	338.80255	338.80251	0.094	6	8	0	0	0	0	3	0	0.0570	0.000	0.875
IC	338.91937	338.91935	0.074	8	9	4	0	1	0	0	1	0.0453	0.444	1.000
IC	338.97352	338.97349	0.089	12	10	5	0	0	0	0	1	0.0399	0.500	1.300
IC	340.82216	340.82212	0.094	4	8	3	0	0	1	2	0	0.0690	0.375	0.625
IC	342.80145	342.80139	0.181	2	7	4	0	0	1	2	0	0.0958	0.571	0.429
IC	342.82811	342.82808	0.079	5	7	4	0	1	0	2	0	0.0915	0.571	0.857
IC	348.8717	348.87166	0.107	7	10	4	0	0	0	2	0	0.0366	0.400	0.800
IC	362.86962	362.86955	0.176	9	11	2	0	1	0	2	0	0.0378	0.182	0.909
IC	362.88732	362.88731	0.036	9	11	4	0	0	0	2	0	0.0366	0.364	0.909
IC	370.83272	370.83269	0.073	6	9	4	0	0	1	2	0	0.0958	0.444	0.778
IC	372.84835	372.84834	0.025	8	9	4	0	0	1	2	0	0.1405	0.444	1.000
IC-PI-HS	252.93669	252.93671	-0.079	6	6	3	0	0	0	0	1	0.0283	0.500	1.167
PI-HS	222.92612	222.92615	-0.129	4	5	2	0	0	0	0	1	0.0226	0.400	1.000
PI-HS	236.94176	236.9418	-0.143	6	6	2	0	0	0	0	1	0.0226	0.333	1.167
PI-HS	332.96296	332.96293	0.093	10	11	4	0	0	0	0	1	0.2015	0.364	1.000
PI	302.95239	302.95236	0.081	8	10	3	0	0	0	0	1	0.0950	0.300	0.900
HS-IC	266.91597	266.91598	-0.026	4	6	4	0	0	0	0	1	0.0313	0.667	0.833

HS-IC	266.95236	266.95236	-0.001	8	7	3	0	0	0	0	1	0.0283	0.429	1.286
HS-IC	268.93162	268.93163	-0.045	6	6	4	0	0	0	0	1	0.0363	0.667	1.167
HS-IC	280.93166	280.93163	0.117	6	7	4	0	0	0	0	1	0.0313	0.571	1.000
HS-IC	282.9109	282.91089	0.014	4	6	5	0	0	0	0	1	0.0399	0.833	0.833
HS-IC	287.03277	287.03279	-0.077	12	12	6	0	0	1	0	0	0.0470	0.500	1.083
HS-IC	308.96294	308.96293	0.058	10	9	4	0	0	0	0	1	0.0313	0.444	1.222
HS-IC	310.9422	310.94219	0.025	8	8	5	0	0	0	0	1	0.0399	0.625	1.125
HS-IC	312.79084	312.79082	0.054	0	6	3	0	0	1	2	0	0.0690	0.500	0.167
HS-IC	324.95788	324.95784	0.127	10	9	5	0	0	0	0	1	0.0399	0.556	1.222
HS-IC	326.8065	326.80647	0.09	2	7	3	0	0	1	2	0	0.0690	0.429	0.429
HS-IC	330.98226	330.98228	-0.06	12	12	6	0	0	0	1	0	0.0953	0.500	1.083
HS-IC	336.99427	336.99423	0.133	14	11	4	0	0	0	0	1	0.0313	0.364	1.364
HS-IC	338.93714	338.93711	0.087	8	9	6	0	0	0	0	1	0.0435	0.667	1.000
HS-IC	351.00988	351.00988	0.022	16	12	4	0	0	0	0	1	0.0313	0.333	1.417
HS-IC	356.81707	356.81704	0.099	4	8	4	0	0	1	2	0	0.0958	0.500	0.625
HS-IC	362.97353	362.97349	0.094	12	12	5	0	0	0	0	1	0.0304	0.417	1.083
HS-IC	366.9684	366.96841	-0.011	12	11	6	0	0	0	0	1	0.0435	0.545	1.182
HS-IC	367.00485	367.00479	0.168	16	12	5	0	0	0	0	1	0.0399	0.417	1.417
HS-IC	376.98916	376.98914	0.036	14	13	5	0	0	0	0	1	0.0304	0.385	1.154
HS	278.98878	278.98875	0.127	12	9	2	0	0	0	0	1	0.0226	0.222	1.444
HS	304.93163	304.93163	0.005	6	9	4	0	0	0	0	1	0.2015	0.444	0.778
HS	318.91092	318.91089	0.088	4	9	5	0	0	0	0	1	0.2195	0.556	0.556
HS	334.97859	334.97858	0.051	12	11	4	0	0	0	0	1	0.0278	0.364	1.182
HS	346.97858	346.97858	-0.001	12	12	4	0	0	0	0	1	0.2015	0.333	1.083
HS	347.93744	347.93744	-0.003	7	10	5	1	0	0	0	1	0.4450	0.500	0.800
HS	348.99428	348.99423	0.151	14	12	4	0	0	0	0	1	0.0278	0.333	1.250
HS	349.95314	349.95309	0.149	9	10	5	1	0	0	0	1	0.0332	0.500	1.000

HS	354.96843	354.96841	0.064	12	10	6	0	0	0	0	1	0.0528	0.600	1.300
HS	358.90583	358.90581	0.075	4	11	6	0	0	0	0	1	0.1223	0.545	0.455
HS	358.94223	358.94219	0.094	8	12	5	0	0	0	0	1	0.1130	0.417	0.750
HS	360.95788	360.95784	0.113	10	12	5	0	0	0	0	1	0.2195	0.417	0.917
HS	360.99418	360.99423	-0.122	14	13	4	0	0	0	0	1	0.2015	0.308	1.154
HS	361.95312	361.95309	0.071	9	11	5	1	0	0	0	1	0.4450	0.455	0.909
HS	363.9688	363.96874	0.153	11	11	5	1	0	0	0	1	0.0332	0.455	1.091
HS	368.94769	368.94767	0.037	10	10	7	0	0	0	0	1	0.0573	0.700	1.100
HS	368.98406	368.98406	0.018	14	11	6	0	0	0	0	1	0.0528	0.545	1.364
HS	372.92149	372.92146	0.082	6	12	6	0	0	0	0	1	0.1223	0.500	0.583
HS	372.95786	372.95784	0.053	10	13	5	0	0	0	0	1	0.1130	0.385	0.846
HS	374.97352	374.97349	0.086	12	13	5	0	0	0	0	1	0.2195	0.385	1.000
HS	377.98439	377.98439	-0.012	13	12	5	1	0	0	0	1	0.0332	0.417	1.167
HS	382.9633	382.96332	-0.071	12	11	7	0	0	0	0	1	0.0573	0.636	1.182
HS	386.9371	386.93711	-0.029	8	13	6	0	0	0	0	1	0.1223	0.462	0.692
HS	386.9735	386.97349	0.012	12	14	5	0	0	0	0	1	0.1130	0.357	0.929
HS	396.97897	396.97897	-0.014	14	12	7	0	0	0	0	1	0.0573	0.583	1.250
US	225.05351	225.05353	-0.091	14	8	5	0	0	1	0	0	0.0160	0.625	1.875
US	170.98543	170.98545	-0.119	4	7	3	0	0	1	0	0	0.0199	0.429	0.714
US	395.22066	395.22059	0.158	36	19	6	0	0	1	0	0	0.0214	0.316	1.947
US	278.95236	278.95236	-0.018	8	8	3	0	0	0	0	1	0.0252	0.375	1.125
US	186.98034	186.98036	-0.118	4	7	4	0	0	1	0	0	0.0278	0.571	0.714
US	334.9561	334.95606	0.103	8	14	5	0	0	0	1	0	0.0294	0.357	0.643
US	321.95817	321.95818	-0.004	9	9	4	1	0	0	0	1	0.0304	0.444	1.111
US	254.95233	254.95236	-0.126	8	6	3	0	0	0	0	1	0.0326	0.500	1.500
US	334.90583	334.90581	0.078	4	9	6	0	0	0	0	1	0.0330	0.667	0.556
US	379.00476	379.00479	-0.076	16	13	5	0	0	0	0	1	0.0343	0.385	1.308

US	376.91638	376.91637	0.012	6	11	7	0	0	0	0	1	0.0356	0.636	0.636
US	377.94805	377.94801	0.116	9	11	6	1	0	0	0	1	0.0360	0.545	0.909
US	294.81225	294.81223	0.068	1	2	1	0	0	0	0	2	0.0426	0.500	1.000
US	336.8353	336.83528	0.064	3	8	5	0	0	0	2	0	0.0446	0.625	0.500
US	350.85094	350.85093	0.052	5	9	5	0	0	0	2	0	0.0446	0.556	0.667
US	352.91641	352.91637	0.112	6	9	7	0	0	0	0	1	0.0472	0.778	0.778
US	299.91969	299.91968	0.037	7	6	3	1	1	0	0	1	0.0584	0.500	1.333
US	313.93536	313.93533	0.073	9	7	3	1	1	0	0	1	0.0584	0.429	1.429
US	327.95101	327.95098	0.1	11	8	3	1	1	0	0	1	0.0584	0.375	1.500
US	396.94254	396.94259	-0.113	10	11	8	0	0	0	0	1	0.0619	0.727	1.000
US	286.92102	286.92106	-0.147	4	9	3	0	0	0	0	1	0.0655	0.333	0.556
US	398.99464	398.99462	0.044	16	12	7	0	0	0	0	1	0.0742	0.583	1.417
US	356.92658	356.92654	0.12	6	12	5	0	0	0	0	1	0.0777	0.417	0.583
US	343.94594	343.9459	0.134	11	8	4	1	1	0	0	1	0.0864	0.500	1.500
US	357.92518	357.92516	0.061	9	8	5	1	1	0	0	1	0.0936	0.625	1.250
US	371.94087	371.94081	0.147	11	9	5	1	1	0	0	1	0.0936	0.556	1.333
US	370.75592	370.75596	-0.094	2	7	3	0	0	0	3	0	0.1087	0.429	0.429
US	372.88844	372.88844	-0.019	6	8	7	0	1	0	0	1	0.1305	0.875	0.875
US	386.90076	386.90072	0.111	4	12	7	0	0	0	0	1	0.1313	0.583	0.417
US	375.1369	375.13686	0.094	24	21	4	0	0	1	0	0	0.1380	0.190	1.190
US	375.04891	375.04884	0.194	16	15	9	0	0	1	0	0	0.1820	0.600	1.133
US	304.96803	304.96801	0.045	10	10	3	0	0	0	0	1	0.1830	0.300	1.100
US	388.95278	388.95276	0.051	10	13	6	0	0	0	0	1	0.2375	0.462	0.846
US	388.91633	388.91637	-0.1	6	12	7	0	0	0	0	1	0.2560	0.583	0.583
US	249.93706	249.93705	0.056	5	6	2	1	0	0	0	1	0.3360	0.333	1.000
US	333.95819	333.95818	0.051	9	10	4	1	0	0	0	1	0.4090	0.400	1.000
<i>3S-1 (3H Flowback and Early Production Water Only)</i>														

US	341.17358	341.17364	-0.175	30	15	6	0	0	1	0	0	0.0251	0.400	2.067
US	265.89557	265.89558	-0.01	1	5	4	1	0	0	0	1	0.0304	0.800	0.400
<i>3S-2 (3H Flowback and Production Water Only)</i>														
IC	344.74032	344.74031	0.045	0	5	3	0	0	0	3	0	0.1595	0.600	0.200
IC	308.84038	308.84036	0.073	3	7	4	0	0	0	2	0	0.0415	0.571	0.571
<i>5S-2 (5H Flowback and Early Production Water Only)</i>														
IC	233.05858	233.05861	-0.13	14	10	4	0	0	1	0	0	0.049	0.400	1.500

Table A3.4 Exact mass [M-H]⁻ lists for selected ion clusters [from all ions appearing in 2 or more samples for a given well]; cluster title corresponding to presence at a given time period and therefore absence at other (i.e., absence from fracturing fluid and produced waters).

3S-1 (3H Flowback and Early Production Water Only)	3S-3 (3H Production Water Only)	3S-2 (3H Flowback and Production Water Only)	5S-2 (5H Flowback and Early Production Water Only)
158.05398	161.02441	180.07471	183.04977
165.03055	170.98543	181.06351	192.06660
166.98421	186.98034	182.05733	207.03321
173.00792	206.96209	190.05095	207.10600
174.02303	214.01233	198.00438	211.08106
176.03867	217.02727	198.04887	216.55089
176.06455	218.99684	201.03920	217.09035
180.03022	219.02429	208.02511	223.05628
180.03833	219.07742	220.99137	224.02000
180.99986	220.14683	222.04411	227.08443
183.04977	220.90099	225.08968	227.97942
186.02303	221.06823	227.07596	229.05061
188.03530	222.89895	228.99895	230.01282
189.01932	222.92612	232.06150	233.05858
197.02777	223.05193	241.01019	236.02000
197.07920	225.05351	242.04923	236.09617
197.15469	230.92980	244.02850	237.07850
198.95626	232.92777	246.04413	237.12609
203.11748	232.97608	253.01760	239.04166
204.03020	234.88028	259.01378	239.09584
206.08224	235.03785	261.00407	239.12081
208.01073	235.89755	261.04382	240.03356
209.05675	236.87822	262.91815	241.03871
211.09901	236.94176	266.05862	243.06761
212.93551	237.90874	266.99686	246.01190
218.04585	238.87524	268.02850	246.04419
218.07510	239.01161	270.03362	247.01675
218.10334	240.99895	271.08565	248.02002
220.03324	242.01283	271.11067	250.00738
223.04678	242.03063	271.11317	251.14175
223.05630	242.97823	274.10847	253.03872
223.07403	244.98582	276.05948	253.06621
223.10090	246.01183	276.08062	254.01284
224.93553	248.89593	276.99897	255.01889
226.95118	248.97193	278.08340	256.07547
227.01846	249.89928	278.08577	260.02340
227.06767	249.93706	279.03329	262.04324
228.03358	250.07543	279.09305	264.04295
228.98120	250.88460	281.13459	266.16078
230.01284	250.89300	286.05841	269.10102
230.92831	250.89389	286.99095	272.04119
233.02775	250.91156	287.04424	272.10560
234.04417	251.89723	290.03873	273.02607

236.02002	252.89095	290.07852	274.06832
236.10088	252.90864	292.04964	275.06733
236.91902	252.90953	292.09416	276.09585
237.02270	252.93669	294.04753	276.99898
238.02131	254.86205	299.07073	277.05529
239.00191	254.90659	300.05138	278.04211
239.00532	254.95233	300.08774	280.04962
239.04172	256.85910	304.99390	280.94399
239.09586	256.85999	308.84038	282.04416
239.12082	258.85706	309.08152	282.99179
239.12329	258.92473	309.08998	283.14705
239.98281	258.94342	310.07550	284.03154
240.02307	258.96115	312.01834	285.11660
240.98122	260.90400	313.09624	286.07211
241.03872	260.92266	315.07551	286.99097
242.03874	262.87526	317.07341	287.09715
244.04779	262.90194	319.02819	287.13226
246.97739	262.91159	319.08870	289.04847
248.02003	262.94989	319.59038	290.03402
248.10091	264.05888	322.02860	291.06225
249.87108	264.86923	323.04422	293.01257
250.11655	264.89085	324.00782	293.05862
250.89832	264.90957	324.05473	293.06114
251.07545	264.92727	325.03541	294.02557
252.01497	266.88793	327.19102	298.07549
252.03695	266.88881	328.06088	299.01974
252.06284	266.90653	328.06897	299.14196
252.09925	266.91597	330.03366	300.04426
252.13221	266.92519	331.03154	300.05138
252.87968	266.95236	333.01082	302.03063
253.02099	267.85184	334.13298	302.05264
254.03061	267.89215	336.07589	303.19997
254.04921	268.88586	339.06567	306.02554
254.98248	268.93162	340.04966	309.08996
255.09071	270.86644	342.06195	309.09244
256.96174	272.94039	344.04118	310.07545
256.99390	274.91965	344.04612	312.03615
256.99813	274.93837	344.74032	312.06288
257.06014	274.95994	348.13814	313.05000
258.00777	275.13227	349.07516	313.09624
259.00955	276.86922	352.08600	317.14282
260.02008	276.91760	354.10165	318.03364
260.19480	278.86711	356.05271	318.03704
260.99301	278.90654	356.12546	319.02822
261.03884	278.92519	357.08610	319.05723
262.04322	278.95236	360.03954	319.59038
262.08019	278.98878	360.09365	320.04930
262.86530	279.85184	360.14860	320.05268
262.91297	280.82774	363.05438	320.11732
263.00539	280.90444	368.08089	321.01081
263.03671	280.93166	370.05686	322.05041
263.05053	280.94403	370.10465	322.21390
263.07723	281.11834	371.12342	322.22340

263.11184	282.82575	372.03949	323.04425
264.04297	282.85695	372.08064	323.05210
264.05471	282.86646	372.12280	324.01841
264.12413	282.91090	373.13598	324.03611
264.93379	282.94727	376.13305	326.07847
265.89557	282.96116	378.05815	327.11191
266.01624	283.95064	378.08642	328.06092
266.05261	284.85492	378.20368	328.08268
266.16078	284.87263	379.61938	328.13055
266.85892	284.94039	380.04455	330.07012
266.89533	284.95911	380.07375	330.10647
267.03663	284.97681	382.02382	331.03155
267.07481	286.05032	382.06017	333.01085
267.12716	286.83022	383.00788	334.02864
269.01591	286.87059	384.08709	334.12250
270.02553	286.92102	384.11215	341.05794
270.97741	286.93835	385.02014	343.10681
271.02482	286.95606	386.08815	344.04116
271.95490	286.97477	386.12784	345.12071
272.00898	287.03277	386.13593	346.06499
272.04119	288.86763	388.07078	348.04762
272.05644	288.93534	388.14019	348.13004
272.95667	288.95403	390.05815	349.08734
273.06037	290.86621	390.12284	349.11403
273.08652	292.12241	391.03408	349.23843
274.21049	292.88184	392.07370	352.05776
274.98668	292.88580	394.08937	353.03037
275.06734	292.89524	394.19520	355.05405
276.01498	292.91250	395.13811	355.10998
276.09584	292.92217	396.03949	356.04122
277.05526	293.04894	396.10488	359.16556
278.91308	293.05460	396.16980	360.03614
278.94948	293.96333	397.17152	360.03951
279.00024	294.81225	398.09959	360.09357
279.03663	294.87980		360.15800
279.04788	294.88373		362.05513
279.07096	294.92014		364.03915
279.13351	294.94729		364.09906
280.02849	294.98368		365.01509
280.03189	295.94117		365.10782
280.04964	296.10021		365.63488
280.06827	296.87777		366.04674
280.94527	296.91715		366.08644
281.03524	296.92656		366.14104
282.04755	297.09241		367.04602
283.03154	297.93916		368.11724
283.04932	298.07675		370.05688
283.05718	298.81155		370.06832
283.07088	298.93283		370.09319
283.12209	298.95602		370.10466
284.00904	299.81495		370.10712
284.14196	299.91969		370.13295
284.95664	299.93616		371.13810

284.99308	300.79082		372.03615
285.11662	300.82719		372.04760
286.03571	300.85786		372.08062
286.97233	300.95400		372.09117
287.02648	301.81287		372.14862
287.06584	302.80660		373.11728
287.10223	302.80747		376.16942
287.96761	302.82518		378.20366
288.01834	302.85582		379.61937
288.22618	302.95239		380.08079
288.95158	303.02772		380.12119
289.04661	303.81080		381.06162
290.03402	304.78673		382.09649
290.04210	304.80453		382.10039
290.11149	304.82312		383.07320
290.91311	304.84549		383.08712
290.98589	304.85287		384.05729
291.12717	304.86416		384.07246
292.00990	304.93163		386.05178
296.02341	304.96803		386.07288
296.02682	306.18258		387.61681
296.06319	306.84342		388.07553
297.98833	306.86112		388.08851
298.02471	306.90147		388.14014
298.97230	306.98631		388.14835
299.01976	308.85905		389.01499
299.10221	308.89943		389.01834
299.98411	308.92995		390.04668
300.98797	308.96295		390.05473
301.96548	310.77124		390.05810
301.98322	310.85703		390.14065
302.10679	310.87471		390.16395
302.94950	310.89645		391.03400
302.98165	310.94220		394.04967
304.06564	311.84168		394.19524
304.99728	312.79084		396.08390
305.92401	312.81759		396.10485
306.02893	313.93536		399.16946
306.90802	314.78879		399.21770
306.92734	314.82519		
307.10166	314.86157		
307.91982	316.12314		
308.01293	316.76509		
308.06321	316.78672		
309.01084	316.82297		
309.05846	316.92221		
309.13773	318.78381		
310.03908	318.91092		
310.07885	318.92016		
310.08487	320.19825		
310.88520	320.91711		
310.92156	321.01814		
311.02649	321.95818		

311.10470	322.89343		
311.14013	322.91505		
312.00397	322.93276		
312.02651	322.97860		
312.05136	322.99090		
312.84671	323.18978		
313.04212	323.84167		
313.05001	323.87803		
313.15579	323.94554		
313.98324	324.85400		
313.99768	324.92149		
315.98111	324.95788		
315.99891	325.14792		
316.01329	326.10343		
316.02138	326.76616		
316.05445	326.80650		
316.12716	327.95102		
317.05026	328.80445		
317.14282	328.82218		
317.23337	328.84082		
318.02890	328.89879		
318.99517	329.80779		
319.03164	329.82551		
319.13334	330.80239		
319.93966	330.81045		
320.11734	330.82009		
320.12538	330.83783		
320.92369	330.89677		
320.93905	330.91449		
320.94302	330.96462		
321.01082	330.98226		
321.93546	331.07837		
321.94387	331.82342		
322.03913	332.76002		
322.04246	332.77261		
322.07552	332.79949		
322.11258	332.81803		
322.13300	332.83573		
322.19523	332.91315		
322.97071	332.96296		
322.97571	333.82139		
323.02654	333.95819		
323.03774	334.77055		
323.93123	334.78826		
324.01838	334.81512		
324.05811	334.83832		
324.79978	334.85606		
324.90083	334.90583		
324.93513	334.95610		
325.00574	334.97859		
325.04214	335.94553		
325.05002	335.98199		
325.05987	336.76763		

325.13264	336.78619		
326.01962	336.83530		
326.03060	336.85403		
326.03739	336.90906		
326.06703	336.99427		
326.96728	337.05105		
326.98160	337.96125		
327.00364	338.78331		
327.11190	338.80255		
327.99888	338.83326		
328.00700	338.85192		
328.02141	338.86966		
328.13841	338.91937		
328.16822	338.93714		
328.98286	338.97352		
328.99937	339.16023		
329.01930	339.89077		
329.07646	340.16363		
329.07799	340.78116		
329.08134	340.82216		
329.11276	340.83122		
329.96040	340.86758		
329.99680	340.91512		
330.00064	341.88862		
330.01115	342.80145		
330.01454	342.82010		
330.02556	342.82811		
330.99355	343.88663		
330.99521	343.94594		
331.09216	344.00819		
331.09698	344.10986		
331.95619	344.79637		
331.96313	344.79936		
332.07382	344.81804		
332.15039	344.82606		
332.23123	344.83575		
332.99150	346.77469		
333.00750	346.79727		
333.95530	346.81512		
334.02859	346.82402		
334.03913	346.87473		
334.11264	346.94226		
334.12250	346.97858		
334.14103	347.93744		
335.02648	347.97396		
336.05480	348.22143		
336.09178	348.77257		
336.95494	348.79437		
337.05337	348.87170		
337.89610	348.99428		
338.00424	349.73956		
338.02350	349.95314		
338.03402	350.85094		

338.04211	351.00989		
338.05675	351.94049		
338.06321	351.97689		
338.10684	352.84889		
338.12790	352.86758		
338.88011	352.88530		
338.95080	352.91641		
338.99671	353.95611		
339.01462	354.77972		
339.04920	354.84681		
339.05774	354.96843		
339.89188	355.15514		
340.01329	356.81707		
340.03528	356.84529		
340.05307	356.92659		
340.89577	357.92518		
341.01928	358.73824		
341.04491	358.81503		
341.07643	358.90583		
341.11523	358.94223		
341.17358	359.09520		
341.20667	360.10501		
342.01454	360.75498		
342.02891	360.77697		
342.03704	360.81288		
342.05095	360.82291		
342.09832	360.95788		
342.99858	360.99418		
343.00958	361.95312		
343.05271	362.23702		
343.06064	362.77495		
343.09209	362.86962		
343.09370	362.88732		
343.15979	362.97353		
343.97603	363.00612		
344.03019	363.80546		
345.07287	363.96880		
345.08610	364.11840		
345.12070	364.77201		
346.00942	364.88524		
346.02041	365.10886		
346.02388	365.95618		
346.02859	366.86456		
346.11320	366.88327		
346.19527	366.96840		
347.00787	367.00485		
347.02314	367.04594		
347.05214	368.86250		
347.15339	368.94769		
347.95319	368.98406		
348.04762	370.75592		
348.80332	370.77461		
349.00576	370.82302		

349.08644	370.83272		
349.11403	371.94087		
350.05514	372.05813		
350.07037	372.75393		
350.10750	372.77169		
351.06900	372.79033		
351.91174	372.82096		
351.92946	372.83064		
352.01330	372.84835		
352.05304	372.88844		
352.07238	372.92149		
352.14360	372.95786		
352.20580	373.19657		
352.91113	373.85168		
352.91510	374.23705		
352.97803	374.75187		
353.04833	374.78831		
353.06484	374.81889		
353.21812	374.82864		
353.90755	374.84631		
354.01457	374.97352		
354.96555	375.04891		
354.97390	375.13690		
355.00973	375.84968		
355.05404	376.25273		
355.06061	376.72207		
356.03017	376.74985		
356.04122	376.84429		
356.99224	376.86196		
357.03980	376.91638		
357.07131	376.98916		
357.12242	377.13393		
358.02045	377.84763		
358.02872	377.94805		
358.03195	377.95610		
358.98690	377.98439		
359.02987	377.99255		
359.05216	378.72003		
359.10172	378.73776		
359.12489	378.76543		
359.97096	378.82813		
360.04429	378.84130		
360.15803	378.86461		
360.97160	378.90092		
361.03877	379.00476		
361.04208	379.72340		
361.93247	379.97178		
361.96884	380.00819		
362.05516	380.73570		
362.12076	380.76636		
363.01803	380.99220		
363.02136	381.72138		
364.09727	382.71599		

364.99413	382.73370		
365.92739	382.96330		
365.94515	384.71300		
365.99105	385.00581		
366.06525	385.79358		
366.08642	386.80991		
366.13880	386.90077		
368.00816	386.93710		
368.03408	386.97350		
368.04122	387.79165		
368.07757	388.74881		
368.08900	388.91633		
368.11000	388.95278		
368.84381	390.74676		
369.11013	391.04922		
369.86818	393.95103		
370.00941	395.22066		
371.08706	396.87175		
371.13808	396.94254		
372.00731	396.97897		
372.03614	398.86961		
372.04422	398.99464		
372.14860	399.10445		
373.00920			
373.06780			
373.07106			
373.10419			
373.11732			
373.12527			
373.98659			
374.02295			
375.01803			
375.02137			
375.08673			
375.09666			
375.27524			
375.94810			
376.03107			
376.03914			
376.04249			
376.04959			
377.03697			
377.06271			
378.02888			
378.10249			
379.00342			
379.03410			
379.05267			
379.12567			
379.62735			
380.03405			
380.08080			
380.11818			

380.23710			
381.02519			
381.06161			
381.10783			
381.11016			
382.05688			
382.09649			
382.10047			
382.15422			
383.00452			
383.05548			
383.12585			
383.14997			
383.16218			
383.21092			
383.22869			
383.88379			
384.03613			
384.04435			
384.10884			
384.12026			
384.16987			
385.10263			
385.10484			
385.13898			
385.14145			
385.87963			
386.09629			
386.99952			
387.00281			
387.08343			
387.08675			
387.11984			
387.14088			
387.18599			
387.61686			
388.03106			
388.04250			
388.07555			
388.84888			
389.01502			
389.06270			
389.10236			
389.13543			
389.96372			
390.05484			
390.11226			
390.14871			
391.04748			
392.03404			
393.05759			
393.06830			
393.15875			

394.04163			
394.06011			
394.15418			
395.00798			
395.04088			
396.07579			
397.02007			
397.12929			
397.13898			
397.14143			
398.05175			
398.18545			
399.00270			
399.08196			
399.09963			

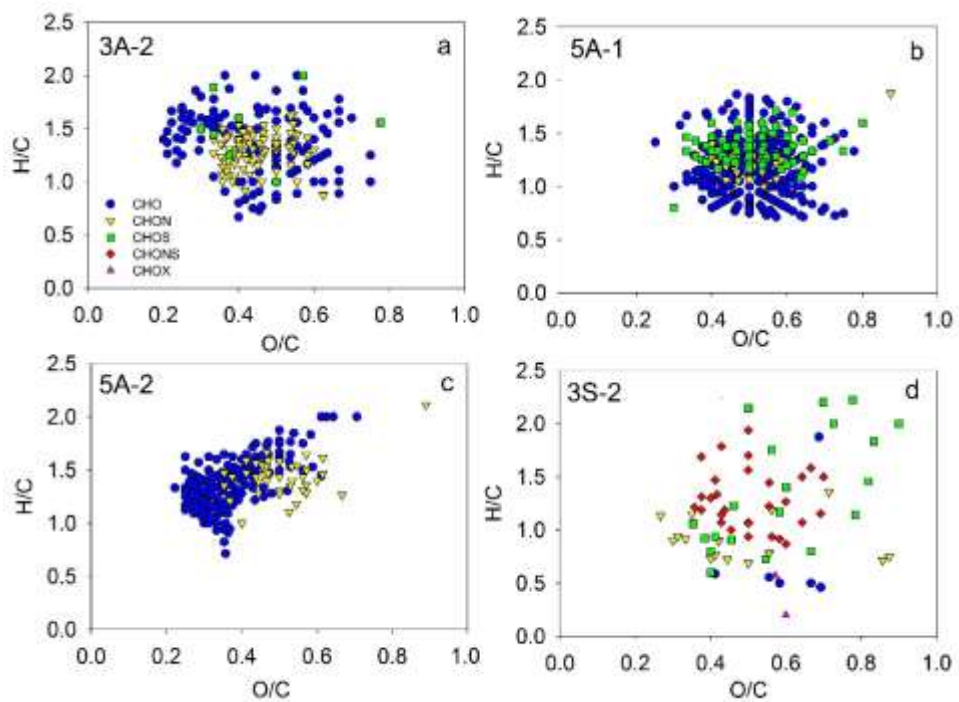


Figure A3.8 Distribution of formulas assigned to ions present in clusters described in **Table A3.4** not shown in **Figure 3.2**.

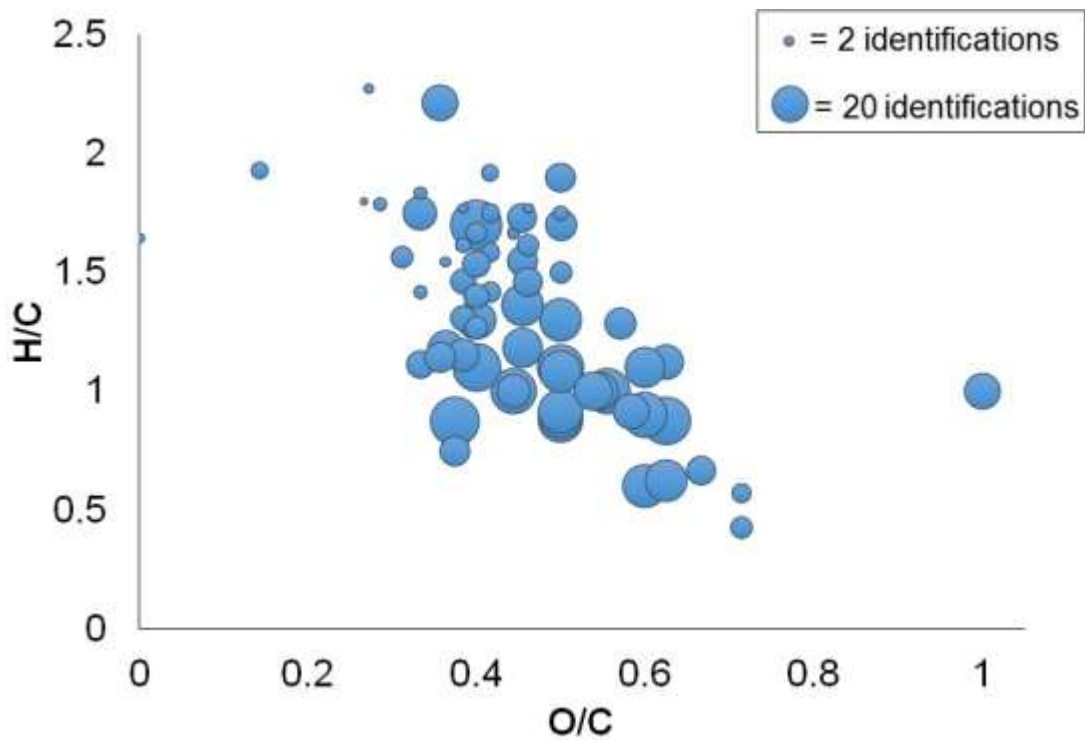


Figure A3.9 Van Krevelen diagram of iodinated formulas assigned to m/z ions identified in fluid samples.

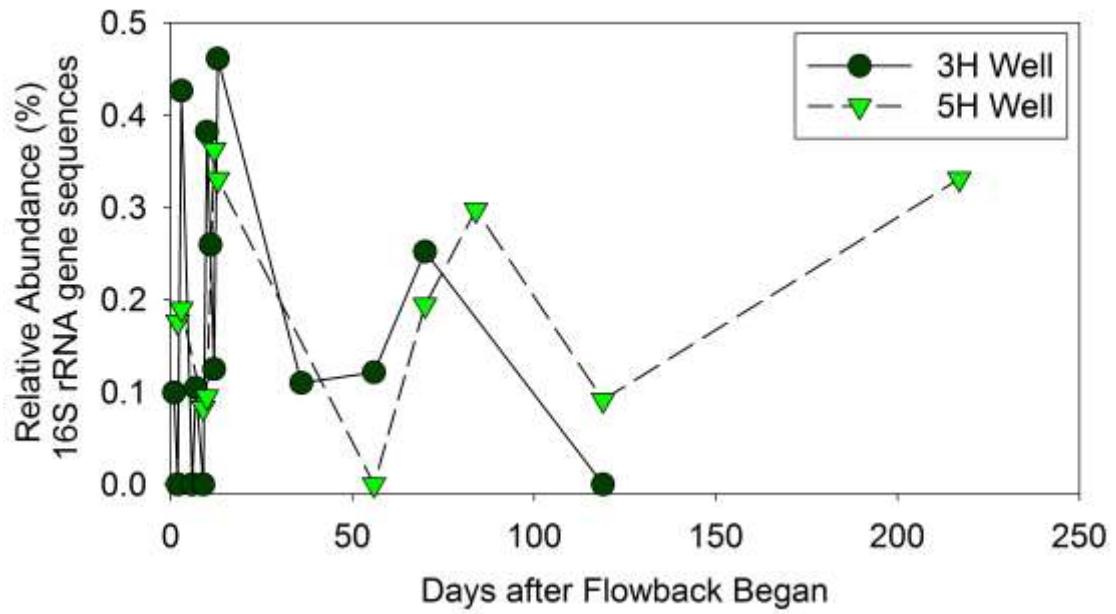


Figure A3.10 *Roseovarius* spp. percent abundance of total 16S rRNA gene sequences in 3H and 5H wells (unpublished data from Kelly Wrighton using methods from Cluff et al., 2014; Daly et al., 2016).

Appendix 4

Table A4.1 Water quality data for acute toxicity test on early flowback fluids. DO = dissolved oxygen.

Pre-animal		12:02 PM				Free Chlorine
		5/9/17				
% of Whole Effluent	Sample Replicate	pH	Conductivity (uS)	Temp (C)	DO (mg/L)	
0	Combined	7.2	313	24	8.53	
6.25%	Combined	6.62	324	23.6	8.56	
12.50%	Combined	6.69	325	23.2	8.49	
25%	Combined	6.64	321	23.4	9.17	
50%	Combined	6.68	321	23.2	8.82	
100%	Combined	6.75	248	23.3	9.24	0.025
48-Hr		12:55PM				
		5/11/17				
% of Whole Effluent	Sample Replicate	pH	Conductivity (uS)	Temp (C)	DO (mg/L)	
0	A	7.16	536	24.2	7.96	
0	B	7.12	407	24.1	8.5	
0	C	6.89	407	23.8	8.47	
0	D	6.82	659	24	8.4	
6.25%	A	6.75	313	24.1	8.37	
6.25%	B	6.94	398	23.9	8.42	
6.25%	C	6.95	394	24.3	8.31	
6.25%	D	6.81	384	24	8.35	
12.50%	A	6.84	266	24.2	8.31	
12.50%	B	6.79	380	24.3	8.24	
12.50%	C	6.88	415	24.5	8.27	
12.50%	D	6.82	478	24.4	8.25	
25%	A	6.87	545	24.4	8.1	
25%	B	6.89	405	24.5	8.24	
25%	C	6.95	388	24.7	8.26	
25%	D	6.98	404	24.5	8.21	
50%	A	7.04	405	24.6	8.23	
50%	B	6.99	420	24.8	8.2	
50%	C	7.02	411	24.8	8.21	
50%	D	6.99	447	24.8	8.3	
100%	A	7.02	463	24.6	8.21	
100%	B	7.05	399	24.8	8.14	
100%	C	7.17	393	24.8	8.12	
100%	D	7.13	454	24.8	8.13	

Table A4.2 Water quality data for acute toxicity test on potassium chloride control run alongside early flowback fluid test. DO = dissolved oxygen.

12:02 PM						
Pre-animal			5/9/17			
Concentration- KCl Control (mg/L)	Replicate	pH	Conductivity (uS)	Temp (C)	DO (mg/ L)	Free Chlorine (mg/L)
0	Combined	7.2	313	24	8.53	
50	Combined	6.94	418	23.8	9.08	
150	Combined	6.78	609	23	9.17	
300	Combined	6.74	885	23.4	9.04	
600	Combined	6.69	1470	23.3	9.07	0.01
12:55PM						
48-Hr			5/11/17			
Concentration- KCl Control (mg/L)	Replicate	pH	Conductivity (uS)	Temp (C)	DO (mg/ L)	
0	A	7.16	536	24.2	7.96	
0	B	7.12	407	24.1	8.5	
0	C	6.89	407	23.8	8.47	
0	D	6.82	659	24	8.4	
50	A	7.01	491	24	8.51	
50	B	7	514	24.2	8.38	
50	C	7.07	555	24.8	8.15	
50	D	7.08	584	24.5	8.3	
150	A	7.03	701	24.8	8.27	
150	B	7.04	679	24.7	8.33	
150	C	7.08	742	24.7	8.15	
150	D	7.11	744	24.8	8.26	
300	A	7.04	1240	24.9	8.17	
300	B	7.03	1110	25.1	8.17	
300	C	7.1	1180	25.3	8.12	
300	D	7.12	1100	25.1	8.12	
600	A	7.03	2160	25	8.1	
600	B	7.03	2440	25	8.09	
600	C	7.08	2160	25	8.12	
600	D	7.19	NA	25.1	NA	

Table A4.3 Water quality data for acute toxicity test on late flowback fluids. DO = dissolved oxygen.

Pre-animal		10:30AM 5/31/17					Free Chlorine
% of Whole Effluent	Sample Replicate	pH	Conductivity (uS)	Temp (C)	DO (mg/L)	(mg/L)	
0	Combined	7.73	307	24.3	8.48	0	
6.25%	Combined	8.18	300	23.4	8.23		
12.50%	Combined	8.11	292	23.5	8.26		
25%	Combined	8.01	295	23.8	8.3		
50%	Combined	7.91	298	23.8	8.43		
100%	Combined	7.88	300	23.7	8.58	0.01	

48-Hr		12:00PM 6/2/17				
% of Whole Effluent	Sample Replicate	pH	Conductivity (uS)	Temp (C)	DO (mg/L)	
0%	A	8.29	343	23.9	8.3	
0%	B	8.3	339	24.1	8.3	
0%	C	8.31	344	24.2	8.3	
0%	D	8.35	341	24.3	8.3	
6.25%	A	8.38	358	23.8	8.3	
6.25%	B	8.4	340	24.3	8.3	
6.25%	C	8.4	362	23.7	8.3	
6.25%	D	8.43	347	23.5	8.3	
12.5%	A	8.4	358	23.5	8.3	
12.5%	B	8.43	342	24	8.3	
12.5%	C	8.4	344	24.1	8.3	
12.5%	D	8.47	338	24.2	8.3	
25%	A	8.42	346	24	8.62	
25%	B	8.39	353	23.9	8.63	
25%	C	8.42	339	24	8.56	
25%	D	8.43	343	24.6	8.45	
50%	A	8.4	334	24.6	8.45	
50%	B	8.42	335	24.7	8.38	
50%	C	8.38	335	24.8	8.34	
50%	D	8.4	366	24.4	8.42	
100%	A	8.4	346	24.7	8.33	
100%	B	8.41	321	24.8	8.32	
100%	C	8.42	335	24.6	8.36	
100%	D	8.4	337	24.6	8.38	

Table A4.4 Water quality data for acute toxicity test on potassium chloride control run alongside early flowback fluid test. DO = dissolved oxygen.

Pre-animal		10:30AM 5/31/17					Free Chlorine
KCl Control (mg/L)	Sample Replicate	pH	Conductivity (uS)	Temp (C)	DO (mg/L)	(mg/L)	
0	Combined	7.73	307	24.3	8.48	0	
50	Combined	7.98	400	24.9	8.43		
150	Combined	8.07	585	24.7	8.42		
300	Combined	8.1	875	24.9	8.4		
600	Combined	8.17	1430	24.8	8.53	0.03	
48-Hr		12:00PM 6/2/17					
KCl Control (mg/L)	Sample Replicate	pH	Conductivity (uS)	Temp (C)	DO (mg/L)		
0	A	8.29	343	23.9	8.3		
0	B	8.3	339	24.1	8.3		
0	C	8.31	344	24.2	8.3		
0	D	8.35	341	24.3	8.3		
50	A	8.41	442	24.8	8.31		
50	B	8.38	462	24.5	8.4		
50	C	8.39	427	24.7	8.4		
50	D	8.4	452	24.6	8.36		
150	A	8.16	636	24.3	8.47		
150	B	8.24	625	24.4	8.45		
150	C	8.24	638	24.4	8.45		
150	D	8.28	622	24.5	8.44		
300	A	8.28	927	24	8.58		
300	B	8.3	977	24.1	8.56		
300	C	8.32	915	24.5	8.46		
300	D	8.34	923	24.3	8.5		
600	A	8.19	1590	24.1	8.5		
600	B	8.32	1490	24.7	8.52		
600	C	8.33	1580	24.3	8.58		
600	D	8.38	1560	24.2	8.59		

Table A4.5 Water quality data for chronic toxicity test on early flowback fluids. DO = dissolved oxygen. DO and pH measurements were taken before and after each daily static renewal.

Negative Control (0% FF)	Temp (C)	DO init (mg/L)	DO final (mg/L)	pH init	pH final	Conductivity (uS)
Day 0	23	8.4	8.25	7.9	8.5	295
Day 1	23.7	8.58	8.4	7.5	8.6	295
Day 2	24	8.52	8.22	7.6	8.4	298
Day 3	23.4	8.66	8.29	7.6	8.4	297
Day 4	23.1	8.61	NA	7.6	8.6	297
Day 5	23	8.73	8.06	8.1	8.7	296
Day 6	24.4	8.42	8.22	8.6	8.6	307
Day 7	24.3	8.36	8.27	7.6	8.5	306
Day 8	23	8.47	8.1	7.5	8.6	295

100% FF	Temp (C)	DO init (mg/L)	DO final (mg/L)	pH init	pH final	Conductivity (uS)
Day 0	23.6	8.66	8.35	7.8	8.4	304
Day 1	24	8.6	8.34	8.1	8.5	303
Day 2	24.1	8.63	8.27	8	8.4	297
Day 3	23.2	8.63	8.44	8	8.3	298
Day 4	23.4	8.61	8.61	8	8.6	299
Day 5	23.2	8.66	8.21	8.2	8.6	298
Day 6	23.6	8.43	8.17	8.5	8.6	290
Day 7	23.9	8.38	8.87	8.1	8.5	293
Day 8	23.1	8.65	8	8	8.6	299

50% FF	Temp (C)	DO init (mg/L)	DO final (mg/L)	pH init	pH final	Conductivity (uS)
Day 0	23.5	8.63	8.18	7.7	8.4	301
Day 1	24.1	8.62	8.43	8	8.5	305
Day 2	24.2	8.58	8.29	8	8.4	301
Day 3	23.4	8.67	8.46	8	8.4	300
Day 4	23.4	8.6	8.54	8	8.6	304
Day 5	23.8	8.68	8.26	8.2	8.6	312
Day 6	24.2	8.48	8.18	8.5	8.5	306
Day 7	24.4	8.34	9	8.2	8.7	188
Day 8	23.1	8.65	8.01	8	8.6	297

25% FF	Temp (C)	DO init (mg/L)	DO final (mg/L)	pH init	pH final	Conductivity (uS)
Day 0	23.5	8.66	8.34	7.8	8.4	297
Day 1	23.9	8.57	8.48	8	8.5	305
Day 2	24.4	8.54	8.34	7.9	8.5	303
Day 3	23.4	8.58	8.51	7.9	8.4	304
Day 4	23.3	8.57	8.58	8	8.6	307
Day 5	24	8.7	8.28	8.2	8.5	313
Day 6	24.4	8.45	8.16	8.6	8.5	312
Day 7	24.3	8.37	8.78	8	8.6	304
Day 8	23.1	8.62	8	7.9	8.5	300

12.5% FF	Temp (C)	DO init (mg/L)	DO final (mg/L)	pH init	pH final	Conductivity (uS)
Day 0	23.4	8.7	8.37	7.8	8.4	290
Day 1	24	8.65	8.57	7.9	8.5	303
Day 2	24.3	8.5	8.41	7.9	8.4	303
Day 3	23.4	8.6	8.54	7.8	8.4	303
Day 4	23.2	8.59	8.62	7.9	8.6	306
Day 5	24	8.69	8.34	8.2	8.5	310
Day 6	24.4	8.44	8.45	8.6	8.5	209
Day 7	24.3	8.35	8.84	8	8.5	310
Day 8	23.5	8.42	8.06	7.9	8.6	301

6.25% FF	Temp (C)	DO init (mg/L)	DO final (mg/L)	pH init	pH final	Conductivity (uS)
Day 0	23.2	8.76	8.27	7.9	8.4	298
Day 1	23.9	8.68	8.4	7.8	8.6	305
Day 2	24.2	8.49	8.35	7.8	8.3	301
Day 3	23.4	8.62	8.58	7.8	8.5	304
Day 4	23.1	8.63	8.65	7.8	8.6	308
Day 5	23.9	8.73	8.33	8.1	8.6	309
Day 6	24.4	8.43	8.38	8.6	8.4	306
Day 7	24.3	8.37	8.84	7.8	8.6	308
Day 8	24	8.47	8	7.8	8.5	323

KCl Control (150 mg /L)	Temp (C)	DO init (mg/L)	DO final (mg/L)	pH init	pH final	Conductivity (uS)
Day 0	23	8.7	8.29	7.5	8.2	583
Day 1	24	8.55	8.56	7.9	8.4	591
Day 2	24.1	8.32	8.34	7.6	8.2	585
Day 3	23	8.57	8.41	7.5	8	587
Day 4	23.5	8.61	8.29	7.8	8.4	603
Day 5	23.5	8.28	8.02	7.8	8.5	612
Day 6	23.4	8.58	8.42	8.2	8.4	585
Day 7	24	8.45	8.62	7.7	8.4	590
Day 8	23.8	8.57	8	7.4	8.5	615

Table A4.6 *Daphnia magna* acute toxicity test results early flowback and potassium chloride (KCl) control. Individual replicates contained 5 daphnids. *Minimum control survival rate of 0.9 not met.

Acute Survival Rate Late Flowback

NOEC = 100%

LOEC > 100%

LC50 > 100%

Replicate	Concentration (percent of whole effluent)					
	0	6.25	12.5	25	50	100
1	0.8	1	1	1	0.8	0.8
2	0.8	1	0.8	1	1	1
3	0.8	0.8	1	1	1	1
4	1	1	0.8	1	1	0.8
Average	0.85*	0.95	0.9	1	0.95	0.9
Standard Deviation	0.10	0.10	0.12	0.00	0.10	0.12
Dunnett Test		NS	NS	NS	NS	NS

Acute Survival Rate KCl Control

NOEC = 300 mg/L

LOEC = 600 mg/L

LC50 = 490 mg/L (95% CI = 433 - 534)

Replicate	Concentration (mg/L)				
	0	50	150	300	600
1	0.8	1	0.8	0.6	0.2
2	0.8	0.6	1	1	0.2
3	0.8	1	0.8	1	0.2
4	1	0.6	1	0.8	0.4
Average	0.85	0.8	0.9	0.85	0.25
Standard Deviation	0.10	0.23	0.12	0.19	0.10
Dunnett Test		NS	NS	NS	Y

Table A4.7 *Daphnia magna* acute toxicity test results early flowback and potassium chloride (KCl) control. Individual replicates contained 5 daphnids.

Acute Survival Rate Early Flowback

NOEC = 100%

LOEC > 100%

LC50 > 100%

Replicate	Concentration (percent of whole effluent)					
	0	6.25	12.5	25	50	100
1	1	0.8	0.8	0.8	1	0.8
2	1	0.8	1	0.6	1	1
3	1	0.8	0.8	1	1	1
4	1	1	1	1	1	1
Average	1	0.85	0.9	0.85	1	0.95
Standard Deviation	0.00	0.10	0.12	0.19	0.00	0.10
Dunnett Test		NS	NS	NS	NS	NS

Acute Survival Rate KCl Control

NOEC = 150 mg/L

LOEC = 300 mg/L

LC50 > 600 mg/L

Replicate	Concentration (mg/L)				
	0	50	150	300	600
1	1	1	0.6	0.6	0.8
2	1	1	1	0.8	0.6
3	1	1	1	0.6	0.8
4	1	1	1	1	0.4
Average	1	1	0.9	0.75	0.65
Standard Deviation	0.00	0.00	0.20	0.19	0.19
Dunnett Test		NS	NS	Y	Y

Table A4.8 *Ceriodaphnia dubia* chronic toxicity test results. Individual replicates contained one daphnid. *Minimum number of young control criteria not met.

Chronic Survival Rate Early Flowback

NOEC = 100%

LOEC >100%

Replicate	Concentrations (% of whole effluent)						KCl Control
	0	6.25	12.5	25	50	100	
1	1	1	1	1	1	1	1
2	1	1	1	1	0	1	1
3	1	1	0	1	1	1	0
4	1	1	1	1	1	1	1
5	1	1	0	1	1	1	1
6	1	1	1	1	1	1	1
7	1	1	1	0	1	1	1
8	1	1	1	1	1	0	1
9	1	1	1	1	0	1	1
10	0	1	1	1	1	1	1
Total	9	10	8	9	8	9	9
Steel Test		NS	NS	NS	NS	NS	NS

Chronic Number of Young Early Flowback

IC25 >100%

Replicate	Concentrations (% of whole effluent)						KCl Control
	0	6.25	12.5	25	50	100	
1	9	6	6	12	11	15	12
2	8	12	0	11	0	9	12
3	1	9	9	12	4	13	0
4	4	0	9	13	15	5	5
5	11	5	0	9	4	6	10
6	4	11	10	14	12	8	10
7	4	13	8	0	13	12	9
8	9	10	13	7	0	0	8
9	5	11	10	14	0	10	10
10	0	20	10	9	9	2	6
Total	55*	97	75	101	68	80	82
Dunnett test		NS	NS	NS	NS	NS	NS

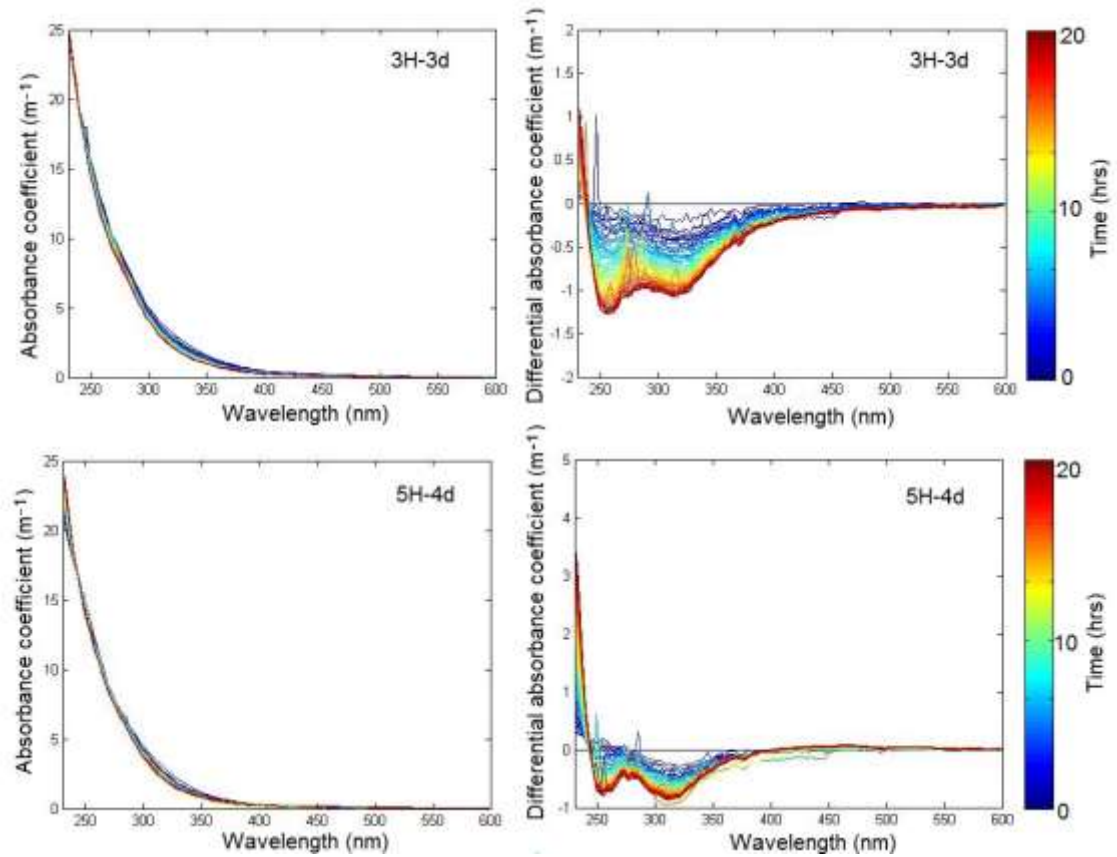


Figure A4.1 Change in absorbance of early flowback shale gas wastewaters from the 3H and 5H wells. Individual lines represent spectral scans taken every 20 minutes.

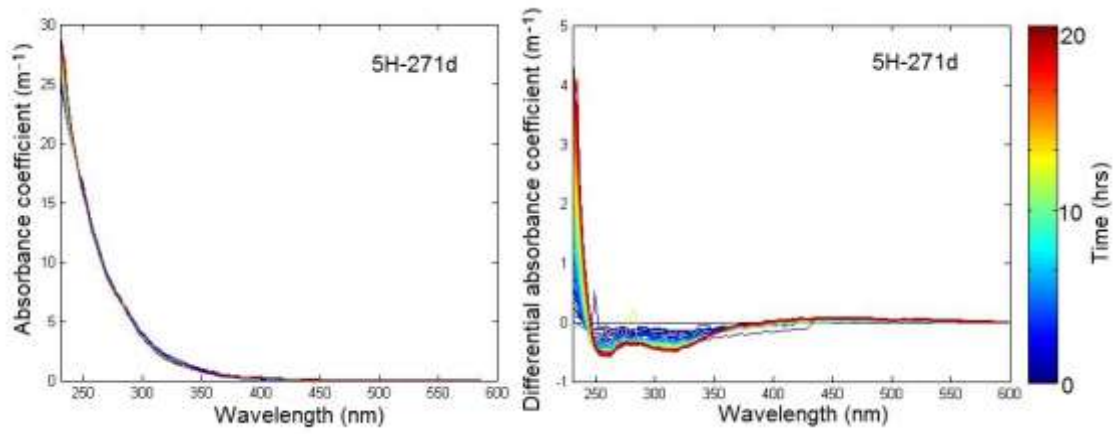


Figure A4.2 Change in absorbance of nine month old shale gas wastewaters from the 3H and 5H wells. Individual lines represent spectral scans taken every 20 minutes.

Table A4.6 Linear regression of PARAFAC component fluorescence change during 20 h photoirradiation. *Fmax2 and Fmax4 irradiation curves are more appropriately modeled using a single exponential decay model and a double exponential decay model, respectively (**Table A4.7**). Strike-through is used to designate samples with significant error in linear regression.

Sample ID	PARAFAC Component	R ²	b	Standard Error b	m (h ⁻¹)	Standard Error m	% Error m
3H-3d	Fmax1	0.815	0.127	0.00117	0.00164	0.000104	6%
3H-3d	Fmax2	0.973	0.105	0.000772	-0.00314	0.0000687	-2%
3H-3d	Fmax3	0.685	0.169	0.000668	-0.000662	0.0000595	-9%
3H-3d	Fmax4*	0.952	0.0435	0.00459	-0.00138	0.0000408	-3%
5h_4d	Fmax1	0.923	0.104	0.000353	-0.000817	0.0000309	-4%
5h_4d	Fmax2	0.946	0.0812	0.000534	-0.00149	0.0000467	-3%
5h_4d	Fmax3	0.22	0.077	0.000623	-0.00022	0.0000545	-25%
5h_4d	Fmax4*	0.868	0.0353	0.00055	-0.000939	0.0000482	-5%
5h_61d	Fmax1	0.0459	0.0969	0.000394	0.0000574	0.0000342	60%
5h_61d	Fmax2	0.985	0.0738	0.000423	-0.00229	0.0000371	-2%
5h_61d	Fmax3	0.835	0.0898	0.000662	-0.000992	0.000058	-6%
5h_61d	Fmax4*	0.935	0.0359	0.000433	-0.0011	0.0000379	-3%
3h_66d	Fmax1	0.00519	0.0897	0.00134	0.0000647	0.000118	182%
3h_66d	Fmax2	0.918	0.0447	0.000829	-0.00184	0.0000725	-4%
3h_66d	Fmax3	0.884	0.121	0.00113	-0.00209	0.000099	-5%
3h_66d	Fmax4*	0.949	0.0261	0.000354	-0.00102	0.000031	-3%
5h_271d	Fmax1	0.915	0.123	0.00046	-0.00101	0.0000403	-4%
5h_271d	Fmax2	0.953	0.0958	0.000565	-0.0017	0.0000495	-3%
5h_271d	Fmax3	0.648	0.129	0.00643	-0.000582	0.0000562	-10%
5h_271d	Fmax4*	0.823	0.0339	0.000697	-0.001	0.000061	-6%

Table A4.10 Single and double exponential decay functions ($F_t = F_1e^{-k_1t} + F_2$) ($F_t = F_1e^{-k_1t} + F_2e^{-k_2t} + F_3$) fit for PARAFAC component Fmax2 and Fmax4 fluorescence.

Fmax2	R²	F₂	Error F₂	F₁	Error F₁	k₁	Error k₁
3H-3d	0.97	-0.3168	0.4209	0.4226	0.4201	0.008	0.0086
5H_4d	0.9705	0.0432	0.0033	0.0415	0.0029	0.0654	0.0093
5H_61d	0.9925	-0.0184	0.0094	0.0948	0.0091	0.0331	0.0045
3H_66d	0.9402	-0.0076	0.0081	0.0559	0.0074	0.0553	0.0133
5H_271d	0.0762	0.0505	0.0038	0.0489	0.0035	0.0608	0.0083

Fmax4	R²	F₃	Error F₃	F₁	Error F₁	k₁	Error k₁
3H-3d	0.9934	-0.0013	0.0093	0.0063	0.0015	0.6462	0.2316
5H_4d	0.9953	0.0167	0.0005	0.0075	0.0005	1.6739	0.25
5H_61d	0.9975	-0.511	0.0366	0.01	0.0004	0.9061	0.0795
3H_66d	0.9839	-0.0578	0.678	0.083	0.0672	0.0126	0.0119
5H_271d	0.9926	0.0164	0.0004	0.0078	0.0008	2.1425	0.4453

Fmax4	F₂	Error F₂	k₂	Error k₂
3H-3d	0.0445	0.0078	0.0406	0.0141
5H_4d	0.0207	0.0003	0.1012	0.0071
5H_61d	0.0851	0.0362	0.0123	0.0061
3H_66d	0.007	0.0009	1.2421	0.3408
5H_271d	0.0217	0.0004	0.1404	0.009

Table A4.11 Ions identified to be consistently *increasing* after 20 hr photoirradiation with possible formula assignment.

Measured Exact Mass	Theoretical Exact Mass	Error (ppm)	C	H Ion	O	N	S	Cl	Br	I	O/C	H/C	DBE
165.01935	165.01933	0.078	8	5	4	0	0	0	0	0	0.50	0.75	6
171.10269	171.10267	0.098	9	15	3	0	0	0	0	0	0.33	1.78	2
195.02991	195.0299	0.053	9	7	5	0	0	0	0	0	0.56	0.89	6
217.07174	217.07176	-0.107	9	13	6	0	0	0	0	0	0.67	1.56	3
222.92614	222.92615	-0.025	5	4	2	0	0	0	0	1	0.40	1.00	3.5
222.92614	222.92615	-0.025	5	4	2	0	0	0	0	1	0.40	1.00	3.5
243.051	243.05103	-0.116	10	11	7	0	0	0	0	0	0.70	1.20	5
243.051	243.05103	-0.116	10	11	7	0	0	0	0	0	0.70	1.20	5
245.06667	245.06668	-0.043	10	13	7	0	0	0	0	0	0.70	1.40	4
251.05609	251.05611	-0.08	12	11	6	0	0	0	0	0	0.50	1.00	7
253.08482	253.08483	-0.017	10	18	5	0	0	1	0	0	0.50	1.90	2
255.05099	255.05103	-0.148	11	11	7	0	0	0	0	0	0.64	1.09	6
255.05099	255.05103	-0.148	11	11	7	0	0	0	0	0	0.64	1.09	6
268.10383	268.10379	0.129	9	18	8	1	0	0	0	0	0.89	2.11	1
276.93286	276.93282	0.129	12	6	1	0	1	0	1	0	0.08	0.58	10
276.93672	276.93671	0.031	8	6	3	0	0	0	0	1	0.38	0.88	5.5
276.93672	276.93671	0.031	8	6	3	0	0	0	0	1	0.38	0.88	5.5
281.07006	281.07005	0.043	10	17	7	0	1	0	0	0	0.70	1.80	2
281.14283	281.14282	0.04	12	25	5	0	1	0	0	0	0.42	2.17	0
284.96866	284.96867	-0.037	7	7	6	2	0	2	0	0	0.86	1.14	6
287.07726	287.07724	0.041	12	15	8	0	0	0	0	0	0.67	1.33	5
293.06669	293.06668	0.046	14	13	7	0	0	0	0	0	0.50	1.00	8
296.90155	296.90152	0.091	14	2	1	0	1	0	1	0	0.07	0.21	14
307.19153	307.19148	0.138	18	27	4	0	0	0	0	0	0.22	1.56	5
313.07851	313.07851	0.026	11	21	6	0	2	0	0	0	0.55	2.00	1
313.14459	313.14453	0.186	19	21	4	0	0	0	0	0	0.21	1.16	9
320.96297	320.96293	0.14	10	10	4	0	0	0	0	1	0.40	1.10	5.5
320.96297	320.96293	0.14	10	10	4	0	0	0	0	1	0.40	1.10	5.5
323.07726	323.07724	0.056	15	15	8	0	0	0	0	0	0.53	1.07	8
325.09293	325.09289	0.106	15	17	8	0	0	0	0	0	0.53	1.20	7
325.16907	325.16904	0.099	14	29	6	0	1	0	0	0	0.43	2.14	0
331.10349	331.10346	0.091	14	19	9	0	0	0	0	0	0.64	1.43	5
335.07725	335.07724	0.025	16	15	8	0	0	0	0	0	0.50	1.00	9
336.88858	336.88851	0.181	9	2	8	0	2	1	0	0	0.89	0.33	9
339.07219	339.07216	0.078	15	15	9	0	0	0	0	0	0.60	1.07	8
353.07316	353.07315	0.033	12	22	2	2	0	0	0	1	0.17	1.92	2.5
353.07316	353.07315	0.033	12	22	2	2	0	0	0	1	0.17	1.92	2.5
353.08781	353.08781	0.011	16	17	9	0	0	0	0	0	0.56	1.13	8
355.11165	355.11162	0.075	15	26	1	2	0	3	0	0	0.07	1.80	5
365.0878	365.08781	-0.021	17	17	9	0	0	0	0	0	0.53	1.06	9
371.09838	371.09837	0.011	16	19	10	0	0	0	0	0	0.63	1.25	7
374.09152	374.09151	0.027	15	20	8	1	1	0	0	0	0.53	1.40	6
375.18133	375.18131	0.046	21	27	6	0	0	0	0	0	0.29	1.33	8

377.08779	377.08781	-0.059	18	17	9	0	0	0	0	0	0.50	1.00	10
383.09838	383.09837	0.023	17	19	10	0	0	0	0	0	0.59	1.18	8
384.85789	384.85786	0.075	13	3	5	0	1	1	1	0	0.38	0.31	13
386.85589	386.85586	0.085	6	7	6	2	0	3	1	0	1.00	1.33	6
386.85589	386.85592	-0.075	11	11	1	0	0	2	2	0	0.09	1.09	8
404.87592	404.87594	-0.045	10	12	2	0	0	1	1	1	0.20	1.30	5.5
404.87592	404.87595	-0.067	9	4	8	2	1	3	0	0	0.89	0.56	10
405.11908	405.11911	-0.085	20	21	9	0	0	0	0	0	0.45	1.10	10
425.14531	425.14532	-0.029	20	25	10	0	0	0	0	0	0.50	1.30	8
425.18172	425.18171	0.023	21	29	9	0	0	0	0	0	0.43	1.43	7
428.84525	428.84529	-0.11	11	5	5	2	0	3	1	0	0.45	0.55	12
428.84525	428.84519	0.14	18	3	2	0	2	1	1	0	0.11	0.22	18
428.84525	428.84529	-0.11	11	5	5	2	0	3	1	0	0.45	0.55	12
428.84525	428.84519	0.14	18	3	2	0	2	1	1	0	0.11	0.22	18
435.16607	435.16606	0.032	22	27	9	0	0	0	0	0	0.41	1.27	9
488.30276	488.30274	0.036	22	48	4	3	0	2	0	0	0.18	2.23	1
514.32458	514.3246	-0.046	35	45	0	1	0	1	0	0	0.00	1.31	14

Table A4.12 Ions identified to be consistently *decreasing* after 20 hr photoirradiation with possible formula assignment.

ExpMass	ThMass	ErrPPM	HIon	C	O	N	S	Cl	Br	I	O/C	H/C	DBE
171.0663	171.06628	0.09	11	8	4	0	0	0	0	0	0.50	1.50	3
171.0663	171.06628	0.09	11	8	4	0	0	0	0	0	0.50	1.50	3
173.11834	173.11832	0.097	17	9	3	0	0	0	0	0	0.33	2.00	1
175.06122	175.0612	0.105	11	7	5	0	0	0	0	0	0.71	1.71	2
179.035	179.03498	0.077	7	9	4	0	0	0	0	0	0.44	0.89	6
187.13399	187.13397	0.085	19	10	3	0	0	0	0	0	0.30	2.00	1
189.07686	189.07685	0.06	13	8	5	0	0	0	0	0	0.63	1.75	2
189.11325	189.11323	0.089	17	9	4	0	0	0	0	0	0.44	2.00	1
197.04555	197.04555	0.024	9	9	5	0	0	0	0	0	0.56	1.11	5
199.00706	199.00706	0.014	7	8	4	0	1	0	0	0	0.50	1.00	5
199.13397	199.13397	0.009	19	11	3	0	0	0	0	0	0.27	1.82	2
200.09284	200.09283	0.023	14	9	4	1	0	0	0	0	0.44	1.67	3
209.04553	209.04555	-0.078	9	10	5	0	0	0	0	0	0.50	1.00	6
211.06118	211.0612	-0.07	11	10	5	0	0	0	0	0	0.50	1.20	5
223.06118	223.0612	-0.078	11	11	5	0	0	0	0	0	0.45	1.09	6
223.09756	223.09758	-0.089	15	12	4	0	0	0	0	0	0.33	1.33	5
226.07209	226.0721	-0.047	12	10	5	1	0	0	0	0	0.50	1.30	5
226.07209	226.0721	-0.047	12	10	5	1	0	0	0	0	0.50	1.30	5
227.05609	227.05611	-0.095	11	10	6	0	0	0	0	0	0.60	1.20	5
235.07424	235.07426	-0.076	16	10	4	0	0	1	0	0	0.40	1.70	3
236.0776	236.07758	0.074	14	8	7	1	0	0	0	0	0.88	1.88	2
237.07683	237.07685	-0.079	13	12	5	0	0	0	0	0	0.42	1.17	6
239.05611	239.05611	-0.036	11	11	6	0	0	0	0	0	0.55	1.09	6
243.16017	243.16018	-0.055	23	13	4	0	0	0	0	0	0.31	1.85	2
245.04891	245.04892	-0.055	13	10	5	0	1	0	0	0	0.50	1.40	4
248.89596	248.89596	0.01	3	7	3	0	0	1	1	0	0.43	0.57	7
253.08482	253.08483	-0.017	18	10	5	0	0	1	0	0	0.50	1.90	2
253.10814	253.10815	-0.039	17	13	5	0	0	0	0	0	0.38	1.38	5
253.14452	253.14453	-0.041	21	14	4	0	0	0	0	0	0.29	1.57	4
256.96566	256.96569	-0.121	8	7	2	2	0	3	0	0	0.29	1.29	6
257.13945	257.13945	-0.003	21	13	5	0	0	0	0	0	0.38	1.69	3
257.13945	257.13945	-0.003	21	13	5	0	0	0	0	0	0.38	1.69	3
259.1551	259.1551	-0.015	23	13	5	0	0	0	0	0	0.38	1.85	2
261.1344	261.13436	0.133	21	12	6	0	0	0	0	0	0.50	1.83	2
262.99486	262.99488	-0.066	14	7	0	2	1	3	0	0	0.00	2.14	3
265.07176	265.07176	-0.029	13	13	6	0	0	0	0	0	0.46	1.08	7
267.0445	267.0445	-0.007	11	11	4	2	1	0	0	0	0.36	1.09	7
267.0445	267.0445	-0.007	11	11	4	2	1	0	0	0	0.36	1.09	7
268.10383	268.10379	0.129	18	9	8	1	0	0	0	0	0.89	2.11	1
277.02078	277.02079	-0.04	10	13	1	2	1	1	0	0	0.08	0.85	10

277.10817	277.10815	0.081	17	15	5	0	0	0	0	0	0.33	1.20	7
279.02374	279.02375	-0.012	16	10	4	0	0	0	1	0	0.40	1.70	3
283.11873	283.11871	0.062	19	14	6	0	0	0	0	0	0.43	1.43	5
285.10134	285.10135	-0.023	21	10	7	0	1	0	0	0	0.70	2.20	0
285.17076	285.17075	0.054	25	15	5	0	0	0	0	0	0.33	1.73	3
285.17076	285.17075	0.054	25	15	5	0	0	0	0	0	0.33	1.73	3
287.12891	287.12888	0.085	19	17	4	0	0	0	0	0	0.24	1.18	8
292.11908	292.11905	0.119	18	15	5	1	0	0	0	0	0.33	1.27	7
292.11908	292.11905	0.119	18	15	5	1	0	0	0	0	0.33	1.27	7
293.10308	293.10306	0.06	17	15	6	0	0	0	0	0	0.40	1.20	7
293.13947	293.13945	0.057	21	16	5	0	0	0	0	0	0.31	1.38	6
294.87975	294.87972	0.081	9	8	0	0	1	0	2	0	0.00	1.25	5
294.93784	294.93783	0.037	9	9	4	0	0	1	1	0	0.44	1.11	6
296.85902	296.85899	0.106	7	7	1	0	1	0	2	0	0.14	1.14	5
296.85902	296.85899	0.106	7	7	1	0	1	0	2	0	0.14	1.14	5
298.81156	298.81156	0.019	2	6	2	0	0	1	2	0	0.33	0.50	7
301.16569	301.16566	0.092	25	15	6	0	0	0	0	0	0.40	1.73	3
305.1031	305.10306	0.115	17	16	6	0	0	0	0	0	0.38	1.13	8
305.16062	305.16058	0.145	25	14	7	0	0	0	0	0	0.50	1.86	2
308.85903	308.85899	0.142	7	8	1	0	1	0	2	0	0.13	1.00	6
311.04999	311.04996	0.079	20	11	5	0	0	0	1	0	0.45	1.91	2
313.16569	313.16566	0.082	25	16	6	0	0	0	0	0	0.38	1.63	4
315.18135	315.18131	0.114	27	16	6	0	0	0	0	0	0.38	1.75	3
317.06671	317.06668	0.107	13	16	7	0	0	0	0	0	0.44	0.88	10
317.10311	317.10306	0.14	17	17	6	0	0	0	0	0	0.35	1.06	9
317.11616	317.11613	0.108	22	15	5	0	0	1	0	0	0.33	1.53	5
317.12423	317.12419	0.103	21	14	8	0	0	0	0	0	0.57	1.57	4
317.13542	317.13543	-0.023	21	13	7	2	0	0	0	0	0.54	1.69	4
319.13181	319.13178	0.107	24	15	5	0	0	1	0	0	0.33	1.67	4
322.88031	322.88031	0.002	10	5	2	2	0	1	2	0	0.40	2.20	3
327.08523	327.08522	0.01	20	12	8	0	0	1	0	0	0.67	1.75	3
328.75665	328.75663	0.061	0	4	1	2	0	0	3	0	0.25	0.25	7
329.17587	329.17583	0.116	25	20	4	0	0	0	0	0	0.20	1.30	8
329.17587	329.17583	0.116	25	20	4	0	0	0	0	0	0.20	1.30	8
332.87677	332.87675	0.088	7	10	3	0	0	0	2	0	0.30	0.80	8
333.11108	333.11104	0.105	22	15	6	0	0	1	0	0	0.40	1.53	5
337.11402	337.11402	-0.016	21	13	10	0	0	0	0	0	0.77	1.69	3
337.14236	337.14234	0.061	26	15	6	0	0	1	0	0	0.40	1.80	3
339.16609	339.16606	0.081	27	14	9	0	0	0	0	0	0.64	2.00	1
343.10347	343.10346	0.045	19	15	9	0	0	0	0	0	0.60	1.33	6
343.17626	343.17623	0.078	27	17	7	0	0	0	0	0	0.41	1.65	4

344.11737	344.11733	0.093	22	15	6	1	1	0	0	0	0.40	1.53	5
349.0929	349.09289	0.02	17	17	8	0	0	0	0	0	0.47	1.06	9
349.14238	349.14234	0.094	26	16	6	0	0	1	0	0	0.38	1.69	4
355.21264	355.21261	0.064	31	19	6	0	0	0	0	0	0.32	1.68	4
359.09031	359.09031	0.011	20	16	7	0	0	1	0	0	0.44	1.31	7
359.09031	359.09031	0.011	20	16	7	0	0	1	0	0	0.44	1.31	7
359.11365	359.11363	0.047	19	19	7	0	0	0	0	0	0.37	1.05	10
359.13476	359.13476	-0.003	23	16	9	0	0	0	0	0	0.56	1.50	5
361.09291	361.09289	0.055	17	18	8	0	0	0	0	0	0.44	1.00	10
375.12159	375.12161	-0.036	24	17	7	0	0	1	0	0	0.41	1.47	6
375.158	375.15799	0.008	28	18	6	0	0	1	0	0	0.33	1.61	5
376.14606	376.14605	0.021	26	12	12	1	0	0	0	0	1.00	2.25	0
377.21809	377.21809	-0.001	33	18	8	0	0	0	0	0	0.44	1.89	2
383.1923	383.19227	0.064	31	16	10	0	0	0	0	0	0.63	2.00	1
395.09836	395.09837	-0.038	19	18	10	0	0	0	0	0	0.56	1.11	9
399.20248	399.20244	0.095	31	20	8	0	0	0	0	0	0.40	1.60	5
403.13984	403.13984	-0.016	23	21	8	0	0	0	0	0	0.38	1.14	10
403.13984	403.13984	-0.016	23	21	8	0	0	0	0	0	0.38	1.14	10
405.19184	405.19188	-0.086	29	22	7	0	0	0	0	0	0.32	1.36	8
419.16897	419.16895	0.042	32	16	10	0	0	1	0	0	0.63	2.06	1
420.17227	420.17227	0.007	30	14	13	1	0	0	0	0	0.93	2.21	0
427.16097	427.16097	-0.017	27	20	10	0	0	0	0	0	0.50	1.40	7
427.21844	427.21849	-0.109	35	18	11	0	0	0	0	0	0.61	2.00	1
429.19774	429.19775	-0.044	33	17	12	0	0	0	0	0	0.71	2.00	1
453.20492	453.20494	-0.04	34	24	6	0	0	1	0	0	0.25	1.46	8
463.19517	463.19517	0.01	36	18	11	0	0	1	0	0	0.61	2.06	1

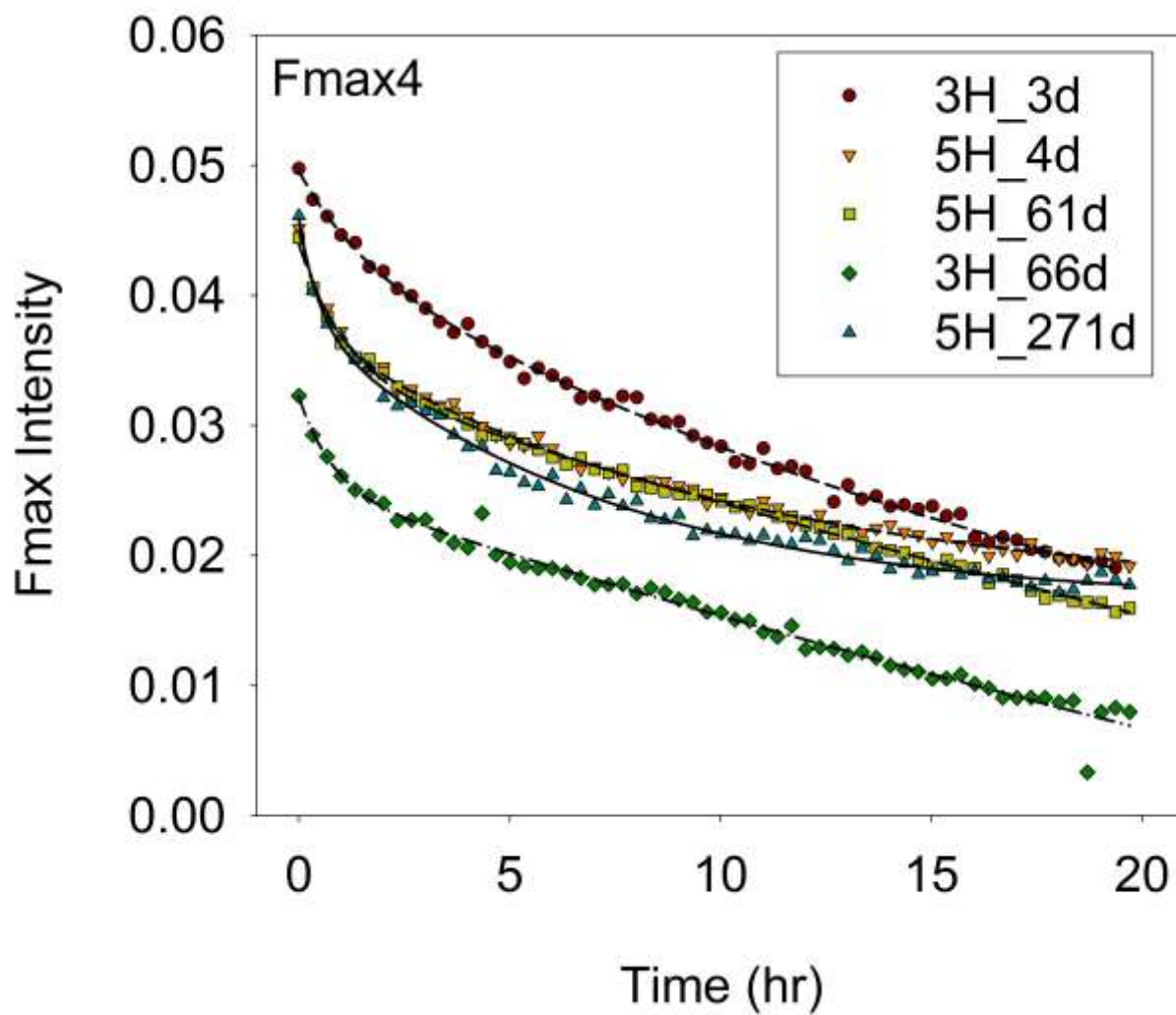


Figure A4.3 Fitted PARAFAC component Fmax4 fluorescence curves.

Appendix 5

Table A5.1 Names and locations of all Garrett County, MD streamwater sampling locations. Bolded sites were collected seasonally, all others were collected annually.

MD-DNR Site Code	Stream Name	LAT	LONG	Elevation (ft)
CASS-101-D	Piney Creek UT	39.7131	-79.0113	2441
CASS-103-D	Twomile Run	39.6759	-79.0620	2495
CASS-105-D	Meadow Run	39.6871	-79.1002	2616
GEOR-101-D	Mill Run	39.5481	-79.0658	2068
PRUN-301-D	Nydegger Run	39.2975	-79.3502	2339
SAVA-101-D	Savage River UT	39.6460	-79.0170	2276
SAVA-202-D	Big Run	39.5743	-79.1598	1959
SAVA-204-S	Crabtree Creek	39.5036	-79.1557	1590
SAVA-301-D	Savage River	39.6419	-79.0218	2302
SAVA-302-D	Savage River	39.6432	-79.0200	2264
YOUG-102-D	Youghiogheny River UT	39.6968	-79.3809	1600
YOUG-103-D	Youghiogheny River UT	39.6968	-79.3823	1590
YOUG-104-D	Buffalo Run UT	39.6863	-79.4101	1485
YOUG-105-D	Laurel Run	39.3826	-79.4913	2394
YOUG-106-D	Salt Block Run	39.5655	-79.4684	2512
YOUG-201-D	Mill Run	39.7105	-79.3699	1511
YOUG-301-D	Buffalo Run	39.6889	-79.4214	1566
YOUG-302-D	Cherry Creek	39.3686	-79.4541	2401
YOUG-432-S	Bear Creek	39.6425	-79.2798	2251

Table A5.2 Fracturing fluid, flowback fluid, and produced water samples by state (WV, PA, OH) and location (A, B). Numbers are given when samples were collected from the same location at multiple time points. ^a Unknown fluid type are samples were collected by a fracking wastewater treatment company and are likely dominated by produced waters. ^b Synthetic mixture typical of Marcellus Shale region described previously (Kekacs et al., 2015).

Sample ID	Fluid Type
WV-A1	Fracturing Fluid
WV-A1	Fracturing Fluid
WV-A2	Flowback Fluid
WV-A3	Flowback Fluid
WV-A4	Flowback Fluid
WV-A5	Flowback Fluid
WV-A6	Flowback Fluid
WV-A7	Flowback Fluid
WV-A8	Produced Water
WV-A9	Produced Water
WV-A10	Produced Water
WV-A11	Produced Water
WV-A12	Produced Water
WV-A13	Produced Water
WV-A14	Produced Water
WV-B1	Fracturing Fluid
WV-B1	Fracturing Fluid
WV-B2	Flowback Fluid
WV-B3	Flowback Fluid
WV-B4	Flowback Fluid
WV-B5	Flowback Fluid
WV-B6	Produced Water
WV-B7	Produced Water
WV-B8	Produced Water
WV-C1	Unknown
WV-D1	Unknown
WV-E1	Unknown
WV-F1	Produced Water
PA-A1	Unknown
PA-B1	Unknown
PA-C1	Unknown
PA-D1	Unknown
PA-E1	Unknown
OH-A1	Recycled Flowback Fluid

OH-A2	Recycled Flowback Fluid
OH-A3	Recycled Flowback Fluid
OH-A4	Recycled Flowback Fluid
OH-A5	Recycled Flowback Fluid
OH-A6	Recycled Flowback Fluid
OH-B1	Synthetic Fracturing Fluid

Table A5.3. All surfactant exact masses found in hydraulic fracturing fluid and wastewater but absent from stream water samples.

Exact m/z	Neutral Assigned Formula	Conventional name
242.22458	C15H30O2	n-propyl dodecanoate; propyl laurate
255.105491	C13H19NaO3S	4-(n-heptyl)benzenesulfonic acid sodium
264.20893	C17H28O2	BNP-EO-1; branched nonylphenol (ethoxylate)1
282.1678532	C12H26O7	PEG-6EO
287.9762294	C10H8O6S2	naphthalene-1,5-disulfonate
292.18859	C14H28O6	n-octyl-beta-D-glucoside
308.2351449	C19H32O3	NPEO2
315.2773441	C18H37N1O3	C13DEA
320.21989	C16H32O6	n-decylglucoside
334.2541658	C18H38S1O3	C18-SAS
339.199391	C19H31NaO3S	LAS-xC13; x-(4-sulfophenyl)tridecane sodium salt
341.178656	C18H29NaO4S	n-dodecylsulfonic acid, 3-phenoxy, sodium
348.2698159	C19H40S1O3	C19-SAS
352.2613596	C21H36O4	NPEO3
353.215041	C20H33NaO3S	2,5-diheptylbenzenesulfonic acid sodium
366.2228657	C21H34O3S1	C15-DATS
366.261755	C18H38O7	LH-EO-6; linear hexanol (ethoxylate)6
369.209956	C20H33NaO4S	n-tetradecylsulfonic acid, 3-phenoxy, sodium
370.2202827	C16H34O9	PEG-8EO
371.3399443	C22H45N1O3	C17DEA
380.2385157	C22H36O3S1	C16-DATS
382.25667	C18H38O8	AEO
382.271925	C22H38O5	LOP-EO-4.5; linear octylphenol (ethoxylate)4.5
384.235935	C17H36O9	AEO
392.3137891	C21H44O6	C11-AEO-5
394.2541658	C23H38O3S1	C17-DATS
394.293055	C20H42O7	LO-EO-6; linear octanol (ethoxylate)6
396.287575	C23H40O5	LNP-EO-4; linear nonylphenol (ethoxylate)4
398.251585	C18H38O9	AEO
408.2698159	C24H40O3S1	C18-DATS
408.308705	C21H44O7	LN-EO6; nonanol (ethoxylate)6
410.28797	C20H42O8	AEO
414.2464974	C18H38O10	PEG-9EO
422.2854659	C25H42O3S1	C19-DATS
424.228345	C23H36O5S1	STA-12C
424.30362	C21H44O8	AEO
426.282885	C20H42O9	AEO
426.29814	C24H42O6	BOP-EO-5; branched octylphenol (ethoxylate)5
428.26215	C19H40O10	AEO
434.3607393	C24H50O6	C14-AEO-5, LTED-EO-5; linear tetradecanol (ethoxylate)5

436.3400039	C23H48O7	C11-AEO-6
440.1868741	C22H32O7S1	STA-10DC
440.31379	C25H44O6	BNP-EO-5; branched nonylphenol (ethoxylate)5
442.2025242	C22H34O7S1	SPA-14DC
460.412775	C27H56O5	PEG
470.2913392	C22H46O8S1	C14-AE4S
472.288365	C21H44O11	AEO
474.428425	C28H58O5	PEG
484.3069892	C23H48O8S1	C15-AE4S
484.340005	C27H48O7	LNP-EO-6; linear nonylphenol (ethoxylate)6
486.2862538	C22H46O9S1	C12-AE5S
488.40769	C28H56O6	OL-EO-5.5; oleyl (ethoxylate)5.5
498.3404	C24H50O10	AEO
500.301906	C23H48O9S	1-pentadecanol -15-(EO)4-sulfate
504.43899	C29H60O6	PEG
512.35605	C25H52O10	AEO
514.3175539	C24H50O9S1	C14-AE5S
514.35057	C28H50O8	LOP-EO-7; linear octylphenol (ethoxylate)7
516.31458	C23H48O12	PEG
518.45464	C30H62O6	PEG
520.4339043	C29H60O7	C17-AEO-6
526.3717	C26H54O10	LO-EO-9; linear octanol (ethoxylate)9
530.3124685	C24H50O10S1	C12-AE6S
534.4495543	C30H62O7	C18-AEO-6
540.38735	C27H56O10	AEO
542.3488541	C26H54O9S1	C16-AE5S
546.3251417	C24H50O13	PEG-12EO
556.382265	C27H56O11	AEO
558.3437687	C26H54O10S1	C14-AE6S
558.376785	C30H54O9	LOP-EO-8.5; linear octylphenol (ethoxylate)8.5
560.340795	C25H52O13	PEG
562.480855	C32H66O7	PEG
564.460119	C31H64O8	C17-AEO-7
570.397915	C28H58O11	LO-EO-10; linear octanol (ethoxylate)10
572.3594187	C27H56O10S1	C15-AE6S
572.392435	C31H56O9	LNP-EO-8; linear nonylphenol (ethoxylate)8
578.4757691	C32H66O8	C18-AEO-7
584.413565	C29H60O11	AEO
586.39283	C28H58O11	PEG
590.3513564	C26H54O14	PEG-13EO
598.4292128	C30H62O11	C10-AEO-10
602.3699834	C28H58O11S1	C14-AE7S
606.50707	C34H70O8	PEG
612.4448629	C31H64O11	C11-AEO-10
614.42413	C30H62O12	PEG
616.41865	C33H60O10	BNP-EO-9; branched nonylphenol (ethoxylate)09

622.5019838	C34H70O9	C18-AEO-8
623.473425	C33H67ClO10	LTD-EO-10-Cl; linear tridecanol (ethoxylate)10 chloride
626.460513	C32H66O11	C12-AEO-10
634.359816	C28H58O13S	1-dodecanol -12-(EO)8-sulfate
634.3775712	C28H58O15	PEG-14EO
642.4554276	C32H66O12	C10-AEO-11
642.627458	C39H82N2O4	1,2-propanediamine distearate
656.4710776	C33H68O12	C11-AEO-11
658.429215	C35H62O11	LNP-EO-9ac; linear nonylphenol (ethoxylate)9 acetate
660.4118482	C31H64O12S1	C15-AE8S
664.403395	C33H60O13P	BNP-EO-9-P; branched nonylphenol (ethoxylate)9 phosphate
674.4274983	C32H66O12S1	C16-AE8S
676.4067629	C31H64O13S1	C13-AE9S
678.40379	C30H62O16	PEG
686.4816423	C34H70O13	C10-AEO-12
690.4224129	C32H66O13S1	C14-AE9S
692.41944	C31H64O16	PEG
694.5595	C38H78O10	PEG
702.47656	C34H70O14	PEG
738.585715	C40H82O11	PEG
750.4435423	C34H70O15S1	C12-AE11S
750.461305	C34H70O17	PEG

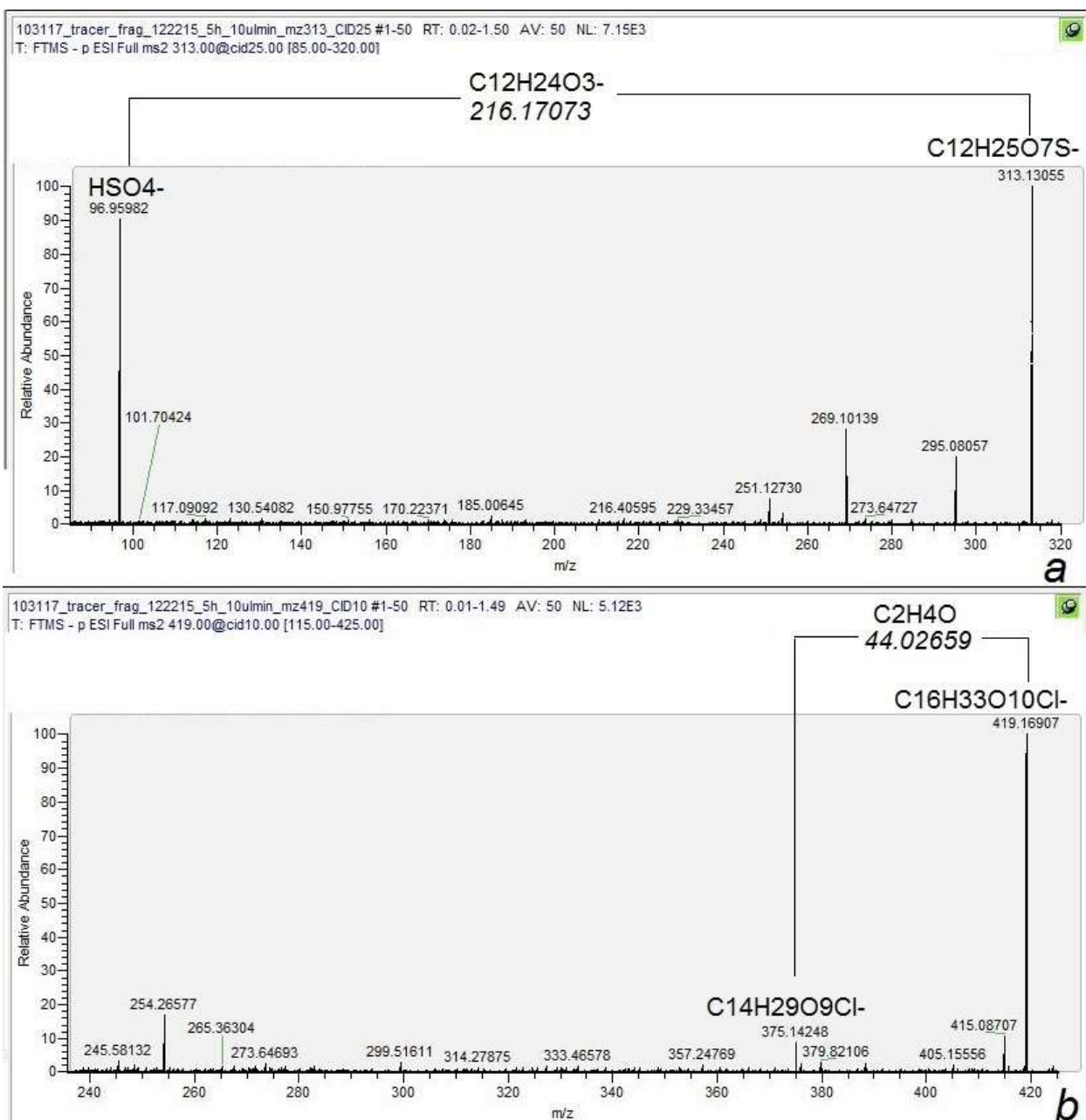


Figure A5.1 Fragmentation spectra of selected sulfonated (a) and chlorinated (b) tracer ions, tracer ions are the parent/highest intensity peak in the mass spectra. Fragmentation was performed using an Orbitrap mass spectrometer on a 1 m/z window using a collision induced dissociation values of 25 (a) and 10 (b). Exact mass error of approximately 6ppm is seen in observed peaks, however, mass differences between individual peaks provide much more precise values for understanding fragments.

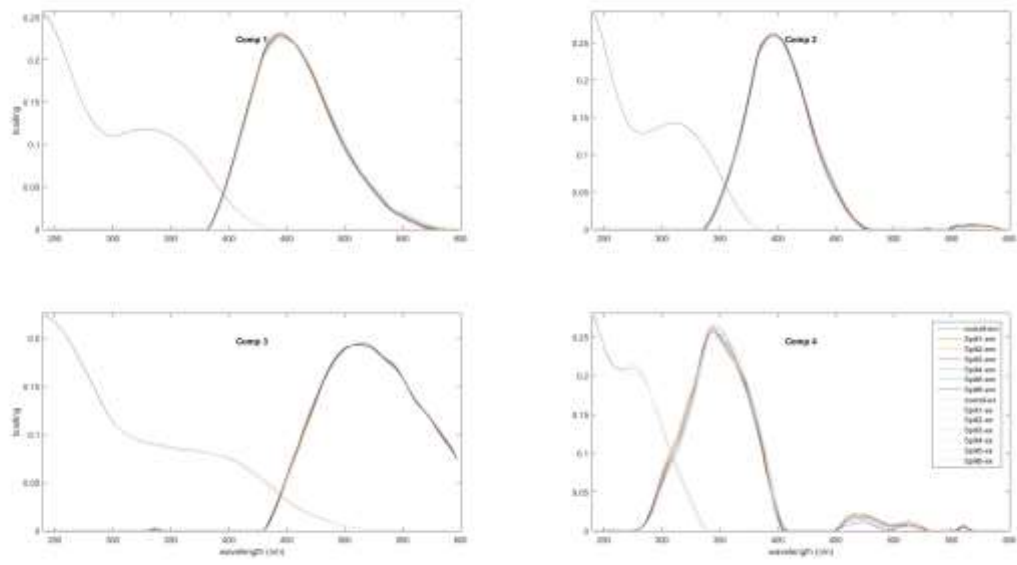


Figure A5.2 Split-half validation of 4-component PARAFAC model.

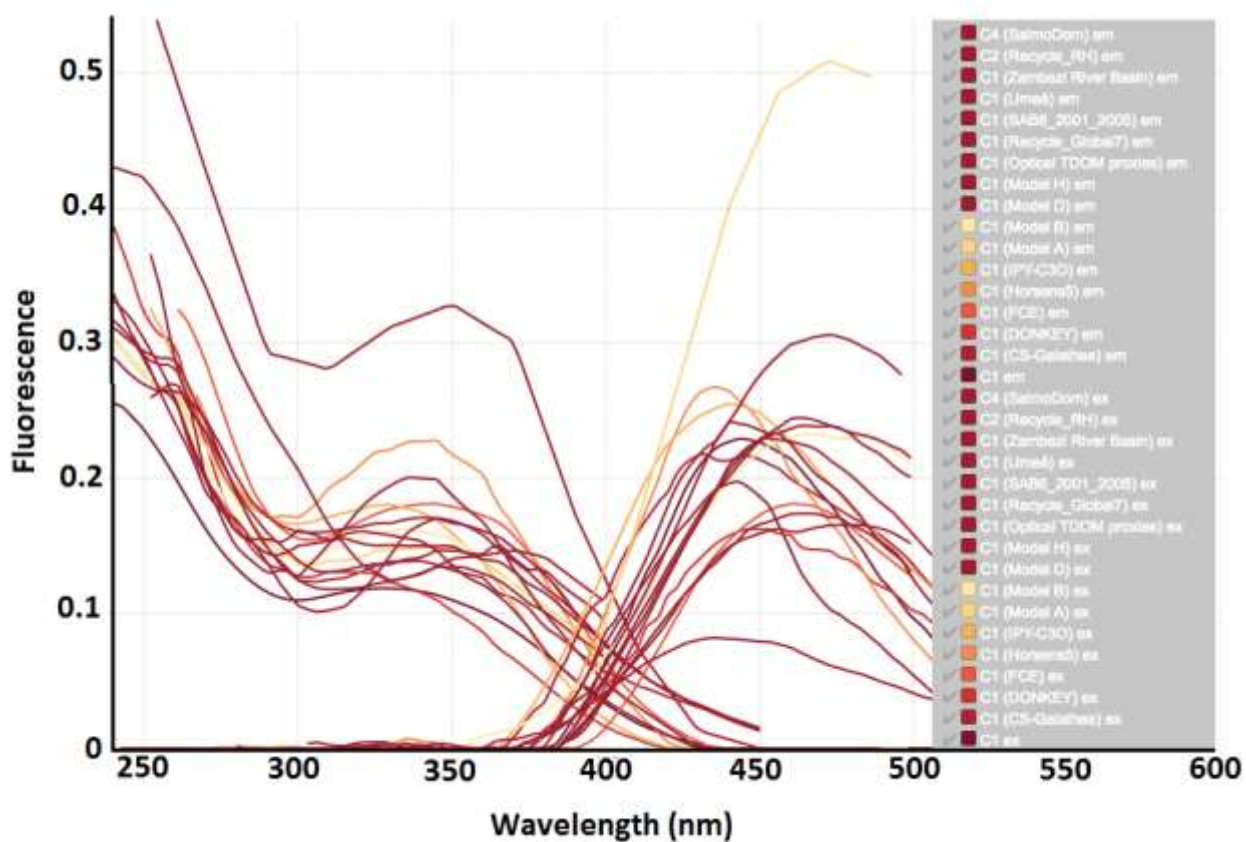


Figure A5.3 Comparison of PARAFAC model to OpenFluor database (C1). This study given plotted as “C1 ex” and “C1 em.” All other PARAFAC models listed can be found in the OpenFluor database (Murphy et al., 2014).

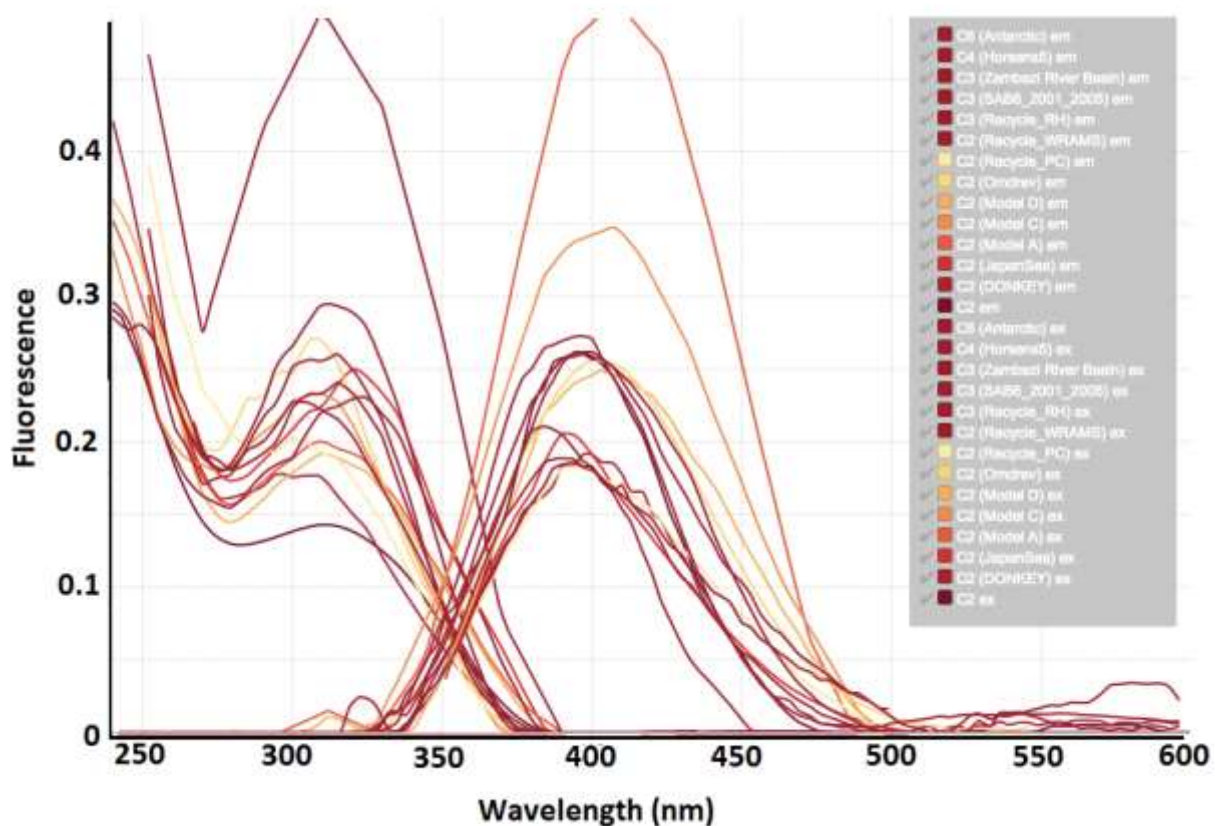


Figure A5.4 Comparison of PARAFAC model to OpenFluor database (C2). This study given plotted as “C2 ex” and “C2 em.” All other PARAFAC models listed can be found in the OpenFluor database (Murphy et al., 2014).

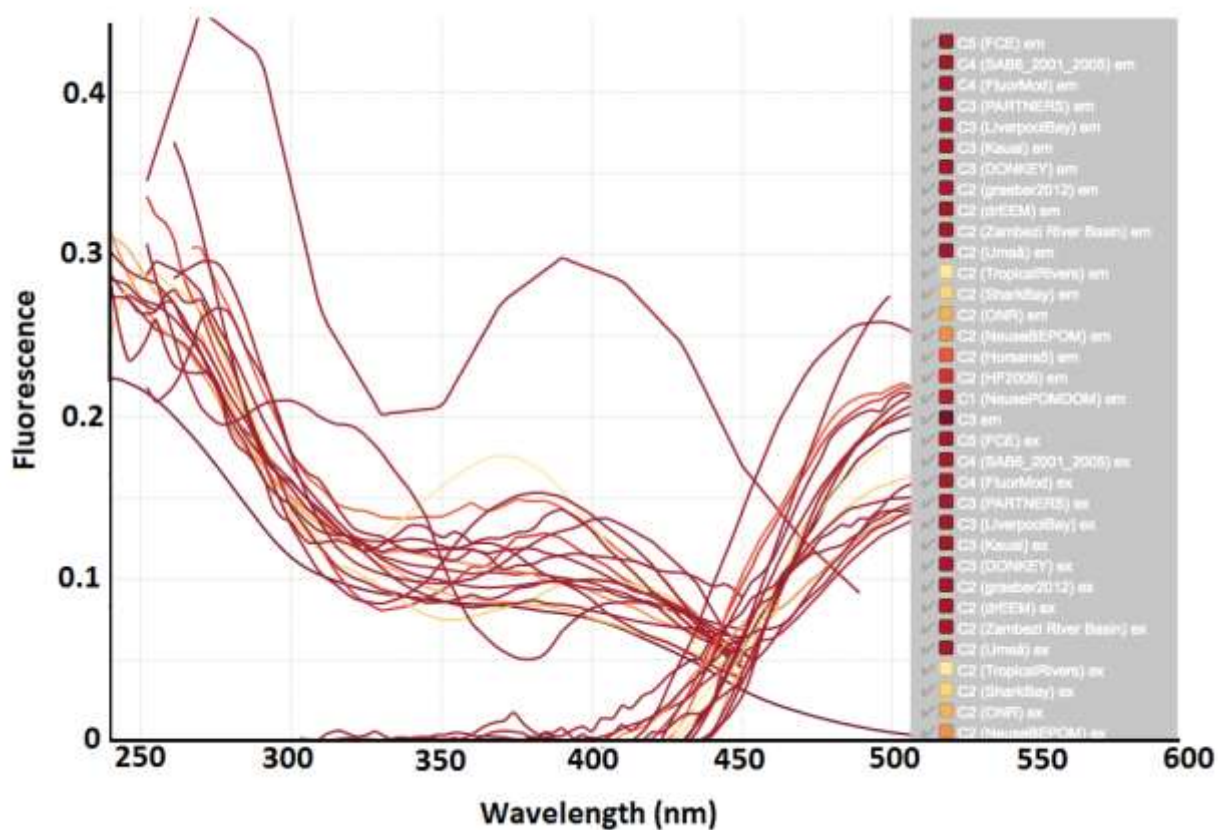


Figure A5.5 Comparison of PARAFAC model to OpenFluor database (C3). This study given plotted as “C3 ex” and “C3 em.” All other PARAFAC models listed can be found in the OpenFluor database (Murphy et al., 2014).

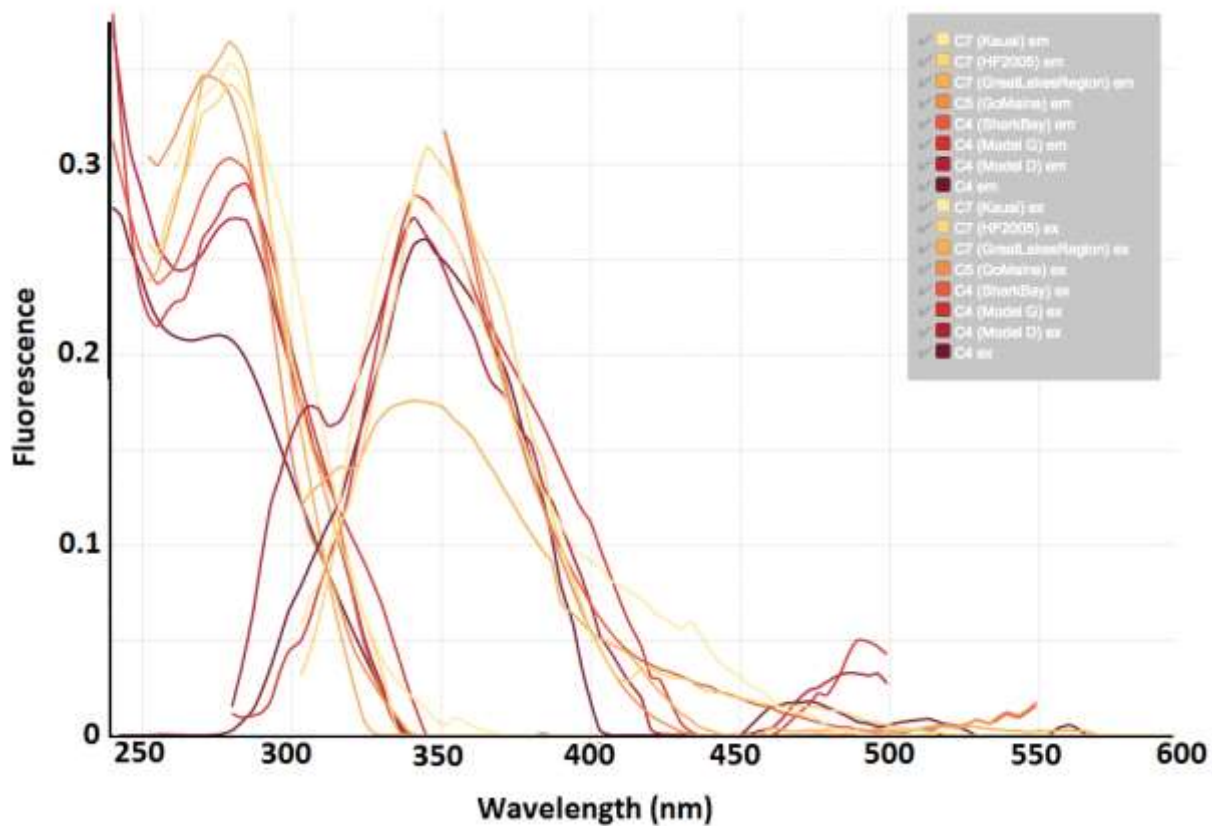


Figure A5.6 Comparison of PARAFAC model to OpenFluor database (C4). This study given plotted as “C4 ex” and “C4 em.” All other PARAFAC models listed can be found in the OpenFluor database (Murphy et al., 2014).

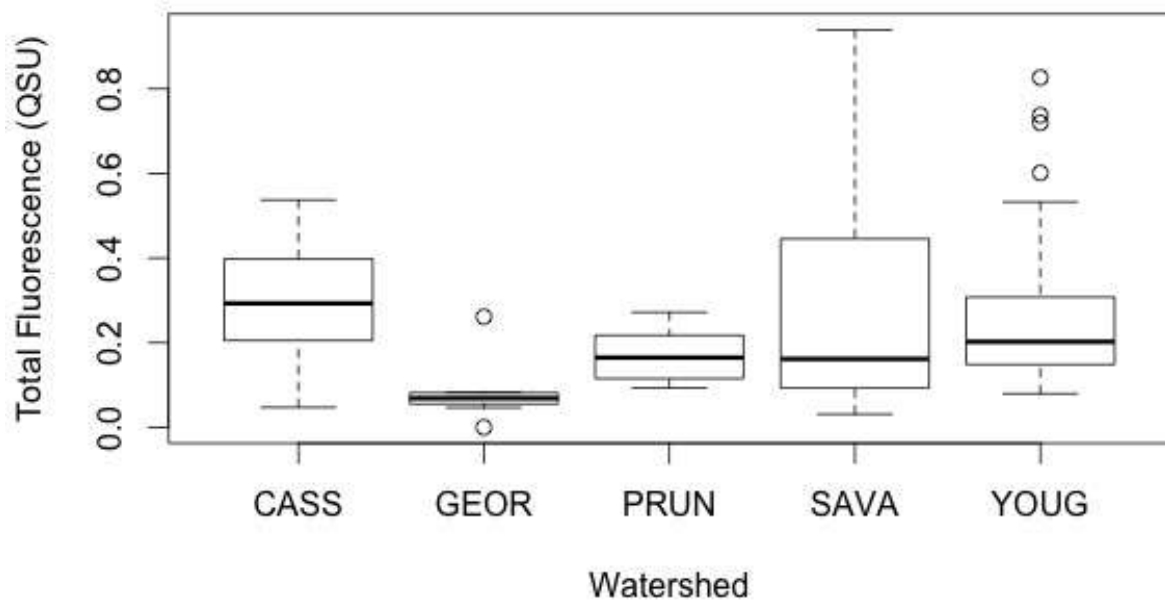


Figure A5.7 Comparison of total fluorescence by watershed from 4 PARAFAC components across all stream water samples.

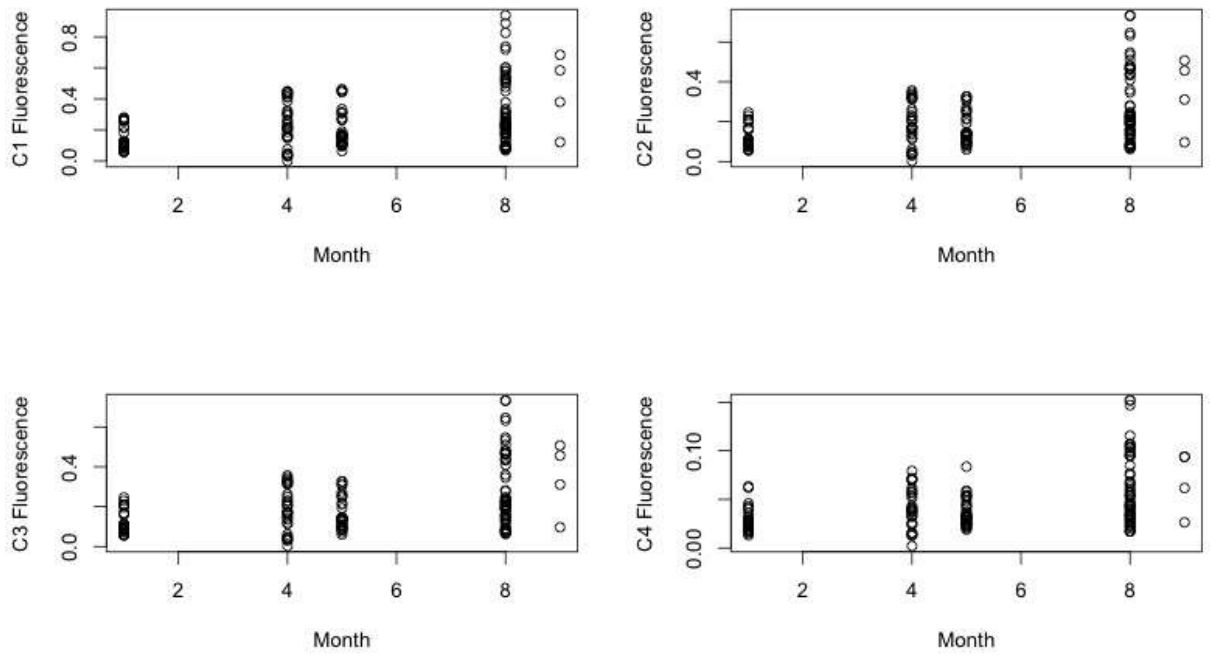


Figure A5.8 Comparison of fluorescence from individual PARAFAC components (C1, C2, C3, C4) by month across all stream water samples.

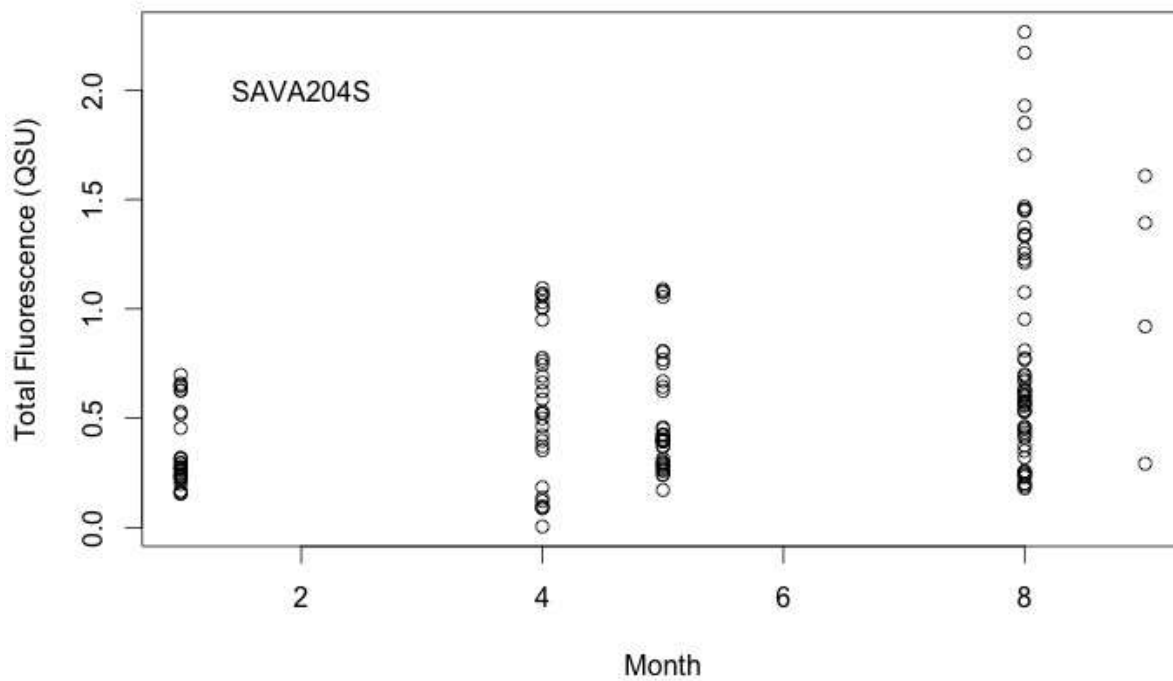


Figure A5.9 Total fluorescence from 4 PARAFAC components in individual stream water sites across months.

References

- 2016 Oil and Gas Annual Report, 2016. . Pennsylvania Department of Environmental Protection.
- Abdullah, K., Malloy, T., Stenstrom, M.K., Suffet, I.H. (Mel), 2017. Toxicity of acidization fluids used in California oil exploration. *Toxicol. Environ. Chem.* 99, 78–94. <https://doi.org/10.1080/02772248.2016.1160285>
- Abualfaraj, N., Gurian, P.L., Olson, M.S., 2014. Characterization of Marcellus Shale Flowback Water. *Environ. Eng. Sci.* 140716083132007. <https://doi.org/10.1089/ees.2014.0001>
- Akob, D.M., Cozzarelli, I.M., Dunlap, D.S., Rowan, E.L., Lorah, M.M., 2015. Organic and inorganic composition and microbiology of produced waters from Pennsylvania shale gas wells. *Appl. Geochem.* 60, 116–125. <https://doi.org/10.1016/j.apgeochem.2015.04.011>
- Akob, D.M., Mumford, A.C., Orem, W., Engle, M.A., Klinges, J.G., Kent, D.B., Cozzarelli, I.M., 2016. Wastewater Disposal from Unconventional Oil and Gas Development Degrades Stream Quality at a West Virginia Injection Facility. *Environ. Sci. Technol.* 50, 5517–5525. <https://doi.org/10.1021/acs.est.6b00428>
- Allen-King, R.M., Grathwohl, P., Ball, W.P., 2002. New modeling paradigms for the sorption of hydrophobic organic chemicals to heterogeneous carbonaceous matter in soils, sediments, and rocks. *Adv. Water Resour.* 25, 985–1016.
- Amachi, S., Muramatsu, Y., Akiyama, Y., Miyazaki, K., Yoshiki, S., Hanada, S., Kamagata, Y., Ban-nai Tadaaki, Shinoyama, H., Fujii, T., 2005. Isolation of Iodide-Oxidizing Bacteria from Iodide-Rich Natural Gas Brines and Seawaters. *Microb. Ecol.* 49, 547–557. <https://doi.org/10.1007/s00248-004-0056-0>
- Bae, E., Na, J.-G., Chung, S.H., Kim, H.S., Kim, S., 2010. Identification of about 30 000 Chemical Components in Shale Oils by Electrospray Ionization (ESI) and Atmospheric Pressure Photoionization (APPI) Coupled with 15 T Fourier Transform Ion Cyclotron Resonance Mass Spectrometry (FT-ICR MS) and a Comparison to Conventional Oil. *Energy Fuels* 24, 2563–2569. <https://doi.org/10.1021/ef100060b>
- Bae, E., Yeo, I.J., Jeong, B., Shin, Y., Shin, K.-H., Kim, S., 2011. Study of Double Bond Equivalents and the Numbers of Carbon and Oxygen Atom Distribution of Dissolved Organic Matter with Negative-Mode FT-ICR MS. *Anal. Chem.* 83, 4193–4199. <https://doi.org/10.1021/ac200464q>

- Barati, R., Liang, J.-T., 2014. A review of fracturing fluid systems used for hydraulic fracturing of oil and gas wells. *J. Appl. Polym. Sci.* 131, 40735. <https://doi.org/10.1002/app.40735>
- Barbot, E., Vidic, N.S., Gregory, K.B., Vidic, R.D., 2013. Spatial and Temporal Correlation of Water Quality Parameters of Produced Waters from Devonian-Age Shale following Hydraulic Fracturing. *Environ. Sci. Technol.* 47, 2562–2569. <https://doi.org/10.1021/es304638h>
- Bell, E.A., Poynor, T.E., Newhart, K.B., Regnery, J., Coday, B.D., Cath, T.Y., 2017. Produced water treatment using forward osmosis membranes: Evaluation of extended-time performance and fouling. *J. Membr. Sci.* 525, 77–88. <https://doi.org/10.1016/j.memsci.2016.10.032>
- Bibby, K.J., Brantley, S.L., Reible, D.D., Linden, K.G., Mouser, P.J., Gregory, K.B., Ellis, B.R., Vidic, R.D., 2013. Suggested Reporting Parameters for Investigations of Wastewater from Unconventional Shale Gas Extraction. *Environ. Sci. Technol.* 47, 13220–13221. <https://doi.org/10.1021/es404960z>
- Booker, A.E., Borton, M.A., Daly, R.A., Welch, S.A., Nicora, C.D., Hoyt, D.W., Wilson, T., Purvine, S.O., Wolfe, R.A., Sharma, S., Mouser, P.J., Cole, D.R., Lipton, M.S., Wrighton, K.C., Wilkins, M.J., 2017. Sulfide Generation by Dominant *Halanaerobium* Microorganisms in Hydraulically Fractured Shales. *mSphere* 2, e00257–17. <https://doi.org/10.1128/mSphereDirect.00257-17>
- Boutegrabet, L., Kanawati, B., Gebefügi, I., Peyron, D., Cayot, P., Gougeon, R.D., Schmitt-Kopplin, P., 2012. Attachment of Chloride Anion to Sugars: Mechanistic Investigation and Discovery of a New Dopant for Efficient Sugar Ionization/Detection in Mass Spectrometers. *Chem. - Eur. J.* 18, 13059–13067. <https://doi.org/10.1002/chem.201103788>
- Brüchert, V., 1998. Early diagenesis of sulfur in estuarine sediments: The role of sedimentary humic and fulvic acids. *Geochim. Cosmochim. Acta* 62, 1567–1586.
- Brusseau, M.L., 1994. Transport of reactive contaminants in heterogeneous porous media. *Rev. Geophys.* 32, 285–313.
- Burr, D.A., Sudicky, E.A., Naff, R.L., 1994. Nonreactive and reactive solute transport in three-dimensional heterogeneous porous media: Mean displacement, plume spreading, and uncertainty. *Water Resour. Res.* 30, 791–815.
- Callbeck, C.M., Agrawal, A., Voordouw, G., 2013. Acetate Production from Oil under Sulfate-Reducing Conditions in Bioreactors Injected with Sulfate and Nitrate. *Appl. Environ. Microbiol.* 79, 5059–5068. <https://doi.org/10.1128/AEM.01251-13>
- Calza, P., Massolino, C., Pelizzetti, E., Minero, C., 2008. Solar driven production of toxic halogenated and nitroaromatic compounds in natural seawater. *Sci. Total Environ.* 398, 196–202. <https://doi.org/10.1016/j.scitotenv.2008.03.023>

- Carr, T., 2017. Marcellus Shale Energy and Environment Laboratory (MSEEL): Subsurface Reservoir Characterization and Engineered Completion.
- Chapman, E.C., Capo, R.C., Stewart, B.W., Kirby, C.S., Hammack, R.W., Schroeder, K.T., Edenborn, H.M., 2012. Geochemical and Strontium Isotope Characterization of Produced Waters from Marcellus Shale Natural Gas Extraction. *Environ. Sci. Technol.* 46, 3545–3553. <https://doi.org/10.1021/es204005g>
- Chen, H., Abdulla, H.A.N., Sanders, R.L., Myneni, S.C.B., Mopper, K., Hatcher, P.G., 2014. Production of Black Carbon-like and Aliphatic Molecules from Terrestrial Dissolved Organic Matter in the Presence of Sunlight and Iron. *Environ. Sci. Technol. Lett.* 1, 399–404. <https://doi.org/10.1021/ez5002598>
- Chen, H., Hou, A., Corilo, Y.E., Lin, Q., Lu, J., Mendelssohn, I.A., Zhang, R., Rodgers, R.P., McKenna, A.M., 2016. 4 Years after the *Deepwater Horizon* Spill: Molecular Transformation of Macondo Well Oil in Louisiana Salt Marsh Sediments Revealed by FT-ICR Mass Spectrometry. *Environ. Sci. Technol.* 50, 9061–9069. <https://doi.org/10.1021/acs.est.6b01156>
- Cluff, M.A., Hartsock, A., MacRae, J.D., Carter, K., Mouser, P.J., 2014. Temporal Changes in Microbial Ecology and Geochemistry in Produced Water from Hydraulically Fractured Marcellus Shale Gas Wells. *Environ. Sci. Technol.* 48, 6508–6517. <https://doi.org/10.1021/es501173p>
- Coble, P.G., 2007. Marine optical biogeochemistry: the chemistry of ocean color. *Chem. Rev.* 107, 402–418.
- Coble, P.G., 1996. Characterization of marine and terrestrial DOM in seawater using excitation-emission matrix spectroscopy. *Mar. Chem.* 51, 325–346.
- Coday, B.D., Xu, P., Beaudry, E.G., Herron, J., Lampi, K., Hancock, N.T., Cath, T.Y., 2014. The sweet spot of forward osmosis: Treatment of produced water, drilling wastewater, and other complex and difficult liquid streams. *Desalination* 333, 23–35. <https://doi.org/10.1016/j.desal.2013.11.014>
- Connor, J.A., Walker, K., Molofsky, L., Baca, E., Gie, E., McHugh, T., 2016. Comment on “Impact to Underground Sources of Drinking Water and Domestic Wells from Production Well Stimulation and Completion Practices in the Pavillion, Wyoming, Field”. *Environ. Sci. Technol.* 50, 10769–10770.
- Cooper, W.J., Zika, R.G., Petasne, R.G., Fischer, A.M., 1988. Sunlight-Induced Photochemistry of Humic Substances in Natural Waters: Major Reactive Species, in: Suffet, I.H., MacCarthy, P. (Eds.), *Aquatic Humic Substances*. American Chemical Society, Washington, DC, pp. 333–362.
- Cottrell, B.A., Gonsior, M., Isabelle, L.M., Luo, W., Perraud, V., McIntire, T.M., Pankow, J.F., Schmitt-Kopplin, P., Cooper, W.J., Simpson, A.J., 2013. A regional

- study of the seasonal variation in the molecular composition of rainwater. *Atmos. Environ.* 77, 588–597. <https://doi.org/10.1016/j.atmosenv.2013.05.027>
- Cozzarelli, I.M., Skalak, K.J., Kent, D.B., Engle, M.A., Bentham, A., Mumford, A.C., Haase, K., Farag, A., Harper, D., Nagel, S.C., Iwanowicz, L.R., Orem, W.H., Akob, D.M., Jaeschke, J.B., Galloway, J., Kohler, M., Stoliker, D.L., Jolly, G.D., 2017. Environmental signatures and effects of an oil and gas wastewater spill in the Williston Basin, North Dakota. *Sci. Total Environ.* 579, 1781–1793. <https://doi.org/10.1016/j.scitotenv.2016.11.157>
- Criquet, J., Rodriguez, E.M., Allard, S., Wellauer, S., Salhi, E., Joll, C.A., von Gunten, U., 2015. Reaction of bromine and chlorine with phenolic compounds and natural organic matter extracts – Electrophilic aromatic substitution and oxidation. *Water Res.* 85, 476–486. <https://doi.org/10.1016/j.watres.2015.08.051>
- Dahm, K.G., Guerra, K.L., Xu, P., Drewes, J.E., 2011. Composite Geochemical Database for Coalbed Methane Produced Water Quality in the Rocky Mountain Region. *Environ. Sci. Technol.* 45, 7655–7663. <https://doi.org/10.1021/es201021n>
- Dahm, K.G., Van Straaten, C.M., Munakata-Marr, J., Drewes, J.E., 2013. Identifying Well Contamination through the use of 3-D Fluorescence Spectroscopy to Classify Coalbed Methane Produced Water. *Environ. Sci. Technol.* 47, 649–656. <https://doi.org/10.1021/es303866k>
- Daly, R.A., Borton, M.A., Wilkins, M.J., Hoyt, D.W., Kountz, D.J., Wolfe, R.A., Welch, S.A., Marcus, D.N., Trexler, R.V., MacRae, J.D., Krzycki, J.A., Cole, D.R., Mouser, P.J., Wrighton, K.C., 2016. Microbial metabolisms in a 2.5-km-deep ecosystem created by hydraulic fracturing in shales. *Nat. Microbiol.* 1, 16146. <https://doi.org/10.1038/nmicrobiol.2016.146>
- Damsté, J.S.S., van Koert, E.R., Kock-van Dalen, A.C., de Leeuw, J.W., Schenck, P.A., 1989. Characterisation of highly branched isoprenoid thiophenes occurring in sediments and immature crude oils. *Org. Geochem.* 14, 555–567.
- Darrah, T.H., Vengosh, A., Jackson, R.B., Warner, N.R., Poreda, R.J., 2014. Noble gases identify the mechanisms of fugitive gas contamination in drinking-water wells overlying the Marcellus and Barnett Shales. *Proc. Natl. Acad. Sci.* 111, 14076–14081.
- De Hoon, M.J.L., Imoto, S., Nolan, J., Miyano, S., 2004. Open Source Clustering Software. *Bioinformatics* 20, 1453–1454.
- Dembitsky, V.M., 2006. Biogenic Iodine and Iodine-Containing Metabolites. *Nat. Prod. Commun.* 1, 139 – 175.
- DiGiulio, D.C., Jackson, R.B., 2016a. Impact to Underground Sources of Drinking Water and Domestic Wells from Production Well Stimulation and Completion Practices

in the Pavillion, Wyoming, Field. *Environ. Sci. Technol.* 50, 4524–4536.
<https://doi.org/10.1021/acs.est.5b04970>

DiGiulio, D.C., Jackson, R.B., 2016b. Response to Comment on “Impact to Underground Sources of Drinking Water and Domestic Wells from Production Well Stimulation and Completion Practices in the Pavillion, Wyoming Field”. *Environ. Sci. Technol.* 50, 10771–10772. <https://doi.org/10.1021/acs.est.6b04300>

DiGiulio, D.C., Richard T. Wilkin, Carlyle Miller, Gregory Oberley, 2011. Investigation of Ground Water Contamination near Pavilion, Wyoming (Draft No. EPA 600/R-00/000). US Environmental Protection Agency.

Ding, G., Zhang, X., Yang, M., Pan, Y., 2013. Formation of new brominated disinfection byproducts during chlorination of saline sewage effluents. *Water Res.* 47, 2710–2718. <https://doi.org/10.1016/j.watres.2013.02.036>

Dittmar, T., Koch, B., Hertkorn, N., Kattner, G., 2008. A simple and efficient method for the solid-phase extraction of dissolved organic matter (SPE-DOM) from seawater. *Limnol. Ocean. Methods* 6, 230–235.

Drewes, J., T. Cath, J. Debroux, J. Veil, 2009. An Integrated Framework for Treatment and Management of Produced Water: Technical Assessment of Produced Water Treatment Technologies (No. RPSEA Project 07122-12.).

Drilling Productivity Report For key tight oil and shale regions, 2017a. . U.S. Energy Information Administration.

Drollette, B.D., Hoelzer, K., Warner, N.R., Darrah, T.H., Karatum, O., O’Connor, M.P., Nelson, R.K., Fernandez, L.A., Reddy, C.M., Vengosh, A., Jackson, R.B., Elsner, M., Plata, D.L., 2015. Elevated levels of diesel range organic compounds in groundwater near Marcellus gas operations are derived from surface activities. *Proc. Natl. Acad. Sci.* 112, 13184–13189.
<https://doi.org/10.1073/pnas.1511474112>

Dvorski, S.E.-M., Gonsior, M., Hertkorn, N., Uhl, J., Müller, H., Griebler, C., Schmitt-Kopplin, P., 2016. Geochemistry of Dissolved Organic Matter in a Spatially Highly Resolved Groundwater Petroleum Hydrocarbon Plume Cross-Section. *Environ. Sci. Technol.* 50, 5536–5546. <https://doi.org/10.1021/acs.est.6b00849>

Einsiedl, F., Mayer, B., Schäfer, T., 2008. Evidence for Incorporation of H₂S in Groundwater Fulvic Acids from Stable Isotope Ratios and Sulfur K-edge X-ray Absorption Near Edge Structure Spectroscopy. *Environ. Sci. Technol.* 42, 2439–2444. <https://doi.org/10.1021/es7025455>

Elliott, E.G., Ettinger, A.S., Leaderer, B.P., Bracken, M.B., Deziel, N.C., 2017. A systematic evaluation of chemicals in hydraulic-fracturing fluids and wastewater for reproductive and developmental toxicity. *J. Expo. Sci. Environ. Epidemiol.* 27, 90–99.

- Elsner, M., Hoelzer, K., 2016. Quantitative Survey and Structural Classification of Hydraulic Fracturing Chemicals Reported in Unconventional Gas Production. *Environ. Sci. Technol.* 50, 3290–3314. <https://doi.org/10.1021/acs.est.5b02818>
- Energy Policy Act of 2005.
- Engle, M.A., Rowan, E.L., 2014. Geochemical evolution of produced waters from hydraulic fracturing of the Marcellus Shale, northern Appalachian Basin: A multivariate compositional data analysis approach. *Int. J. Coal Geol.* 126, 45–56. <https://doi.org/10.1016/j.coal.2013.11.010>
- Estrada, J.M., Bhamidimarri, R., 2016. A review of the issues and treatment options for wastewater from shale gas extraction by hydraulic fracturing. *Fuel* 182, 292–303. <https://doi.org/10.1016/j.fuel.2016.05.051>
- Evaluation of Impacts to Underground Sources of Drinking Water by Hydraulic Fracturing of Coalbed Methane Reservoirs, 2004. . US Environmental Protection Agency.
- F.W. McLafferty, F. Turecek, 1993. *Interpretation of Mass Spectra*, 4th Edition. ed. University Science Books, Mill Valley, VA.
- Fakhru'l-Razi, A., Pendashteh, A., Abdullah, L.C., Biak, D.R.A., Madaeni, S.S., Abidin, Z.Z., 2009. Review of technologies for oil and gas produced water treatment. *J. Hazard. Mater.* 170, 530–551. <https://doi.org/10.1016/j.jhazmat.2009.05.044>
- Fellman, J.B., Hood, E., Spencer, R.G.M., 2010. Fluorescence spectroscopy opens new windows into dissolved organic matter dynamics in freshwater ecosystems: A review. *Limnol. Ocean.* 55, 2452–2462. <https://doi.org/10.4319/lo.2010.55.6.2452>
- Ferdelman, T.G., Church, T.M., Luther, G.W., 1991. Sulfur enrichment of humic substances in a Delaware salt marsh sediment core. *Geochim. Cosmochim. Acta* 55, 979–988.
- Fernández-Ramos, C., Ballesteros, O., Zafra-Gómez, A., Camino-Sánchez, F.J., Blanc, R., Navalón, A., Pérez-Trujillo, J.P., Vílchez, J.L., 2014. Evaluation of the levels of alcohol sulfates and ethoxysulfates in marine sediments near wastewater discharge points along the coast of Tenerife Island. *Mar. Pollut. Bull.* 79, 107–113. <https://doi.org/10.1016/j.marpolbul.2013.12.031>
- Ferrar, K.J., Michanowicz, D.R., Christen, C.L., Mulcahy, N., Malone, S.L., Sharma, R.K., 2013. Assessment of Effluent Contaminants from Three Facilities Discharging Marcellus Shale Wastewater to Surface Waters in Pennsylvania. *Environ. Sci. Technol.* 130314103725000. <https://doi.org/10.1021/es301411q>
- Ferrer, I., Thurman, E.M., 2015a. Chemical constituents and analytical approaches for hydraulic fracturing waters. *Trends Environ. Anal. Chem.* 5, 18–25. <https://doi.org/10.1016/j.teac.2015.01.003>

- Ferrer, I., Thurman, E.M., 2015b. Analysis of hydraulic fracturing additives by LC/Q-TOF-MS. *Anal. Bioanal. Chem.* 407, 6417–6428. <https://doi.org/10.1007/s00216-015-8780-5>
- Fontenot, B.E., Hunt, L.R., Hildenbrand, Z.L., Carlton Jr., D.D., Oka, H., Walton, J.L., Hopkins, D., Osorio, A., Bjorndal, B., Hu, Q.H., Schug, K.A., 2013. An Evaluation of Water Quality in Private Drinking Water Wells Near Natural Gas Extraction Sites in the Barnett Shale Formation. *Environ. Sci. Technol.* 47, 10032–10040. <https://doi.org/10.1021/es4011724>
- FracFocus, website: fracfocus.org, 2017.
- Freedman, D.E., Riley, S.M., Jones, Z.L., Rosenblum, J.S., Sharp, J.O., Spear, J.R., Cath, T.Y., 2017. Biologically active filtration for fracturing flowback and produced water treatment. *J. Water Process Eng.* 18, 29–40. <https://doi.org/10.1016/j.jwpe.2017.05.008>
- Fuse, H., Inoue, H., Murakami, K., Takimura, O., Yamaoka, Y., 2003. Production of free and organic iodine by *Roseovarius* spp. *FEMS Microbiol. Lett.* 229, 189–194. [https://doi.org/10.1016/S0378-1097\(03\)00839-5](https://doi.org/10.1016/S0378-1097(03)00839-5)
- Getzinger, G.J., O'Connor, M.P., Hoelzer, K., Drollette, B.D., Karatum, O., Deshusses, M.A., Ferguson, P.L., Elsner, M., Plata, D.L., 2015. Natural Gas Residual Fluids: Sources, Endpoints, and Organic Chemical Composition after Centralized Waste Treatment in Pennsylvania. *Environ. Sci. Technol.* 49, 8347–8355. <https://doi.org/10.1021/acs.est.5b00471>
- Gilmore, K.R., Hupp, R.L., Glathar, J., 2014. Transport of Hydraulic Fracturing Water and Wastes in the Susquehanna River Basin, Pennsylvania. *J. Environ. Eng.* 140, B4013002. [https://doi.org/10.1061/\(ASCE\)EE.1943-7870.0000810](https://doi.org/10.1061/(ASCE)EE.1943-7870.0000810)
- Gong, T., Zhang, X., 2015. Detection, identification and formation of new iodinated disinfection byproducts in chlorinated saline wastewater effluents. *Water Res.* 68, 77–86. <https://doi.org/10.1016/j.watres.2014.09.041>
- Gonsior, M., Mitchelmore, C., Heyes, A., Harir, M., Richardson, S.D., Petty, W.T., Wright, D.A., Schmitt-Kopplin, P., 2015. Bromination of Marine Dissolved Organic Matter following Full Scale Electrochemical Ballast Water Disinfection. *Environ. Sci. Technol.* 49, 9048–9055. <https://doi.org/10.1021/acs.est.5b01474>
- Gonsior, M., Peake, B.M., Cooper, W.T., Podgorski, D., D'Andrilli, J., Cooper, W.J., 2009. Photochemically Induced Changes in Dissolved Organic Matter Identified by Ultrahigh Resolution Fourier Transform Ion Cyclotron Resonance Mass Spectrometry. *Environ. Sci. Technol.* 43, 698–703. <https://doi.org/10.1021/es8022804>
- Gonsior, M., Schmitt-Kopplin, P., Stavklint, H., Richardson, S.D., Hertkorn, N., Bastviken, D., 2014. Changes in Dissolved Organic Matter during the Treatment

Processes of a Drinking Water Plant in Sweden and Formation of Previously Unknown Disinfection Byproducts. *Environ. Sci. Technol.* 48, 12714–12722. <https://doi.org/10.1021/es504349p>

- Gonsior, M., Valle, J., Schmitt-Kopplin, P., Hertkorn, N., Bastviken, D., Luek, J., Harir, M., Bastos, W., Enrich-Prast, A., 2016. Chemodiversity of dissolved organic matter in the Amazon Basin. *Biogeosciences* 13, 4279–4290. <https://doi.org/10.5194/bg-13-4279-2016>
- Gonsior, M., Zwartjes, M., Cooper, W.J., Song, W., Ishida, K.P., Tseng, L.Y., Jeung, M.K., Rosso, D., Hertkorn, N., Schmitt-Kopplin, P., 2011a. Molecular characterization of effluent organic matter identified by ultrahigh resolution mass spectrometry. *Water Res.* 45, 2943–2953. <https://doi.org/10.1016/j.watres.2011.03.016>
- Gonsior, M., Zwartjes, M., Cooper, W.J., Song, W., Ishida, K.P., Tseng, L.Y., Jeung, M.K., Rosso, D., Hertkorn, N., Schmitt-Kopplin, P., 2011b. Molecular characterization of effluent organic matter identified by ultrahigh resolution mass spectrometry. *Water Res.* 45, 2943–2953. <https://doi.org/10.1016/j.watres.2011.03.016>
- Gregory, K.B., Vidic, R.D., Dzombak, D.A., 2011. Water Management Challenges Associated with the Production of Shale Gas by Hydraulic Fracturing. *Elements* 7, 181–186. <https://doi.org/10.2113/gselements.7.3.181>
- Gribble, G.W., 2010. Naturally Occurring Organohalogen Compounds- A Comprehensive Update. Springer Wien New York, Germany.
- Gross, S.A., Avens, H.J., Banducci, A.M., Sahmel, J., Panko, J.M., Tvermoes, B.E., 2013. Analysis of BTEX groundwater concentrations from surface spills associated with hydraulic fracturing operations. *J. Air Waste Manag. Assoc.* 63, 424–432. <https://doi.org/10.1080/10962247.2012.759166>
- Haluszczak, L.O., Rose, A.W., Kump, L.R., 2013. Geochemical evaluation of flowback brine from Marcellus gas wells in Pennsylvania, USA. *Appl. Geochem.* 28, 55–61. <https://doi.org/10.1016/j.apgeochem.2012.10.002>
- Hao, Z., Yin, Y., Cao, D., Liu, J., 2017. Probing and Comparing the Photobromination and Photoiodination of Dissolved Organic Matter by Using Ultra-High-Resolution Mass Spectrometry. *Environ. Sci. Technol.* 51, 5464–5472. <https://doi.org/10.1021/acs.est.6b03887>
- Harkness, J.S., Dwyer, G.S., Warner, N.R., Parker, K.M., Mitch, W.A., Vengosh, A., 2015. Iodide, Bromide, and Ammonium in Hydraulic Fracturing and Oil and Gas Wastewaters: Environmental Implications. *Environ. Sci. Technol.* 49, 1955–1963. <https://doi.org/10.1021/es504654n>

- Hayes, T., 2009. Sampling and Analysis of Water Streams Associated with the Development of Marcellus Shale Gas (Final Report). Gas Technology Institute.
- He, Y., Flynn, S.L., Folkerts, E.J., Zhang, Y., Ruan, D., Alessi, D.S., Martin, J.W., Goss, G.G., 2017a. Chemical and toxicological characterizations of hydraulic fracturing flowback and produced water. *Water Res.* 114, 78–87. <https://doi.org/10.1016/j.watres.2017.02.027>
- He, Y., Folkerts, E.J., Zhang, Y., Martin, J.W., Alessi, D.S., Goss, G.G., 2017b. Effects on Biotransformation, Oxidative Stress, and Endocrine Disruption in Rainbow Trout (*Oncorhynchus mykiss*) Exposed to Hydraulic Fracturing Flowback and Produced Water. *Environ. Sci. Technol.* 51, 940–947. <https://doi.org/10.1021/acs.est.6b04695>
- Helms, J.R., Mao, J., Stubbins, A., Schmidt-Rohr, K., Spencer, R.G.M., Hernes, P.J., Mopper, K., 2014. Loss of optical and molecular indicators of terrigenous dissolved organic matter during long-term photobleaching. *Aquat. Sci.* 76, 353–373. <https://doi.org/10.1007/s00027-014-0340-0>
- Helms, J.R., Stubbins, A., Ritchie, J.D., Minor, E.C., Kieber, D.J., Mopper, K., 2008. Absorption spectral slopes and slope ratios as indicators of molecular weight, source, and photobleaching of chromophoric dissolved organic matter. *Limnol. Ocean.* 53, 955–969.
- Hertkorn, N., Frommberger, M., Witt, M., Koch, B.P., Schmitt-Kopplin, P., Perdue, E.M., 2008. Natural Organic Matter and the Event Horizon of Mass Spectrometry. *Anal. Chem.* 80, 8908–8919. <https://doi.org/10.1021/ac800464g>
- Herzsprung, P., Hertkorn, N., Friese, K., Schmitt-Kopplin, P., 2010. Photochemical degradation of natural organic sulfur compounds (CHOS) from iron-rich mine pit lake pore waters - an initial understanding from evaluation of single-elemental formulae using ultra-high-resolution mass spectrometry. *Rapid Commun. Mass Spectrom.* 24, 2909–2924. <https://doi.org/10.1002/rcm.4719>
- Herzsprung, P., von Tümpling, W., Hertkorn, N., Harir, M., Büttner, O., Bravidor, J., Friese, K., Schmitt-Kopplin, P., 2012. Variations of DOM Quality in Inflows of a Drinking Water Reservoir: Linking of van Krevelen Diagrams with EEMF Spectra by Rank Correlation. *Environ. Sci. Technol.* 46, 5511–5518. <https://doi.org/10.1021/es300345c>
- Hickenbottom, K.L., Hancock, N.T., Hutchings, N.R., Appleton, E.W., Beaudry, E.G., Xu, P., Cath, T.Y., 2013. Forward osmosis treatment of drilling mud and fracturing wastewater from oil and gas operations. *Desalination* 312, 60–66. <https://doi.org/10.1016/j.desal.2012.05.037>
- Hildenbrand, Z.L., Carlton, D.D., Fontenot, B.E., Meik, J.M., Walton, J.L., Taylor, J.T., Thacker, J.B., Korlie, S., Shelor, C.P., Henderson, D., Kadjo, A.F., Roelke, C.E., Hudak, P.F., Burton, T., Rifai, H.S., Schug, K.A., 2015. A Comprehensive

- Analysis of Groundwater Quality in The Barnett Shale Region. *Environ. Sci. Technol.* 49, 8254–8262. <https://doi.org/10.1021/acs.est.5b01526>
- Hildenbrand, Z.L., Carlton, D.D., Fontenot, B.E., Meik, J.M., Walton, J.L., Thacker, J.B., Korlie, S., Shelor, C.P., Kadjo, A.F., Clark, A., Usenko, S., Hamilton, J.S., Mach, P.M., Verbeck, G.F., Hudak, P., Schug, K.A., 2016. Temporal variation in groundwater quality in the Permian Basin of Texas, a region of increasing unconventional oil and gas development. *Sci. Total Environ.* 562, 906–913. <https://doi.org/10.1016/j.scitotenv.2016.04.144>
- Hladik, M.L., Focazio, M.J., Engle, M., 2014. Discharges of produced waters from oil and gas extraction via wastewater treatment plants are sources of disinfection by-products to receiving streams. *Sci. Total Environ.* 466-467, 1085–1093. <https://doi.org/10.1016/j.scitotenv.2013.08.008>
- Hoelzer, K., Sumner, A.J., Karatum, O., Nelson, R.K., Drollette, B.D., O'Connor, M.P., D'Ambro, E.L., Getzinger, G.J., Ferguson, P.L., Reddy, C.M., Elsner, M., Plata, D.L., 2016. Indications of Transformation Products from Hydraulic Fracturing Additives in Shale-Gas Wastewater. *Environ. Sci. Technol.* 50, 8036–8048. <https://doi.org/10.1021/acs.est.6b00430>
- Horai, H., Arita, M., Kanaya, S., Nihei, Y., Ikeda, T., Suwa, K., Ojima, Y., Tanaka, Kenichi, Tanaka, S., Aoshima, K., Oda, Y., Kakazu, Y., Kusano, M., Tohge, T., Matsuda, F., Sawada, Y., Hirai, M.Y., Nakanishi, H., Ikeda, K., Akimoto, N., Maoka, T., Takahashi, H., Ara, T., Sakurai, N., Suzuki, H., Shibata, D., Neumann, S., Iida, T., Tanaka, Ken, Funatsu, K., Matsuura, F., Soga, T., Taguchi, R., Saito, K., Nishioka, T., 2010. MassBank: a public repository for sharing mass spectral data for life sciences. *J. Mass Spectrom.* 45, 703–714. <https://doi.org/10.1002/jms.1777>
- Hosen, J.D., McDonough, O.T., Febria, C.M., Palmer, M.A., 2014. Dissolved Organic Matter Quality and Bioavailability Changes Across an Urbanization Gradient in Headwater Streams. *Environ. Sci. Technol.* 48, 7817–7824. <https://doi.org/10.1021/es501422z>
- Hughey, C.A., Hendrickson, C.L., Rodgers, R.P., Marshall, A.G., Qian, K., 2001. Kendrick Mass Defect Spectrum: A Compact Visual Analysis for Ultrahigh-Resolution Broadband Mass Spectra. *Anal. Chem.* 73, 4676–4681. <https://doi.org/10.1021/ac010560w>
- Ishii, S.K.L., Boyer, T.H., 2012. Behavior of Reoccurring PARAFAC Components in Fluorescent Dissolved Organic Matter in Natural and Engineered Systems: A Critical Review. *Environ. Sci. Technol.* 46, 2006–2017. <https://doi.org/10.1021/es2043504>
- Jackson, R.B., Vengosh, A., Darrah, T.H., Warner, N.R., Down, A., Poreda, R.J., Osborn, S.G., Zhao, K., Karr, J.D., 2013. Increased stray gas abundance in a subset of

- drinking water wells near Marcellus shale gas extraction. *Proc. Natl. Acad. Sci.* 110, 11250–11255. <https://doi.org/10.1073/pnas.1221635110>
- Jang, E., Jeong, S., Chung, E., 2017. Application of three different water treatment technologies to shale gas produced water. *Geosystem Eng.* 20, 104–110. <https://doi.org/10.1080/12269328.2016.1239553>
- Jiang, M., Hendrickson, C.T., VanBriesen, J.M., 2014. Life Cycle Water Consumption and Wastewater Generation Impacts of a Marcellus Shale Gas Well. *Environ. Sci. Technol.* 48, 1911–1920. <https://doi.org/10.1021/es4047654>
- Kahrilas, G.A., Blotevogel, J., Corrin, E.R., Borch, T., 2016. Downhole Transformation of the Hydraulic Fracturing Fluid Biocide Glutaraldehyde: Implications for Flowback and Produced Water Quality. *Environ. Sci. Technol.* 50, 11414–11423. <https://doi.org/10.1021/acs.est.6b02881>
- Kahrilas, G.A., Blotevogel, J., Stewart, P.S., Borch, T., 2015. Biocides in Hydraulic Fracturing Fluids: A Critical Review of Their Usage, Mobility, Degradation, and Toxicity. *Environ. Sci. Technol.* 49, 16–32. <https://doi.org/10.1021/es503724k>
- Kamel, A., Shah, S.N., 2009. Effects of salinity and temperature on drag reduction characteristics of polymers in straight circular pipes. *J. Pet. Sci. Eng.* 67, 23–33. <https://doi.org/10.1016/j.petrol.2009.02.004>
- Kassotis, C.D., Tillitt, D.E., Davis, J.W., Hormann, A.M., Nagel, S.C., 2014. Estrogen and Androgen Receptor Activities of Hydraulic Fracturing Chemicals and Surface and Ground Water in a Drilling-Dense Region. *Endocrinology* 155, 897–907. <https://doi.org/10.1210/en.2013-1697>
- Kekacs, D., Drollette, B.D., Brooker, M., Plata, D.L., Mouser, P.J., 2015. Aerobic biodegradation of organic compounds in hydraulic fracturing fluids. *Biodegradation*. <https://doi.org/10.1007/s10532-015-9733-6>
- Kellerman, A.M., Dittmar, T., Kothawala, D.N., Tranvik, L.J., 2014. Chemodiversity of dissolved organic matter in lakes driven by climate and hydrology. *Nat. Commun.* 5. <https://doi.org/10.1038/ncomms4804>
- Keranen, K.M., Savage, H.M., Abers, G.A., Cochran, E.S., 2013. Potentially induced earthquakes in Oklahoma, USA: Links between wastewater injection and the 2011 Mw 5.7 earthquake sequence. *Geology* 41, 699–702. <https://doi.org/10.1130/G34045.1>
- Khan, N.A., Engle, M., Dungan, B., Holguin, F.O., Xu, P., Carroll, K.C., 2016. Volatile-organic molecular characterization of shale-oil produced water from the Permian Basin. *Chemosphere* 148, 126–136. <https://doi.org/10.1016/j.chemosphere.2015.12.116>

- Kim, D., Amy, G.L., Karanfil, T., 2015. Disinfection by-product formation during seawater desalination: A review. *Water Res.* 81, 343–355. <https://doi.org/10.1016/j.watres.2015.05.040>
- Kim, S., Omur-Ozbek, P., Dhanasekar, A., Prior, A., Carlson, K., 2016. Temporal analysis of flowback and produced water composition from shale oil and gas operations: Impact of frac fluid characteristics. *J. Pet. Sci. Eng.* 147, 202–210. <https://doi.org/10.1016/j.petrol.2016.06.019>
- Kim, W.-Y., 2013. Induced seismicity associated with fluid injection into a deep well in Youngstown, Ohio: INDUCED SEISMICITY IN YOUNGSTOWN, OHIO. *J. Geophys. Res. Solid Earth* 118, 3506–3518. <https://doi.org/10.1002/jgrb.50247>
- King, S.M., Leaf, P.A., Olson, A.C., Ray, P.Z., Tarr, M.A., 2014. Photolytic and photocatalytic degradation of surface oil from the Deepwater Horizon spill. *Chemosphere* 95, 415–422. <https://doi.org/10.1016/j.chemosphere.2013.09.060>
- Koch, B.P., Dittmar, T., Witt, M., Kattner, G., 2007. Fundamentals of Molecular Formula Assignment to Ultrahigh Resolution Mass Data of Natural Organic Matter. *Anal. Chem.* 79, 1758–1763. <https://doi.org/10.1021/ac061949s>
- Kondash, A., Vengosh, A., 2015. Water Footprint of Hydraulic Fracturing. *Environ. Sci. Technol. Lett.* 150918090943001. <https://doi.org/10.1021/acs.estlett.5b00211>
- Kondash, A.J., Albright, E., Vengosh, A., 2017a. Quantity of flowback and produced waters from unconventional oil and gas exploration. *Sci. Total Environ.* 574, 314–321. <https://doi.org/10.1016/j.scitotenv.2016.09.069>
- Kondash, A.J., Albright, E., Vengosh, A., 2017b. Quantity of flowback and produced waters from unconventional oil and gas exploration. *Sci. Total Environ.* 574, 314–321. <https://doi.org/10.1016/j.scitotenv.2016.09.069>
- Lavonen, E.E., Gonsior, M., Tranvik, L.J., Schmitt-Kopplin, P., Köhler, S.J., 2013. Selective Chlorination of Natural Organic Matter: Identification of Previously Unknown Disinfection Byproducts. *Environ. Sci. Technol.* 47, 2264–2271. <https://doi.org/10.1021/es304669p>
- LEAF vs. U.S. EPA. US Court of Appeals, 11th Circuit. No. 95-6501., 1997.
- Lee, J., 2015. Conventional Vs. Unconventional. Oil & Gas Blog. www.croftsystems.net/oil-gas-blog/conventional_vs._unconventional
- Lester, Y., Ferrer, I., Thurman, E.M., Sitterley, K.A., Korak, J.A., Aiken, G., Linden, K.G., 2015. Characterization of hydraulic fracturing flowback water in Colorado: Implications for water treatment. *Sci. Total Environ.* 512-513, 637–644. <https://doi.org/10.1016/j.scitotenv.2015.01.043>

- Lester, Y., Sharpless, C.M., Mamane, H., Linden, K.G., 2013. Production of Photo-oxidants by Dissolved Organic Matter During UV Water Treatment. *Environ. Sci. Technol.* 47, 11726–11733. <https://doi.org/10.1021/es402879x>
- Lester, Y., Yacob, T., Morrissey, I., Linden, K.G., 2014. Can We Treat Hydraulic Fracturing Flowback with a Conventional Biological Process? The Case of Guar Gum. *Environ. Sci. Technol. Lett.* 1, 133–136. <https://doi.org/10.1021/ez4000115>
- Li, H.-P., Yeager, C.M., Brinkmeyer, R., Zhang, S., Ho, Y.-F., Xu, C., Jones, W.L., Schwehr, K.A., Otosaka, S., Roberts, K.A., Kaplan, D.I., Santschi, P.H., 2012. Bacterial Production of Organic Acids Enhances H₂O₂-Dependent Iodide Oxidation. *Environ. Sci. Technol.* 46, 4837–4844. <https://doi.org/10.1021/es203683v>
- Li, Y., Harir, M., Lucio, M., Kanawati, B., Smirnov, K., Flerus, R., Koch, B.P., Schmitt-Kopplin, P., Hertkorn, N., 2016. Proposed Guidelines for Solid Phase Extraction of Suwannee River Dissolved Organic Matter. *Anal. Chem.* 88, 6680–6688. <https://doi.org/10.1021/acs.analchem.5b04501>
- Llewellyn, G.T., Dorman, F., Westland, J.L., Yoxtheimer, D., Grieve, P., Sowers, T., Humston-Fulmer, E., Brantley, S.L., 2015. Evaluating a groundwater supply contamination incident attributed to Marcellus Shale gas development. *Proc. Natl. Acad. Sci.* 112, 6326 – 6330. <https://doi.org/10.1073/pnas.1420279112>
- Lobo, F.L., Wang, H., Huggins, T., Rosenblum, J., Linden, K.G., Ren, Z.J., 2016. Low-energy hydraulic fracturing wastewater treatment via AC powered electrocoagulation with biochar. *J. Hazard. Mater.* 309, 180–184. <https://doi.org/10.1016/j.jhazmat.2016.02.020>
- Lu, J., Wu, J., Ji, Y., Kong, D., 2015. Transformation of bromide in thermo activated persulfate oxidation processes. *Water Res.* 78, 1–8. <https://doi.org/10.1016/j.watres.2015.03.028>
- Luek, J.L., Gonsior, M., 2017. Organic Compounds in Hydraulic Fracturing Fluids and Wastewaters: A Review. *Water Res.* 123, 536–548. <https://doi.org/10.1016/j.watres.2017.07.012>
- Luek, J.L., Schmitt-Kopplin, P., Mouser, P.J., Petty, W.T., Richardson, S.D., Gonsior, M., 2017. Halogenated Organic Compounds Identified in Hydraulic Fracturing Wastewaters Using Ultrahigh Resolution Mass Spectrometry. *Environ. Sci. Technol.* 51, 5377–5385. <https://doi.org/10.1021/acs.est.6b06213>
- Lutz, B.D., Lewis, A.N., Doyle, M.W., 2013. Generation, transport, and disposal of wastewater associated with Marcellus Shale gas development: RAPID COMMUNICATION. *Water Resour. Res.* 49, 647–656. <https://doi.org/10.1002/wrcr.20096>

- Mackay, D.M., Freyberg, D.L., Roberts, P.V., Cherry, J.A., 1986. A Natural Gradient Experiment on Solute Transport in a Sand Aquifer 1. Approach and Overview of Plume Movement. *Water Resour. Res.* 22, 2017–2029.
- Maguire-Boyle, S.J., Barron, A.R., 2014. Organic compounds in produced waters from shale gas wells. *Env. Sci Process. Impacts* 16, 2237–2248.
<https://doi.org/10.1039/C4EM00376D>
- Maillard, J.-Y., 2002. Bacterial target sites for biocide action. *J. Appl. Microbiol.* 92.
- Maloney, K.O., Yoxtheimer, D.A., 2012. Production and Disposal of Waste Materials from Gas and Oil Extraction from the Marcellus Shale Play in Pennsylvania. *Environ. Pr.* 14, 278–287. <https://doi.org/10.1017/S146604661200035X>
- Marshall, A.G., Hendrickson, C.L., 2008. High-Resolution Mass Spectrometers. *Annu. Rev. Anal. Chem.* 1, 579–599.
<https://doi.org/10.1146/annurev.anchem.1.031207.112945>
- Matzek, L.W., Carter, K.E., 2016. Activated persulfate for organic chemical degradation: A review. *Chemosphere* 151, 178–188.
<https://doi.org/10.1016/j.chemosphere.2016.02.055>
- Mauter, M.S., Palmer, V.R., 2014. Expert Elicitation of Trends in Marcellus Oil and Gas Wastewater Management. *J. Environ. Eng.* 140, B4014004.
[https://doi.org/10.1061/\(ASCE\)EE.1943-7870.0000811](https://doi.org/10.1061/(ASCE)EE.1943-7870.0000811)
- McHugh, T., Molofsky, L., Daus, A., Connor, J., 2014. Comment on “An Evaluation of Water Quality in Private Drinking Water Wells Near Natural Gas Extraction Sites in the Barnett Shale Formation”. *Environ. Sci. Technol.* 48, 3595–3596.
<https://doi.org/10.1021/es405772d>
- McHugh, T., Molofsky, L., Fitzgerald, L., Connor, J., 2016. Comment on “A Comprehensive Analysis of Groundwater Quality in The Barnett Shale Region”. *Environ. Sci. Technol.* 50, 496–497. <https://doi.org/10.1021/acs.est.5b05067>
- McLaughlin, M.C., Borch, T., Blotvogel, J., 2016. Spills of Hydraulic Fracturing Chemicals on Agricultural Topsoil: Biodegradation, Sorption, and Co-contaminant Interactions. *Environ. Sci. Technol.*
<https://doi.org/10.1021/acs.est.6b00240>
- Methods for Measuring the Acute Toxicity of Effluents and Receiving Waters to Freshwater and Marine Organisms. 5th Edition (No. EPA-821-R-02-012), 2002a. . U.S. Environmental Protection Agency, Washington, DC.
- Miller, D.J., Huang, X., Li, H., Kasemset, S., Lee, A., Agnihotri, D., Hayes, T., Paul, D.R., Freeman, B.D., 2013. Fouling-resistant membranes for the treatment of flowback water from hydraulic shale fracturing: A pilot study. *J. Membr. Sci.* 437, 265–275. <https://doi.org/10.1016/j.memsci.2013.03.019>

- Miller, J.S., Olejnik, D., 2001. Photolysis of polycyclic aromatic hydrocarbons in water. *Water Res.* 35, 233–243.
- Mohan, A.M., Bibby, K.J., Lipus, D., Hammack, R.W., Gregory, K.B., 2014. The Functional Potential of Microbial Communities in Hydraulic Fracturing Source Water and Produced Water from Natural Gas Extraction Characterized by Metagenomic Sequencing. *PLoS ONE* 9, e107682. <https://doi.org/10.1371/journal.pone.0107682>
- Morales-Cid, G., Gebefugi, I., Kanawati, B., Harir, M., Hertkorn, N., Rosselló-Mora, R., Schmitt-Kopplin, P., 2009. Automated microextraction sample preparation coupled on-line to FT-ICR-MS: application to desalting and concentration of river and marine dissolved organic matter. *Anal. Bioanal. Chem.* 395, 797–807. <https://doi.org/10.1007/s00216-009-3025-0>
- Moulin, V., Reiller, P., Amekraz, B., Moulin, C., 2001. Direct characterization of iodine covalently bound to fulvic acids by electrospray mass spectrometry. *Rapid Commun. Mass Spectrom.* 15, 2488–2496. <https://doi.org/10.1002/rcm.503>
- Mouser, P.J., Borton, M., Darrah, T.H., Hartsock, A., Wrighton, K.C., 2016. Hydraulic fracturing offers view of microbial life in the deep terrestrial subsurface. *FEMS Microbiol. Ecol.* 92, fiw166. <https://doi.org/10.1093/femsec/fiw166>
- Müller, V., 2008. Bacterial fermentation. *Encyclopedia of Life Sciences.*
- Murali Mohan, A., Hartsock, A., Bibby, K.J., Hammack, R.W., Vidic, R.D., Gregory, K.B., 2013a. Microbial Community Changes in Hydraulic Fracturing Fluids and Produced Water from Shale Gas Extraction. *Environ. Sci. Technol.* 47, 13141–13150. <https://doi.org/10.1021/es402928b>
- Murali Mohan, A., Hartsock, A., Hammack, R.W., Vidic, R.D., Gregory, K.B., 2013b. Microbial communities in flowback water impoundments from hydraulic fracturing for recovery of shale gas. *FEMS Microbiol. Ecol.* 86, 567–580. <https://doi.org/10.1111/1574-6941.12183>
- Murphy, K.R., Stedmon, C.A., Graeber, D., Bro, R., 2013. Fluorescence spectroscopy and multi-way techniques. *PARAFAC. Anal. Methods* 5, 6557. <https://doi.org/10.1039/c3ay41160e>
- Murphy, K.R., Stedmon, C.A., Wenig, P., Bro, R., 2014. OpenFluor– an online spectral library of auto-fluorescence by organic compounds in the environment. *Anal. Methods* 6, 658. <https://doi.org/10.1039/c3ay41935e>
- Niazhen, L., Ming, L., Shicheng, Z., 2015. Flowback patterns of fractured shale gas wells. *Nat. Gas Ind. B* 2, 247–251. <https://doi.org/10.1016/j.ngib.2015.07.017>
- Nicot, J.-P., Scanlon, B.R., 2012. Water Use for Shale-Gas Production in Texas, U.S. *Environ. Sci. Technol.* 46, 3580–3586. <https://doi.org/10.1021/es204602t>

- Oetjen, K., Chan, K.E., Gulmark, K., Christensen, J.H., Blotevogel, J., Borch, T., Spear, J.R., Cath, T.Y., Higgins, C.P., 2018. Temporal characterization and statistical analysis of flowback and produced waters and their potential for reuse. *Sci. Total Environ.* 619-620, 654–664. <https://doi.org/10.1016/j.scitotenv.2017.11.078>
- Orem, W., Tatu, C., Varonka, M., Lerch, H., Bates, A., Engle, M., Crosby, L., McIntosh, J., 2014. Organic substances in produced and formation water from unconventional natural gas extraction in coal and shale. *Int. J. Coal Geol.* 126, 20–31. <https://doi.org/10.1016/j.coal.2014.01.003>
- Orem, W., Varonka, M., Crosby, L., Haase, K., Loftin, K., Hladik, M., Akob, D.M., Tatu, C., Mumford, A., Jaeschke, J., Bates, A., Schell, T., Cozzarelli, I., 2017. Organic geochemistry and toxicology of a stream impacted by unconventional oil and gas wastewater disposal operations. *Appl. Geochem.* 80, 155–167. <https://doi.org/10.1016/j.apgeochem.2017.02.016>
- Osborn, Stephen G., Vengosh, A., Warner, N.R., Jackson, R.B., 2011. Methane contamination of drinking water accompanying gas-well drilling and hydraulic fracturing. *Proc. Natl. Acad. Sci.* 108, 8172–8176.
- Osborn, S. G., Vengosh, A., Warner, N.R., Jackson, R.B., 2011. Methane contamination of drinking water accompanying gas-well drilling and hydraulic fracturing. *Proc. Natl. Acad. Sci.* 108, 8172–8176. <https://doi.org/10.1073/pnas.1100682108>
- Pan, Y., Li, W., An, H., Cui, H., Wang, Y., 2016. Formation and occurrence of new polar iodinated disinfection byproducts in drinking water. *Chemosphere* 144, 2312–2320. <https://doi.org/10.1016/j.chemosphere.2015.11.012>
- Parker, K.M., Zeng, T., Harkness, J., Vengosh, A., Mitch, W.A., 2014. Enhanced Formation of Disinfection Byproducts in Shale Gas Wastewater-Impacted Drinking Water Supplies. *Environ. Sci. Technol.* 48, 11161–11169. <https://doi.org/10.1021/es5028184>
- Patterson, L.A., Konschnik, K.E., Wiseman, H., Fargione, J., Maloney, K.O., Kiesecker, J., Nicot, J.-P., Baruch-Mordo, S., Entekin, S., Trainor, A., Saiers, J.E., 2017. Unconventional Oil and Gas Spills: Risks, Mitigation Priorities, and State Reporting Requirements. *Environ. Sci. Technol.* 51, 2563–2573. <https://doi.org/10.1021/acs.est.6b05749>
- Peters, K.E., Walters, C.C., Moldowan, J.M., 2005. *The Biomarker Guide*, 2nd Ed. ed. Cambridge University Press, Cambridge, UK.
- Peuravuori, J., Pihlaja, K., 1997. Molecular size distribution and spectroscopic properties of aquatic humic substances. *Anal. Chim. Acta* 337, 133–149.
- Piotrowski, P.K., Weggler, B.A., Barth-Naftilan, E., Kelly, C.N., Zimmermann, R., Saiers, J.E., Dorman, F.L., 2018. Non-Targeted chemical characterization of a Marcellus shale gas well through GC × GC with scripting algorithms and high-

resolution time-of-flight mass spectrometry. *Fuel* 215, 363–369.
<https://doi.org/10.1016/j.fuel.2017.11.026>

- Plewa, M.J., Wagner, E.D., Muellner, M.G., Hsu, K.-M., Richardson, S.D., 2008. Comparative Mammalian Cell Toxicity of N-DBPs and C-DBPs, in: Karanfil, T., Krasner, S.W., Westerhoff, P., Xie, Y. (Eds.), *Disinfection By-Products in Drinking Water*. American Chemical Society, Washington, DC, pp. 36–50.
- Plewa, M.J., Wagner, E.D., Richardson, S.D., Thruston, A.D., Woo, Y.-T., McKague, A.B., 2004. Chemical and Biological Characterization of Newly Discovered Iodoacid Drinking Water Disinfection Byproducts. *Environ. Sci. Technol.* 38, 4713–4722. <https://doi.org/10.1021/es049971v>
- Postigo, C., Cojocariu, C.I., Richardson, S.D., Silcock, P.J., Barcelo, D., 2016. Characterization of iodinated disinfection by-products in chlorinated and chloraminated waters using Orbitrap based gas chromatography-mass spectrometry. *Anal. Bioanal. Chem.* 408, 3401–3411.
<https://doi.org/10.1007/s00216-016-9435-x>
- Radović, J.R., Aeppli, C., Nelson, R.K., Jimenez, N., Reddy, C.M., Bayona, J.M., Albaigés, J., 2014. Assessment of photochemical processes in marine oil spill fingerprinting. *Mar. Pollut. Bull.* 79, 268–277.
<https://doi.org/10.1016/j.marpolbul.2013.11.029>
- Rahm, B.G., Bates, J.T., Bertoia, L.R., Galford, A.E., Yoxtheimer, D.A., Riha, S.J., 2013. Wastewater management and Marcellus Shale gas development: Trends, drivers, and planning implications. *J. Environ. Manage.* 120, 105–113.
<https://doi.org/10.1016/j.jenvman.2013.02.029>
- Ray, P.Z., Chen, H., Podgorski, D.C., McKenna, A.M., Tarr, M.A., 2014. Sunlight creates oxygenated species in water-soluble fractions of Deepwater horizon oil. *J. Hazard. Mater.* 280, 636–643. <https://doi.org/10.1016/j.jhazmat.2014.08.059>
- Regnery, J., Coday, B.D., Riley, S.M., Cath, T.Y., 2016. Solid-phase extraction followed by gas chromatography-mass spectrometry for the quantitative analysis of semi-volatile hydrocarbons in hydraulic fracturing wastewaters. *Anal Methods* 8, 2058–2068. <https://doi.org/10.1039/C6AY00169F>
- Richardson, S.D., Fasano, F., Ellington, J.J., Crumley, F.G., Buettner, K.M., Evans, J.J., Blount, B.C., Silva, L.K., Waite, T.J., Luther, G.W., McKague, A.B., Miltner, R.J., Wagner, E.D., Plewa, M.J., 2008. Occurrence and Mammalian Cell Toxicity of Iodinated Disinfection Byproducts in Drinking Water. *Environ. Sci. Technol.* 42, 8330–8338. <https://doi.org/10.1021/es801169k>
- Richardson, S.D., Thruston, A.D., Collette, T.W., Patterson, K.S., Lykins, B.W., Majetich, G., Zhang, Y., 1994. Multispectral identification of chlorine dioxide disinfection byproducts in drinking water. *Environ. Sci. Technol.* 28, 592–599.

- Richardson, S.D., Thruston, A.D., Rav-Acha, C., Groisman, L., Popilevsky, I., Juraev, O., Glezer, V., McKague, A.B., Plewa, M.J., Wagner, E.D., 2003. Tribromopyrrole, Brominated Acids, and Other Disinfection Byproducts Produced by Disinfection of Drinking Water Rich in Bromide. *Environ. Sci. Technol.* 37, 3782–3793. <https://doi.org/10.1021/es030339w>
- Richardson, S.D., Thruston Jr, A.D., Caughran, T.V., Chen, P.H., Collette, T.W., Schenck, K.M., Lykins Jr, B.W., Rav-Acha, C., Glezer, V., 2000. Identification of new drinking water disinfection by-products from ozone, chlorine dioxide, chloramine, and chlorine, in: *Environmental Challenges*. Springer, pp. 95–102.
- Riley, S.M., Oliveira, J.M.S., Regnery, J., Cath, T.Y., 2016. Hybrid membrane bio-systems for sustainable treatment of oil and gas produced water and fracturing flowback water. *Sep. Purif. Technol.* 171, 297–311. <https://doi.org/10.1016/j.seppur.2016.07.008>
- Rogers, J.D., Burke, T.L., Osborn, S.G., Ryan, J.N., 2015. A framework for identifying organic compounds of concern in hydraulic fracturing fluids based on mobility and persistence in groundwater. *Environ. Sci. Technol. Lett.* 150515152302002. <https://doi.org/10.1021/acs.estlett.5b00090>
- Rosenblum, J., Nelson, A.W., Ruyle, B., Schultz, M.K., Ryan, J.N., Linden, K.G., 2017a. Temporal characterization of flowback and produced water quality from a hydraulically fractured oil and gas well. *Sci. Total Environ.* 596-597, 369–377. <https://doi.org/10.1016/j.scitotenv.2017.03.294>
- Rosenblum, J., Thurman, E.M., Ferrer, I., Aiken, G., Linden, K.G., 2017b. Organic Chemical Characterization and Mass Balance of a Hydraulically Fractured Well: From Fracturing Fluid to Produced Water over 405 Days. *Environ. Sci. Technol.* 51, 14006–14015. <https://doi.org/10.1021/acs.est.7b03362>
- Rosenblum, J.S., Sitterley, K.A., Thurman, E.M., Ferrer, I., Linden, K.G., 2016. Hydraulic fracturing wastewater treatment by coagulation-adsorption for removal of organic compounds and turbidity. *J. Environ. Chem. Eng.* 4, 1978–1984. <https://doi.org/10.1016/j.jece.2016.03.013>
- Rosenfeld, B., Simon, E., 1950. THE MECHANISM OF THE BUTANOL-ACETONE FERMENTATION I. THE RÔLE OF PYRUVATE AS AN INTERMEDIATE. *J. Biol. Chem.* 186, 395–404.
- Roullier-Gall, C., Witting, M., Tziotis, D., Ruf, A., Gougeon, R.D., Schmitt-Kopplin, P., 2015. Integrating analytical resolutions in non-targeted wine metabolomics. *Tetrahedron* 71, 2983–2990. <https://doi.org/10.1016/j.tet.2015.02.054>
- Rozell, D.J., Reaven, S.J., 2012. Water Pollution Risk Associated with Natural Gas Extraction from the Marcellus Shale: Marcellus Shale Water Pollution Risk. *Risk Anal.* 32, 1382–1393. <https://doi.org/10.1111/j.1539-6924.2011.01757.x>

- Saba, T., Orzechowski, M., 2011. Lack of data to support a relationship between methane contamination of drinking water wells and hydraulic fracturing. *Proc. Natl. Acad. Sci.* 108, E663–E663.
- Schon, S.C., 2011. Hydraulic fracturing not responsible for methane migration. *Proc. Natl. Acad. Sci.* 108, E664–E664.
- Schuytema, G.S., Nebeker, A.V., Stutzman, T.W., 1997. Salinity tolerance of *Daphnia magna* and potential use for estuarine sediment toxicity tests. *Arch. Environ. Contam. Toxicol.* 33, 194–198.
- Schwarzenbach, R.P., Gschwend, P.M., Imboden, D.M., 2003. *Environmental Organic Chemistry*, 2nd ed. Wiley-Interscience.
- Schymanski, E.L., Jeon, J., Gulde, R., Fenner, K., Ruff, M., Singer, H.P., Hollender, J., 2014a. Identifying Small Molecules via High Resolution Mass Spectrometry: Communicating Confidence. *Environ. Sci. Technol.* 140129110454000. <https://doi.org/10.1021/es5002105>
- Schymanski, E.L., Singer, H.P., Longrée, P., Loos, M., Ruff, M., Stravs, M.A., Ripollés Vidal, C., Hollender, J., 2014b. Strategies to Characterize Polar Organic Contamination in Wastewater: Exploring the Capability of High Resolution Mass Spectrometry. *Environ. Sci. Technol.* 48, 1811–1818. <https://doi.org/10.1021/es4044374>
- Shaffer, D.L., Arias Chavez, L.H., Ben-Sasson, M., Romero-Vargas Castrillón, S., Yip, N.Y., Elimelech, M., 2013. Desalination and Reuse of High-Salinity Shale Gas Produced Water: Drivers, Technologies, and Future Directions. *Environ. Sci. Technol.* 47, 9569–9583. <https://doi.org/10.1021/es401966e>
- Shakeri Yekta, S., Gonsior, M., Schmitt-Kopplin, P., Svensson, B.H., 2012. Characterization of Dissolved Organic Matter in Full Scale Continuous Stirred Tank Biogas Reactors Using Ultrahigh Resolution Mass Spectrometry: A Qualitative Overview. *Environ. Sci. Technol.* 46, 12711–12719. <https://doi.org/10.1021/es3024447>
- Shale gas and oil plays, Lower 48 States, 2016a. . U.S. Energy Information Administration.
- Short-term Methods for Estimating the Chronic Toxicity of Effluents and Receiving Waters to Freshwater Organisms. 4th Edition. (No. EPA-821-R-02-013), 2002b. . US Environmental Protection Agency, Washington, DC.
- Sleighter, R.L., Chen, H., Wozniak, A.S., Willoughby, A.S., Caricasole, P., Hatcher, P.G., 2012. Establishing a Measure of Reproducibility of Ultrahigh-Resolution Mass Spectra for Complex Mixtures of Natural Organic Matter. *Anal. Chem.* 121026123639009. <https://doi.org/10.1021/ac3018026>

- Sleighter, R.L., Chin, Y.-P., Arnold, W.A., Hatcher, P.G., McCabe, A.J., McAdams, B.C., Wallace, G.C., 2014a. Evidence of Incorporation of Abiotic S and N into Prairie Wetland Dissolved Organic Matter. *Environ. Sci. Technol. Lett.* 1, 345–350. <https://doi.org/10.1021/ez500229b>
- Sleighter, R.L., Cory, R.M., Kaplan, L.A., Abdulla, H.A.N., Hatcher, P.G., 2014b. A coupled geochemical and biogeochemical approach to characterize the bioreactivity of dissolved organic matter from a headwater stream: Biogeochemistry & Lability of Stream DOM. *J. Geophys. Res. Biogeosciences* 119, 1520–1537. <https://doi.org/10.1002/2013JG002600>
- Smith, E.M., Plewa, M.J., Lindell, C.L., Richardson, S.D., Mitch, W.A., 2010. Comparison of Byproduct Formation in Waters Treated with Chlorine and Iodine: Relevance to Point-of-Use Treatment. *Environ. Sci. Technol.* 44, 8446–8452. <https://doi.org/10.1021/es102746u>
- Soares, A., Guieysse, B., Jefferson, B., Cartmell, E., Lester, J.N., 2008. Nonylphenol in the environment: A critical review on occurrence, fate, toxicity and treatment in wastewaters. *Environ. Int.* 34, 1033–1049. <https://doi.org/10.1016/j.envint.2008.01.004>
- Soeder, D.J., Sharma, S., Pekney, N., Hopkinson, L., Dilmore, R., Kutchko, B., Stewart, B., Carter, K., Hakala, A., Capo, R., 2014. An approach for assessing engineering risk from shale gas wells in the United States. *Int. J. Coal Geol.* 126, 4–19. <https://doi.org/10.1016/j.coal.2014.01.004>
- Stedmon, C.A., Bro, R., 2008. Characterizing dissolved organic matter fluorescence with parallel factor analysis: a tutorial. *Limnol. Ocean. Methods* 6, 572–579.
- Stedmon, C.A., Markager, S., Bro, R., 2003. Tracing dissolved organic matter in aquatic environments using a new approach to fluorescence spectroscopy. *Mar. Chem.* 82, 239–254. [https://doi.org/10.1016/S0304-4203\(03\)00072-0](https://doi.org/10.1016/S0304-4203(03)00072-0)
- Steinberg, S.M., Kimble, G.M., Schmett, G.T., Emerson, D.W., Turner, M.F., Rudin, M., 2008. Abiotic reaction of iodate with sphagnum peat and other natural organic matter. *J. Radioanal. Nucl. Chem.* 277, 185–191. <https://doi.org/10.1007/s10967-008-0728-1>
- Stenson, A.C., Marshall, A.G., Cooper, W.T., 2003. Exact Masses and Chemical Formulas of Individual Suwannee River Fulvic Acids from Ultrahigh Resolution Electrospray Ionization Fourier Transform Ion Cyclotron Resonance Mass Spectra. *Anal. Chem.* 75, 1275–1284. <https://doi.org/10.1021/ac026106p>
- Stream Monitoring in Marcellus Shale Region, 2017. Maryland Department of Natural Resources.
- Stringfellow, W.T., Domen, J.K., Camarillo, M.K., Sandelin, W.L., Borglin, S., 2014. Physical, chemical, and biological characteristics of compounds used in hydraulic

- fracturing. *J. Hazard. Mater.* 275, 37–54.
<https://doi.org/10.1016/j.jhazmat.2014.04.040>
- Strong, L.C., Gould, T., Kasinkas, L., Sadowsky, M.J., Aksan, A., Wackett, L.P., 2013. Biodegradation in Waters from Hydraulic Fracturing: Chemistry, Microbiology, and Engineering. *J. Environ. Eng.* 140, B4013001.
- Sun, M., Lowry, G.V., Gregory, K.B., 2013. Selective oxidation of bromide in wastewater brines from hydraulic fracturing. *Water Res.* 47, 3723–3731.
<https://doi.org/10.1016/j.watres.2013.04.041>
- Tamtam, F., Chiron, S., 2012. New insight into photo-bromination processes in saline surface waters: The case of salicylic acid. *Sci. Total Environ.* 435-436, 345–350.
<https://doi.org/10.1016/j.scitotenv.2012.07.015>
- Taylor, N.S., Weber, R.J.M., White, T.A., Viant, M.R., 2010. Discriminating between Different Acute Chemical Toxicities via Changes in the Daphnid Metabolome. *Toxicol. Sci.* 118, 307–317. <https://doi.org/10.1093/toxsci/kfq247>
- Thacker, J., Carlton, D., Hildenbrand, Z., Kadjo, A., Schug, K., 2015. Chemical Analysis of Wastewater from Unconventional Drilling Operations. *Water* 7, 1568–1579.
<https://doi.org/10.3390/w7041568>
- Thurman, E.M., Ferrer, I., Blotvogel, J., Borch, T., 2014. Analysis of Hydraulic Fracturing Flowback and Produced Waters Using Accurate Mass: Identification of Ethoxylated Surfactants. *Anal. Chem.* 86, 9653 – 9661.
<https://doi.org/10.1021/ac502163k>
- Thurman, E.M., Ferrer, I., Rosenblum, J., Linden, K., Ryan, J.N., 2017. Identification of polypropylene glycols and polyethylene glycol carboxylates in flowback and produced water from hydraulic fracturing. *J. Hazard. Mater.* 323, 11–17.
<https://doi.org/10.1016/j.jhazmat.2016.02.041>
- Timko, S.A., Gonsior, M., Cooper, W.J., 2015a. Influence of pH on fluorescent dissolved organic matter photo-degradation. *Water Res.* 85, 266–274.
<https://doi.org/10.1016/j.watres.2015.08.047>
- Timko, S.A., Maydanov, A., Pittelli, S.L., Conte, M.H., Cooper, W.J., Koch, B.P., Schmitt-Kopplin, P., Gonsior, M., 2015b. Depth-dependent photodegradation of marine dissolved organic matter. *Front. Mar. Sci.* 2.
<https://doi.org/10.3389/fmars.2015.00066>
- U.S. EIA, 2015a. U.S. Crude Oil and Natural Gas Proved Reserves, Year-end 2015. U.S. Energy Information Administration, Washington, DC.
- U.S. EIA, 2015b. Drilling Productivity Report. U.S. Energy Information Administration.

- U.S. EIA, 2016b. Annual Energy Outlook 2016 Early Release: Annotated Summary of Two Cases; DOE/EIA-0373ER. U.S. Energy Information Administration: Washington, D.C.
- U.S. EIA, 2017. Annual Energy Outlook. U.S. Energy Information Administration: Washington, D.C.
- U.S. EPA, 2016. Hydraulic Fracturing for Oil and Gas: Impacts from the Hydraulic Fracturing Water Cycle on Drinking Water Resources in the United States (Final Report). (No. EPA/600/R-16/236F). U.S. Environmental Protection Agency, Washington, DC.
- U.S. EPA, 2015a. Retrospective Case Study in Northeastern Pennsylvania: Study of the Potential Impacts of Hydraulic Fracturing on Drinking Water Resources (No. EPA/600/R-14/088). US Environmental Protection Agency.
- U.S. EPA, 2015b. Retrospective Case Study in Killdeer, North Dakota: Study of the Potential Impacts of Hydraulic Fracturing on Drinking Water Resources (No. EPA/600/R-14/103). US Environmental Protection Agency.
- U.S. EPA, 2015c. Retrospective Case Study in the Raton Basin, Colorado: Study of the Potential Impacts of Hydraulic Fracturing on Drinking Water Resources (No. EPA/600/R-14/091). US Environmental Protection Agency.
- U.S. EPA, 2015d. Retrospective Case Study in Southwestern Pennsylvania Study of the Potential Impacts of Hydraulic Fracturing on Drinking Water Resources (No. EPA/600/R-14/084). US Environmental Protection Agency.
- U.S. EPA, 2015e. Retrospective Case Study in Wise County, Texas: Study of the Potential Impacts of Hydraulic Fracturing on Drinking Water Resources (No. EPA/600/R-14/090). US Environmental Protection Agency.
- Van Krevelen, D.W., 1950. Graphical-statistical method for the study of structure and reaction processes of coal. *Fuel* 29, 269 – 284.
- Vaughan, P.P., Wilson, T., Kamerman, R., Hagy, M.E., McKenna, A., Chen, H., Jeffrey, W.H., 2016. Photochemical changes in water accommodated fractions of MC252 and surrogate oil created during solar exposure as determined by FT-ICR MS. *Mar. Pollut. Bull.* 104, 262–268. <https://doi.org/10.1016/j.marpolbul.2016.01.012>
- Veil, J., 2015. U.S. Produced water volumes and management practices in 2012. Ground Water Protection Council, Oklahoma City, OK.
- Vengosh, A., Jackson, R.B., Warner, N., Darrah, T.H., Kondash, A., 2014. A Critical Review of the Risks to Water Resources from Unconventional Shale Gas Development and Hydraulic Fracturing in the United States. *Environ. Sci. Technol.* 48, 8334–8348. <https://doi.org/10.1021/es405118y>

- Vengosh, A., Kondash, A., Harkness, J., Lauer, N., Warner, N., Darrah, T.H., 2017. The Geochemistry of Hydraulic Fracturing Fluids. *Procedia Earth Planet. Sci.* 17, 21–24. <https://doi.org/10.1016/j.proeps.2016.12.011>
- Vidic, R.D., Brantley, S.L., Vandenbossche, J.M., Yoxtheimer, D., Abad, J.D., 2013. Impact of Shale Gas Development on Regional Water Quality. *Science* 340, 1235009–1235009. <https://doi.org/10.1126/science.1235009>
- Walker, A., Lucio, M., Pfitzner, B., Scheerer, M.F., Neschen, S., de Angelis, M.H., Hartmann, A., Schmitt-Kopplin, P., 2014. Importance of Sulfur-Containing Metabolites in Discriminating Fecal Extracts between Normal and Type-2 Diabetic Mice. *J. Proteome Res.* 13, 4220–4231. <https://doi.org/10.1021/pr500046b>
- Wang, J.Y., Holditch, S.A., McVay, D.A., 2012. Effect of gel damage on fracture fluid cleanup and long-term recovery in tight gas reservoirs. *J. Nat. Gas Sci. Eng.* 9, 108–118. <https://doi.org/10.1016/j.jngse.2012.05.007>
- Wang, L., Kong, D., Ji, Y., Lu, J., Yin, X., Zhou, Q., 2017. Transformation of iodide and formation of iodinated by-products in heat activated persulfate oxidation process. *Chemosphere* 181, 400–408. <https://doi.org/10.1016/j.chemosphere.2017.04.076>
- Wang, X., Wang, J., Zhang, Yahe, Shi, Q., Zhang, H., Zhang, Yu, Yang, M., 2016. Characterization of unknown iodinated disinfection byproducts during chlorination/chloramination using ultrahigh resolution mass spectrometry. *Sci. Total Environ.* 554-555, 83–88. <https://doi.org/10.1016/j.scitotenv.2016.02.157>
- Warner, N.R., Christie, C.A., Jackson, R.B., Vengosh, A., 2013. Impacts of Shale Gas Wastewater Disposal on Water Quality in Western Pennsylvania. *Environ. Sci. Technol.* 131002090059009. <https://doi.org/10.1021/es402165b>
- Warner, N.R., Darrah, T.H., Jackson, R.B., Millot, R., Kloppmann, W., Vengosh, A., 2014. New Tracers Identify Hydraulic Fracturing Fluids and Accidental Releases from Oil and Gas Operations. *Environ. Sci. Technol.* 48, 12552–12560. <https://doi.org/10.1021/es5032135>
- Warner, N.R., Jackson, R.B., Darrah, T.H., Osborn, S.G., Down, A., Zhao, K., White, A., Vengosh, A., 2012a. Geochemical evidence for possible natural migration of Marcellus Formation brine to shallow aquifers in Pennsylvania. *Proc. Natl. Acad. Sci.* 109, 11961–11966.
- Warner, N.R., Jackson, R.B., Darrah, T.H., Osborn, S.G., Down, A., Zhao, K., White, A., Vengosh, A., 2012b. Geochemical evidence for possible natural migration of Marcellus Formation brine to shallow aquifers in Pennsylvania. *Proc. Natl. Acad. Sci.* 109, 11961–11966.

- Weingarten, M., Ge, S., Godt, J.W., Bekins, B.A., Rubinstein, J.L., 2015. High-rate injection is associated with the increase in US mid-continent seismicity. *Science* 348, 1336–1340.
- Werne, J.P., Lyons, T.W., Hollander, D.J., Schouten, S., Hopmans, E.C., Sinninghe Damsté, J.S., 2008. Investigating pathways of diagenetic organic matter sulfurization using compound-specific sulfur isotope analysis. *Geochim. Cosmochim. Acta* 72, 3489–3502. <https://doi.org/10.1016/j.gca.2008.04.033>
- Westerhoff, P., Chao, P., Mash, H., 2004. Reactivity of natural organic matter with aqueous chlorine and bromine. *Water Res.* 38, 1502–1513. <https://doi.org/10.1016/j.watres.2003.12.014>
- Wolford, R., 2011. Characterization of organics in marcellus shale flowback and produced waters. Pennsylvania State University.
- Xie, P., Ma, J., Liu, W., Zou, J., Yue, S., 2015. Impact of UV/persulfate pretreatment on the formation of disinfection byproducts during subsequent chlorination of natural organic matter. *Chem. Eng. J.* 269, 203–211. <https://doi.org/10.1016/j.cej.2015.01.043>
- Xu, C., Chen, H., Sugiyama, Y., Zhang, S., Li, H.-P., Ho, Y.-F., Chuang, C., Schwehr, K.A., Kaplan, D.I., Yeager, C., Roberts, K.A., Hatcher, P.G., Santschi, P.H., 2013. Novel molecular-level evidence of iodine binding to natural organic matter from Fourier transform ion cyclotron resonance mass spectrometry. *Sci. Total Environ.* 449, 244–252. <https://doi.org/10.1016/j.scitotenv.2013.01.064>
- Yost, E.E., Stanek, J., DeWoskin, R.S., Burgoon, L.D., 2016. Overview of Chronic Oral Toxicity Values for Chemicals Present in Hydraulic Fracturing Fluids, Flowback, and Produced Waters. *Environ. Sci. Technol.* 50, 4788–4797. <https://doi.org/10.1021/acs.est.5b04645>
- Zhang, H., Zhang, Y., Shi, Q., Ren, S., Yu, J., Ji, F., Luo, W., Yang, M., 2012. Characterization of low molecular weight dissolved natural organic matter along the treatment trait of a waterworks using Fourier transform ion cyclotron resonance mass spectrometry. *Water Res.* 46, 5197–5204. <https://doi.org/10.1016/j.watres.2012.07.004>
- Zhang, S., Wang, P., Fu, X., Chung, T.-S., 2014. Sustainable water recovery from oily wastewater via forward osmosis-membrane distillation (FO-MD). *Water Res.* 52, 112–121. <https://doi.org/10.1016/j.watres.2013.12.044>
- Zhou, Z., Liu, Z., Guo, L., 2013. Chemical evolution of Macondo crude oil during laboratory degradation as characterized by fluorescence EEMs and hydrocarbon composition. *Mar. Pollut. Bull.* 66, 164–175. <https://doi.org/10.1016/j.marpolbul.2012.09.028>

Ziemkiewicz, P., 2013. Characterization of liquid waste streams from shale gas development. *AGH Drill. Oil Gas* 30, 297.
<https://doi.org/10.7494/drill.2013.30.1.297>

Ziemkiewicz, P.F., He, Y.T., 2015. Evolution of water chemistry during Marcellus Shale gas development: A case study in West Virginia. *Chemosphere* 134, 224–231.
<https://doi.org/10.1016/j.chemosphere.2015.04.040>

Jenna Luek
Curriculum Vitae
146 Williams Street
Solomons, Maryland 20688
412-605-4898

Education

- ❖ **Chesapeake Biological Lab, University of Maryland Center for Environmental Science**, Solomons, MD (2013 – present), Cumulative GPA: 3.82/4.0
Ph.D. Candidate, Marine, Estuarine, and Environmental Science – Environmental Chemistry
Dissertation: Characterization of organic compounds in hydraulic fracturing fluids
- ❖ **Virginia Institute of Marine Science, College of William and Mary**, Gloucester Point, VA (2010 – 2013)
Master's of Science, Marine Science, Cumulative GPA: 3.79/4.0
Thesis: Submarine groundwater discharge to the York River estuary
- ❖ **Chatham University**, Pittsburgh, PA (2006 –2010)
Bachelor's of Science, Chemistry, Environmental Studies, Cumulative GPA: 3.97/4.0
Thesis: Persistent Organic Pollutants in the Atlantic and Southern Oceans and Oceanic Atmosphere

Peer Reviewed Publications

- ❖ **Luek, J.L.**, Thompson, K.T., Larsen, R.K., Heyes, A.H, Gonsior, M. 2017. Sulfate-reducing bacteria produce high levels of chromophoric dissolved organic matter. *Scientific Reports* 7: 8829. DOI: 10.1038/s41598-017-09223-z
- ❖ **Luek, J.L.**, Gonsior, M. 2017. A Review of Organic Compounds in Hydraulic Fracturing Fluids and Wastewaters. *Water Research* 123, 536-548. DOI:10.1016/j.watres.2017.07.012
- ❖ Zhao, Z., Gonsior M., **Luek, J.**, Timko, S., Ianiri, H., Hertkorn, N., Schmitt-Kopplin, P., Fang, X., Zeng, Q., Jiao, N., Chen, F. 2017. Picocyanobacteria and Deep-Ocean Fluorescent Dissolved Organic Matter share Similar Optical Properties. *Nature Communications* 8:15284, DOI: 10.1038/ncomms15284.
- ❖ Gonsior, M., **Luek, J.L.**, Schmitt-Kopplin, P., Grebmeier, J.M., Cooper, L.W. 2017. Optical Properties and Molecular Diversity of Dissolved Organic Matter in the Bering and Chukchi Seas. *Deep Sea Research II*, in press. DOI: 10.1016/j.dsr2.2017.01.003
- ❖ **Luek, J.L.**, Schmitt-Kopplin, P., Mouser, P., Richardson, S.D., Petty, W.T., Gonsior, M. 2017. Halogenated organics identified in produced waters using ultrahigh resolution mass spectrometry. *Environmental Science & Technology* 51, 5377-5385.
- ❖ **Luek, J.L.**, Dickhut, R.M., Cochran, M.A., Falconer, R.L., Kylin, H. 2017. Persistent organic pollutants in the Atlantic and Southern Oceans and oceanic atmosphere. *Science of the Total Environment* 583, 64-71.

- ❖ Gonsior, M., Valle, J., Schmitt-Kopplin, P., Hertkorn, N., Bastviken, D., **Luek, J.**, Harir, M., Bastos, W., and Enrich-Prast, A., 2016. Chemodiversity of Dissolved Organic Matter in the Amazon Basin, *Biogeosciences* 13, 4279–4290.
- ❖ Khairy, M.A., **Luek, J.L.**, Dickhut, R.M., Lohmann, R., 2016. Levels, Sources and Chemical Fate of Persistent Organic Pollutants in the Atmosphere and Snow along the Western Antarctic Peninsula. *Environmental Pollution* 216, 304-313.
- ❖ Beck, A.J., Kellum, A.A., **Luek, J.L.**, Cochran, M.A., 2016. Chemical flux associated with spatially and temporally variable submarine groundwater discharge, and chemical modification in the subterranean estuary at Gloucester Point, VA (USA). *Estuaries and Coasts* 39, 1-12.
- ❖ O'Connor, A.E., **Luek, J.L.**, McIntosh, H.A., Beck, A.J., 2015. Geochemistry of Redox-Sensitive Trace Elements in a Shallow Subterranean Estuary. *Marine Chemistry* 172, 70-81.
- ❖ **Luek, J.L.**, Beck, A.J., 2014. Submarine groundwater discharge to the York River estuary: quantifying groundwater flux and potential for biogeochemical cycling. *Marine Chemistry* 165, 55-65.

Reviewed Journals

Environmental Science: Processes and Impacts, Environmental Science and Technology, Science of the Total Environment, Water Research, Water Science and Technology

Recent Awards

- ❖ College of Computer, Mathematical, and Natural Sciences Dean's Fellowship, UMD (2017)
- ❖ SETAC Student Travel Award (2017)
- ❖ DAAD (German Academic Exchange Service) Short Term Research Proposal (2016)
- ❖ National High Magnetic Field Lab FT-ICR Facility (2016)
- ❖ Best Student Poster, MEES Colloquium, College Park, MD (2016)
- ❖ Best Student Poster, MEES Colloquium, Annapolis, MD (2015)
- ❖ Graduate Education Council Travel Award, CBL (2014, 2015, 2017)
- ❖ Graduate Education Council Ruth Mathes Scholarship (2013 – 2015)
- ❖ College of Computer, Mathematical, and Natural Sciences Dean's Fellowship, UMD (2013-2014)

Community Activities

- ❖ Member, Calvert County Environmental Commission (2016 – present)
- ❖ Patuxent River Women's Rugby Club (2015 – present), Youth Coach (2017)
- ❖ CBL Representative, UMCES Graduate Student Council, Chesapeake Biological Lab (2014 – 2016) Chair (2015)
- ❖ UMCES Representative, Maryland Higher Education Council Student Advisory Committee (2014 - 2015)
- ❖ Lead Organizer, Chesapeake Biological Lab 5K Run for Research (2014)
- ❖ VIMS Community Garden (2011 – 2013) Co-Founder, Co-Chair, and member of Board of Directors (2011 –2013)
- ❖ Volunteer, Historic Harmony, Harmony, PA (May 2000 – present)